# HYDROLYTIC DEGRADATION OF NEAT AND MODIFIED POLY(LACTIC ACID) WITH NANOPARTICLES AND CHAIN EXTENDERS BY WATER-ETHANOL SOLUTIONS

By

Fabiola Maria Iñiguez Franco

A DISSERTATION

Submitted to
Michigan State University
in partial fulfillment of the requirements
for the degree of

Packaging – Doctor of Philosophy

2018

## ABSTRACT

HYDROLYTIC DEGRADATION OF NEAT AND MODIFIED POLY(LACTIC ACID) WITH NANOPARTICLES AND CHAIN EXTENDERS BY WATER-ETHANOL SOLUTIONS

By

Fabiola Maria Iñiguez Franco

Poly(lactic acid) (PLA), a biobased polymer, has been used for applications in the medical, agriculture and food packaging industries. During its life cycle, PLA can be exposed to different environments including water and alcohol solutions promoting its hydrolytic degradation. Depending on the application, degradation can be an advantage or a disadvantage. Hydrolysis can be used as an advantage for converting PLA back to its monomer via chemical recycling. In the case of long service life applications, hydrolysis can be a disadvantage because controlling the resistance to degradation is essential. Incorporation of nanoparticles and chain extenders can be used to expand PLA applications. This work aimed to evaluate the hydrolytic degradation of PLA by water-ethanol solutions, to use hydrolysis in water-ethanol solutions for facilitating chemical recycling of PLA, and to understand the effect of adding nanoparticles and chain extenders on the hydrolysis of PLA.

The parameters and factors affecting the hydrolysis of PLA in water-ethanol solutions were studied. Experimental studies of the concurrent induced crystallization and hydrolytic degradation of PLA films were performed at 40 °C in contact with water, 50% ethanol, and 95% ethanol. PLA films in contact with 50% ethanol showed faster degradation due to a competitive effect between swelling by the presence of ethanol, and the hydrolysis by water sorption molecules starting the degradation reactions.

The chemical recycling of PLA induced by hydrolysis and swelling of 50%ethanol solutions at moderate temperatures were also assessed. The kinetic parameters governing the chemical recycling, rate constant, and activation energy ($E_a$) were quantified. Analysis of the molecular weight distribution of PLA was performed to estimate the rate of hydrolysis. A reparameterization of the Arrhenius equation was proposed for a better estimation of the $E_a$ with a low correlation coefficient between parameters. The $E_a$ values obtained were 104.74 and 96.27 kJ/mol for water and 50% ethanol solution, respectively.

The effect of adding organomodified montmorillonite (OMMT) on the hydrolytic degradation of PLA in water, 50% ethanol, and 95% ethanol was quantified. The change in molecular weight, crystallinity, release of lactic acid, and release of surfactant were monitored. PLA-nanocomposite film exposed to 50% ethanol had a faster rate of degradation. No difference in the rate of degradation was found with OMMT incorporation into the PLA. The clay released from PLA-OMMT films during hydrolysis in 50% ethanol was 0.58% wt. of the initial amount of nanoclay in the PLA film at 90 days.

Finally, the effect of the addition of an epoxy-acrylic additive as a chain extender on the hydrolysis of PLA was studied. Addition of the chain extender increased the dynamic moduli of PLA and the onset decomposition temperature. These results were attributed to the branched structure of PLA resulting from the chain extender. The hydrolysis of PLA in 50% ethanol solution was decreased by the presence of the chain extender, changing the degradation mechanism from bulk to surface erosion.

This dissertation is dedicated to my beloved parents and siblings

## ACKNOWLEDGMENTS

I would like to thank to the Mexican Council of Science and Technology (CONACyT) for the scholarship assistant during my studies at Michigan State University, and also to the Mexican Secretariat of Public Education (SEP) and the Government of Mexico for providing financial support throughout my Ph.D.

I would like to express my sincere gratitude to my advisor Dr. Rafael Auras for continuous support during my Ph.D. studies, for his motivation, patience, and immense knowledge. I could not have imagined having a better advisor and mentor. I am really grateful for being accepted as part of his group. His guidance helped me in my research, and he provided enormous support for my personal and professional growth.

I would like to extend my gratitude to my thesis committee. To Dr. Maria Rubino for her guidance and support. To Dr. Kirk Dolan for his enormous knowledge and timeless support in all of the parameter estimation topics. Taking his class was very valuable for my thesis. My sincere thanks to Dr. Susan Selke for her help and insightful comments for improving this research. My deepest thanks to Dr. Herlinda Soto-Valdez for continuing to be a part of this journey, her guidance as my master's advisor, brought me to Michigan State University.

My sincere thanks also go to Dr. Daniel Holmes for his help with the NMR studies, for his patient explanations with this regard and his support in establishing methodologies for this research. I am grateful to Dr. Gary Burgess for his time and contribution in this thesis. Also, I gratefully acknowledge the help of the Mass Spectrometry & Metabolomics Core Facility at MSU for their assistance with the

developments of the chromatography methods. I am also thankful to the faculty and staff of the School of Packaging at MSU.

I would like to extend my gratitude to all my friends Hayati, Edgar, Jiyon, Jin, Pom, Kim, Rebeca, Abraham, Javi, Felipe and Marco for all the great times together and for their support and for being part of my family far from my hometown.

Thanks to Matthew Faber for his love and emotional support that he has provided in the last years, thanks for making this journey better.

Thanks to my amazing parents, Maria de Jesus Franco Gómez and Gilberto Iñiguez Covarrubias, for being an inspiration in my life, for always being there for me, and for their unconditional support and love. Thanks to my siblings Pau, Jouss and Gil; my best friends, for their encourage and love. I love my family I could not do this without them.

## TABLE OF CONTENTS

## LIST OF TABLES

## LIST OF FIGURES

## KEY TO ABBREVIATIONS

| | |
|---|---|
| $AF_4$ | asymmetrical flow field-flow fractionation |
| CAPS | 3-(cyclohexylamino)-1-propanesulfonic acid |
| $CDCl_3$ | chloroform-D |
| CF | crystalline fraction |
| $^{13}C$ NMR | carbon nuclear magnetic resonance |
| *D* | diffusion coefficient |
| D-NMR | deuterium NMR |
| $D_2O$ | deuterium oxide |
| DMA | dynamic mechanical analysis |
| DMF | N,N-Dimethylformamide |
| DSC | differential scanning calorimetry |
| $E_a$ | activation energy |
| EHP | electrically heated plate |
| EoL | end of life |
| FDA | Food and Drug Administration |
| FV | free volume |
| *G** | complex modulus |
| *G′* | storage modulus |
| *G″* | loss modulus |
| GFAAS | graphite furnace atomic absorption spectrometry |
| gHMBC | gradient heteronuclear multiple bond correlation |

| | |
|---|---|
| GPC | gel permeation chromatograph |
| $^1$H-NMR | proton nuclear magnetic resonance |
| $H_2O$ | water |
| HDI | hexamethylene diisocyanate |
| HEPES | N-(2-Hydroxyethyl)piperazine-N′-(2-ethanesulfonic acid) |
| HPLC | high-performance liquid chromatography |
| ICP-MS | inductively coupled plasma mass spectrometry |
| $k$ | rate constant |
| $k_{ref}$ | rate constant at $T_{ref}$ |
| LA | lactic acid |
| LDH-$C_{12}$ | laurate-modified Mg-Al layered double hydroxide |
| MAF | mobile amorphous fraction |
| MALS | multi-angle light-scattering |
| MK10 | montmorillonite K10 |
| MK5 | montmorillonite K5 |
| MMT | montmorillonite |
| $M_n$ | number average molecular weight |
| $M_{no}$ | initial $M_n$ |
| $M_V$ | viscosity average molecular weight |
| $M_w$ | weight average molecular weight |
| *MWD* | molecular weight distribution |
| NMR | nuclear magnetic resonance |

| | |
|---|---|
| $\eta^*$ | complex viscosity |
| OMMT | organomodified montmorillonite |
| PA | polyamide |
| PA6 | polyamide 6 |
| PBAT | poly(butylene-adipate-co-terephtalate) |
| PBS | poly(butylene succinate) |
| PBSA | poly[(butylene succinate)-co-adipate] |
| PCDI | poly(carbodiimide) (PCDI) |
| *PDI* | polydispersity index |
| PDLA | poly(D-lactic acid); poly(D-lactide) |
| PDLLA | poly(DL-lactic acid); poly(DL-lactide) |
| PE | polyethylene |
| PET | poly(ethylene terephthalate) |
| $pH_{ref}$ | reference pH |
| $pH_{sim}$ | pH simulation |
| PLA | poly(lactic acid) |
| PLLA | poly(L-lactic acid); poly(L-lactide) |
| PMDA | pyromellitic dianhydride |
| PP | polypropylene |
| QAC | organomodifier, surfactant |
| RAF | rigid amorphous fraction |
| RH | relative humidity |
| RMSE | root mean square error |

| | |
|---|---|
| SC | sensitivity coefficient |
| SEC | size exclusion chromatography |
| SIC | solvent induced crystallization |
| SSC | scaled sensitivity coefficient |
| $t$ | time |
| $T$ | temperature |
| $T_c$ | crystallization temperature |
| $T_{cc}$ | cold-crystallization temperature |
| TEM | transmission electron microscopy |
| $T_g$ | glass transition temperature |
| TGA | thermal gravimetric analysis |
| THF | tetrahydrofuran |
| $T_m$ | melting temperature |
| TNPP | tris(nonylphenyl)phosphite |
| $T_{onset}$ | onset decomposition temperatures |
| TPS | thermoplastic starch |
| $T_{ref}$ | reference temperature |
| $T_{sim}$ | temperature simulation |
| $X_c$ | degree of crystallinity |
| XRD | X-ray diffraction study |

# CHAPTER 1

# Introduction

## 1.0 Background and motivations

As pressure for circular and biobased economies are increasing, production of plastics from fossil resources is no longer considered sustainable, and production of novel plastics from renewable resources is increasingly gaining acceptance. Among these new bioplastics, poly(lactic acid), PLA, is one of the main polymers. Not only because it is produced from renewable resources such as corn or cassava starch, but because it has lower environmental footprint and is also providing the opportunity to be disposed to a new end of life scenario, composting [1, 2].

PLA is a linear aliphatic thermoplastic polyester, in which lactic acid (LA) is the precursor obtained from the fermentation of corn or potato sugar [1]. The world production capacity of PLA is 150,000 metric tons, and additional production plants are being developed [3]. PLA is being used in a number of broad and diverse industries such as medical, pharmaceutical, clothing, packaging and agriculture industries since it is biocompatible with the human body, is degradable, has good wicking, breathability, optical, mechanical and barrier properties. However, in using PLA in these industries for different applications, it is exposed to water and organic solvents. The presence of water and/or organic solvents promotes hydrolytic degradation and structural changes in PLA. Under moist conditions the ester groups of the main chain are hydrolytically degraded leading to a decrease in molecular weight and the release of low molecular weight, soluble oligomers and monomers [1, 4]. On the other hand, when PLA is

exposed to organic solvents such as ethanol, the molecules plasticize, swell and crystallization is induced [5-8].

In medical applications, PLA has been widely used in implants, surgical sutures, controlled delivery systems, and tissue culture [9-12]. As a medical implant, the degradation of PLA over time is favorable, avoiding the surgical removal step. However, the rate of PLA degradation may cause defense reactions from the human host. For instance, during the hydrolysis of PLA, the *pH* of cells/tissue is reduced due to the release of LA that accumulates leading to inflammation of the tissue. Toxicity effects may occur during long-term use [13]. Although a large amount of research was conducted regarding the degradation of PLA for medical applications [14-17], full understanding of the degradation mechanisms of PLA in the medical field environment is still needed.

Both the use of implantable biomaterials and the importance of the sterilization techniques to avoid infections associated with the medical devices have been increasing. The impact of the sterilization method is critical for the success of the device since it will dictate the material bulk and surface properties [18]. Use of steam to sterilize PLA can lead to hydrolysis because of the high temperatures, high relative humidity and pressure. Ethanol soaking is another technique that has been applied for the disinfection of PLA electrospun material for tissue engineering. However, the employment of ethanol on PLA has an effect on its physico-chemical properties such as morphology, crystallinity, surface topography, and mechanical properties [18, 19]. Due to its degradation, PLA can be used for drug release. In these surroundings, PLA can be exposed to aqueous or biological media [20-22]. The media in contact with PLA is

important since the interaction with PLA will dictate the mechanism of drug release including drug dissolution, diffusion through the polymer matrix, swelling of the polymer and its surface or bulk erosion [22].

PLA is suitable for fiber and textile applications. In the automotive industry, PLA fiber has gained attention for car interior parts such as carpets and floor mats [23]. PLA has been also investigated as an alternative for apparel manufacturing due to its wicking properties and breathability [24]. However, in such applications PLA could also be exposed to organic solvents, which may change its morphology and under high temperature and moisture conditions will degrade.

In agriculture, PLA has been considered as a plastic to protect soils from erosion, plants from insects and birds, and as a material for the controlled release of herbicides [25-28]. However, the implementation of PLA in the agriculture field is still in the early stages due to its cost. Studies have shown that PLA limits the food sources for microorganisms to initiate the biodegradation process at low temperatures when it is used as a mulch film due to the relatively high glass transition temperature ($T_g$) and low available amorphous region [25]. Thus, commercialized PLA-based mulch films, most of them made of PLA blends, have plasticizers or LA oligomers, which accelerate the hydrolysis process due to the free volume that they provide in the PLA polymer matrix, allowing faster water diffusion and accessibility of the microorganisms [29, 30].

In food packaging, PLA can be found as films, sheets and rigid thermoform containers for short shelf life products [1, 2, 31, 32]. For fresh products or beverages, PLA is exposed to humid environments or it can be in direct contact with food products with high content of water like juices, but also with cold-chain dairy products or alcoholic

beverages. To ensure the safety of using polymers like PLA for food packaging applications, migration studies are required where PLA is exposed to food simulants under specific conditions of temperature and time to simulate food exposure conditions. For instance, 95% ethanol, 50% ethanol or pure water are commonly used as food simulants for fatty, alcoholic and watery liquid products [33, 34]. Thus, PLA has numerous challenges to overcome the hydrolytic degradation under these different environmental conditions to provide the required properties for packaged food containers during their lifetime.

The hydrolytic degradation of PLA is not always considered as a disadvantage. One of the applications of the hydrolysis of PLA during its end of life scenario is for chemical recycling purposes, that is a depolymerization method that converts PLA back to its monomer for new PLA production with the similar properties of virgin PLA [35, 36]. The depolymerization of PLA and other polymers is generally performed at high temperatures using toxic solvents (*i.e.* toluene, chloroform, tetrahydrofuran (THF)) [4, 35, 37, 38]. Other methods have been applied through solvolysis of PLA by transesterification with alcohol to lactate esters [39-41]. The use of an aqueous phase at high temperatures has been investigated [42, 43]. However, it is important to control the temperature since temperatures higher than the melting temperature ($T_m$) of PLA can trigger racemization and decomposition of LA. Therefore, chemical recycling using "green" solvents at moderate temperatures should be economically viable to safely recover PLA.

As aforementioned the versatility of PLA has led to broad applications. Depending on the application, degradation of PLA can be an advantage or a

disadvantage. In the case of applications for long service life, for instance as a packaging material, controlling the resistance to hydrolytic degradation is important since the properties of the container must remain intact during the shelf life of the product to maintain the quality of the product. Several studies have been conducted to improve PLA properties to expand its applications, but also to avoid the thermal degradation of PLA during processing. These achievements have reached by blending PLA with nanoscale particles and also with the addition of chain extenders to control the thermal degradation of PLA during melt processing [44-55].

In recent years, the addition of nanoscale particles has gained greater attention due to the significant improvement of material properties since the interface interactions between the polymer matrix and the nanofiller are maximized, enhancing the polymer properties [48]. PLA-nanocomposites based on layered nanoclays, in particular montmorillonite (MMT), have attracted attention since addition of MMT can improve PLA properties, such as mechanical, thermal and barrier properties [56]. Modification of the surface of MMT is necessary to promote the interaction between the clay and PLA. For that, cations located in the galleries of the silicate layers are exchanged by organomodifiers or surfactants making PLA compatible with the clay, so good dispersion of the layered silicates within the polymer matrix can be obtained and PLA properties enhanced [57]. PLA-nanocomposites based on organomodified MMT (OMMT) have been extensively studied in terms of mechanical, thermal and barrier properties. However, the effect of the organo-clay fillers on the hydrolytic degradation of PLA-nanocomposites has scarcely been addressed since the impact of the OMMT in

such process will dictate the durability of PLA materials in different environments potentially compromising its end use.

Even though research involving the influence of OMMT on the hydrolytic degradation of PLA-nanocomposites in water and phosphate buffered solutions has been reported [58-60], the applications of nanocomposites also involve different environments, for instance organic compounds or different media for food applications (*e.g.*, juices, alcoholic beverages, cold-chain dairy products). Applications involving the direct contact of nanocomposites to food products have created concerns about the potential release of nanoparticles into food systems where their safety should be ensured [61, 62].

Studies have addressed the release of nanoparticles and organomodifiers from different nanocomposites exposed to different conditions, using polymers such as polypropylene (PP) and polyamide (PA) [63, 64]. Theories have been used to describe the migration process of nanoparticles from polymeric packaging materials into food systems [65]. However, PLA-nanocomposites have to be treated differently since PLA is a polymer susceptible to hydrolytic degradation under moist conditions and the exposure to certain compounds leads to structural changes that could affect the release behavior of PLA-nanocomposite compounds.

Understanding the effects of different environments including water-solvent solutions on the hydrolysis of PLA and the effect of engineered nanoparticles is crucial to evaluate the stability of PLA during its lifetime and to address the safety of these materials. To fill the missing gap, research must be conducted to understand the release of PLA-nanocomposite compounds during the hydrolytic degradation of PLA.

Furthermore, the PLA hydrolysis process in different water-solvent solutions must be considered based on the final application of PLA since the impact of the nanoparticles will dictate the durability of PLA-nanocomposites.

The incorporation of chain extenders into PLA during melt processing has being widely studied since PLA is susceptible to thermal degradation during processing. Different factors can affect the degradation during processing such as moisture content, residual metal catalyst, oxygen and processing temperature [66]. Chain extenders reconnect cleaved chains, increasing the molecular weight of the polymer. The main mechanism of stabilization in this case is the chain extension resulting from the formation of either longer linear chains or long branched chains. The incorporation of epoxy based chain extenders (*i.e.* Joncryl®) into PLA increased the molecular weight and improved the rheological, mechanical and thermal properties [49, 50, 67-71]. However, the effect of adding epoxy chain extenders on the hydrolytic degradation of PLA is not well understood.

## 1.1 Overall goal and objectives

The overall goal of this dissertation is to evaluate the hydrolytic degradation of PLA by water-ethanol solutions, the use of this system to be applied in the chemical recycling of PLA, and the effect of adding nanoparticles and chain extenders on the hydrolytic degradation of PLA. To accomplish the main goal, different objectives have to be addressed.

1) To understand the parameters and factor affecting the hydrolysis of PLA by water-ethanol solutions.

2) To understand and to analyze the hydrolytic degradation of PLA by water-ethanol solutions for the purpose of chemical recycling at moderate temperatures.
3) To understand the effect of the nanoparticles and the surfactant on the hydrolytic degradation of PLA-nanocomposites, and the connection between the transport of water-ethanol solutions through the PLA-nanocomposite and the release of the nanoparticles and the surfactant.
4) To understand the effect of adding chain extenders into PLA during processing and its effect on the hydrolytic degradation of modified PLA.

## 1.2 Dissertation overview

To answer the objectives of this dissertation this document is organized in the following manner. Chapter 2 provides a critical literature review detailing the hydrolytic degradation mechanism of PLA, the parameters controlling the hydrolysis process, the chemical recycling of PLA, a detailed description of the addition of nanoparticles into PLA and the effect on the hydrolytic degradation, and a review of the use of chain extenders into PLA.

Chapter 3 is a version of a published article that presents the results to understand the concurrent effect of the solvent induced crystallization (SIC) and the hydrolytic degradation of PLA when it is exposed to different water-ethanol solutions at 40 °C. At the end of the chapter as an appendix, the supporting information is presented that enhanced the main article.

Chapter 4 is a version of the accepted article to a journal that investigates and analyzes the hydrolytic degradation of PLA in water-ethanol solutions for being used for chemical recycling at moderate temperatures, estimating the kinetic parameters, rate

constant and activation energy that determines the hydrolysis of PLA in these solutions. An appendix is presented at the end of the chapter as supporting information.

Chapter 5 is a version of a published article that explores the effect of adding nanoparticles and surfactant on the hydrolytic degradation at 40 °C of PLA-nanocomposites in water-ethanol solutions and the interaction between PLA, nanoclay and solvent. An appendix is presented at the end of the chapter as supporting information.

Chapter 6 is a version of a submitted article that studies the effect of adding chain extenders during PLA processing and the effect on the hydrolytic degradation of PLA in water-ethanol solution at 80 °C with the purpose of modifying the hydrolysis mechanism of the polymer.

Chapter 7 summarizes all the work in this dissertation and concludes with future work recommendations.

## REFERENCES

## REFERENCES


[1] R. Auras, B. Harte, S. Selke, An overview of polylactides as packaging materials, Macromol. Biosci. 4 (2004) 835-864.

[2] E. Castro-Aguirre, F. Iñiguez-Franco, H. Samsudin, X. Fang, R. Auras, Poly (lactic acid)—Mass production, processing, industrial applications, and end of life, Adv. Drug Deliv. Rev. 107 (2016) 333-366.

[3] E.T. Vink, S. Davies, Life Cycle Inventory and Impact Assessment Data for 2014 Ingeo™ Polylactide Production, Industrial Biotechnology 11 (2015) 167-180.

[4] H. Tsuji, Hydrolytic Degradation, in: R. Auras, L.-T. Lim, S. Selke, H. Tsuji (Eds.), Poly(lactic acid). Synthesis, Structures, Properties, Processing, and Applications, John Wiley & Sons, Inc., New Jersey, 2010, pp. 345-381.

[5] H. Tsuji, K. Sumida, Poly (L‐lactide): v. effects of storage in swelling solvents on physical properties and structure of poly (L‐lactide), J. Appl. Polym. Sci. 79 (2001) 1582-1589.

[6] S. Sato, D. Gondo, T. Wada, S. Kanehashi, K. Nagai, Effects of various liquid organic solvents on solvent‐induced crystallization of amorphous poly (lactic acid) film, J. Appl. Polym. Sci. 129 (2013) 1607-1617.

[7] N. Wu, S. Lang, H. Zhang, M. Ding, J. Zhang, Solvent-Induced Crystallization Behaviors of PLLA Ultrathin Films Investigated by RAIR Spectroscopy and AFM Measurements, J. Phys. Chem. B 118 (2014) 12652-12659.

[8] J. Gao, L. Duan, G. Yang, Q. Zhang, M. Yang, Q. Fu, Manipulating poly (lactic acid) surface morphology by solvent-induced crystallization, Applied Surface Science 261 (2012) 528-535.

[9] K.E. Uhrich, S.M. Cannizzaro, R.S. Langer, K.M. Shakesheff, Polymeric systems for controlled drug release, Chem. Rev. 99 (1999) 3181-3198.

[10] J.-Y. Park, I.-H. Lee, Controlled release of ketoprofen from electrospun porous polylactic acid (PLA) nanofibers, J. Polym. Res. 18 (2011) 1287-1291.

[11] Y. Ikada, H. Tsuji, Biodegradable polyesters for medical and ecological applications, Macromol. Rapid Commun. 21 (2000) 117-132.

[12] N. Bleach, K. Tanner, M. Kellomäki, P. Törmälä, Effect of filler type on the mechanical properties of self-reinforced polylactide–calcium phosphate composites, J. Mater. Sci. Mater. Med. 12 (2001) 911-915.

[13] S. Suzuki, Y. Ikada, Medical Applications, in: R. Auras, L.T. Lim, S. Selke, H. Tsuji (Eds.), Poly(lactic acid). Synthesis, Structures, Properties, Processing, and Applications, Wiley Publishers, New Jersey, 2010, pp. 443-456.

[14] S. Li, S. McCarthy, Further investigations on the hydrolytic degradation of poly (DL-lactide), Biomaterials 20 (1999) 35-44.

[15] A. Reed, D. Gilding, Biodegradable polymers for use in surgery—poly (glycolic)/poly (lactic acid) homo and copolymers: 2. In vitro degradation, Polymer 22 (1981) 494-498.

[16] B. Gupta, N. Revagade, J. Hilborn, In vitro degradation of dry‐jet‐wet spun poly (lactic acid) monofilament and knitted scaffold, J. Appl. Polym. Sci. 103 (2007) 2006-2012.

[17] E. Vey, C. Roger, L. Meehan, J. Booth, M. Claybourn, A.F. Miller, A. Saiani, Degradation mechanism of poly (lactic-co-glycolic) acid block copolymer cast films in phosphate buffer solution, Polym. Degrad. Stab. 93 (2008) 1869-1876.

[18] M. Ahmed, G. Punshon, A. Darbyshire, A.M. Seifalian, Effects of sterilization treatments on bulk and surface properties of nanocomposite biomaterials, Journal of Biomedical Materials Research Part B: Applied Biomaterials (2013).

[19] Z. Pan, J. Ding, Poly (lactide-co-glycolide) porous scaffolds for tissue engineering and regenerative medicine, Interface focus 2 (2012) 366-377.

[20] C.G. Pitt, M.M. Gratzl, A.R. Jeffcoat, R. Zweidinger, A. Schindler, Sustained drug delivery systems II: Factors affecting release rates from poly (ε‐caprolactone) and related biodegradable polyesters, Journal of Pharmaceutical Sciences 68 (1979) 1534-1538.

[21] M.-K. Lai, R.-C. Tsiang, Microencapsulation of acetaminophen into poly (L-lactide) by three different emulsion solvent-evaporation methods, J. Microencapsulation 22 (2005) 261-274.

[22] L. Zhang, C. Long, J. Pan, Y. Qian, A Dissolution‐Diffusion Model and Quantitative Analysis of Drug Controlled Release from Biodegradable Polymer Microspheres, The Canadian Journal of Chemical Engineering 84 (2006) 558-566.

[23] Ford researchers aim to create greener, lighter plastics. http://www.reliableplant.com/Read/20034/ford-researchers-aim-to-create-greener,-lighter-plastics, 2015 (accessed Sept 2nd).

[24] D. Farrington, J. Lunt, S. Davies, R. Blackburn, Poly (lactic acid) fibers, in: R. Blackburn (Ed.), Biodegradable and sustainable fibres, Woodhead Publishing Limeted, Cambridge, England, 2005, pp. 191-220.

[25] D.G. Hayes, S. Dharmalingam, L.C. Wadsworth, K.K. Leonas, C. Miles, D. Inglis, Biodegradable agricultural mulches derived from biopolymers, in: C.S. Kishan Khemani (Ed.), Degradable polymers and materials: Principles and practice, American Chemical Society, Washington, DC, 2012, pp. 201-223.

[26] K.M. Nampoothiri, N.R. Nair, R.P. John, An overview of the recent developments in polylactide (PLA) research, Bioresour. Technol. 101 (2010) 8493-8501.

[27] R.G. Sinclair, Slow-release pesticide system. Polymers of lactic and glycolic acids as ecologically beneficial, cost-effective encapsulating materials, Environ. Sci. Technol. 7 (1973) 955-956.

[28] Y.-N. Chang, R.E. Mueller, E.L. Iannotti, Use of low MW polylactic acid and lactide to stimulate growth and yield of soybeans, Plant Growth Regul. 19 (1996) 223-232.

[29] M. Hakkarainen, S. Karlsson, A.C. Albertsson, Influence of low molecular weight lactic acid derivatives on degradability of polylactide, J. Appl. Polym. Sci. 76 (2000) 228-239.

[30] S.R. Andersson, M. Hakkarainen, A.-C. Albertsson, Tuning the polylactide hydrolysis rate by plasticizer architecture and hydrophilicity without introducing new migrants, Biomacromolecules 11 (2010) 3617-3623.

[31] NatureWorks. NatureWorks PLA helps Delhaize extend environmentally-friendly packaging to belgian costumers. http://www.pressreleasefinder.com/NatureWorks/NWPR001/en/, 2018 (accessed 01/03/2018).

[32] NatureWorks. SPAR Austria enhances freshness of produce with NatureWorks PLA. http://www.pressreleasefinder.com/NatureWorks/NWPR015/en/, 2018 (accessed 01/03/2018).

[33] FDA. Guidance for Industry: Preparation of Premarket Submissions for Food Contact Substances: Chemistry Recommendations. Food and Drug Administration. http://www.fda.gov/Food/GuidanceRegulation/GuidanceDocumentsRegulatoryInformation/IngredientsAdditivesGRASPackaging/ucm081818.htm - iid1a, 2015 (accessed 09/15/2015).

[34] 10/2011/EU Commission regulation on plastic materials and articles intended to come into contact with food. The European Commission., Official Journal of the European Union 12 (2011) 15.11.2011.

[35] K. Hamad, M. Kaseem, F. Deri, Recycling of waste from polymer materials: An overview of the recent works, Polym. Degrad. Stab. 98 (2013) 2801-2812.

[36] V. Piemonte, S. Sabatini, F. Gironi, Chemical recycling of PLA: a great opportunity towards the sustainable development?, J. Polym. Environ. 21 (2013) 640-647.

[37] K. Okamoto, K. Toshima, S. Matsumura, Degradation of poly (lactic acid) into repolymerizable oligomer using montmorillonite K10 for chemical recycling, Macromol. Biosci. 5 (2005) 813-820.

[38] Y. Tsuneizumi, M. Kuwahara, K. Okamoto, S. Matsumura, Chemical recycling of poly (lactic acid)-based polymer blends using environmentally benign catalysts, Polym. Degrad. Stab. 95 (2010) 1387-1393.

[39] F.A. Leibfarth, N. Moreno, A.P. Hawker, J.D. Shand, Transforming polylactide into value‐added materials, J. Polym. Sci. A Polym. Chem. 50 (2012) 4814-4822.

[40] P. Coszach, J.-C. Bogaert, J. Willocq, Chemical recycling of PLA by alcoholysis. United States Patent 848675 B2, in, 2013.

[41] A.C. Sánchez, S.R. Collinson, The selective recycling of mixed plastic waste of polylactic acid and polyethylene terephthalate by control of process conditions, Eur. Polym. J. 47 (2011) 1970-1976.

[42] H. Tsuji, H. Daimon, K. Fujie, A new strategy for recycling and preparation of poly (L-lactic acid): hydrolysis in the melt, Biomacromolecules 4 (2003) 835-840.

[43] H. Tsuji, T. Saeki, T. Tsukegi, H. Daimon, K. Fujie, Comparative study on hydrolytic degradation and monomer recovery of poly (L-lactic acid) in the solid and in the melt, Polym. Degrad. Stab. 93 (2008) 1956-1963.

[44] H. Liu, J. Zhang, Research progress in toughening modification of poly (lactic acid), J. Polym. Sci. Part B Polym. Phys. 49 (2011) 1051-1083.

[45] H. Balakrishnan, A. Hassan, M. Imran, M.U. Wahit, Toughening of polylactic acid nanocomposites: A short review, Polym. Plast. Technol. Eng. 51 (2012) 175-192.

[46] S. Detyothin, A. Kathuria, W. Jaruwattanayon, S.E.M. Selke, R. Auras, Poly(lactic acid) Blends, in: R. Auras, L.T. Lim, S. Selke, H. Tsuji (Eds.), Poly(lactic acid).

Synthesis, Structures, Properties, Processing, and Applications, John Wiley & Sons, Inc., New Jersey, 2010, pp. 227-266.

[47] S.B. Ghosh, S. Bandyopadhyay-Ghosh, M. Sain, Composites, in: R. Auras, L.T. Lim, S. Selke, H. Tsuji (Eds.), Poly(lactic acid). Synthesis, Structures, Properties, Processing, and Applications, John Wiley & Sons, Inc., New Jersey, 2010, pp. 293-307.

[48] S.S. Ray, Nanocomposites, in: R. Auras, L.T. Lim, S. Selke, H. Tsuji (Eds.), Poly(lactic acid). Synthesis, Structures, Properties, Processing, and Applications, John Wiley & Sons, Inc., New Jersey, 2010, pp. 311-321.

[49] N. Najafi, M. Heuzey, P. Carreau, P.M. Wood-Adams, Control of thermal degradation of polylactide (PLA)-clay nanocomposites using chain extenders, Polym. Degrad. Stab. 97 (2012) 554-565.

[50] R. Al-Itry, K. Lamnawar, A. Maazouz, Improvement of thermal stability, rheological and mechanical properties of PLA, PBAT and their blends by reactive extrusion with functionalized epoxy, Polym. Degrad. Stab. 97 (2012) 1898-1914.

[51] H.J. Lehermeier, J.R. Dorgan, Melt rheology of poly (lactic acid): Consequences of blending chain architectures, Polym. Eng. Sci. 41 (2001) 2172-2184.

[52] L. Yang, X. Chen, X. Jing, Stabilization of poly (lactic acid) by polycarbodiimide, Polym. Degrad. Stab. 93 (2008) 1923-1929.

[53] S.I. Woo, B.O. Kim, H.S. Jun, H.N. Chang, Polymerization of aqueous lactic acid to prepare high molecular weight poly (lactic acid) by chain-extending with hexamethylene diisocyanate, Polymer bulletin 35 (1995) 415-421.

[54] J. Tuominen, J. Kylmä, J. Seppälä, Chain extending of lactic acid oligomers. 2. Increase of molecular weight with 1, 6-hexamethylene diisocyanate and 2, 2′ -bis (2-oxazoline), Polymer 43 (2002) 3-10.

[55] M. Villalobos, A. Awojulu, T. Greeley, G. Turco, G. Deeter, Oligomeric chain extenders for economic reprocessing and recycling of condensation plastics, Energy 31 (2006) 3227-3234.

[56] S.S. Ray, K. Yamada, M. Okamoto, K. Ueda, New polylactide-layered silicate nanocomposites. 2. Concurrent improvements of material properties, biodegradability and melt rheology, Polymer 44 (2003) 857-866.

[57] S.S. Ray, M. Okamoto, Polymer/layered silicate nanocomposites: a review from preparation to processing, Prog. Polym. Sci. 28 (2003) 1539-1641.

[58] K. Fukushima, D. Tabuani, M. Dottori, I. Armentano, J. Kenny, G. Camino, Effect of temperature and nanoparticle type on hydrolytic degradation of poly (lactic acid) nanocomposites, Polym. Degrad. Stab. 96 (2011) 2120-2129.

[59] Q. Zhou, M. Xanthos, Nanoclay and crystallinity effects on the hydrolytic degradation of polylactides, Polym. Degrad. Stab. 93 (2008) 1450-1459.

[60] M.-A. Paul, C. Delcourt, M. Alexandre, P. Degée, F. Monteverde, P. Dubois, Polylactide/montmorillonite nanocomposites: study of the hydrolytic degradation, Polym. Degrad. Stab. 87 (2005) 535-542.

[61] Q. Chaudhry, M. Scotter, J. Blackburn, B. Ross, A. Boxall, L. Castle, R. Aitken, R. Watkins, Applications and implications of nanotechnologies for the food sector, Food additives and contaminants 25 (2008) 241-258.

[62] C. Silvestre, D. Duraccio, S. Cimmino, Food packaging based on polymer nanomaterials, Prog. Polym. Sci. 36 (2011) 1766-1782.

[63] Y. Xia, M. Rubino, R. Auras, Release of nanoclay and surfactant from polymer–clay nanocomposites into a food simulant, Environ. Sci. Technol. 48 (2014) 13617-13624.

[64] R. Nigmatullin, F. Gao, V. Konovalova, Polymer-layered silicate nanocomposites in the design of antimicrobial materials, J. Mater. Sci. 43 (2008) 5728-5733.

[65] P. Simon, Q. Chaudhry, D. Bakos, from polymer packaging to food–a physicochemical view, J. Food Nutr. Res. 47 (2008) 105-113.

[66] H. Nishida, Thermal Degradation, in: R. Auras, L.-T. Lim, S. Selke, H. Tsuji (Eds.), Poly(lactic acid). Synthesis, Structures, Properties, Processing, and Applications, John Wiley & Sons, Inc., New Jersey, 2010, pp. 401-412.

[67] S.R. Rathi, E.B. Coughlin, S.L. Hsu, C.S. Golub, G.H. Ling, M.J. Tzivanis, Maintaining structural stability of poly (lactic acid): effects of multifunctional epoxy based reactive oligomers, Polymers 6 (2014) 1232-1250.

[68] Q. Meng, M.-C. Heuzey, P.J. Carreau, Control of thermal degradation of polylactide/clay nanocomposites during melt processing by chain extension reaction, Polym. Degrad. Stab. 97 (2012) 2010-2020.

[69] W. Dong, B. Zou, Y. Yan, P. Ma, M. Chen, Effect of Chain-Extenders on the Properties and Hydrolytic Degradation Behavior of the Poly (lactide)/Poly (butylene adipate-co-terephthalate) Blends, International journal of molecular sciences 14 (2013) 20189-20203.

[70] Y.-M. Corre, J. Duchet, J. Reignier, A. Maazouz, Melt strengthening of poly (lactic acid) through reactive extrusion with epoxy-functionalized chains, Rheol. Acta 50 (2011) 613-629.

[71] R. Al-Itry, K. Lamnawar, A. Maazouz, Reactive extrusion of PLA, PBAT with a multi-functional epoxide: Physico-chemical and rheological properties, Eur. Polym. J. 58 (2014) 90-102.

# CHAPTER 2

## Literature Review

### 2.0 Introduction: Poly(lactic acid) – PLA

Conventional polymers are mostly made from chemicals that are mainly derived from fossil fuels and after their consumption are discarded, creating environmental concerns as increasing greenhouse gas emissions and pollution. In this regard, the development of biodegradable polymers derived from biobased resources has gained great attention. Poly(lactic acid) (PLA) is an aliphatic polyester derived from renewable resources such as corn and potatoes with lower environmental impact than fossil derived polymers and offering alternative disposal routes (*e.g.,* composting) [1]. **Figure 2.1** shows that the interest and the number of published research studies of PLA have increased in the last 25 years.

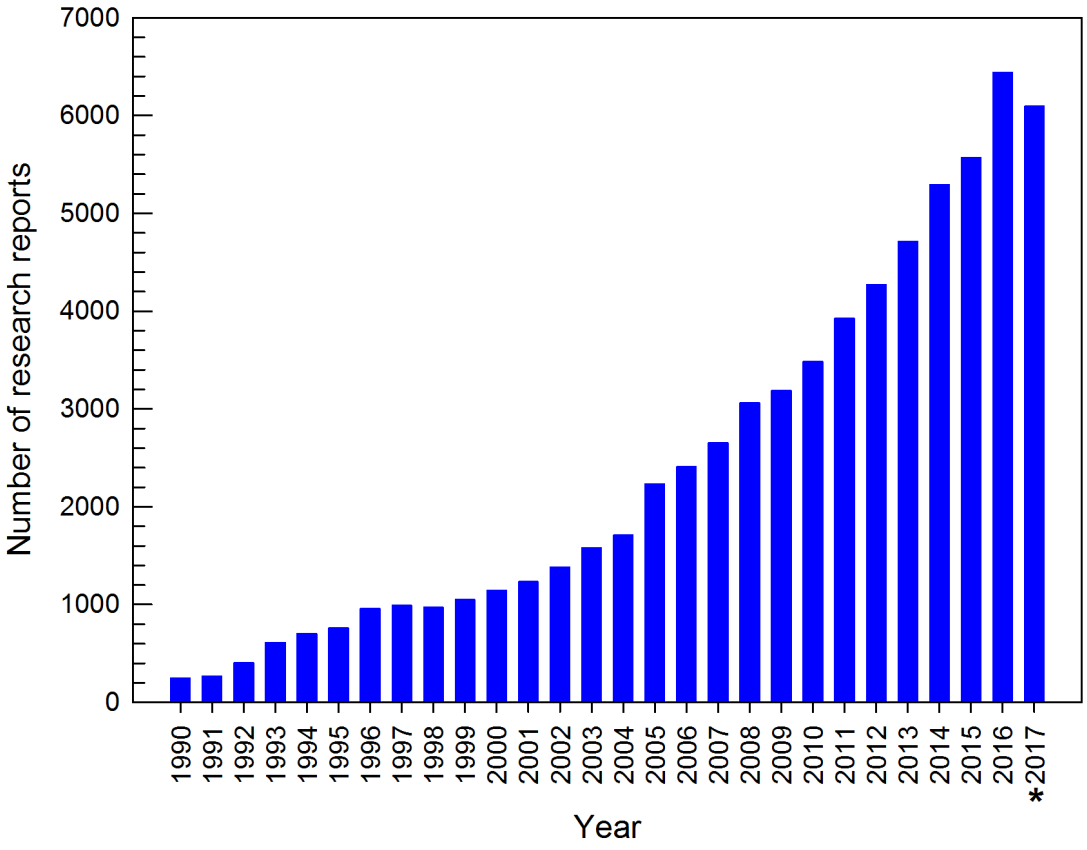


**Figure 2.1** Number of research reports published since 1990 based on a Web of Science search using keywords “PLA”, “PLLA”, “PDLA”, “polylactic acid”, “polylactide”, and “poly(lactic acid)”. * Data until 03/01/18.

PLA has been used in diverse industries for different applications, such as medical, clothing, packaging and agriculture. For medical applications, PLA can be found as suture material, stents and drug delivery systems [2-4]; in agriculture, as mulch film to protect soils and plants [5]. and in packaging industries as films and rigid thermoformed containers for food and non-food products [6].

PLA properties depend on the polymer architecture (*i.e.,* stereochemical makeup) and molecular weight [1]. PLA is synthetized from lactic acid (LA) or lactide, which are chiral molecules having different enantiomers: L- and D-LA or L- and D-lactide (**Figure 2.2**) [7]. High molecular weight PLA is produced from different combinations of LA or lactide enantiomers amounts. PLA comprises by isotactic sequences of L-LA or L-lactide and D-LA or D-lactide are referred to PLLA and PDLA, respectively. When PLA is formed by *meso*-lactide, or a mixture of L-LA or D-LA (or L- and D-lactide), or racemic mixture (50:50) of L-LA and D-LA (or L- and D-lactide) is represented by the term PDLLA. PLA derived from greater than 92% L-LA can be semicrystalline, while PLA from 50 to 92% L-LA is amorphous [1]. The stereochemical architecture of PLA controls the degree of crystallinity, and therefore the degradation behavior.

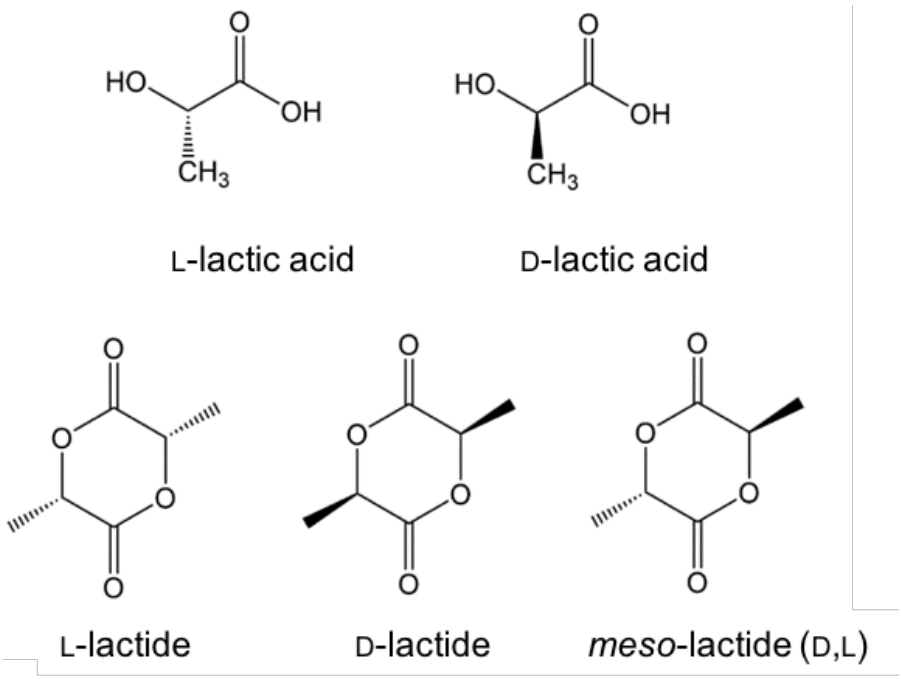


**Figure 2.2** Chemical structure of L(+), D(-) lactic acid, L-lactide, D-lactide and stereocomplex.

## 2.1 Hydrolytic degradation of PLA

Degradation of polymers occurs under normal conditions during their lifetime when they are exposed to the environment and sometimes is the limiting factor for their end use [8]. Degradation is defined as the loss of properties leading to failure of the material. These changes occur mainly through main chain scission induced by a variety of environmental agents such as temperature, water, microorganisms, oxygen or light [8, 9].

Degradation of PLA proceeds by different mechanisms such as chemical hydrolysis, oxidation, microbial, enzymatic and thermal degradation. PLA degrades primarily by hydrolysis of ester groups in the polymer backbone under moist conditions

[1, 10]. The degradation mechanism and rate depend on the chemical and physical properties of the material including diffusivity, porosity and morphology. It is also important to consider besides the material properties, the media in which the polymer is exposed, meaning that temperature, *pH*, solutes or microbes can affect the degradation behavior of PLA based materials [10, 11].

Hydrolytic degradation of PLA starts with chain scission of the ester groups in the presence of water, according to the below reaction, resulting in the reduction of molecular weight and release of soluble oligomers and monomers [10]:

$$-COO + H_2O \rightarrow -COOH + HO^-$$

Hydrolytic degradation of polyesters is partially controlled by the rate of water diffusion. Water molecules diffuse first into the amorphous regions, cleaving the ester bonds, since the amorphous areas are less organized than crystalline regions and water penetrates more easily. Then, the hydrolysis continues at the boundary of the crystalline domains once the amorphous regions are degraded, leading to an increase in the mass loss rate [10]. During hydrolytic degradation the number of carboxylic acid chain ends increases, making the hydrolysis a self-catalyzed reaction due to the accumulation of the acidic polymer fragments in the specimens [12-14].

### 2.1.1 Mechanism

The material degradation mechanism of PLA can be either surface or bulk erosion. The difference between the two mechanisms is due to the competition between the diffusion of water molecules into PLA and the reaction that leads to the hydrolysis of PLA [12]. Surface erosion proceeds when the degradation rate is much higher than the diffusion of water molecules and the hydrolysis mainly occurs on the surface, where an

insignificant dependence of the rate of weight loss per unit surface area on thickness is exhibited (**Figure 2.3**) [15]. In contrast, bulk erosion is a homogenous degradation mechanism where the diffusion rate of water molecules is higher than the hydrolysis rate of the ester bonds of the material [10]. During bulk erosion, the ester bonds cleave randomly, generating carboxyl groups that accelerate the degradation and a decrease of molecular weight is observed over the degradation time [16, 17]. The homogeneous degradation mechanism can be divided into three stages: (1) absorption of water into the PLA matrix, (2) decrease of molecular weight without weight loss, and (3) weight loss due to the release of water-soluble oligomers and monomers [10, 16, 18, 19].

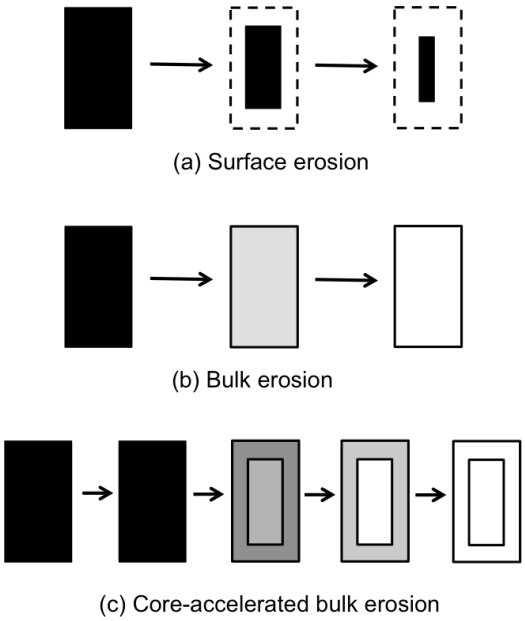


**Figure 2.3** Hydrolytic degradation mechanisms, adapted from Tsuji [10].

Different factors can determine the mechanism of the hydrolytic degradation, for instance, the thickness of the material, PLA molecular architecture or *pH* of the media as will be discussed in the next section. Generally, PLA proceeds via bulk erosion when

thickness is lower than 0.5 – 2 mm and surface erosion when the dimension is higher than 7.4 mm [20]. When material thickness is between 0.5 – 2 mm and 7.4 mm, PLA hydrolysis is mostly via core-accelerated bulk erosion (**Figure 2.3**) due to the oligomers and monomers with high catalytic effect trapped and accumulated in the core of the material where the hydrolysis begins [21].

Molecular architecture, linear or branched, can affect the hydrolytic degradation mechanism behavior and rate because of the number of terminal hydroxyl groups per unit mass. In theory, a branched PLA with higher number of hydroxyl groups than a linear polymer, is expected to have faster hydrolysis reactions, which can attract more water molecules and the cleavage of ester bonds occurs. However, the terminal hydroxyl groups can form hydrogen bonds with the next terminal hydroxyl group preventing them from interacting with water molecules to start hydrolysis reactions with the ester groups around the terminal hydroxyl groups. This interaction will restrict chain mobility as well disturbing the diffusion of water molecules into the PLA matrix and therefore delay the hydrolytic degradation resulting in surface erosion [22]. Tsuji and Hayashi [22] studied the hydrolytic degradation of linear 2-arms and branched 4-arms PDLLA where the 4-arms resulted in degradation via surface erosion due to its larger number of terminal hydroxyl groups, and the 2-arms degraded via bulk erosion.

### 2.1.2 Parameters controlling hydrolytic degradation

#### *2.1.2.1 pH*

The hydrolysis mechanism depends on the *pH* of the media due to the different susceptibility of the ester groups in lactic acid oligomers (**Figure 2.4**). In acidic conditions the hydrolysis proceeds via chain-end scission, whereas in alkaline media

the mechanism takes place via backbiting or intramolecular transesterification to form lactide units and lactic acid as by-products [23].

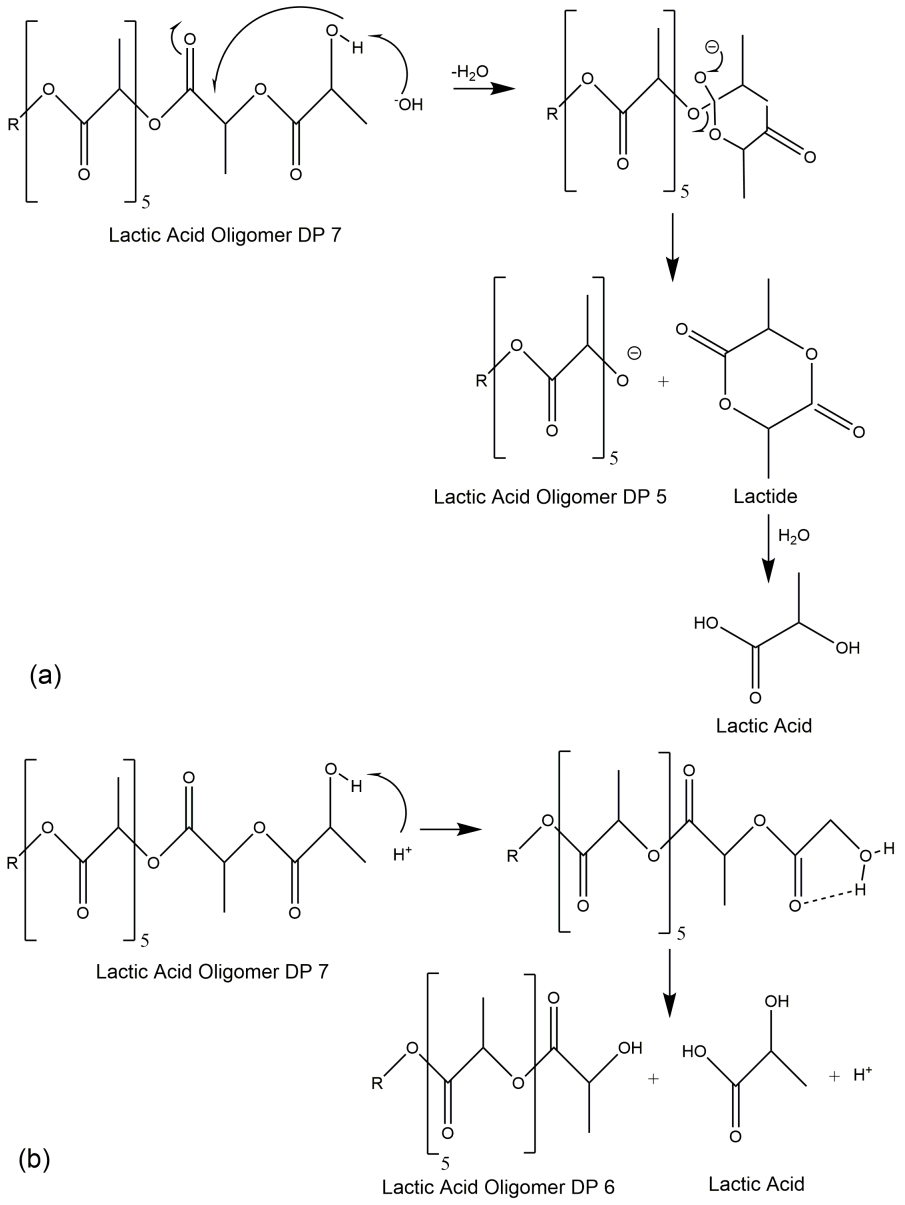


**Figure 2.4** Hydrolytic chain cleavage mechanisms of PLA in alkaline (a) and acidic (b) media, adapted from De Jong et al. [23].

The *pH* of the media contacting the polymer influences the rate of hydrolysis of PLA. PLA chains are more easily degraded in strong acidic and basic media where the

presence of hydronium ($H_3O^+$) and hydroxide ($OH^-$) ions catalyzes the cleavage of ester bonds [12, 24-26]. When PLA is exposed to basic conditions, the carbonyl carbon atoms of the polymer are susceptible to attack by the hydroxide ions where the hydrolytic degradation and the molecular weight reduction are more significant than in acid solutions [24, 25].

Studies have shown that the hydrolytic degradation of PLA immersed in neutral and acid aqueous medium proceeds via a bulk erosion mechanism, resulting in the decrease of molecular weight with degradation time where the autocatalysis is an important factor for this type of erosion [16, 17, 20]. Yuan et al. [16, 17] showed that PLLA fibers faced bulk degradation in a neutral medium at 37 °C where the process was slow, and the changes in properties were not detected in a short time. In the study of hydrolysis of PLA at *pH* 7.4 by von Burkersroda et al. [20] a bulk erosion mechanism was found. During bulk erosion at neutral *pH* the polymer take up water homogeneously and causes the degradation of polymer chains all over the matrix creating free carboxylic acid groups. These carboxylic acid groups lead to a decrease of *pH* inside the polymer, accelerating the degradation inside the polymer bulk. Since the surface is at neutral *pH*, a *pH* gradient is created that slows down the degradation of the polymer at the surface and the surface layer breaks when a critical osmotic pressure forms inside the polymer matrix due to the accumulation of by-products and then release of degradation products [20]. In the case of PLA exposed at acidic conditions von Burkersroda et al. [20] studied the hydrolysis at *pH* 2 where the degradation was already acid catalyzed and found no *pH* gradient buildup as in the case of neutral *pH*

and therefore degradation took place homogenously. So, autocatalysis is an important factor for the bulk erosion mechanism.

Degradation of PLA in contact with alkaline solutions proceeds via surface erosion [15, 20]. In this case, the hydroxyl ions present at the surface of the material are probably consumed by the carboxyl groups, products from PLA degradation taking place at the film surface, without diffusing into the PLA core [15]. Von Burkersroda et al. [23] showed in the study of PLA hydrolyisis at *pH* 13 a linear erosion profile and a constant molecular weight throughout the erosion. Yuan et al. [17] reported that in dilute alkaline solutions, PLA can exhibit surface and bulk degradation where the viscosity-average molecular weight and mass of PLA fibers decreased gradually with degradation time, but in concentrated alkaline solutions when PLA has surface erosion, the viscosity-average molecular weight did not drop.

#### 2.1.2.2 Temperature

Hydrolytic degradation of PLA also depends on the temperature to which the polymer is exposed. The rate of hydrolysis of PLA increases with temperature due to the faster polymer chain scission of the ester bonds [12, 27-29]. When temperatures are above the glass transition temperature ($T_g$) the rate of degradation is enhanced by the mobility of the polymer chains increasing the diffusion of water molecules into the polymer matrix and starting the hydrolysis reactions where the formation of carboxyl groups increases [18, 30-32].

At elevated temperatures the molecular weight and thermal characteristics of PLA are affected. Mitchell and Hirt [29] found that samples of PLA at 60 °C showed a higher polydispersity index (*PDI*) than at 40 °C attributed to the faster degradation of the

amorphous region. It has been shown that when the temperature of the environment in which PLA is exposed increases, the thermal properties such as $T_g$, melting temperature ($T_m$) and crystallization temperature ($T_c$) decrease [29, 32]. The drop in $T_g$ can be explained by the reduction of molecular weight and the plasticizing effect of lactic acid oligomers during hydrolysis [32]. $T_m$ and $T_c$ are also shifted to lower temperatures due to the fragmentation of polymer chains along with the reduction in molecular weight and the susceptibility of amorphous regions to hydrolysis [29, 32].

To study the effect of temperature on the hydrolytic degradation of PLA, the activation energy ($E_a$) is commonly used to describe how the kinetic rate of the reactions changes with temperature. The $E_a$ is described by the Arrhenius equation and is usually estimated by linearizing the equation using the natural logarithm. Different authors have estimated the $E_a$ for the hydrolytic degradation of PLA in different environments within a range of 36 to 110 kJ/mol [25, 29, 30, 33-38]. These environments include water, high-pressure steam, 100% relative humidity (RH), neutral, basic and acidic media as shown in **Table 2.1**. Depending on the media and the environment these values change. When PLA is exposed to temperatures above $T_g$ the chain mobility is enhanced allowing the diffusion of water into the polymer and therefore affecting the hydrolysis rate. So, it is expected that experiments performed above $T_g$ result in ready hydrolytic degradation and lower $E_a$. However, some authors have estimated the $E_a$ using a range of temperature below and above $T_g$ that could affect the final estimation.

**Table 2.1** $E_a$ values reported in literature for the hydrolytic degradation of PLA in different environment at different temperature range.

| Environment | Temperature, °C | $E_a$, kJ/mol | Reference |
|---|---|---|---|
| *pH* 7.4 | 37 – 70 | 100.5<br>102.7 | [30] |
| *pH* 7.4 | 21 – 45 | 83.26<br>83.68 | [25] |
| *pH* 7.4 | 37 – 97 | 75.2 | [39] |
| *pH* 10.5 | 50 – 70 | 110<br>100 | [34] |
| *pH* 2 | 40 – 120 | 58<br>73 | [33] |
| Water | 140 – 180 | 36.85<br>53.23 | [38] |
| Water | 120 – 160<br>170 – 250 | 69.6<br>49.6 | [40] |
| Water | 180 – 350 | 51.05 | [36] |
| 100% RH | 40 – 80 | 110.04<br>93.72 | [29] |
| High-pressure steam | 100 – 130 | 87.2 | [37] |

#### 2.1.2.3 PLA stereoisomers

The properties of PLA can be controlled by the amount of isomers, and therefore the hydrolysis rate of the material as well. Tsuji [41] studied the effect of L-lactide content, tacticity, and enantiomeric polymer blending on the hydrolysis of PLA films. Non-blended PDLLA, PLLA, PDLA films and PLLA/PDLA (1/1) blend (stereocomplex) film were processed in an amorphous state and exposed to hydrolysis in a phosphate-buffered solution *(pH* 7.4) at 37 °C for 24 months. Results showed that the hydrolysis decreased in the following order: nonblended PDLLA > nonblended PLLA > nonblended PDLA > PLLA/PDLA(1/1) blend. The high hydrolyzability of the nonblended PDLLA chains compared with the nonblended PLLA and PDLA was attributed to the lower regularity. The low regularity of PDLLA films decreased the intermolecular interaction making it more susceptible to the attack of water molecules. The retarded hydrolysis of PLLA/PDLA/(1/1) blend film compared with the nonblended films was ascribed to the strong intermolecular interactions between PLLA and PDLA chains.

#### 2.1.2.4 Molecular weight

Molecular weight of PLA is an important parameter that influences the hydrolytic degradation of the polymer: the lower the molecular weight, the faster the rate of hydrolysis. When PLA has low molecular weight the polymer has higher molecular mobility, and higher density of hydrophilic terminal carboxyl and hydroxyl groups that enhance degradation. Furthermore, with the high density of the catalytic terminal carboxyl group the formation of monomers and water-soluble oligomers during hydrolysis is probably higher. All factors mentioned above should be noticeable at PLA molecular weight lower than $1 \times 10^4$ g/mol [10].

Saha and Tsuji [42] studied the effect of molecular weight and D-lactide units on the hydrolytic degradation of PLLA in phosphate-buffered solution at 37 °C (**Figure 2.5**). Different PLLA films were exposed to hydrolysis PLLA1 (number average molecular weight ($M_n$) = 4.09 x $10^5$ g/mol and D-lactide = 0%), PLLA2 ($M_n$ = 1.22 x $10^5$ g/mol and D-lactide = 1.2%) and PLLA3 ($M_n$ = 8.07 x $10^4$ g/mol and D-lactide = 0.2%). The hydrolytic degradation rate constant *k* of PLLA increased with increasing D-lactide. They found that the effect of the amount of D-lactide on the hydrolysis was higher than that of $M_n$ in the first period (0 – 32 weeks). On the contrary, from 32 – 60 weeks neither D-lactide nor $M_n$ affected the rate of degradation. Other studies on the hydrolysis of PLLA films and copolymer of L-lactide with D-lactide [P(LLA-DLA) (77/23)] from Saha and Tsuji were performed (**Figure 2.5**) [43]. They found that the hydrolysis rate was faster for P(LLA-DLA) than for PLLA. The rate constant increased with the increasing water absorption.

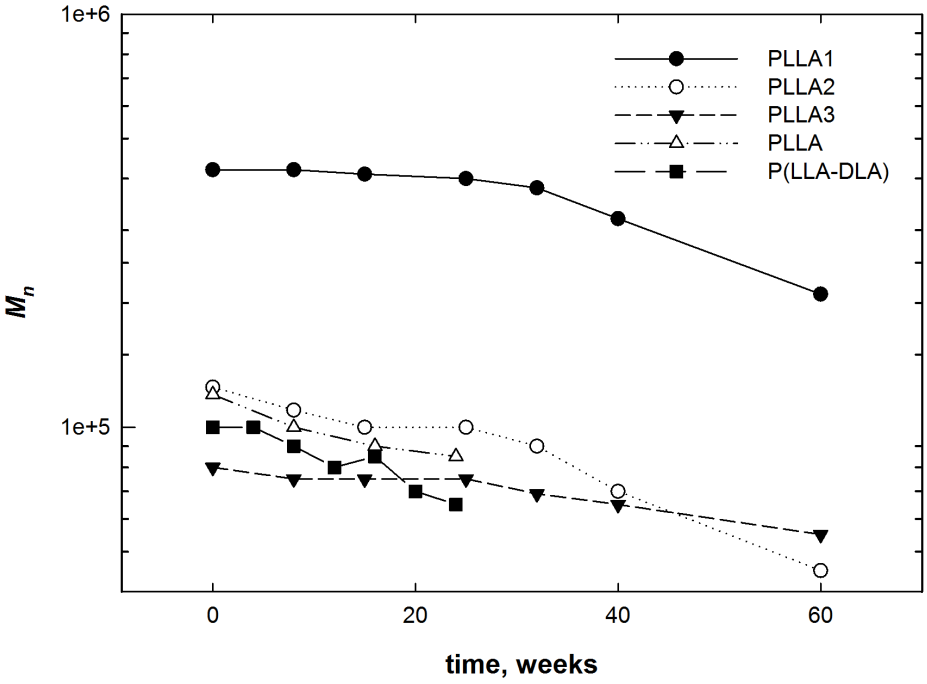


**Figure 2.5** Change in $M_n$ during hydrolytic degradation of amorphous PLLA with high and low molecular weights (PLLA1 and PLLA, respectively), and different ratios of D-lactide (PLLA2 [1.2% D-lactide], PLLA3 [0.2% D-lactide], P(LLA-DLA) [77/23]) in phosphate-buffered solutions at 37 °C, adapted from Saha and Tsuji [42, 43].

Çelikkaya et al. [44] determined the rate of the hydrolytic degradation of PDLLA with different molecular weights ($M_n$ = 7,300, 12,100 and 21,900 g/mol) (**Figure 2.6**). It was found that PDLLA with low $M_n$ degraded faster than PDLLA with higher $M_n$. This behavior was explained by the easy penetration of water molecules within the polymer matrix with low molecular weight due to the lower entanglement and the higher hydrophilicity caused by the high number of carboxyl and hydroxyl end groups.

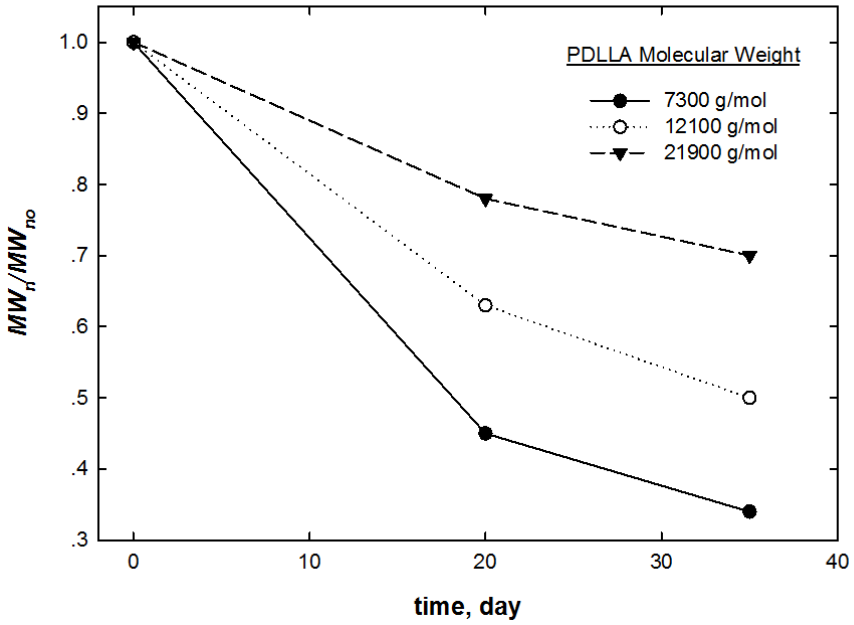


**Figure 2.6** Hydrolytic degradation of PDLLA with different molecular weights in phosphate-buffered solutions at 37 °C, adapted from Çelikkaya et al. [44].

### 2.1.3 Structural changes

#### 2.1.3.1 Crystallinity

PLA crystallinity has been studied where crystal structures have been reported such as *α, α′* (*δ*), *β* and *γ* related to the crystallization conditions [45]. The crystal structure *α*-form, which is an orthorhombic unit cell of parameters $a$ = 1.066 nm, $b$ = 0.616 nm, and $c$ = 2.888 nm, can be obtained from solution casting, melt crystallization and annealing of the glassy state [46-48]. This crystal form with a $T_m$ = 185 °C and $T_c$ near 140-155 °C is a more stable crystal than the *β*-form, a trigonal unit cell of parameters $a = b$ = 1.052 nm and $c$ = 0.88 nm, with a $T_m$ = 175 °C and $T_c$ < 120 °C [47, 49, 50]. The *β*-form can be obtained by stretching *α*-form crystals at high temperatures

and high draw ratio [51]. The *α′*-form or the *δ*-form is a pseudo-hexagonal unit cell of parameters $a = b = 0.62$ nm and $c = 2.88$ nm, which is more disordered in conformation and packing mode of chains than the *α*-form that has a crystal formation below $T_c$ = 80 °C [47, 52, 53]. The *γ*-form is an orthorhombic unit cell of parameters $a = 0.995$ nm, $b = 0.625$ nm, and $c = 0.880$ nm that is produced by epitaxial crystallization in hexamethylbenzene around $T_c$ = 140 °C [50]. Generally, the study of PLA crystalline structures is carried out using X-ray diffraction techniques. The main diffraction peaks and their respective reflections for *α* [54-58], *β* [57] and *α′*-form crystals [55, 56] are presented in **Table 2.2**.

**Table 2.2** Diffraction peaks of *α*, *β*, *α′*-form crystals, as reported by [54-58].

| ***Crystal form*** | ***Diffraction peaks*** | ***Reflections*** |
|---|---|---|
| *α* | 12.5° | 101 |
| | 14.7° | 010 |
| | 16.7° | 110/200 |
| | 19.1° | 100/203 |
| | 22.5° | 102/210 |
| *β* | 16.5° | 110 |
| | 18.8° | 111 |
| | 24.5° | 112 |
| | 28.8° | 300 |
| *α′* | 14.6° | 010 |
| | 16.5° | 110/200 |
| | 18.9° | 203 |
| | 22.3° | 015 |
| | 24.5° | 206 |
| | 28.8° | 018 |

The morphological structure of PLA has an important role in the hydrolytic mechanism. The crystalline morphology of semi-crystalline PLA can be described by a model containing three phases according to the degree of coupling. The three phases include the crystalline phase corresponding to the crystalline fraction (CF), and the non-

crystalline phase that is subdivided into mobile (MAF) and the rigid (RAF) amorphous fractions [59, 60]. **Figure 2.7** shows a schematic representation of these domains. RAF is the amorphous region between crystalline regions and contains three different types of chains: tie chains, folding chains, and chains with a free end. MAF is the completely amorphous areas outside of spherulites [10]. It is important to mention that RAF has reduced mobility while MAF has a rubbery character and therefore the free volume (FV) hole size and distribution differ [61-63]. It has been reported that RAF is formed of low insufficiently decoupled tie chains between the amorphous and the crystalline region obstructing the relaxation, which increases the local diffusion of small molecules in PLA matrix. This characteristic causes the formation of a high number of small FV holes that accelerate the diffusion of water molecules [62] having an important role in the hydrolytic degradation of PLA.

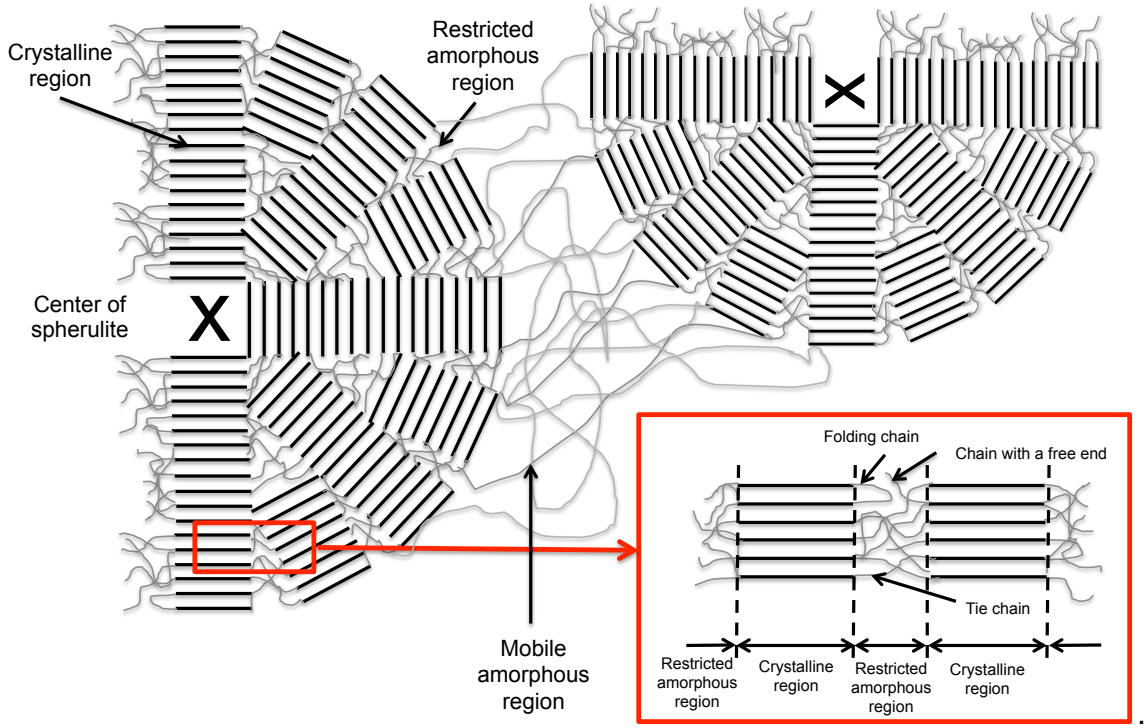


**Figure 2.7** Schematic representation of crystalline morphology of semi-crystalline PLA: crystalline phase corresponding to CF, and the non-crystalline phase corresponding to MAF and RAF, adapted from Sonchaeng et al. [64].

During hydrolysis the chains of the amorphous regions are less resistant to hydrolysis compared to the crystalline regions due to the easy access of water molecules into amorphous areas, where the cleavage of the ester bonds starts releasing water-soluble oligomers and monomers [10]. After the hydrolysis of the amorphous regions, the crystalline regions remaining are called “crystalline residues”, which are degraded in the last stage where the effect of the crystalline thickness is crucial (**Figure 2.8**). The time required to hydrolyze the crystalline residues increases with an increase in their initial molecular weight [10]. Therefore, due to the different

regions in the PLA matrix and their susceptibilities to hydrolytic degradation, PLA structure and crystallinity will change over time.

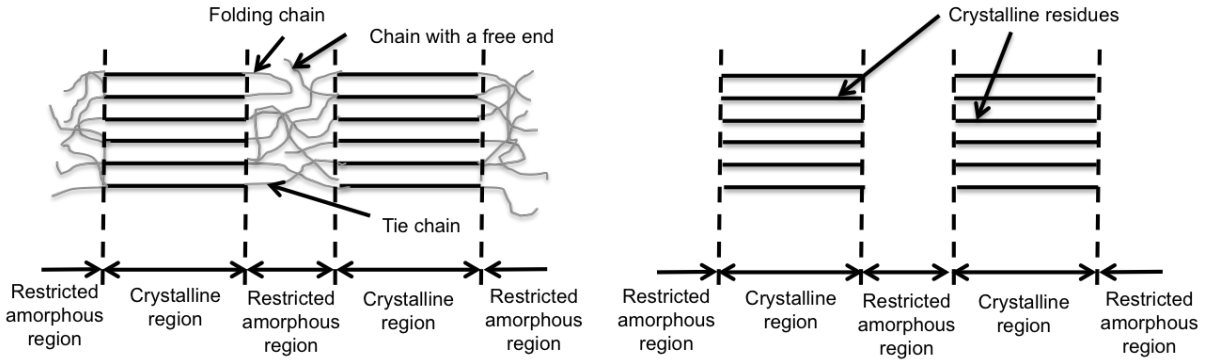


(a) Before hydrolytic degradation

(b) After hydrolytic degradation

**Figure 2.8** Schematic representation of PLA structure (a) before and (b) after hydrolytic degradation, adapted from Tsuji [10].

To describe the isothermal crystallization process the Avrami theory has been applied to study the crystallization kinetics of polymers [65, 66] as below:

$$1 - X_t = exp(Kt^n) \qquad \text{(Eq. 2.1)}$$

where $X_t$ is the relative crystallinity, $t$ is time, and $K$ and $n$ represent the crystallization rate constant and the Avrami exponent, respectively. $K$ is a growth rate constant that considers the nucleation and the growth rate parameters, while $n$ is a mechanism constant that depends on the growth dimension and form of nucleation [65]. An $n$ value close to 3 is correlated to a spherical structure resulting from the process of instantaneous nucleation controlled by diffusion. Non-integral $n$ values show a

combination of thermal and athermal nucleation mechanisms [67]. Generally, the *n* values reported in literature are around 2 and 4 for PLA [65, 68, 69].

During hydrolytic degradation PLA suffers structural changes [18, 42, 70]. Zhang et al. [18] studied the morphological behavior during hydrolysis of two types of PLA: semicrystalline (1.4% D-lactic acid) and amorphous polymer (12% D-lactic acid). The molecular weight of both PLA polymers decreased during the degradation time while the percentage of crystallinity increased, although amorphous PLA degraded much faster than semicrystalline PLA. During degradation, *α*-form crystals were mainly formed in both PLA structures. The main reason for the formation of crystals in amorphous PLA is chain orientation and morphological rearrangement that occurs in PLA when the molecular weight decreases during the degradation process. With the decrease in molecular weight, the short PLA chains have the ability to form crystalline structures.

The thickness of PLA materials has an effect on the crystallinity during the hydrolysis of the polymer. It has been shown that the crystallinity of PLLA fibers with different diameters increases over the hydrolysis process, in which fibers with small diameters have higher crystallinity suggesting faster degradation than fibers with bigger diameters [16, 29]. During the degradation time, there is a gradual increase in molecular regularity due to the decrease of molecular entanglements, which is reflected in the crystallinity. The faster the hydrolysis is, the faster is the rearrangement of PLA segments. Similarly, Tsuji and Ikada [26] concluded that the rate of weight loss per unit surface area of PLLA films decreased linearly with the increase in PLLA crystallinity.

Temperature is a main parameter that influences the hydrolytic degradation rate and therefore the residual crystallinity of PLA materials. Mitchell and Hirt [29] found that

the crystallinity of PLA fibers exposed to 80 °C at 100% RH increased rapidly between 5 and 6 days (~ 73%) comparing to those exposed at 40 and 60 °C (~ 15% and ~ 40%, respectively). The *PDI* of samples also was affected during hydrolysis where samples tested at 40 °C showed a lower increase in the *PDI* than samples tested at 60 °C where the *PDI* changed from 2.0 originally to 4.0 at day 7. The increase in *PDI* was explained by the degradation of the amorphous region where high temperatures drive faster hydrolysis.

#### 2.1.3.2 Swelling

The stability or durability of PLA when it is exposed to different environments such as water and/or organic solvents is crucial when PLA is used as a container, bottle or other vessel. The exposure to different solvent solutions can lead to structural changes in PLA that can modify the rate of hydrolysis. Swelling of the polymer is one of the structural changes that PLA can experience when it is in contact with organic solvents [71, 72].

The swelling of a polymeric material occurs when the solvent molecules diffuse and are absorbed into the amorphous region, where the amount of solvent ad/absorbed increases according to the affinity with the polymer [72]. The swelling is reflected in the softening of the polymer, resulting in the movement and the alignment of the polymer chains, which may induce crystallization [54, 71]. Different polymers experience SIC when they absorb organic solvents, such as poly(ethylene terephthalate), poly(methyl methacrylate), polycarbonate of bisphenol A and poly(styrene) [73-77].

SIC is controlled by the transport of the organic solvent in glassy polymers. According to Ouyang et al. the transport of acetone in PET induces crystallization in

three stages [75, 78]. The first stage is the transport of the solvent by diffusion, which is controlled by the concentration gradient. The second stage involves the dramatic increase of swelling in the polymer by the solvent and primary crystallization takes place where a large amount of crystals are formed by the release of internal stress. Finally, the third stage of SIC involves secondary crystallization when the system is saturated and the rate of crystallization decreases.

The density of the polymer is affected by the SIC. It has been shown that high swelling of PLA depends on the organic solvent permeation through the polymer, inducing a reduction in the PLA density leading to porous structures [54]. Sato et al. [54] found that the density of amorphous PLA (L/D ranged from 96.0/4.0 to 96.8/3.2) decreased with increasing crystallinity due to solvent exposure and no linear relationship was observed between crystallinity and film density. Usually, crystalline polymers are denser than amorphous, but in the case of PLA crystallized by organic solvents the crystals are more dispersed than amorphous polymers.

Tsuji and Sumida [72] studied the degree of swelling of PLLA when it was exposed to ethanol at 25 °C for 7 days. They found that swelling with ethanol reached an equilibrium after 20 min of immersion and the $T_m$ and the crystallinity of PLA increased by that time. Pitt and Zhong-wei [71] determined the effect of water (*pH* 7.4), ethanol and pentanol at 37 °C. They found that crystallization of PLLA occurred during degradation in ethanol, causing alignment of polymer chains after 20 days, indicating the plasticization effect of ethanol, while the degree of crystallinity remained unchanged in the presence of water during 80 days of exposure. It is important to mention that the degree of polymer crystallinity affects the rate of hydrolytic degradation since hydrolysis

depends on the diffusion of water molecules through amorphous regions to start the cleavage of ester bonds.

Tsai et al. [79] showed in the study of physical changes and sorption/desorption behavior of amorphous and semi-crystalline PLLA exposed to water, methanol and ethanol at 37 °C that water in the glassy structure had a plasticizing effect. However, the plasticization was not sufficient to induce cold-crystallization. In the case of ethanol they induced cold-crystallization in PLLA showing a complex sorption and desorption kinetics due to the progressing cold-crystallization on sorption. In the analysis of the crystallization kinetics using the Avrami equation (**Eq. 2.1**) the *n* values were found to be very low, 0.5 and 1 for ethanol and methanol, respectively. These low values suggested restricted crystal growth in terms of chain mobility and dimensionality.

When PLA has been exposed to different solvents, SIC has led to the formation of different crystals. Tsai et al. [79] found that methanol and ethanol induced the formation of *α'*-form crystals at 37 °C. Sato et al. [54] found a mixture of *α*- and *β*-form when PLA was exposed to 60 inorganic solvents at 35 °C for 24 h. They concluded that crystallinity is not dependent of the organic solvent but on the degree of swelling. When films had crystallinity between 0 – 5% they mainly had *β*-form crystals. On the other hand, samples with crystallinity ranging around 25% formed a mixture of *α*- and *β*-form, and samples with crystallinity around 40% had *α*-form crystals.

Other studies investigated the crystalline complex formation of new crystals "ε-form" in PLLA in contact with low molecular weight compounds, such as five-membered ring (cyclopentanone, 1,3-dioxolane, $\gamma$ -butyrolactone and THF) and *N,N*-dimethylformamide (DMF) below room temperature. The ε-crystals had an orthorhombic

unit cell with parameters $a$ = 1.5 – 1.6 nm, $b$ = 1.2 – 1.3 nm and $c$ = 2.8 – 2.9 nm. Further research is needed to fully understand the swelling and SIC of PLA by different solvents.

## 2.2 Chemical recycling: Application of hydrolytic degradation

As stated above, PLA is susceptible to hydrolytic degradation, so this can be effectively used for the chemical recycling of PLA to its monomer [1]. One of the preferable recovering routes of PLA as many other polymers is recycling, which can be either mechanical or chemical [6]. Mechanical recycling includes recovering, sorting, regrinding and reprocessing of PLA [80]. However, this process results in the deterioration of PLA physical properties where the molecular weight is reduced due to the exposure to high temperatures and shear during reprocessing of PLA [81]. On the other hand, chemical recycling of PLA recovers the LA by hydrolysis which can then be used as a raw material for new PLA production with the same properties as virgin materials [81, 82].

Different chemical recycling methods have been used to recover PLA; one is hydrolysis or solvolysis to obtain L-LA or D-LA oligomers, and another is the depolymerization of PLA to cyclic dimer, L-lactide. Some patents have been granted for the depolymerization of PLA by hydrolysis or solvolysis [83-85]. The conditions used for the chemical recycling of PLA to give high yield of monomers in short period and avoid the removal of catalysts and additives to save energy and cost must be closely monitored. During the depolymerization of PLA it is important to avoid the racemization and decomposition of LA, and also to consider the optical purity of the degraded PLA and the LA formed [36]. Chemical recycling of PLA has been conducted with different

solutions, such as water, alcohols and other organic solvents, which are explained in more detail in the following section.

### 2.2.1 Water

Water has been used as solvent for chemical recycling to avoid the use of catalysts and additives. Brake and Subramanian [83] rapidly hydrolyzed PLA with water to water-soluble monomers and oligomers in 3 and 0.5 h at 120 and 170 °C, respectively. However, the yield of formed LA, the optical purity of the PLA used and the optical purity of the LA formed were not characterized. This is important since racemization and decomposition of LA can occur at high temperatures.

Tsuji et al. [36] studied the hydrolysis of PLLA in the melt in high-temperature and high-pressure water at the temperature range of 180 – 350 °C with no catalyst resulting in homogeneous and random hydrolysis via bulk erosion mechanism. They investigated the formation, racemization and decomposition of LA. A yield of 90% was obtained at 250 °C in 10 – 20 min. When the temperature increased to 350 °C, the yield decreased due to the dramatic racemization and decomposition of the monomers. Tsuji et al. [40] also investigated the difference of performing the hydrolysis in the melt (170 – 190 °C) and in the solid state (120 – 150 °C). The hydrolysis was homogeneous and random via a bulk erosion mechanism. Crystalline residues were formed below 140 °C but not at degradation temperatures above 170 °C. The presence of crystalline residues could slow the decrease of the $M_n$ in the late stages. The LA yield exceeding 95% was obtained at the range of temperature studied, but the difference was the time to get the maximum yield.

### 2.2.2 Alcohols

Chemical recycling by solvolysis of PLA by transesterification with alcohol to lactate esters is an alternative process that has been applied by several authors. The use of catalysts was necessary in this process. Sánchez and Collinson [86] studied the chemical recycling by alcoholysis of PLA in methanol and ethanol using zinc acetate as a catalyst (**Figure 2.9**). They found that better yields were achieved in the catalyzed methanolysis than ethanolysis since the methanol molecule is a better nucleophile than ethanol due to its smaller size and higher dielectric constants; therefore, the reaction with the carbonyl is faster. Leibfarth et al. [87] reported the organocatalytic recycling of postconsumer PLA into lactate esters using triazabicyclodecene in the presence of alcohols (*i.e.,* methanol, ethanol, butanol). The depolymerization of PLA was completed in minutes at room temperature, retaining the stereochemistry of the lactates.

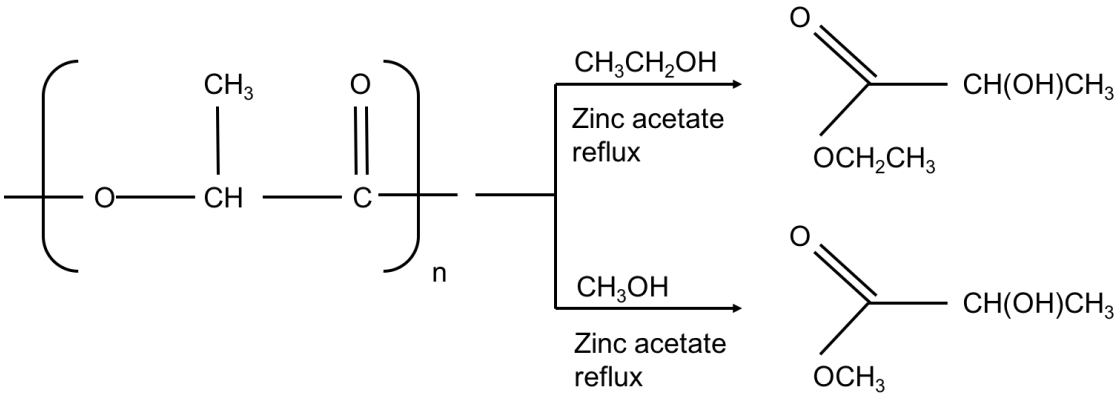


**Figure 2.9** Alcoholysis of PLA, adapted from Sánchez and Collinson [86].

### 2.2.3 Other organic solvents

Other different organic solvents besides alcohols have been applied for PLA chemical recycling. Gironi et al. [88] used acetone and ethyl lactate without catalysts to

study the dissolution behavior of PLA at different water concentrations, finding that acetone based solvents were more effective in solubilizing PLA. One of their conclusions was that the increase of water concentration in the solvent phase, determines a reduction of the solvent power and a reduction of the mass transport coefficient for the two solvents tested.

Okamoto et al. [89] degraded PLLA (weight average molecular weight ($M_w$) = 120 000 Da) by montmorillonite K10 (MK10) in toluene at 100 °C for 6 h resulting in oligomers with $M_w$ of a few hundreds in a yield greater than 90%. No isomerization of L-LA occurred and the degradation was accelerated by the addition of a small amount of ethanol in toluene using anhydrous MK10 to produce oligomers with ethyl ester end groups. Chloroform, hexane and *o*-xylene were used by Takahashi et al. [90] for the degradation of PDLLA, PDLA and PLLA using the enzyme lipase as a catalyst to produce cyclic oligomers. They found that adding a small amount of water to the *o*-xylene solution significantly accelerated the enzymatic degradation of PLLA. Toluene, xylene, and chloroform have also been used for the chemical recycling of PLA via controlled degradation with protic (macro) molecules (*e.g.* diols, dipentaerythriol, diamines, adipic acid or oligo(ethylene glycol)) using catalysts [91]. Although the use of enzymes as catalysts can help the degradation of PLA at low temperatures, the application of enzymes is generally dependent on factors such as their stability and solubility in an organic solvent and substrate specificity of the enzyme [90, 92]. Other factors can limit the degradation conditions, such as temperature, solvent and polymer concentration.

Chemical recycling of PLA based polymer blends has been reported by Tsuneizumi et al. [93] for PLA/polyethylene (PE) and PLA/poly(butylene succinate) (PBS) blends using clay catalysts and enzymes for selective chemical recycling. Two routes were applied for PLA/PE blends. The first route was the direct separation of PLA and PE due to their different solubilities in toluene followed by chemical recycling of PLA using montmorillonite K5 clay (MK5). The second route was selective degradation of PLA in the blend by MK5 in toluene at 100 °C forming LA oligomers with low molecular weight. The PE was recovered by the re-precipitation method. Similar procedures were used for PLA/PBS blends. The first route was the direct separation of PLA and PBS by their solubility in toluene; and the second route was sequential degradation of the blend using lipase to degrade PBS and then PLA was degraded by MK5.

## 2.3 Modification of PLA

### 2.3.1 Nanoparticles: organomodified montmorillonite (OMMT)

Nanocomposites are materials where at least one of the particles incorporated is of nanometric size. In general, three different categories of nanofillers exist, which are distinguished by the number of nanometric dimensions that they have. Nanotubes or whiskers are elongated nanofillers with two dimensions in the nanometer range. Isodimensional nanoparticles (*i.e.* spherical particles) are particles where the three dimensions are nanometric. Plate-like nanofiller is a layered material with a thickness on the order of 1 nm with an aspect ratio around 25 with the other two dimensions. Layered silicates are among the most popular plate-like nanofillers, such as smectic clays, graphene sheets and layered double hydroxides [94, 95].

#### 2.3.1.1 Characteristics

##### 2.3.1.1.1 Structure and properties

Montmorillonite (MMT) is a clay that belongs to a layered smectite group, also known as 2:1 phillosilicates, which consists of several stacked layers with a thickness of 1 nm and lateral dimensions from 30 nm to several microns. The crystal structure consists of two silica tetrahedral sheets fused to an edge-shared octahedral sheet of aluminum (**Figure 2.10**) [94, 96]. The aspect ratio is about 10-1000 and the surface area is in the range of 750 $m^2/g$ [97]. The parallel layers are linked together by van der Waals forces with a gap between the layers known as the gallery or interlayer. The clay layer is negatively charged, which is counterbalanced by exchangeable cations such as $Na^+$, $K^+$, $Li^+$ and $Ca^{2+}$ located within the galleries of the silicate layers. The cations are not strongly bound to the clay surface, and therefore can be replaced with other molecules (*e.g.,* polar compounds) [95, 98]. The general chemical formula of MMT is $(M + \times nH_2O)\left(Al_{(4-y)}Mg_y\right)Si_8O_{20}(OH)_4$ where $M \quad (M = Na^+, Ca^{2+}, Mg^{2+}, etc.)$ is the interlayer cation [99].

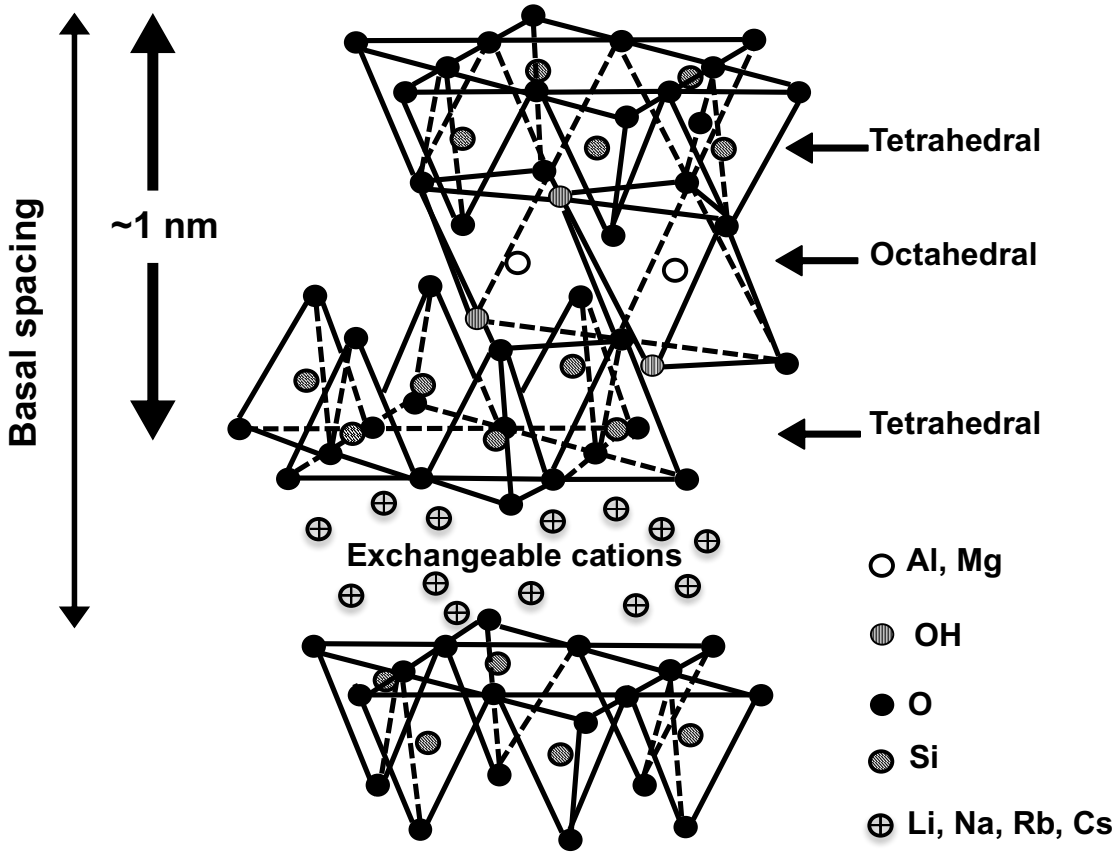


**Figure 2.10** Structure of 2:1 layered silicates, adapted from Ray and Okamoto [96].

#### 2.3.1.1.2 Surface modification

MMT is a hydrophilic clay, making it poorly suited to interact with hydrophobic or less hydrophilic polymers like PLA, and therefore a modified surface is necessary by exchanging the cations in the galleries for organic surfactants including primary, secondary, tertiary or quaternary alkylammonium or alkylphosphonium cations [96]. Since the interlayer height of clay before modification is relatively small, the long chain of alkylammonium cations decrease the surface energy of MMT and the interlayer spacing expands, enhancing the interaction between the clay and the polymer resulting in a well dispersed clay within the polymer matrix (**Figure 2.11**) [98]. When a nanoclay

has been modified, it is common to identify it as an organoclay. For instance, when MMT has been exposed to surface modification, it could be called organomodifed MMT (OMMT). **Table 2.3** shows common organomodifier names, structures and commercial names used for preparing PLA nanocomposites.

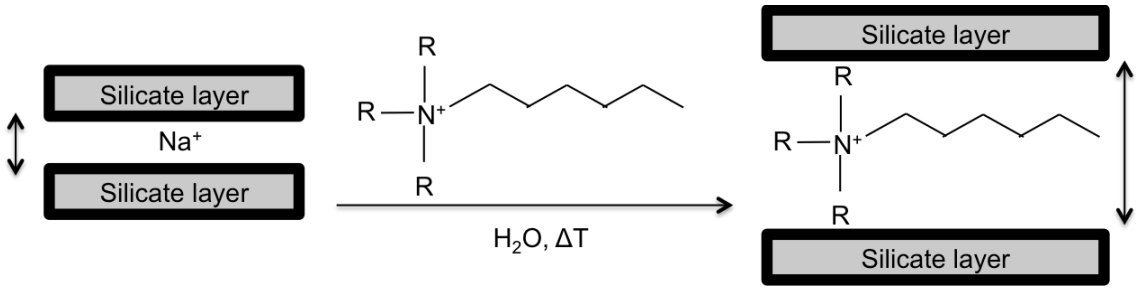


**Figure 2.11** Organomodification of layered silicates with quaternary ammonium, adapted from Raquez et al. [95].

**Table 2.3** Common modified montmorillonites used for PLA-nanocomposites, adapted from Souza et al. [100].

| Modifier | Structure | Commercial name |
|---|---|---|
| Methyl, tallow, bis-2-hydroxyethyl, quaternary | 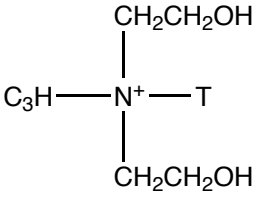 | CLOISITE 30B/Southern Clay Products |
| Dimethyl, dehydrogenated tallow, 2-ethylhexyl quaternary ammonium | 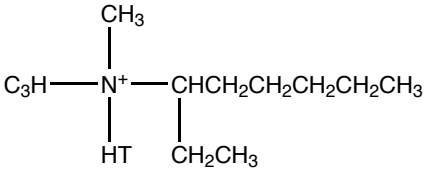 | CLOISITE 25A/Southern Clay Products |
| Dimethyl, dihydrogenated tallow, quaternary ammonium | 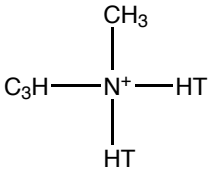 | CLOISITE 20A/Southern Clay Products<br>CLOISITE 15A/Southern Clay Products |
| Methyl, dihydrogenated tallow, quaternary ammonium | 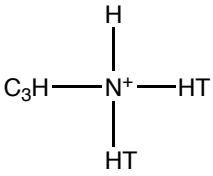 | CLOISITE 93A/Southern Clay Products |
| Octadecyl ammonium | 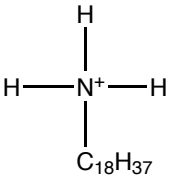 | NANOMER 1.30P/Nanocor |
| Stearyl dihydroxyethyl ammonium | 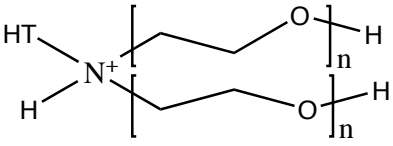 | NANOFIL 804/Süd-Chemie |

**Table 2.3 (Cont'd)**

| Modifier | Structure | Commercial name |
|---|---|---|
| Dimethyl benzyl hydrogenated tallow ammonium | 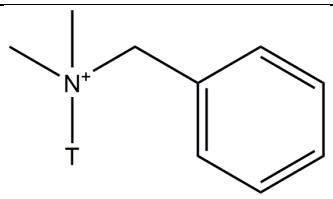 | DELLITE 43B |

*T is tallow with around 65% $C_{18}$, 30% $C_{16}$ and 5% $C_{14}$

The dispersion of the silicate layers depends on the chemical structure of the organomodifier used in the organoclay. In the case of PLA, the dispersion and de-agglomeration of the layers within the polymer matrix depends on the hydrogen-bonding interaction between the carbonyl groups of PLA chains and the hydroxyl groups in the organomodifier of the organoclay [101]. Furthermore, strong interactions could also occur between the hydroxyl end groups of PLA chains and the MMT platelet surfaces, or the hydroxyl groups of the surfactant in the OMMT [102]. Therefore, the properties of the nanocomposites are highly dependent on the distribution of the silicate layer in the polymer matrix.

#### 2.3.1.1.3 Morphology

The main techniques for the preparation of PLA-clay nanocomposites are *in situ* intercalation, intercalation of polymer from solution and melt intercalation. *In situ* intercalation is when the nanofillers are dispersed in liquid monomer and the monomer is absorbed into the clay interplanar spaces, followed by polymerization. Intercalation of polymer from solution requires the dissolution of the polymer in a solvent capable of solubilizing the polymer and swelling the layers of the nanoclay, followed by the

evaporation of the solvent or precipitation [103, 104]. Melt intercalation, which is the most industrially viable method, involves the direct melt-mixing of dry polymer pellets with the nanoclay powders under shearing action at a temperature above the polymer melting point that facilitates the diffusion of the polymer chains into the clay galleries to achieve a good dispersion of silicate layers within the polymer [105, 106].

The compatibility between the nanoparticles and the polymer matrix is the main issue to obtain a good dispersion of layered silicates, which dictates the final properties of the nanocomposites. When the affinity is low, the silicate layers are not intercalated with the polymer; in other words, the clay particles are not delaminated, resulting in a material with similar properties to micro-composites (**Figure 2.12**). On the contrary, when affinity exists the results are either intercalated or exfoliated nanocomposite. Intercalated nanocomposites are normally when the polymer chains are inserted between the silicate layers, leading to the reinforcement of the material. Exfoliated nanocomposites occur when each individual layer is dispersed within the polymer and the structure is fully delaminated, resulting in the maximal property enhancement [96, 107]. Therefore, to achieve miscibility of layered silicates with biodegradable polymers such as PLA, it is necessary to modify the hydrophilic silicate surface to an organophilic one.

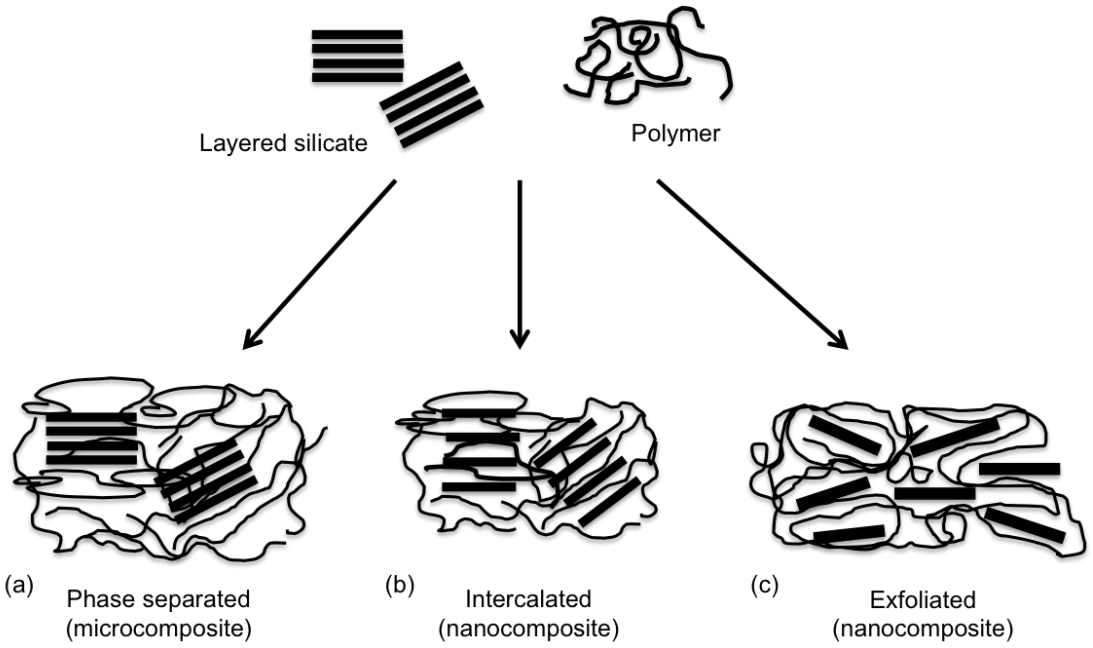


**Figure 2.12** Types of nanocomposites derived from interaction between clays and polymers, adapted from Alexandre and Dubois [108].

#### 2.3.1.1.4 Benefits of PLA-nanocomposite

PLA-nanocomposites have improved properties compared to neat PLA, such as mechanical, thermal, and barrier properties. Mechanical properties are enhanced due to strong interfacial interaction or adhesion between the nanoclay and the polymer matrix and the level of intercalation [109]. The improvement of tensile modulus, as a mechanical property, is also attributed to the presence of small tactoids and the absence of agglomerates, rather than exfoliation [110]. Regarding barrier properties, the presence of clay in the polymer increases the dwelling times of the penetrant around accessible clays, and therefore, the barrier properties of the polymer are improved [111].

Ray et al. [112] prepared PLA-OMMT nanocomposites with loadings of 4, 5 and 7 wt%. The silicate layers were intercalated and well distributed in the PLA matrix. To

determine the dispersion of the clays, X-ray diffraction and transmission electron microscope analyses were performed. All the nanocomposites showed an increase in storage modulus, flexural modulus, flexural strength, heat distortion temperature, and gas barrier properties compared to neat PLA (**Table 2.4**). Maiti et al. [113], studied the enhancement of PLA properties incorporating OMMT (3.8 wt%), where the $O_2$ gas permeability of PLA was decreased from 3.31 to 2.00 $x10^{-24}$ kg m $m^{-2}$ $s^{-1}$ $Pa^{-1}$. Lewitus et al. [114] observed that when OMMT was incorporated at 5% loading level into PLLA films the tensile modulus and the elongation increased by 30 and 40%, respectively, and the cold-crystallization temperature ($T_{cc}$) decreased by 15 °C due to the nucleation effect, compared to neat PLLA.

**Table 2.4** Comparison of material properties between neat PLA and PLA-OMMT nanocomposites with different amounts of OMMT, adapted from Ray et al. [112].

| **Material properties** | **PLA** | **PLA-OMMT (4%)** | **PLA-OMMT (5%)** | **PLA-OMMT (7%)** |
|---|---|---|---|---|
| Modulus (GPa) | 4.8 | 5.5 | 5.6 | 5.8 |
| Strength (MPa) | 86 | 134 | 122 | 105 |
| Distortion al break (%) | 1.9 | 3.1 | 2.6 | 2 |
| $P_{PLA\text{-}OMMT}/P_{PLA}$ * | 1 | 0.88 | 0.85 | 0.81 |

* $P_{PLA\text{-}OMMT}/P_{PLA}$: Relative permeability coefficient of $O_2$

#### 2.3.1.2 Hydrolytic degradation

PLA properties are enhanced when layered silicate nanoparticles are incorporated in the polymer matrix as compared with the unfilled PLA and its microcomposites. However, these engineered nanoparticles have an effect on the hydrolytic degradation of PLA and depending on the final application, the influence of the nanoparticles on the hydrolysis process could be favorable or not.

Several authors have studied the hydrolytic degradation of PLA-nanocomposites based on MMT. Zhou and Xanthos [34] studied the accelerated hydrolytic degradation of amorphous (PDLLA) and semicrystalline PLLA (6% D-lactide) containing unmodified and organically modified MMT between 50 and 70 °C. The effects of polymer type on the degradation rate constant showed that the unfilled PDLLA and its composites displayed higher hydrolysis than unfilled PLLA and its composites. The reason was due to the amount of crystalline regions that reduce the mobility of polymer chains and FV, and therefore the water absorption. Nanocomposites showed higher degradation rates than the unfilled PLA, and the degradation of the unmodified MMT (microcomposites), was slightly lower than unfilled polymer. The study demonstrated that high dispersion of the particles in the nanocomposites accelerates the hydrolytic degradation.

The water uptake of nanocomposites has a great influence on hydrolysis rates compared with neat polymers. Zhou and Xanthos [34] observed a higher amount of water absorbed by PLA nanocomposites comparing with pristine PLA. When nanoparticles are incorporated in PLA, their large water sorption capacity increase the water sorption of the nanocomposites. Also, organomodified MMT, which was treated with hydrophobic organic compounds, lost the capacity of neutralizing the carboxylic

groups formed by the cleavage of polymer chains during hydrolysis.

The effect of organomodifier or surfactant has also been studied. Paul et al. [115] studied the hydrolytic degradation in phosphate buffer solution (*pH* 7.4) of two PLA-OMMT nanocomposites based on different surfactants, one more hydrophobic (Cloisite®25A) and the other more hydrophilic (Cloisite®30B). After five months, the reduction in $M_n$ of unfilled PLA was 41.6%, while the nanocomposites made with Cloisite®25A and Cloisite®30B were 71.2% and 79.2%, respectively. In the presence of Cloisite®30B, the $T_g$ of PLA started to decrease after one month, while the $T_g$ of PLA with Cloisite®25A decreased only after more than two and a half months due to the reduction in $M_n$ and the plasticizing effect of LA oligomers formed during degradation. The more hydrophilic the filler, the faster the hydrolysis. However, is important to mention that the initial $M_n$ of the samples was not the same at the beginning of the experiments, influencing the final results.

Fukushima et al. [116] evaluated two different modified montmorillonites (Cloisite®30B and Nanofil 804) under compost degradation conditions at 40 °C. A considerable reduction in $M_n$ and $M_w$ was shown by PLA-nanocomposites, although the initial $M_n$ for neat PLA, PLA- Cloisite®30B and PLA-Nanofil 804 was different (72,743, 64,270 and 47,528 Da, respectively). The faster degradation of PLA-nanocomposites was attributed to the hydroxyl groups in the clay organic modifiers, where the presence of Cloisite®30B showed higher hydrolysis due to higher dispersion in PLA than Nanofil 804. However, the difference in the initial molecular weight of the samples was not considered.

Araújo et al. [117] evaluated the thermal stability of PLA-based nanocomposites

using three modified MMTs. Different behaviors were shown depending on the chemical structure of the organomodifier. The hydrolysis was enhanced by the presence of Cloisite®30B, which has OH groups that increase the hydrophilicity and therefore displayed better dispersion than Dellite®43B. Hydrolysis of PLA Dellite®43B resulted in less chain scission due to the benzene ring in its chemical structure making it more hydrophobic and with less capability to absorb water than Cloisite®30B and Cloisite®15A. Therefore, the hydrolysis rate depends on the filler dispersion, water uptake and hydrating ability of the fillers.

Hydrolysis of PLA-nanocomposites can be noticed in the degree of crystallinity. DSC results have demonstrated the increase of the crystallinity after the addition of nanoclay and after degradation [27, 114, 117]. The incorporation of clay particles in PLA matrix promotes the crystallization of PLA indicating a nucleating effect [27, 114]. The increase in crystallinity during hydrolytic degradation of PLA-nanocomposites is due to the hydrolysis of PLA chains in the amorphous regions by the easy access of water molecules into those regions [117]. The increase of crystallinity can also be attributed to the plasticization of PLA by water molecules and LA oligomer giving mobility to the polymer allowing the reorganization of the chain and further crystallization [115].

Visible changes in opacity have been observed as a consequence of hydrolytic degradation in PLA-OMMT nanocomposites. Over exposure time of nanocomposites to hydrolysis conditions, the polymer turns white and becomes extremely brittle. The changes in appearance can be attributed to various phenomena, such as light scattering due to the presence of water and degradation products formed during hydrolysis, formation of holes in the bulk of the polymer, or the increase in crystallinity

due to the hydrolysis in the amorphous regions of the PLA matrix [27, 115].

#### 2.3.1.3 Chemical compound release

Nanocomposites have been employed in a wide range of applications due to the improvements on polymer properties. However, during the life cycle of nanocomposites, the nanoclays have the potential to be released. Nanoparticles may be released from packaging materials in direct contact with food, even though the nanoscale components are bound to the material [118, 119]. After use, the nanoparticles also could be released into the surrounding environment reaching plants, wildlife, or humans [120]. Therefore, the evaluation and characterization of migrants from nanocomposites containing clay is important for food safety considerations [121].

Due to the greater surface area per mass of nanoclays compared with larger sized particles of the same nature, ion exchange capacity, and high absorption ability, nanoclays are more reactive to biological systems [122, 123]. Some nanoparticles may cause damage to biological systems since they have the ability to penetrate cellular barriers inducing oxygen radical generation that leads to oxidative reactions in the cell [124, 125]. Also, the organomodifiers or surfactants used in the nanoclays have the potential risk to be toxic to ecosystems, animals and humans [126, 127].

The migration process of nanoparticles may not be the same as migration of small molecules or additives from the polymer matrix. Simon et al. [128] studied the potential rate of migration and equilibrium distribution of nanoparticles from polymeric packaging materials based on physicochemical properties of nanoparticles and polymer materials. The results indicated that the migration of nanoparticles takes place when the particles are very small, with a radius on the order of 1 nm. Meanwhile, the polymer

matrix should be low in viscosity and not interact with the nanoparticles. On the contrary, for bigger nanoparticles in polymer matrices with a relatively high viscosity, such as organomodified MMT, the migration is not likely detectable. However, there is a lack of information to confirm these statements.

Xia et al. [129] evaluated the release of OMMT nanoclay from PP and polyamide 6 (PA6) nanocomposites films in ethanol at 70 °C, in which the release of the nanoparticles was detectable. The release of OMMT was verified by quantifying Si and Al as nanoclay markers using a graphite furnace atomic absorption spectrometry (GFAAS) technique. After 10 days of exposure more nanoclay particles were released from PP films (0.15 mg/L) than from PA6 (0.10 mg/L). The higher release from PP was attributed to the lack of interaction between the nanoclay and the polymer matrix. Thus, the interaction between the nanoparticles with the polymer matrix influences the release to the environment.

Different techniques have been used for the detection of the release of nanoparticles from PLA nanocomposites. For instance, Schmidt et al. [130] assessed the migration of nanoclay from a PLA-OMMT nanocomposite (5% wt. Cloisite®30B). Based on asymmetrical flow field-flow fractionation ($AF_4$) coupled with multi-angle light-scattering (MALS) analysis, migration of particles with a radii range of 50-800 nm was detected in a mixture of 95% ethanol and 5% water. When $AF_4$-MALS with inductively coupled plasma mass spectrometry (ICP-MS) technique was applied, no clay minerals were detectable.

Besides OMMT clay release, other nanoparticles have been studied. Schmidt et al. [131] studied the migration of the major components from PLA/laurate-modified Mg-

Al layered double hydroxide (PLA-LDH-$C_{12}$) films to assess their suitability for use as food contact materials. Three films were tested where LDH-$C_{12}$ was introduced into PLA either by direct compounding with PLA or by dispersion of LDH-$C_{12}$ using a masterbatch technique. All tested films showed migration of LDH using acid digestion followed by ICP-MS detecting Mg. Also, migration of the laurate organomodifier took place. The results were within the migration limits of the European Commission for total migration and specific lauric acid migration of ≤ 10 mg/$dm^2$ [132].

Studies have demonstrated the possible release of the organomodifiers or surfactants when nanoparticles or nanocomposites are exposed to aqueous media. Nigmatullin et al. [133] reported the release of quaternary ammonium compounds from different OMMTs to aqueous media by monitoring electrical conductivity for 6 h. The tested OMMTs were divided into two groups, organoclays with a single long tail of hydrogenated tallow (Cloisite®10A, Cloisite®30B) and with two long tails of hydrogenated tallow (Cloisite®20A, Cloisite®93A, Cloisite®15A). Also, the same study reported the migration of the surfactants when organoclays were incorporated into PA. The release of surfactants from the polymer nanocomposite was slower compared with the release from nanoclays where the release of surfactants with single long tail of hydrogenated tallow was faster than the surfactants with two long tails.

Xia et al. [129] studied the release of surfactant from two types of polymer-clay nanocomposites: PP and PA6. Nanocomposites were exposed to ethanol at 70 °C. The amount of surfactant released into ethanol was 3.5 mg/L from PP nanocomposite and 16.2 mg/L from PA6 nanocomposite. The release of the surfactant from PA6 films was faster than PP due to the swelling effect of ethanol in PA6. The swelling of the polymer

allowed easy access of solvent molecules into the polymer matrix, for the later swelling of the nanoclay particles and then interaction with the surfactant. Compared with nanoclay particles, the authors concluded that surfactant molecules can more easily move within the polymer matrix, following the diffusion behavior of small molecules due to the presences of FV and polymer chain relaxation.

### 2.3.2 Chain extenders

It is well known that PLA is susceptible to thermal degradation during processing at elevated temperatures resulting in an undesired molecular weight reduction and weight loss with a decrease of the rheological and mechanical properties. Different factors might affect the thermal degradation of PLA during melt processing, such as moisture content, residual metal catalysts, processing temperature, and oxygen [134]. Several authors have reported the use of chain extenders to control the thermal degradation of PLA introduced during polymer processing [135-141]. Chain extenders have two or more functional groups that react with the chemical groups formed during the degradation of the polymer. The degraded chains are re-linked, restoring the molecular weight of the polymer [142]. Some of the chain extenders that have been reported in literature are tris(nonylphenyl)phosphite (TNPP) [135], hexamethylene diisocyanate (HDI) [143], 1,6-hexanediol diglycidyl ether (HDE) [144], pyromellitic dianhydride (PMDA) [143], poly(carbodiimide) (PCDI) [135, 145, 146] and epoxy based (*e.g.* Joncryl®) [135, 136, 142-144, 147, 148].

Epoxy based chain extenders have proven to be effective to maintain and increase the molecular weight during PLA processing [135, 136, 147, 149]. Joncryl®, one of the well studied epoxy chain extenders, is an oligomeric copolymer based on

glycidyl methacrylate, styrene and other acrylates with functionality greater than four (**Figure 2.13**) [141, 142]. The molecular weight of PLA processed with an epoxy chain extender increases with the increase in functionality, but no further increase is observed with a functionality greater than 5 [142]. When PLA is degraded during melt processing due to hydrolysis of the ester groups, two new chains are created, each with a carboxylic acid group at one end and at the other end a hydroxyl group. The epoxy groups of the Joncryl® chain extender can theoretically react with the hydroxyl and carboxyl acid groups. However, studies have shown that the reaction is most favorable with the carboxylic acid group due to the strong polymerization of the hydroxyl groups of carboxylic acid [142, 150-152]. A possible reaction between Joncryl® and PLA end groups is shown in **Figure 2.14.**

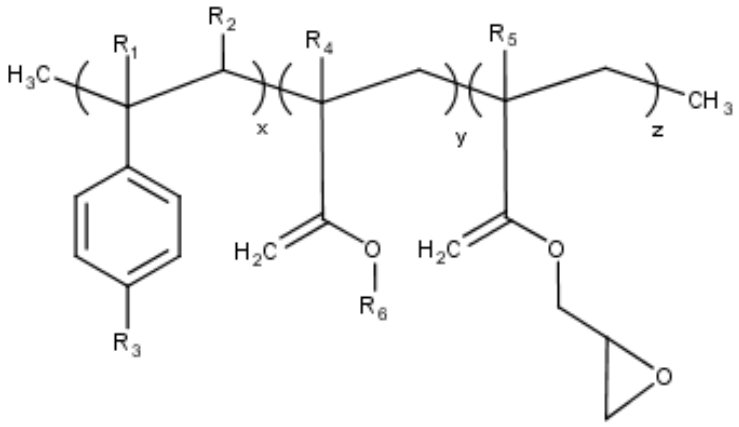


**Figure 2.13** General structure of Joncryl® ADR, where $R_1$ – $R_5$ are H, $CH_3$, a higher alkyl group, or combination of them; $R_6$ is an alkyl group, and x, y and z are each between 1 and 20, adapted from Cailloux et.al. [152]

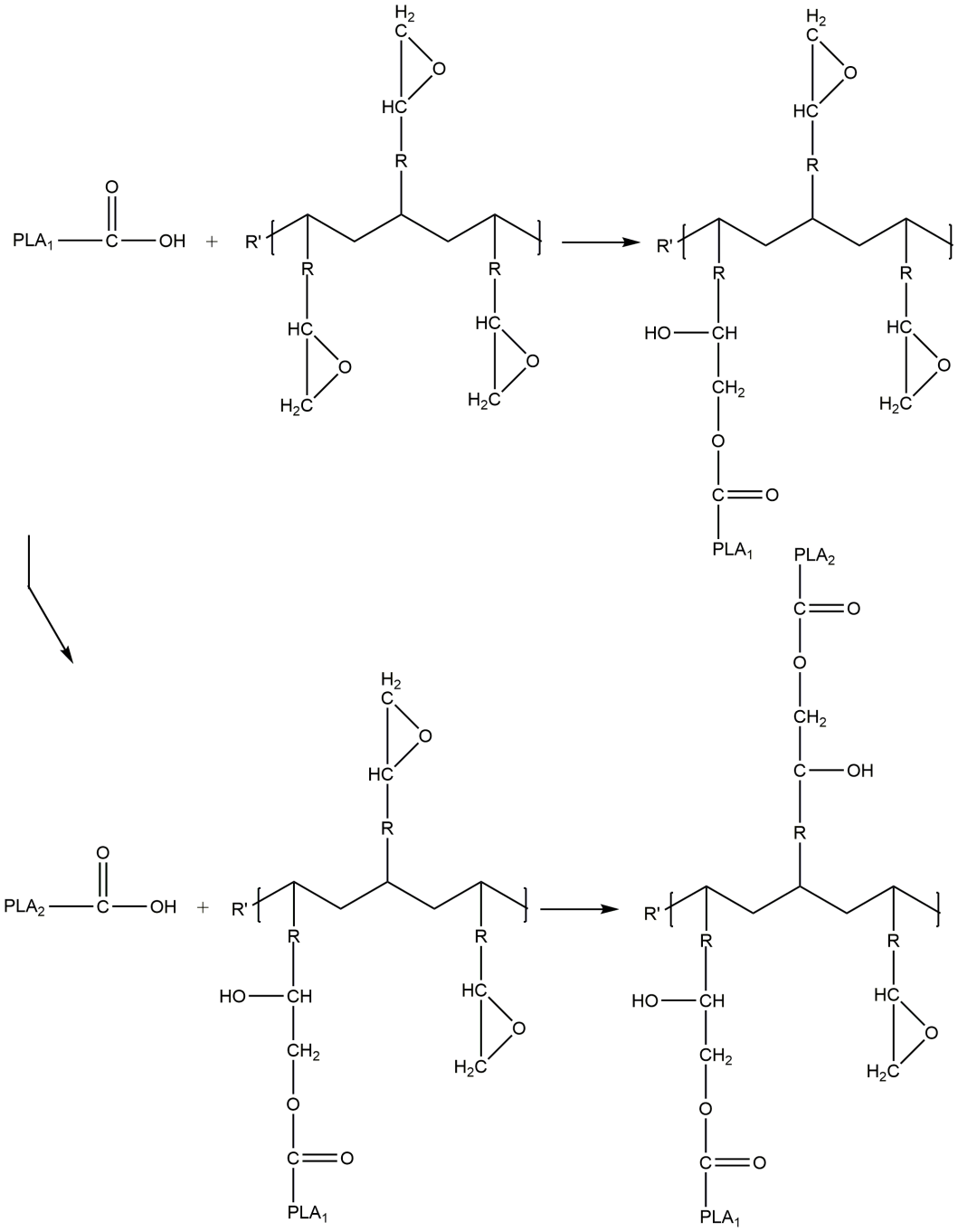


**Figure 2.14** Reaction of Joncryl® and PLA end groups, adapted from Najafi et al. [135].

Different authors have reported the control of thermal degradation of PLA using Joncryl® comparing to the addition of other kind of chain extenders. Najafi et al. [135]

studied three chain extenders into neat PLA and PLA-nanocomposite (2% wt. Cloisite®30B): PCDI (2% wt.), TNPP (1% wt.) and Joncryl®ADR-4368 (1% wt.). Results showed an increase in the molecular weight of PLA with the addition of chain extender having an impact in the rheological and thermal properties. The incorporation of PCDI and TNPP led to the formation of longer linear chains while Joncryl® led to a long chain branched structure. Joncryl®ADR-4368 was the most efficient chain extender among these. The presence of Joncryl® gave a stable viscoelastic response, strongly influencing the rheological properties. The thermal gravimetric analysis showed that the addition of PCDI and TNPP increased the onset temperature for thermal degradation of PLA, attributed to longer chains with a reduced number of chain ends per mass. However, the presence of Joncryl® decreased the onset temperature due to the long branched structures with a higher number of ends per chain than linear systems.

Meng et al. [143] studied the use of HDI (0.5% wt.), PMDA (0.5% wt.) and Joncryl®ADR-4368 (0.5% wt.) in PLA and PLA nanocomposites. HDI has bi-reactive end groups per molecule; therefore, extended PLA molecules with mostly linear structure were obtained. On the other hand, the presence of Joncryl® changed the molecular structure from linear to a branched or cross-linked structure depending on the concentration of Joncryl® and temperature of processing. It was found that Joncryl® and HDI had much higher chain extension than when PMDA was incorporated into PLA. Joncryl® increased the complex viscosity. Also, Joncryl® showed significant thermal stabilization of PLA nanocomposites containing 6% Cloisite®30B.

The presence of Joncryl® has been studied in PLA blends with other polymers, such as poly(butylene-adipate-co-terephtalate) (PBAT) [136, 148, 153], poly[(butylene

succinate)-co-adipate] (PBSA) [154], and thermoplastic starch (TPS). Zhang et al. [149] investigated the addition of Joncryl®ADR-4370S (1% wt.) into a blend of plasticized PLA and TPS and found the improvement of the mechanical properties, for instance the tensile strength, the yield strength and the elongation. In a blend of PLA/PBAT (80/20 w/w), Al-Itry et al. [136] showed that the incorporation of Joncryl®ADR-4368 (0.25, 0.5 and 1% wt.) improved the thermal stability, molecular weight, intrinsic viscosity, shear thinning and elasticity during melt processing due to the formation of extended and branched chains. Molecular weight, melt strength and thermal stability enhancement was also reported by Ojijo and Ray [154] in a blend of PLA/PBSA using Joncryl®ADR-4368, which changed the molecular structure from linear to branched.

Studies of the effect of Joncryl® on the hydrolytic degradation of PLA is limited in the literature. Dong et al. [153] studied the effect of Joncryl®ADR-4370S (1% wt.) in a blend of PLA/PBAT (80/20 w/w) in the hydrolysis of the material in alkaline media at 60 °C. The hydrolysis of the samples was evaluated by weight loss, molecular weight reduction and *pH* variation. They found that the hydrolysis of PLA and its blends went through a gradual diffusion of water, fast hydrolysis of the bulk leading a reduction in molecular weight and further hydrolysis of PLA oligomers. However, the addition of chain extenders in the blend did not noticeably retard the hydrolytic degradation of the PLA matrix. Studies are needed to understand the effect of epoxy chain extenders in the hydrolytic degradation of PLA.

# REFERENCES

## REFERENCES


[1] R. Auras, B. Harte, S. Selke, An overview of polylactides as packaging materials, Macromol. Biosci. 4 (2004) 835-864.

[2] N. Bleach, K. Tanner, M. Kellomäki, P. Törmälä, Effect of filler type on the mechanical properties of self-reinforced polylactide–calcium phosphate composites, J. Mater. Sci. Mater. Med. 12 (2001) 911-915.

[3] Y. Ikada, H. Tsuji, Biodegradable polyesters for medical and ecological applications, Macromol. Rapid Commun. 21 (2000) 117-132.

[4] J.-Y. Park, I.-H. Lee, Controlled release of ketoprofen from electrospun porous polylactic acid (PLA) nanofibers, J. Polym. Res. 18 (2011) 1287-1291.

[5] D.G. Hayes, S. Dharmalingam, L.C. Wadsworth, K.K. Leonas, C. Miles, D. Inglis, Biodegradable agricultural mulches derived from biopolymers, in: C.S. Kishan Khemani (Ed.), Degradable polymers and materials: Principles and practice, American Chemical Society, Washington, DC, 2012, pp. 201-223.

[6] E. Castro-Aguirre, F. Iñiguez-Franco, H. Samsudin, X. Fang, R. Auras, Poly (lactic acid)—Mass production, processing, industrial applications, and end of life, Adv. Drug Deliv. Rev. 107 (2016) 333-366.

[7] X. Jiang, Y. Luo, X. Tian, D. Huang, N. Reddy, Y. Yang, Chemical Structure of Poly(lactic acid), in: R. Auras, L.-T. Lim, S. Selke, H. Tsuji (Eds.), Poly(lactic acid). Synthesis, Structures, Properties, Processing, and Applications, John Wiley & Sons, Inc., New Jersey, 2010, pp. 69-82.

[8] W.L. Hawkins, Polymer Degradation and Stabilization, Springer-Verlag, Berlin, 1984.

[9] R. Muller, Biodegradability of polymers: Regulations and methods of testing. , in: A. Steinbuchel (Ed.), Biopolymer, General Aspects and Special Application, Wiley Publishers, 2008, pp. 366-388.

[10] H. Tsuji, Hydrolytic Degradation, in: R. Auras, L.-T. Lim, S. Selke, H. Tsuji (Eds.), Poly(lactic acid). Synthesis, Structures, Properties, Processing, and Applications, John Wiley & Sons, Inc., New Jersey, 2010, pp. 345-381.

[11] K.M. Nampoothiri, N.R. Nair, R.P. John, An overview of the recent developments in polylactide (PLA) research, Bioresour. Technol. 101 (2010) 8493-8501.

[12] S. Lyu, J. Schley, B. Loy, D. Lind, C. Hobot, R. Sparer, D. Untereker, Kinetics and time-temperature equivalence of polymer degradation, Biomacromolecules 8 (2007) 2301-2310.

[13] I. Grizzi, H. Garreau, S. Li, M. Vert, Hydrolytic degradation of devices based on poly (DL-lactic acid) size-dependence, Biomaterials 16 (1995) 305-311.

[14] Y. Cha, C. Pitt, The acceleration of degradation-controlled drug delivery from polyester microspheres, Journal of controlled release 8 (1989) 259-265.

[15] X. Yuan, A.F. Mak, K. Yao, Surface degradation of poly (L-lactic acid) fibres in a concentrated alkaline solution, Polym. Degrad. Stab. 79 (2003) 45-52.

[16] X. Yuan, A.F. Mak, K. Yao, In vitro degradation of poly (L‐lactic acid) fibers in phosphate buffered saline, J. Appl. Polym. Sci. 85 (2002) 936-943.

[17] X. Yuan, A.F. Mak, K. Yao, Comparative observation of accelerated degradation of poly (L-lactic acid) fibres in phosphate buffered saline and a dilute alkaline solution, Polym. Degrad. Stab. 75 (2002) 45-53.

[18] X. Zhang, M. Espiritu, A. Bilyk, L. Kurniawan, Morphological behaviour of poly (lactic acid) during hydrolytic degradation, Polym. Degrad. Stab. 93 (2008) 1964-1970.

[19] H. Antheunis, J.-C. van der Meer, M. de Geus, W. Kingma, C.E. Koning, Improved mathematical model for the hydrolytic degradation of aliphatic polyesters, Macromolecules 42 (2009) 2462-2471.

[20] F. von Burkersroda, L. Schedl, A. Göpferich, Why degradable polymers undergo surface erosion or bulk erosion, Biomaterials 23 (2002) 4221-4231.

[21] S.M. Li, M. Vert, Biodegradation of aliphatic polyesters, in: G. Scott, G. D (Eds.), Biodegradable Polymers: Principles and Applications, Chapman & Hall, Cambridge, 1995, pp. 43-87.

[22] H. Tsuji, T. Hayashi, Hydrolytic degradation of linear 2-arm and branched 4-arm poly (dl-lactide) s: effects of branching and terminal hydroxyl groups, Polym. Degrad. Stab. 102 (2014) 59-66.

[23] S. De Jong, E.R. Arias, D. Rijkers, C. Van Nostrum, J. Kettenes-Van den Bosch, W. Hennink, New insights into the hydrolytic degradation of poly (lactic acid): participation of the alcohol terminus, Polymer 42 (2001) 2795-2802.

[24] J.H. Jung, M. Ree, H. Kim, Acid-and base-catalyzed hydrolyses of aliphatic polycarbonates and polyesters, Catal. Today 115 (2006) 283-287.

[25] K. Makino, H. Ohshima, T. Kondo, Mechanism of hydrolytic degradation of poly (L-lactide) microcapsules: effects of pH, ionic strength and buffer concentration, J. Microencapsulation 3 (1986) 203-212.

[26] H. Tsuji, Y. Ikada, Properties and morphology of poly (L‐lactide). II. Hydrolysis in alkaline solution, J. Polym. Sci. A Polym. Chem. 36 (1998) 59-66.

[27] K. Fukushima, D. Tabuani, M. Dottori, I. Armentano, J. Kenny, G. Camino, Effect of temperature and nanoparticle type on hydrolytic degradation of poly (lactic acid) nanocomposites, Polym. Degrad. Stab. 96 (2011) 2120-2129.

[28] A. Copinet, C. Bertrand, S. Govindin, V. Coma, Y. Couturier, Effects of ultraviolet light (315 nm), temperature and relative humidity on the degradation of polylactic acid plastic films, Chemosphere 55 (2004) 763-773.

[29] M.K. Mitchell, D.E. Hirt, Degradation of PLA fibers at elevated temperature and humidity, Polym. Eng. Sci. (2014).

[30] N. Weir, F. Buchanan, J. Orr, D. Farrar, G. Dickson, Degradation of poly-L-lactide. Part 2: increased temperature accelerated degradation, Proc. Inst. Mech. Eng. H J. Eng. Med. 218 (2004) 321-330.

[31] S. Li, S. McCarthy, Further investigations on the hydrolytic degradation of poly (DL-lactide), Biomaterials 20 (1999) 35-44.

[32] W. Tham, B. Poh, Z.M. Ishak, W. Chow, Water Absorption Kinetics and Hygrothermal Aging of Poly (lactic acid) Containing Halloysite Nanoclay and Maleated Rubber, J. Polym. Environ. (2015) 1-9.

[33] F. Codari, S. Lazzari, M. Soos, G. Storti, M. Morbidelli, D. Moscatelli, Kinetics of the hydrolytic degradation of poly (lactic acid), Polym. Degrad. Stab. 97 (2012) 2460-2466.

[34] Q. Zhou, M. Xanthos, Nanoclay and crystallinity effects on the hydrolytic degradation of polylactides, Polym. Degrad. Stab. 93 (2008) 1450-1459.

[35] H. Tsuji, K. Ikarashi, In vitro hydrolysis of poly (l-lactide) crystalline residues as extended-chain crystallites. Part I: long-term hydrolysis in phosphate-buffered solution at 37 C, Biomaterials 25 (2004) 5449-5455.

[36] H. Tsuji, H. Daimon, K. Fujie, A new strategy for recycling and preparation of poly (L-lactic acid): hydrolysis in the melt, Biomacromolecules 4 (2003) 835-840.

[37] A.-F. Mohd-Adnan, H. Nishida, Y. Shirai, Evaluation of kinetics parameters for poly (L-lactic acid) hydrolysis under high-pressure steam, Polym. Degrad. Stab. 93 (2008) 1053-1058.

[38] V. Piemonte, F. Gironi, Kinetics of hydrolytic degradation of PLA, J. Polym. Environ. 21 (2013) 313-318.

[39] H. Tsuji, K. Ikarashi, In vitro hydrolysis of poly (l-lactide) crystalline residues as extended-chain crystallites: II. Effects of hydrolysis temperature, Biomacromolecules 5 (2004) 1021-1028.

[40] H. Tsuji, T. Saeki, T. Tsukegi, H. Daimon, K. Fujie, Comparative study on hydrolytic degradation and monomer recovery of poly (L-lactic acid) in the solid and in the melt, Polym. Degrad. Stab. 93 (2008) 1956-1963.

[41] H. Tsuji, Autocatalytic hydrolysis of amorphous-made polylactides: effects of L-lactide content, tacticity, and enantiomeric polymer blending, Polymer 43 (2002) 1789-1796.

[42] S.K. Saha, H. Tsuji, Effects of molecular weight and small amounts of d-lactide units on hydrolytic degradation of poly (l-lactic acid) s, Polym. Degrad. Stab. 91 (2006) 1665-1673.

[43] S.K. Saha, H. Tsuji, Hydrolytic Degradation of Amorphous Films of L‐Lactide Copolymers with Glycolide and D‐Lactide, Macromol. Mater. Eng. 291 (2006) 357-368.

[44] E. Çelikkaya, E.B. Denkbaş, E. Pişkin, Poly (DL‐lactide)/poly (ethylene glycol) copolymer particles. I. Preparation and characterization, J. Appl. Polym. Sci. 61 (1996) 1439-1446.

[45] P. Pan, Y. Inoue, Polymorphism and isomorphism in biodegradable polyesters, Prog. Polym. Sci. 34 (2009) 605-640.

[46] N. Naga, Y. Yoshida, M. Inui, K. Noguchi, S. Murase, Crystallization of amorphous poly (lactic acid) induced by organic solvents, J. Appl. Polym. Sci. 119 (2011) 2058-2064.

[47] T. Kawai, N. Rahman, G. Matsuba, K. Nishida, T. Kanaya, M. Nakano, H. Okamoto, J. Kawada, A. Usuki, N. Honma, Crystallization and melting behavior of poly (L-lactic acid), Macromolecules 40 (2007) 9463-9469.

[48] Y. Srithep, P. Nealey, L.S. Turng, Effects of annealing time and temperature on the crystallinity and heat resistance behavior of injection‐molded poly (lactic acid), Polym. Eng. Sci. 53 (2013) 580-588.

[49] W. Hoogsteen, A. Postema, A. Pennings, G. Ten Brinke, P. Zugenmaier, Crystal structure, conformation and morphology of solution-spun poly (L-lactide) fibers, Macromolecules 23 (1990) 634-642.

[50] L. Cartier, T. Okihara, Y. Ikada, H. Tsuji, J. Puiggali, B. Lotz, Epitaxial crystallization and crystalline polymorphism of polylactides, Polymer 41 (2000) 8909-8919.

[51] D. Sawai, K. Takahashi, A. Sasashige, T. Kanamoto, S.-H. Hyon, Preparation of oriented β-form poly (L-lactic acid) by solid-state coextrusion: effect of extrusion variables, Macromolecules 36 (2003) 3601-3605.

[52] K. Wasanasuk, K. Tashiro, Structural regularization in the crystallization process from the glass or melt of poly (l-lactic acid) viewed from the temperature-dependent and time-resolved measurements of FTIR and wide-angle/small-angle X-ray scatterings, Macromolecules 44 (2011) 9650-9660.

[53] J. Zhang, K. Tashiro, A.J. Domb, H. Tsuji, Confirmation of Disorder $\alpha$ Form of Poly (L‐lactic acid) by the X‐ray Fiber Pattern and Polarized IR/Raman Spectra Measured for Uniaxially‐Oriented Samples, in: Macromolecular symposia, Wiley Online Library, 2006, pp. 274-278.

[54] S. Sato, D. Gondo, T. Wada, S. Kanehashi, K. Nagai, Effects of various liquid organic solvents on solvent‐induced crystallization of amorphous poly (lactic acid) film, J. Appl. Polym. Sci. 129 (2013) 1607-1617.

[55] H. Marubayashi, S. Asai, M. Sumita, Complex crystal formation of poly (l-lactide) with solvent molecules, Macromolecules 45 (2012) 1384-1397.

[56] H.-m. Chen, Y. Shen, J.-h. Yang, T. Huang, N. Zhang, Y. Wang, Z.-w. Zhou, Molecular ordering and $\alpha'$ -form formation of poly (l-lactide) during the hydrolytic degradation, Polymer 54 (2013) 6644-6653.

[57] M. Yasuniwa, S. Tsubakihara, K. Iura, Y. Ono, Y. Dan, K. Takahashi, Crystallization behavior of poly (L-lactic acid), Polymer 47 (2006) 7554-7563.

[58] H. Zhou, T.B. Green, Y.L. Joo, The thermal effects on electrospinning of polylactic acid melts, Polymer 47 (2006) 7497-7505.

[59] E. Zuza, J.M. Ugartemendia, A. Lopez, E. Meaurio, A. Lejardi, J.-R. Sarasua, Glass transition behavior and dynamic fragility in polylactides containing mobile and rigid amorphous fractions, Polymer 49 (2008) 4427-4432.

[60] A. Magoń, M. Pyda, Study of crystalline and amorphous phases of biodegradable poly (lactic acid) by advanced thermal analysis, Polymer 50 (2009) 3967-3973.

[61] J. Del Rio, A. Etxeberria, N. Lopez-Rodriguez, E. Lizundia, J. Sarasua, A PALS contribution to the supramolecular structure of poly (L-lactide), Macromolecules 43 (2010) 4698-4707.

[62] S.F. Nassar, A. Guinault, N. Delpouve, V. Divry, V. Ducruet, C. Sollogoub, S. Domenek, Multi-scale analysis of the impact of polylactide morphology on gas barrier properties, Polymer 108 (2017) 163-172.

[63] G. Dlubek, A.S. Gupta, J. Pionteck, R. Häßler, R. Krause-Rehberg, H. Kaspar, K. Lochhaas, Glass transition and free volume in the mobile (MAF) and rigid (RAF) amorphous fractions of semicrystalline PTFE: a positron lifetime and PVT study, Polymer 46 (2005) 6075-6089.

[64] U. Sonchaeng, F. Iñiguez-Franco, R. Auras, S. Selke, M. Rubino, L.-T. Lim, Poly(lactic acid) mass transfer properties, Prog. Polym. Sci. Submitted (2017).

[65] J. Cai, M. Liu, L. Wang, K. Yao, S. Li, H. Xiong, Isothermal crystallization kinetics of thermoplastic starch/poly (lactic acid) composites, Carbohydrate Polymers 86 (2011) 941-947.

[66] A. Kalkar, V. Deshpande, M. Kulkarni, Isothermal crystallization kinetics of poly (phenylene sulfide)/TLCP composites, Polymer Engineering and Science 49 (2009) 397-417.

[67] A. Kalkar, V. Deshpande, M. Kulkarni, Isothermal crystallization kinetics of poly (phenylene sulfide)/TLCP composites, Polym. Eng. Sci. 49 (2009) 397-417.

[68] G. Papageorgiou, D. Achilias, S. Nanaki, T. Beslikas, D. Bikiaris, PLA nanocomposites: effect of filler type on non-isothermal crystallization, Thermochimica Acta 511 (2010) 129-139.

[69] T. Ke, X. Sun, Melting behavior and crystallization kinetics of starch and poly (lactic acid) composites, Journal of Applied Polymer Science 89 (2003) 1203-1210.

[70] H. Tsuji, A. Mizuno, Y. Ikada, Properties and morphology of poly (L‐lactide). III. Effects of initial crystallinity on long‐term in vitro hydrolysis of high molecular weight poly (L‐lactide) film in phosphate‐buffered solution, J. Appl. Polym. Sci. 77 (2000) 1452-1464.

[71] C.G. Pitt, G. Zhong-wei, Modification of the rates of chain cleavage of poly (ϵ-caprolactone) and related polyesters in the solid state, Journal of controlled release 4 (1987) 283-292.

[72] H. Tsuji, K. Sumida, Poly (L‐lactide): v. effects of storage in swelling solvents on physical properties and structure of poly (L‐lactide), J. Appl. Polym. Sci. 79 (2001) 1582-1589.

[73] S. Lee, Fourteen-year-old aging study of the effect of thickness on methanol transport in crosslinked poly (methyl methacrylate), Journal of materials research 11 (1996) 2403-2405.

[74] S.M. Aharoni, N.S. Murthy, Effects of Solvent-induced Crystallization on the Amorphous Phase of Polycarbonate of bisphenol A), International Journal of Polymeric Materials 42 (1998) 275-283.

[75] W.-H. Lee, H. Ouyang, M.-C. Shih, M.-H. Wu, Kinetics of solvent-induced crystallization of poly (ethylene terephthalate) at the final stage, J. Polym. Res. 10 (2003) 133-137.

[76] K. Tashiro, A. Yoshioka, Molecular mechanism of solvent-induced crystallization of syndiotactic polystyrene glass. 2. Detection of enhanced motion of the amorphous chains in the induction period of crystallization, Macromolecules 35 (2002) 410-414.

[77] H. Ouyang, W.-H. Lee, W. Ouyang, S.-T. Shiue, T.-M. Wu, Solvent-induced crystallization in poly (ethylene terephthalate) during mass transport: Mechanism and boundary condition, Macromolecules 37 (2004) 7719-7723.

[78] H. Ouyang, W.-H. Lee, M.-C. Shih, Three stages of crystallization in poly (ethylene terephthalate) during mass transport, Macromolecules 35 (2002) 8428-8432.

[79] W.-C. Tsai, M. Hedenqvist, Å. Laiback, H. Melin, M. Ngo, M. Trollsås, U. Gedde, Physical changes and sorption/desorption behaviour of amorphous and semi-crystalline PLLA exposed to water, methanol and ethanol, Eur. Polym. J. 76 (2016) 278-293.

[80] C. Chariyachotilert, S.E. Selke, R.A. Auras, S. Joshi, Assessment of the properties of poly (L-lactic Acid) sheets produced with differing amounts of post-consumer recycled poly (L-lactic Acid), J. Plast. Film Sheet. 28 (2012) 314-335.

[81] K. Hamad, M. Kaseem, F. Deri, Recycling of waste from polymer materials: An overview of the recent works, Polym. Degrad. Stab. 98 (2013) 2801-2812.

[82] V. Piemonte, S. Sabatini, F. Gironi, Chemical recycling of PLA: a great opportunity towards the sustainable development?, J. Polym. Environ. 21 (2013) 640-647.

[83] L.D. Brake, N.S. Subramanian, Rapid depolymerization of polyhydroxy acids. United States Patent 5229528, (1993).

[84] P. Coszach, J.-C. Bogaert, J. Willocq, Chemical recycling of PLA by alcoholysis. United States Patent 848675 B2, in, 2013.

[85] P. Coszach, J.-C. Bogaert, J. Willocq, Chemical recycling of PLA by hydrolysis. United States Patent 8431683 B2, in, 2013.

[86] A.C. Sánchez, S.R. Collinson, The selective recycling of mixed plastic waste of polylactic acid and polyethylene terephthalate by control of process conditions, Eur. Polym. J. 47 (2011) 1970-1976.

[87] F.A. Leibfarth, N. Moreno, A.P. Hawker, J.D. Shand, Transforming polylactide into value‐added materials, J. Polym. Sci. A Polym. Chem. 50 (2012) 4814-4822.

[88] F. Gironi, S. Frattari, V. Piemonte, PLA Chemical Recycling Process Optimization: PLA Solubilization in Organic Solvents, J. Polym. Environ. 24 (2016) 328-333.

[89] K. Okamoto, K. Toshima, S. Matsumura, Degradation of poly (lactic acid) into repolymerizable oligomer using montmorillonite K10 for chemical recycling, Macromol. Biosci. 5 (2005) 813-820.

[90] Y. Takahashi, S. Okajima, K. Toshima, S. Matsumura, Lipase‐Catalyzed Transformation of Poly (lactic acid) into Cyclic Oligomers, Macromol. Biosci. 4 (2004) 346-353.

[91] A. Plichta, P. Lisowska, A. Kundys, A. Zychewicz, M. Dębowski, Z. Florjańczyk, Chemical recycling of poly (lactic acid) via controlled degradation with protic (macro) molecules, Polym. Degrad. Stab. 108 (2014) 288-296.

[92] S. Matsumura, Enzyme‐Catalyzed Synthesis and Chemical Recycling of Polyesters, Macromol. Biosci. 2 (2002) 105-126.

[93] Y. Tsuneizumi, M. Kuwahara, K. Okamoto, S. Matsumura, Chemical recycling of poly (lactic acid)-based polymer blends using environmentally benign catalysts, Polym. Degrad. Stab. 95 (2010) 1387-1393.

[94] H.M. De Azeredo, Nanocomposites for food packaging applications, Food Res. Int. 42 (2009) 1240-1253.

[95] J.-M. Raquez, Y. Habibi, M. Murariu, P. Dubois, Polylactide (PLA)-based nanocomposites, Prog. Polym. Sci. 38 (2013) 1504-1542.

[96] S.S. Ray, M. Okamoto, Polymer/layered silicate nanocomposites: a review from preparation to processing, Prog. Polym. Sci. 28 (2003) 1539-1641.

[97] F. Hussain, M. Hojjati, M. Okamoto, R.E. Gorga, Review article: polymer-matrix nanocomposites, processing, manufacturing, and application: an overview, Journal of composite materials 40 (2006) 1511-1575.

[98] Y. Xi, R.L. Frost, H. He, T. Kloprogge, T. Bostrom, Modification of Wyoming montmorillonite surfaces using a cationic surfactant, Langmuir 21 (2005) 8675-8680.

[99] L.d.A. Prado, C. Karthikeyan, K. Schulte, S. Nunes, I.L. de Torriani, Organic modification of layered silicates: structural and thermal characterizations, Journal of Non-Crystalline Solids 351 (2005) 970-975.

[100] P.M.S. Souza, A.R. Morales, M.A. Marin-Morales, L.H.I. Mei, PLA and montmorilonite nanocomposites: properties, biodegradation and potential toxicity, J. Polym. Environ. 21 (2013) 738-759.

[101] M. Pluta, Melt compounding of polylactide/organoclay: structure and properties of nanocomposites, J. Polym. Sci. Part B Polym. Phys. 44 (2006) 3392-3405.

[102] L. Jiang, J. Zhang, M.P. Wolcott, Comparison of polylactide/nano-sized calcium carbonate and polylactide/montmorillonite composites: reinforcing effects and toughening mechanisms, Polymer 48 (2007) 7632-7644.

[103] A.P. Kumar, D. Depan, N.S. Tomer, R.P. Singh, Nanoscale particles for polymer degradation and stabilization—trends and future perspectives, Prog. Polym. Sci. 34 (2009) 479-515.

[104] M. Zanetti, S. Lomakin, G. Camino, Polymer layered silicate nanocomposites, Macromol. Mater. Eng. 279 (2000) 1-9.

[105] P. Krishnamachari, J. Zhang, J. Lou, J. Yan, L. Uitenham, Biodegradable poly (lactic acid)/clay nanocomposites by melt intercalation: a study of morphological, thermal, and mechanical properties, International Journal of Polymer Analysis and Characterization 14 (2009) 336-350.

[106] R.A. Vaia, E.P. Giannelis, Polymer melt intercalation in organically-modified layered silicates: model predictions and experiment, Macromolecules 30 (1997) 8000-8009.

[107] L.-T. Lim, R. Auras, M. Rubino, Processing technologies for poly (lactic acid), Prog. Polym. Sci. 33 (2008) 820-852.

[108] M. Alexandre, P. Dubois, Polymer-layered silicate nanocomposites: preparation, properties and uses of a new class of materials, Materials Science and Engineering: R: Reports 28 (2000) 1-63.

[109] S.-R. Lee, H.-M. Park, H. Lim, T. Kang, X. Li, W.-J. Cho, C.-S. Ha, Microstructure, tensile properties, and biodegradability of aliphatic polyester/clay nanocomposites, Polymer 43 (2002) 2495-2500.

[110] M. Jollands, R.K. Gupta, Effect of mixing conditions on mechanical properties of polylactide/montmorillonite clay nanocomposites, J. Appl. Polym. Sci. 118 (2010) 1489-1493.

[111] X. Fang, O. Vitrac, S. Domenek, V. Ducruet, A tailored approach to optimize the barrier properties of Poly (lactic acid) nanocomposites for food contact purposes, in: Matériaux 2010. 2010-10-182010-10-22, Nantes, FRA, 2010.

[112] S.S. Ray, K. Yamada, M. Okamoto, K. Ueda, New polylactide-layered silicate nanocomposites. 2. Concurrent improvements of material properties, biodegradability and melt rheology, Polymer 44 (2003) 857-866.

[113] P. Maiti, K. Yamada, M. Okamoto, K. Ueda, K. Okamoto, New polylactide/layered silicate nanocomposites: role of organoclays, Chemistry of materials 14 (2002) 4654-4661.

[114] D. Lewitus, S. McCarthy, A. Ophir, S. Kenig, The effect of nanoclays on the properties of PLLA-modified polymers part 1: mechanical and thermal properties, J. Polym. Environ. 14 (2006) 171-177.

[115] M.-A. Paul, C. Delcourt, M. Alexandre, P. Degée, F. Monteverde, P. Dubois, Polylactide/montmorillonite nanocomposites: study of the hydrolytic degradation, Polym. Degrad. Stab. 87 (2005) 535-542.

[116] K. Fukushima, C. Abbate, D. Tabuani, M. Gennari, G. Camino, Biodegradation of poly (lactic acid) and its nanocomposites, Polym. Degrad. Stab. 94 (2009) 1646-1655.

[117] A. Araújo, G. Botelho, M. Oliveira, A. Machado, Influence of clay organic modifier on the thermal-stability of PLA based nanocomposites, Appl. Clay Sci. 88 (2014) 144-150.

[118] C. Silvestre, D. Duraccio, S. Cimmino, Food packaging based on polymer nanomaterials, Prog. Polym. Sci. 36 (2011) 1766-1782.

[119] Q. Chaudhry, M. Scotter, J. Blackburn, B. Ross, A. Boxall, L. Castle, R. Aitken, R. Watkins, Applications and implications of nanotechnologies for the food sector, Food additives and contaminants 25 (2008) 241-258.

[120] F. Gottschalk, B. Nowack, The release of engineered nanomaterials to the environment, Journal of Environmental Monitoring 13 (2011) 1145-1155.

[121] C. Blasco, Y. Picó, Determining nanomaterials in food, TrAC Trends in Analytical Chemistry 30 (2011) 84-99.

[122] C.-F. Chau, S.-H. Wu, G.-C. Yen, The development of regulations for food nanotechnology, Trends in Food Science & Technology 18 (2007) 269-280.

[123] M. Baek, J.-A. Lee, S.-J. Choi, Toxicological effects of a cationic clay, montmorillonite in vitro and in vivo, Molecular & Cellular Toxicology 8 (2012) 95-101.

[124] M. Geiser, B. Rothen-Rutishauser, N. Kapp, S. Schürch, W. Kreyling, H. Schulz, M. Semmler, V.I. Hof, J. Heyder, P. Gehr, Ultrafine particles cross cellular membranes by nonphagocytic mechanisms in lungs and in cultured cells, Environmental health perspectives (2005) 1555-1560.

[125] N. Li, C. Sioutas, A. Cho, D. Schmitz, C. Misra, J. Sempf, M. Wang, T. Oberley, J. Froines, A. Nel, Ultrafine particulate pollutants induce oxidative stress and mitochondrial damage, Environmental health perspectives 111 (2003) 455.

[126] Y. Guang Guo, Behavior and effects of surfactants and their degradation products in the environment, International J. of Environment 32 (2004) 417-431.

[127] S.H. Venhuis, M. Mehrvar, Health effects, environmental impacts, and photochemical degradation of selected surfactants in water, International Journal of photoenergy 6 (2004) 115-125.

[128] P. Simon, Q. Chaudhry, D. Bakos, from polymer packaging to food–a physicochemical view, J. Food Nutr. Res. 47 (2008) 105-113.

[129] Y. Xia, M. Rubino, R. Auras, Release of nanoclay and surfactant from polymer–clay nanocomposites into a food simulant, Environ. Sci. Technol. 48 (2014) 13617-13624.

[130] B. Schmidt, J.H. Petersen, C. Bender Koch, D. Plackett, N.R. Johansen, V. Katiyar, E.H. Larsen, Combining asymmetrical flow field-flow fractionation with light-scattering and inductively coupled plasma mass spectrometric detection for characterization of nanoclay used in biopolymer nanocomposites, Food Additives and Contaminants 26 (2009) 1619-1627.

[131] B. Schmidt, V. Katiyar, D. Plackett, E.H. Larsen, N. Gerds, C.B. Koch, J.H. Petersen, Migration of nanosized layered double hydroxide platelets from polylactide nanocomposite films, Food Additives & Contaminants: Part A 28 (2011) 956-966.

[132] European Union. Commission Directive of 6 August 2002

relating to plastic materials and articles intended to come into contact with foodstuffs., Official Journal of the European Union, L 220/18; amendments: 2004/1/EC, 2004/19/EC, 2005/79/EC, 2007/19/EC, 2008/39/EC (2002).

[133] R. Nigmatullin, F. Gao, V. Konovalova, Polymer-layered silicate nanocomposites in the design of antimicrobial materials, J. Mater. Sci. 43 (2008) 5728-5733.

[134] H. Nishida, Thermal degradation, in: R. Auras, L.T. Lim, S. Selke, H. Tsuji (Eds.), Poly(lactic acid). Synthesis, Structures, Properties, Processing, and Applications, Wiley Publishers, New Jersey, 2010, pp. 401-412.

[135] N. Najafi, M. Heuzey, P. Carreau, P.M. Wood-Adams, Control of thermal degradation of polylactide (PLA)-clay nanocomposites using chain extenders, Polym. Degrad. Stab. 97 (2012) 554-565.

[136] R. Al-Itry, K. Lamnawar, A. Maazouz, Improvement of thermal stability, rheological and mechanical properties of PLA, PBAT and their blends by reactive extrusion with functionalized epoxy, Polym. Degrad. Stab. 97 (2012) 1898-1914.

[137] H.J. Lehermeier, J.R. Dorgan, Melt rheology of poly (lactic acid): Consequences of blending chain architectures, Polym. Eng. Sci. 41 (2001) 2172-2184.

[138] L. Yang, X. Chen, X. Jing, Stabilization of poly (lactic acid) by polycarbodiimide, Polym. Degrad. Stab. 93 (2008) 1923-1929.

[139] S.I. Woo, B.O. Kim, H.S. Jun, H.N. Chang, Polymerization of aqueous lactic acid to prepare high molecular weight poly (lactic acid) by chain-extending with hexamethylene diisocyanate, Polymer bulletin 35 (1995) 415-421.

[140] J. Tuominen, J. Kylmä, J. Seppälä, Chain extending of lactic acid oligomers. 2. Increase of molecular weight with 1, 6-hexamethylene diisocyanate and 2, 2′ -bis (2-oxazoline), Polymer 43 (2002) 3-10.

[141] M. Villalobos, A. Awojulu, T. Greeley, G. Turco, G. Deeter, Oligomeric chain extenders for economic reprocessing and recycling of condensation plastics, Energy 31 (2006) 3227-3234.

[142] S.R. Rathi, E.B. Coughlin, S.L. Hsu, C.S. Golub, G.H. Ling, M.J. Tzivanis, Maintaining structural stability of poly (lactic acid): effects of multifunctional epoxy based reactive oligomers, Polymers 6 (2014) 1232-1250.

[143] Q. Meng, M.-C. Heuzey, P.J. Carreau, Control of thermal degradation of polylactide/clay nanocomposites during melt processing by chain extension reaction, Polym. Degrad. Stab. 97 (2012) 2010-2020.

[144] W. Dong, B. Zou, Y. Yan, P. Ma, M. Chen, Effect of chain-extenders on the properties and hydrolytic degradation behavior of the poly(lactide)/poly(butylene adipate-co-terephthalate) blends, International Journal of Molecular Sciences 14 (2013) 20189-20203.

[145] P. Stloukal, G. Jandikova, M. Koutny, V. Sdlarík, Carbodiimide additve to control hydrolytic stability and biodegradability of PLA, Polym. Test. 54 (2016) 19-28.

[146] P. Stloukal, A. Kalendova, H. Mattausch, S. Laske, C. Holzer, M. Koutny, The influence of a hydrolysis-inhibiting additive on the degradation and biodegradation of PLA and its nanocomposites, Polym. Test. 41 (2015) 124-132.

[147] Y.-M. Corre, J. Duchet, J. Reignier, A. Maazouz, Melt strengthening of poly (lactic acid) through reactive extrusion with epoxy-functionalized chains, Rheol. Acta 50 (2011) 613-629.

[148] R. Al-Itry, K. Lamnawar, A. Maazouz, Reactive extrusion of PLA, PBAT with a multi-functional epoxide: Physico-chemical and rheological properties, Eur. Polym. J. 58 (2014) 90-102.

[149] Y. Zhang, X. Yuan, Q. Liu, A. Hrymak, The effect of polymeric chain extenders on physical properties of thermoplastic starch and polylactic acid blends, J. Polym. Environ. 20 (2012) 315-325.

[150] S. Japon, L. Boogh, Y. Leterrier, J.-A. Månson, Reactive processing of poly (ethylene terephthalate) modified with multifunctional epoxy-based additives, Polymer 41 (2000) 5809-5818.

[151] A. Haralabakopoulos, D. Tsiourvas, C. Paleos, Chain extension of poly (ethylene terephthalate) by reactive blending using diepoxides, J. Appl. Polym. Sci. 71 (1999) 2121-2127.

[152] D.N. Bikiaris, G.P. Karayannidis, Chain extension of polyesters PET and PBT with two new diimidodiepoxides. II, J. Polym. Sci. A Polym. Chem. 34 (1996) 1337-1342.

[153] W. Dong, B. Zou, Y. Yan, P. Ma, M. Chen, Effect of Chain-Extenders on the Properties and Hydrolytic Degradation Behavior of the Poly (lactide)/Poly (butylene adipate-co-terephthalate) Blends, International journal of molecular sciences 14 (2013) 20189-20203.

[154] V. Ojijo, S.S. Ray, Super toughened biodegradable polylactide blends with non-linear copolymer interfacial architecture obtained via facile in-situ reactive compatibilization, Polymer 80 (2015) 1-17.

# CHAPTER 3

## Concurrent Solvent Induced Crystallization and Hydrolytic Degradation of PLA by Water-Ethanol Solutions

A version of this chapter is published as:

F. Iñiguez-Franco, R. Auras, G. Burgess, D. Holmes, X. Fang, M. Rubino, H. Soto-Valdez, Concurrent solvent induced crystallization and hydrolytic degradation of PLA by water-ethanol solutions, Polymer 99 (2016) 315-323.

## 3.0 Abstract

Poly(lactic acid) (PLA) films were immersed in pure water, 50% and 95% ethanol solutions for up to 180 days. The change in molecular weight, sorption of water, sorption of ethanol, and lactic acid released were monitored. Glass transition temperature and percent crystallinity as a function of ethanol content were also measured. PLA experienced faster hydrolytic degradation in contact with 50% than with 95% ethanol or pure water. NMR methodologies were developed to measure sorption of deuterated water and ethanol in PLA. More water was sorbed in 50% ethanol, explaining the higher hydrolysis. During exposure, PLA experienced solvent induced crystallization. Higher percent crystallinity was found in films exposed to 50% ethanol with the formation of α-form crystals. The hydrolysis of PLA was correlated with the release of lactic acid (LA) during exposure. Mathematical models are proposed to explain the concurrent solvent induced crystallization and hydrolytic degradation of PLA.

## 3.1 Introduction

PLA is one of the most widely used biopolymers. It has gained attention in recent years as a promising alternative to polymers from nonrenewable resources. PLA is a linear aliphatic thermoplastic polyester, in which LA is the precursor, obtained from the fermentation of corn sugar [1]. Currently, the world capacity for production of PLA is 150,000 metric tons [2]. The versatility of PLA has led to broad and diverse applications. In the medical field, due to its biocompatibility with the human body, PLA has been used for applications such as sutures, stents and drug delivery systems.[3-6] In agriculture, PLA has been used as a material for the controlled release of herbicides [7-9] or as a

plastic to protect soil and plants from erosion, insects and birds [10]. In packaging, PLA has been used as both a film and a rigid thermoform for containers for food and non-food products [1, 11-13].

Depending on the application, PLA can be exposed to different kinds of media, including water and/or ethanol. In the medical field, it can be in contact with aqueous systems or biological media for drug delivery systems [14-16]. For example, disinfection of electrospun materials for tissue engineering is commonly carried out by ethanol soaking [17-19]. In agriculture, for growth stimulation and the controlled release of pesticides, PLA is in a high relative humidity environment or in direct contact with water [7, 20]. In packaging applications, when PLA is used for beverage and fresh food containers, it could be in direct contact with water or ethanol, or be exposed to humid environments. These types of exposure to various environmental conditions could favor PLA degradation.

PLA degradation leads to changes in mechanical and thermal properties, molecular weight and morphology [21-24]. PLA in the presence of water is susceptible to hydrolytic degradation. The ester groups are hydrolytically degraded, leading to a decrease in molecular weight and the release of low molecular weight soluble oligomers and monomers [1, 25]. Conversely, it has been found that PLA will plasticize and crystallize in the presence of organic solvents, which swell the polymer matrix, increasing chain mobility and inducing solvent induced crystallization (SIC) [23, 26-28]. The SIC behavior has been studied in polymers such as poly(methyl methacrylate) [29], poly(carbonate of bisphenol A) [30], polystyrene [31-33], and poly(ethylene terephthalate) (PET) [34-36], SIC is a complex phenomenon involving many processes,

such as diffusion of solvent molecules, swelling, plasticization and crystallization. Several factors can affect each process involved in SIC. Examples are initial crystallinity, temperature, molecular weight and solvent chemistry [30-36]. In a study of SIC in PLA ultrathin films, Wu et al. found that in the initial diffusion stage, the solvent molecules interact with random PLA coil chains, which increase the motion of the PLA segments [28]. These interactions can lead to either dissolution of the polymer or nucleation, leading to the rearrangement of PLA chains into crystal lattices. Therefore, understanding the concurrent effect of SIC and hydrolytic degradation of the PLA matrix as it is exposed to water-ethanol solutions is of paramount importance to fully control and/or develop its applications and tailor its uses, which was the goal of this work.

## 3.2 Materials and methods

### 3.2.1 Chemicals and Reagents

PLA resin (3.8-4.2% D-LA) was obtained from NatureWorks LLC (Minnetonka, MN, USA) with a weight and number average molecular weight ($M_w$, $M_n$) of 2.35 ± 0.07 x $10^5$ Da and 1.21 ± 0.08 x $10^5$ Da, respectively. Ethanol (high-performance liquid chromatography (HPLC) grade), acetonitrile (HPLC grade), methanol (HPLC grade), and formic acid were supplied by Sigma-Aldrich (St. Louis, MO, USA), tetrahydrofuran (THF) by Pharmco-AAPER (North East, CA, USA), and water (HPLC grade) by J.T. Baker (Center Valley, PA, USA). L(+) LA was purchased from Supelco (Bellefonte, PA, USA). Malonic acid was obtained from Columbus Chemical Industries (Columbus, WI, USA). Deuterium oxide (D, 99.9%) ($D_2O$) and chloroform-D (D, 99.8%) ($CDCl_3$) were purchased from Cambridge Isotope Laboratories (Andover, MA, USA). N,N-Dimethylformamide (DMF) was provided by Avantor Performance Materials (Center

Valley, PA, USA). Water used in the HPLC mobile phase was purified using Milli-Q System from Millipore Corp (Bedford, MA, USA).

### 3.2.2 Production of PLA film

PLA pellets were dried at 60 °C for 24 h under vacuum (85 kPa) and processed in a Randcastle cast film microextruder (Extrusion System, Inc., Cedar Grove, NJ, USA) with a screw of 1.5875 cm diameter, 24/1 L/D ratio extruder, and 34 cc volume. Extrusion temperatures were 193, 212, 215, 215 and 210 °C for zone 1, 2, and 3 transfer tube and die, respectively, with a rotation speed of 60 rpm. The film thickness was 27.9 ± 9.9 μm.

### 3.2.3 Storage experiments

Ten disks 2.0 cm in diameter separated by glass beads on a stainless steel wire were placed in cells containing pure water, 50% ethanol, or 95% ethanol by volume, previously conditioned at 40 °C. The total disk surface area to fluid volume was 1.79 $cm^2$/mL. Degradation and release experiments were conducted at 40 °C using a migration cell as recommended by ASTM D4754-11 [37]. Samples were retrieved at defined times during 6 months to assess $M_w$, $M_n$, water and ethanol sorption, thermal and physical properties, and LA release.

### 3.2.4 PLA molecular weight

At various times throughout the experiments, $M_w$ and $M_n$ were determined by weighing approximately 10 mg of film retrieved from the test cells and dissolved in THF (2 mg/mL). A gel permeation chromatograph (GPC) (Waters 1515, Waters, Milford, MA, USA) equipped with a refractive index detector (Waters 2414) and a series of three

columns of HR Styragel® (HR4, HR3 and HR2) were used (each 7.8 mm × 300 mm, Waters Styragel). An elution of THF at a flow rate of 1 mL/min was applied with a flow rate ramping time of 5 min and a total run time of 45 min. The temperature of the detector and column was 35 °C and the injection volume was 100 µL. A calibration curve was made from polystyrene standards-Shodex SM-105 (Waters, Milford, MA), which contained a molecular weight range of $1.37x10^3$ to $2.48x10^6$ Da. The Mark−Houwink constants for the correction were $K$ = 0.0164 mL/g and $\alpha$ = 0.704 for PLA solutions in THF at 35 °C. The measurements were conducted in triplicate.

### 3.2.5 Water and ethanol sorption

Water and ethanol sorbed by PLA film were measured at 40 °C using migration cells as described in the storage experiments section. In this study, the water ($H_2O$) in the solvents (water, 50% ethanol, 95% ethanol) was replaced with $D_2O$ to avoid contamination from environmental water and interference with measurements. Ethanol sorbed was determined using the $^1$H-NMR (proton nuclear magnetic resonance) technique and water sorbed using D-NMR (Deuterium NMR). Samples of film were taken periodically. For ethanol sorption, the samples were rinsed with $D_2O$ and for water sorption with $H_2O$ to remove the solvent from the surface. For ethanol sorption, samples were dissolved in $CDCl_3$ with DMF as the internal standard, and for water sorption, samples were dissolved in THF with $CDCl_3$ as the internal standard. For ethanol and $D_2O$ sorption measurements, samples were analyzed using a Varian Inova 600 MHz superconducting NMR-Spectrometer equipped with a Nalorac 5 mm PFG switchable probe operating at 599.892 MHz and 92.069 MHz for $^1$H and $^2$H, respectively.

Experiments were conducted in triplicate. Detailed descriptions of the $^{1}$H-NMR and D-NMR experiments are provided in the Appendix 3A.

Ethanol sorption appears to follow Fick's law of diffusion. The analytical solution with constant concentration assumed on both disk faces is [38]:

$$\frac{M_t}{M_\infty} = 1 - \frac{8}{\pi^2}\sum_{n=0}^{\infty}\frac{1}{(2n+1)^2}exp\left(\frac{-D(2n+1)^2\pi^2 t}{l^2}\right) \quad \text{(Eq. 3.1)}$$

where $M_t$ is the amount of ethanol sorbed at time $t$ (g-EtOH/g-PLA), $M_\infty$ is the amount of ethanol at equilibrium (g-EtOH/g-PLA), $t$ is time (s), $l$ is thickness of expanded disk (m) and $D$ is the diffusion coefficient (m$^2$/s). The nonlinear regression (nlin-fit) function in MATLAB® 2011b (MathWorks, Natick, MA) was used to fit **(Eq.** 3.1. This provides an estimate of $M_\infty$ and $D$.

### 3.2.6 Differential scanning calorimetry (DSC)

A differential scanning calorimeter (Q100, TA Instruments New Castle, DE, USA) was used to determine the glass transition temperature ($T_g$), melting temperature ($T_m$), crystallization temperature ($T_c$) and degree of crystallinity ($\%X_c$) of the PLA samples. The samples where cooled from 25 to 5 °C and then run at a temperature range of 5 to 210 °C, with a heating rate of 10 °C/min using liquid nitrogen with a flow rate of 70 mL/min. The first heat scans of the samples are reported. The data obtained were analyzed using the Thermal Analysis Universal 2000 version 4.5A software. Percentage crystallinity was calculated using the heat of fusion of the 100% crystalline for PLA sample of 93.7 J/g [39]. The measurements were conducted in triplicate.

### 3.2.7 X-ray diffraction study (XRD)

XRD analyses were performed using a Bruker AXS D8 Advance X-ray diffractometer (Bruker Co., Billerica, MA, USA) equipped with a Global Mirror filtered Cu Kα radiation source set at 40 kV and 100 mA. Samples were scanned in the 2θ range from 2 ° to 40 ° at a rate of 0.24 °/min and an increment of 0.01 °.

### 3.2.8 Dynamic mechanical analysis (DMA)

To determine the $T_g$ of PLA, the loss factor (tan delta) was measured as a function of temperature when PLA samples were immersed between 4 and 7 days in the various ethanol-water solutions during testing. A TA RSA-G2 Solids Analyzer Immersion System (TA Instruments, New Castle, DE, USA) equipped with a tension geometry at a frequency of 1 Hz was used. The samples where cooled down from 25 to 10, -10, -10, -30, and -60 °C for 0, 25, 50, 75 and 95 % ethanol volume and then heated to 60 °C at a heating constant rate of 5 °C/min using liquid nitrogen. The data obtained was analyzed using the TA Instruments TRIOS software.

### 3.2.9 Lactic acid release

Release of LA into the three different solvent systems (water, 50% ethanol and 95% ethanol) was determined using the migration cell at 40 °C as described in the storage experimental section. Four replicates were performed for each of the solvent systems. LA quantification was carried out since lactide and oligomers are degradation products of PLA that are able to migrate and easily decompose to LA. Modified methods published by Mutsuga et al. and Di Maio et al. were used [40, 41]. Samples containing 0.5 mL of simulant were taken periodically and exposed to alkali hydrolysis. For ethanol solutions, the ethanol was evaporated using a Savant SC110 SpeedVac Concentrator

System (Savant Instruments, Holbrook, NY, USA) and then reconstituted with 0.5 mL of water. Samples were then saponified with 50 µL of 0.2 M sodium hydroxide, followed by heating for 15 minutes in a water bath at 60 °C. After cooling at room temperature, 50 µL of 0.2 M hydrochloric acid was added. LA was analyzed with an LC/MS/MS system with a triple quadrupole/linear ion trap (AB/Sciex QTRAP 3200, Framingham, MA, USA). Separation was carried out on an Ascentis Express C18, 2.7 µm, 100 x 2.1 mm reverse phase column (Sigma-Aldrich, St. Louis, MO, USA.) with a flow rate of 0.2 mL/min. Solvents were A: 1% formic acid and B: methanol. Solvent programming was isocratic for 3 minutes with 1% B, then a linear gradient to 95% B up to 2 minutes, followed by the isocratic mode for 2 minutes. A linear gradient was then carried out in 0.01 minutes to 1% B and held for 3 minutes in the isocratic mode. The oven temperature was 40 °C. Mass spectrometric analyses were performed in the negative-ion mode following the Ambient Pressure Chemical Ionization (APCI) method; the curtain gas was set to 20, gas-1 20 and gas-2 20, with a temperature of 650 °C. The calibration curve was made from 0.25 to 15 µg/mL by treating the LA standard solutions in the same way as the samples and using malonic acid as the internal standard.

### 3.3 Results and discussion

To study the hydrolytic degradation and SIC of PLA by water-ethanol solutions, the change in molecular weight of PLA was analyzed during exposure to determine the rate of hydrolysis caused by the cleavage of the ester bonds. The sorption of water in PLA was studied since hydrolysis depends on the presence of water molecules in the polymer matrix. However, the ethanol molecules in the solvent solutions influenced the water sorption in PLA due to the swelling effect. Swelling studies were carried out and

the initial first order reaction equation for $M_n$ reduction was modified to account the effect of PLA swelling in the rate constant. Crystallinity studies of PLA were performed over the exposure time to assess the concurrent SIC by ethanol molecules along with the hydrolysis of amorphous regions in the polymer matrix by water molecules. Finally, LA release was assessed as the result of the concurrent SIC and hydrolysis of the polymer chains and a model was proposed to predict the LA release when PLA is exposed to water-ethanol solutions.

### 3.3.1 Molecular weight

**Figure 3.1** shows $M_n$ as a function of time for PLA disks immersed in water, 50% ethanol and 95% ethanol at 40 °C. Molecular weight decreased over time, indicating hydrolysis of PLA. However, the change in $M_n$ was different for PLA in the three solutions. A first order reaction relationship was fitted to the experimental data. **Table 3.1** gives the rate constants $k$ ($gmol^{-1}\ d^{-1}$) for each system. The 50% ethanol solution caused the highest rate of decrease of $M_n$ at 0.0223 $gmol^{-1}\ d^{-1}$ ($p<0.05$), followed by 95% ethanol and water at 0.0133 ($p<0.05$) and 0.0059 $gmol^{-1}\ d^{-1}$ ($p<0.05$), respectively. After 120 days, the films in 50% ethanol were no longer intact and dispersed as small fragments in the solvent. The reduction in $M_n$ during exposure is attributed to scission of the ester bond of the polymer chains by water molecules [22, 25]. Optical images of PLA samples immersed in the three different water-ethanol solutions during hydrolytic degradation are presented in **Figure 3B.1**, Appendix 3B.

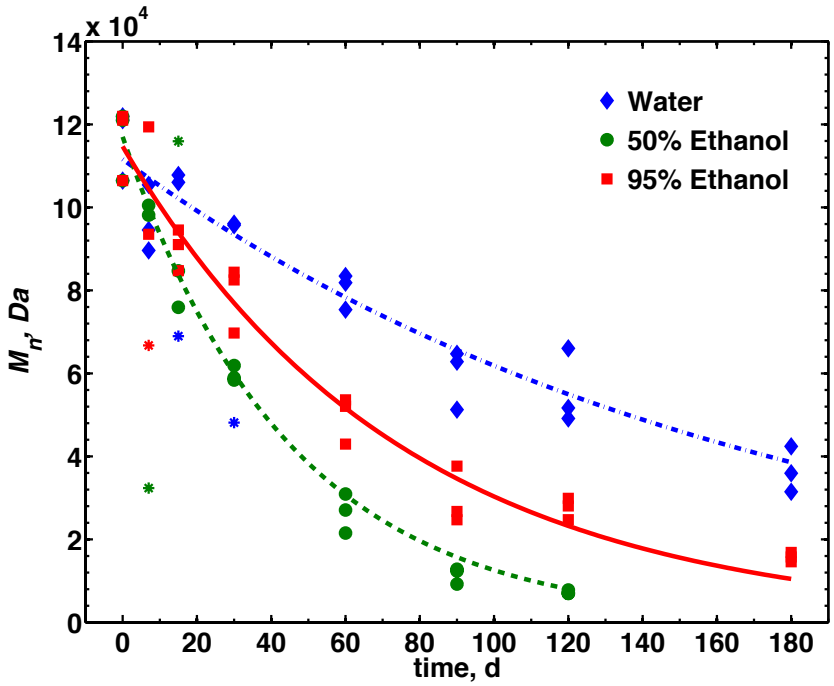


**Figure 3.1** $M_n$ as a function of time during hydrolytic degradation of PLA film immersed in water, 50% ethanol and 95% ethanol at 40 °C. Values indicated as * were considered outliers and therefore no used for fitting of the first order.

**Table 3.1** Rate constants for PLA films at 40 °C in water-ethanol solutions.

| | ***k* (gmol$^{-1}$ d$^{-1}$) for *$H_2O$ or $D_2O$/ethanol solutions*** | | |
|---|---|---|---|
| **Solvent solution** | ***$H_2O$ **** | ***$H_2O$ ***** | ***$D_2O$ ****** |
| Water | 0.0059 ± 0.0004 [a] | 0.0059 | 0.0020 ± 0.0002 [a] |
| 50% Ethanol | 0.0223 ± 0.0010 [b] | 0.0230 | 0.0124 ± 0.0007 [b] |
| 95% Ethanol | 0.0133 ± 0.0004 [c] | 0.0115 | 0.0111 ± 0.0012 [b] |

*Fitting of first order reaction: $M_n = M_{n_o} exp(-kt)$, where $M_n$ is the number average molecular weight at time $t$ and $M_{n_o}$ is the initial $M_n$.

**Fitting of first order reaction with $k$ from **(Eq.** 3.2

***Fitting of first order reaction kinetic. Synthetic data was used for calculations assuming a first order reaction since only the first and last points were measured.

Values with different lower case letters in the same column are statistically different (α=0.05 Tukey-Kramer Test)

Di Miao et al. and Sato et al. evaluated the effect of organic solvents like ethanol in contact with PLA, which swell the polymer matrix and increase chain mobility [26, 41]. The creation of free volume due to swelling allows more water molecules to diffuse in and get sorbed in the PLA matrix. This accelerates the hydrolysis rate. A more complete understanding of the diffusion and sorption of water and ethanol during hydrolytic degradation should help to describe the mechanism of solvent assisted hydrolysis.

### 3.3.2 Water and ethanol sorption

Diffusion of $H_2O$ in PLA has been reported [42-44]. *D* values of 3.53x10$^{-15}$ m$^2$/s at 80% relative humidity (RH) and 1.5x10$^{-11}$ m$^2$/s at 90% RH in vapor systems, and

$2.92x10^{-12}$ $m^2/s$ in immersion conditions were reported for PLA at 40 °C. In our experiment, to simultaneously measure the rate of diffusion and sorption of water in PLA in ethanol solutions created technical challenges since the $H_2O$ peaks overlap with PLA resonances in the $^1$H-NMR spectrum as shown in the Appendix 3A. Furthermore, excluding all extraneous sources of water from NMR measurements to ensure accurate measurements is extremely difficult. In contrast, $D_2O$ does not suffer the same issues and allows for the accurate measurement of sorption. Therefore, $D_2O$ water was used to simulate the diffusion of $H_2O$ in PLA. It is important to recognize that $D_2O$ will cause a different hydrolysis rate in PLA than $H_2O$ as is shown in **Table 3.1**, even though $D_2O$ and $H_2O$ may have the same initial diffusion coefficient as shown in **Figure 3C.1**, Appendix 3C, which shows the rate of diffusion of $H_2O$ vapor and $D_2O$ vapor in PLA. The *k* values will decrease when $H_2O$ is replaced with $D_2O$ since hydrogen isotopes $^1$H in $H_2O$ have been replaced by deuterium isotopes $^2$H, reducing the number of hydroxide (deuteroxide) ions that start the cleavage of the ester bonds.

**Figure 3.2** shows the rate of $D_2O$ sorption by PLA. The concentration of $D_2O$ molecules in PLA was lowest when the films were immersed in $D_2O$ and highest when immersed in 50% ethanol. The higher the concentration of $D_2O$ in the PLA, the faster the hydrolysis by $D_2O$, since there are more molecules of $D_2O$ available to start the cleavage of ester bonds. However, faster cleavage should be expected if $H_2O$ were used due to the reactivity of hydroxyl groups, even though the sorption of $H_2O$ vapor and $D_2O$ vapor into PLA are similar (**Figure 3D.1**, Appendix 3D).

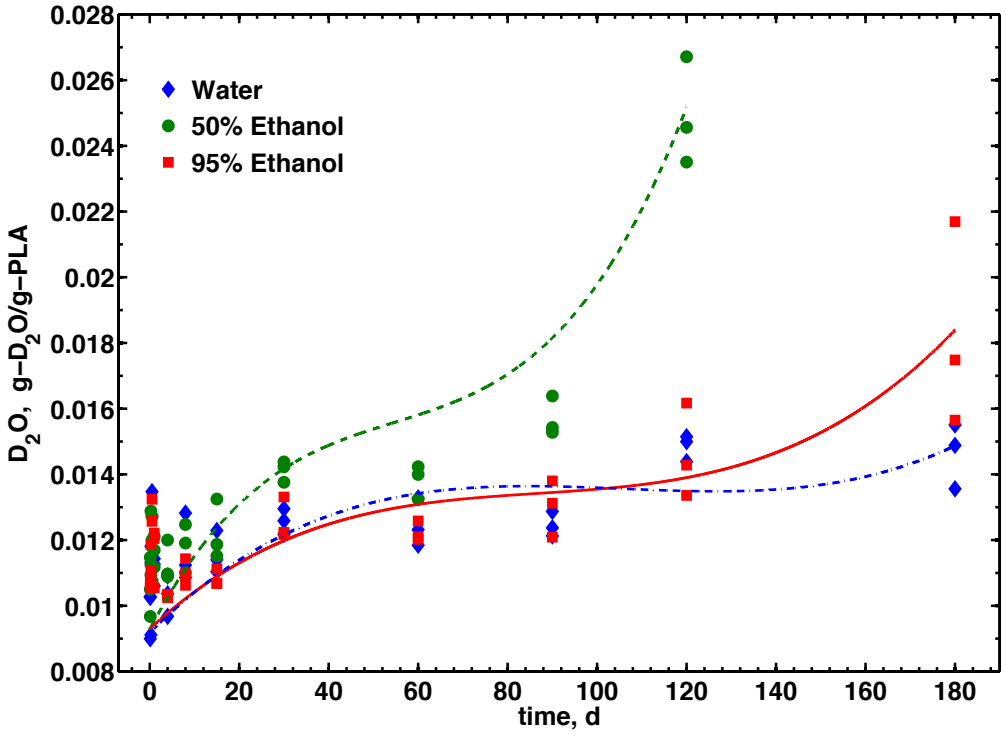


**Figure 3.2** $D_2O$ sorption into PLA films in contact with $D_2O$, 50% ethanol and 95% ethanol at 40 °C. y-axis represents grams of $D_2O$ sorbed divided by grams of PLA remaining in the disk after hydrolysis with $H_2O$. Trend lines are used as visual aid.

**Figure 3E.1**, Appendix 3E shows immediate ethanol sorption in PLA during hydrolysis. Diffusion coefficients were estimated using **(Eq.** 3.1, taking into account the swelled thickness of the PLA films at equilibrium (*i.e.*, the initial thickness was 27.94 μm and the final estimated thicknesses based on expansion for 50% and 95% ethanol were 28.78 and 29.53 μm, respectively). **Table 3.2** shows the estimated parameters. *D* for ethanol in disks immersed in 95% ethanol ($5.88 \times 10^{-14}$ $m^2/s$) was almost twice the *D* for ethanol in disks immersed in 50% ethanol ($2.55 \times 10^{-14}$ $m^2/s$). Also, the amount of ethanol at equilibrium ($M_\infty$) was 160% higher in 95% ethanol than in 50% ethanol.

**Table 3.2** Diffusion coefficients (*D*) and amount of ethanol at equilibrium ($M_\infty$) in PLA films at 40 °C

| Solvent | $D$ x $10^{14}$ ($m^2$/s) | $M_\infty$ (g-EtOH/g-PLA)* |
|---|---|---|
| 50% Ethanol | 0.64 ± 0.1 [a] | 0.03 ± 0.00 [a] |
| 95% Ethanol | 1.47 ± 0.33 [b] | 0.08 ± 0.00 [b] |

Values with different letter within the same column are statistically different (α=0.05 Tukey-Kramer Test)

*Note: grams of ethanol sorbed divided by grams of the PLA disk used for the $^1$H-NMR experiments

Experiments were performed using the $^1$H-NMR technique to study the relationship between ethanol concentration and polymer expansion when PLA films were exposed to different concentrations of ethanol over 24 h. **Figure 3F.1**, Appendix 3F shows the relationship between % expansion of PLA and ethanol fraction (volume of ethanol divided by total volume).

The initial first order reaction, $M_n = M_{n_o} exp(-kt)$, can be modified to account for the effect of PLA swelling. A model based on the assumption that the expansion of the polymer is due to an increase in void space, not expansion of the chains, predicts that the rate constant is:

$$k = \beta \left[ \frac{V_o}{V_d} + \left( 0.06 - \frac{V_o}{V_d} \right) p - 0.06 p^2 \right] \quad \text{(Eq. 3.2)}$$

where $V_o$ is the initial void space in the PLA matrix, $V_d$ is the volume of the disk, $\beta$ is a constant, and $p$ is the ethanol fraction ($p$ = 0, 0.5, 0.95). This model incorporates the

effect of expansion due to ethanol in the rate constant. When $p = 0$ (pure water), $k = \beta V_o/V_d$; and when $p = 1$ (no water), $k = 0$. The details of how the model was derived are presented in the Appendix 3G. Fitting $M_n = M_{n_o} exp(-kt)$ to the experimental data in **Figure 3.1** with *k* defined in **(Eq.** 3.2 gives $\beta = 1.05$ and $V_o/V_d = 0.0056$. Using $V_d = 0.0088\ cm^3$, the initial void space $(V_o)$ in one disk is predicted to be $4.93 \times 10^{-5}$ $cm^3$. Table 1 shows the rate constants using **(Eq.** 3.2.

Setting the derivative of $k$ with respect to $p$ in **(Eq.** 3.2 equal to zero gives the maximum rate of decay in $M_n$. This occurs when the volume fraction of ethanol reaches $p \approx 0.45$ (**Figure 3.3**). At that concentration of ethanol, a competitive balance between swelling and hydrolysis is observed, where the molecules of ethanol swell the polymer and allow the maximum concentration of water into the polymer to start the cleavage of the ester bonds.

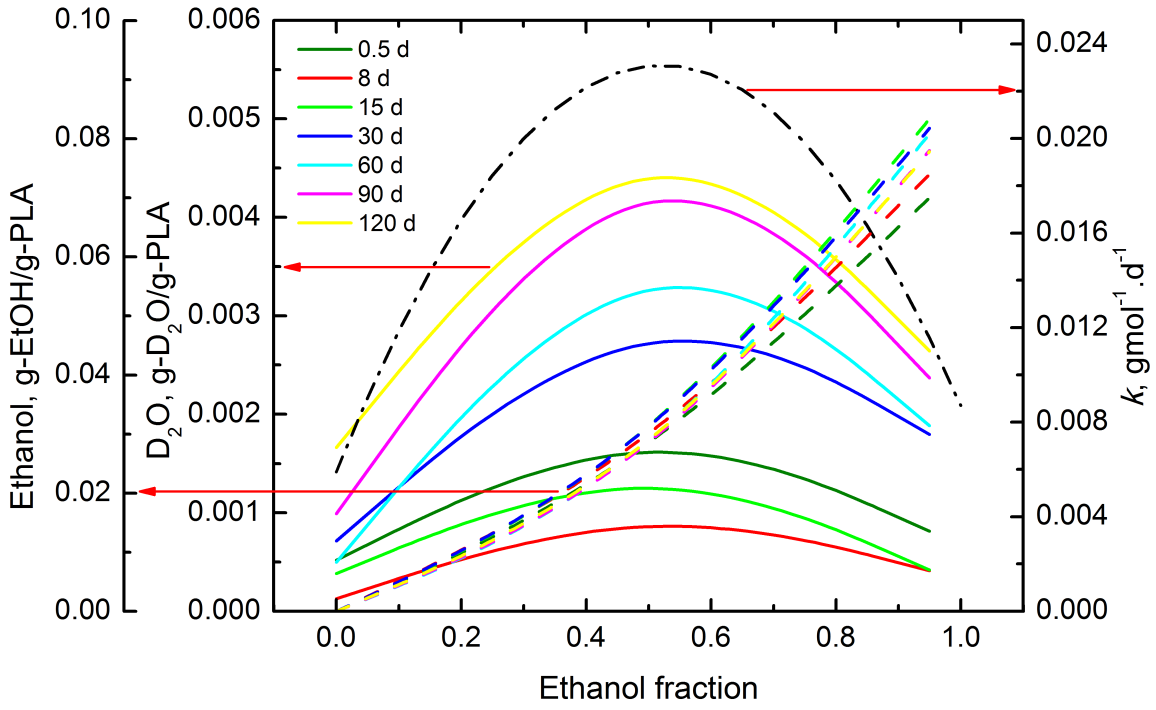


**Figure 3.3** Rate constant for hydrolytic degradation of PLA films fitting first order reaction equation with $k$ from **(Eq.** 3.2 (−•−). $D_2O$ sorption (−) and ethanol sorption (−−) into PLA at different exposure times versus volume fraction of ethanol in solvent solution at 40 °C. $D_2O$ and ethanol sorption lines were obtained from experimental data of PLA immersed in water, 50% ethanol and 95% ethanol at different exposure times.

Hydrolytic degradation of PLA occurs in the amorphous regions since they have a larger void volume than the crystalline regions and water can penetrate amorphous regions more readily [39, 45]. Since hydrolysis reduces the amorphous regions, the degree of crystallinity increases, even though the crystalline regions remain unchanged [25]. On the other hand, exposure of PLA to ethanol causes softening in the polymer, resulting in the movement and realignment of polymer chains, which induces crystallinity [26, 46]. Therefore, it is a combination of structural changes in PLA including

swelling and induced crystallinity when exposed to different combined solvents that affects hydrolysis.

**Figure 3.4** shows the change in $T_g$ of PLA when immersed in different volume fractions of ethanol at 40 °C. The relationship is linear (**Figure 3.4 insert**). The $T_g$ of the PLA films before being exposed to hydrolytic degradation was 59.8 ± 0.5 °C according to the DSC results. PLA films immersed in 100% water had a $T_g$ of 53 °C, but when PLA was immersed in 50% and 95% ethanol, $T_g$ was approximately 36 and 20 °C, respectively. This means that the higher the concentration of ethanol in the solution, the lower the $T_g$ during solvent transport into PLA, where swelling occurs immediately according to **Figure 3E.1**, Appendix 3E. The plasticization effect of ethanol on PLA allows the movement of the polymer chains, inducing alignment so crystallinity can occur.

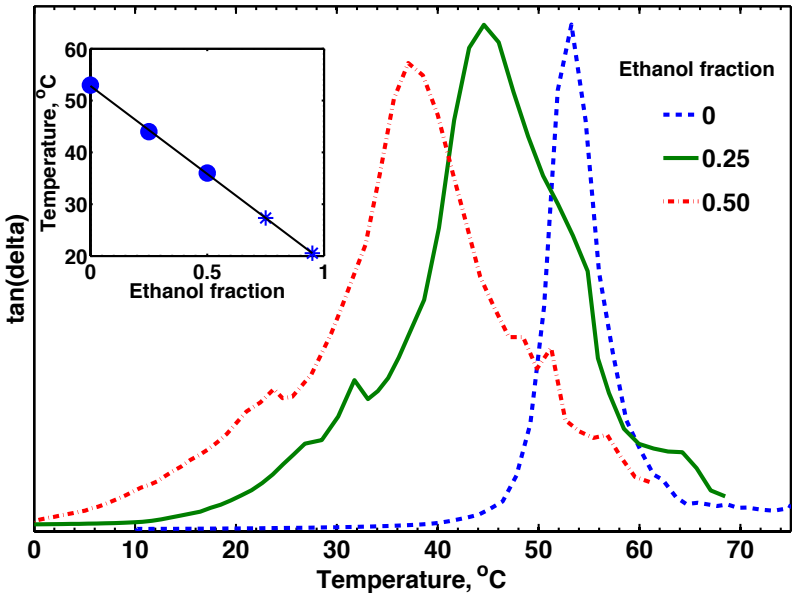


**Figure 3.4** $T_g$ of PLA when immersed in different volume fractions of ethanol at 40 °C from the immersion DMA results. Insert: $T_g$ as a function of $p$ where $T_g$ values (*) were estimated when $p > 0.5$ ($T_g = -0.34p + 52.83$; $R^2$=0.999).

### 3.3.3 Crystallinity

For assessing the crystallinity of PLA during hydrolytic degradation, DSC and XRD techniques were used. DSC was applied to calculate the percent crystallinity and identify changes in $T_m$, $T_c$ and $T_g$ using DSC thermograms. The identification of the type of crystals formed during PLA hydrolysis was performed by the XRD technique.

**Figure 3.5** shows the percent crystallinity ($\%X_c$) obtained by the DSC technique during hydrolytic degradation of PLA as a function of time. The crystallinity of samples exposed to water increased from 2.8 to 7.3% after 6 months of immersion. For PLA films exposed to ethanol solutions, the crystallinity increased dramatically. After the first

15 days of immersion, the crystallinity of PLA in 50% and 95% ethanol was the same, around 26%. After one month, the 50% ethanol samples started showing higher crystallinity. The increase on crystallinity during hydrolytic degradation has also been observed in other systems when PLA has been exposed to different environments and *pH* [21, 47, 48].

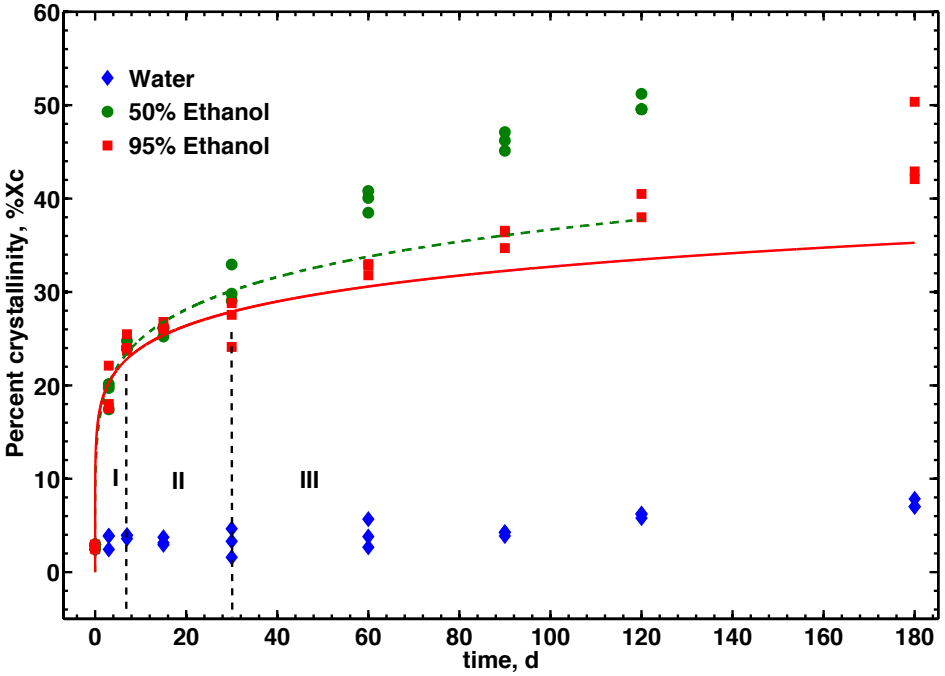


**Figure 3.5** Percent crystallinity during hydrolytic degradation of PLA films immersed in water, 50% and 95% ethanol at 40 °C. Trend lines from fitting Avrami equation **(Eq.** 3.3. Numbers I, II and III indicate the regions corresponding to the different processes of PLA crystallization.

The increase in crystallinity can be explained by the depression of $T_g$ due to the process of SIC. If $T_g$ falls below the test temperature (40 °C), the polymer chains have sufficient mobility and tend to rearrange into a crystalline structure, which is a more

stable configuration.[36] According to Ouyang et al. the transport of acetone in poly(ethylene terephthalate) (PET) induces crystallization in three stages [34, 36]. The first stage is the transport of the solvent by diffusion, which is controlled by the concentration gradient. The second stage involves swelling by the solvent and the third stage is secondary crystallization. In the case of PLA, the second stage present in PET is observed in **Figure 3.5** as the region marked with number I due to the dramatic increase in swelling by ethanol, as measured by the change in film thickness. In this region, primary crystallization takes place, where large amounts of crystallites are formed as a result of relaxation of constraints by the release of internal stress, where chains begin to fold and become crystals [34-36]. When the system is in saturation (region II), the crystallization rate is slow and polymer chains can form small crystals dispersed in the amorphous region, corresponding to a secondary crystallization [34, 36]. After 30 days in 95% ethanol, the crystallinity started to increase (region III). This can be explained by the preferential hydrolysis of the amorphous regions left after secondary crystallization, which increases the net crystalline region as degradation proceeds. For PLA in contact with 50% ethanol, crystallization due to hydrolysis started after 15 days of exposure, resulting in a higher $\%X_c$ than films immersed in 95% ethanol. The higher $\%X_c$ can be explained by the higher solubility of water molecules in the amorphous regions, hydrolyzing them faster and therefore increasing the net crystalline regions.

In order to quantify the crystallization kinetics, the Avrami theory [49, 50] was applied according to:

$$X_c = 1 - exp(-Kt^n) \quad \text{(Eq. 3.3)}$$

where $X_c$ is the relative crystallinity of the polymer, $t$ is time, $K$ the crystallization rate constant, and $n$ is the Avrami exponent. As observed in **Figure 3.5**, the Avrami model fits regions I and II well. The deviation from the Avrami equation in region III is due to the hydrolysis of the amorphous region and not to the formation of new crystals. The Avrami kinetic parameters of crystallinity for 50% ethanol were $K$ = 0.018 $s^{-1}$ and $n$ = 0.20, and for 95% ethanol were $K$ = 0.031 $s^{-1}$ and $n$ = 0.16. Generally, the $n$ values reported in the literature are around 2 and 4 [49, 51, 52]. The low values obtained in this study are in accordance with recently reported values by Tsai et al. where PLA was exposed to methanol and ethanol, giving values of 1 and 0.5, respectively [53]. This is an indication of the uni-dimensional growth of crystals restricted by diffusion of the solvent.

The XRD profiles of PLA films during hydrolytic degradation are shown in **Figure 3.6**. When PLA was immersed in pure water, the profiles showed only broad peaks during hydrolysis. These results indicate that PLA immersed in pure water remained amorphous during hydrolysis. No formation of crystals took place, which is in agreement with the 3% increase in crystallinity during degradation. In contrast, some sharp peaks began to appear after 3 days exposure to 50% and 95% ethanol (**Figure 3.6D** and **3.6E**). The diffraction peaks observed in 6 for ethanol solutions correspond to the formation of α-form crystals (orthorhombic unit cell with parameters a=1.06 nm, b=0.61 nm, and c=2.88 nm) [54]. In 50% ethanol, diffraction peaks at 14.8°, 16.8°, 19.1° and 22.4° were observed. In 95% ethanol, the diffraction peaks were in the same range as in 50% ethanol. They were 14.8°, 16.7°, 19.1° and 22.2°, corresponding to the 010, 110/200, 100/203 and 102/210 plane reflections, respectively [26, 55-58]. The

appearance of crystals in PLA after 3 days exposure to ethanol solutions indicates that SIC took place in the early stages corresponding to primary crystallization (region I). At all times, the diffraction peaks were the same, meaning the same kind of crystals were formed during secondary crystallization (region II) and were present during the entire degradation of the amorphous regions (region III). Zhang, et al. [59] studied the morphology behavior of amorphous PLA during hydrolysis in neutral conditions, and semicrystalline PLA in acid and alkaline environments where α-form crystals were mainly formed and remained during the degradation process.

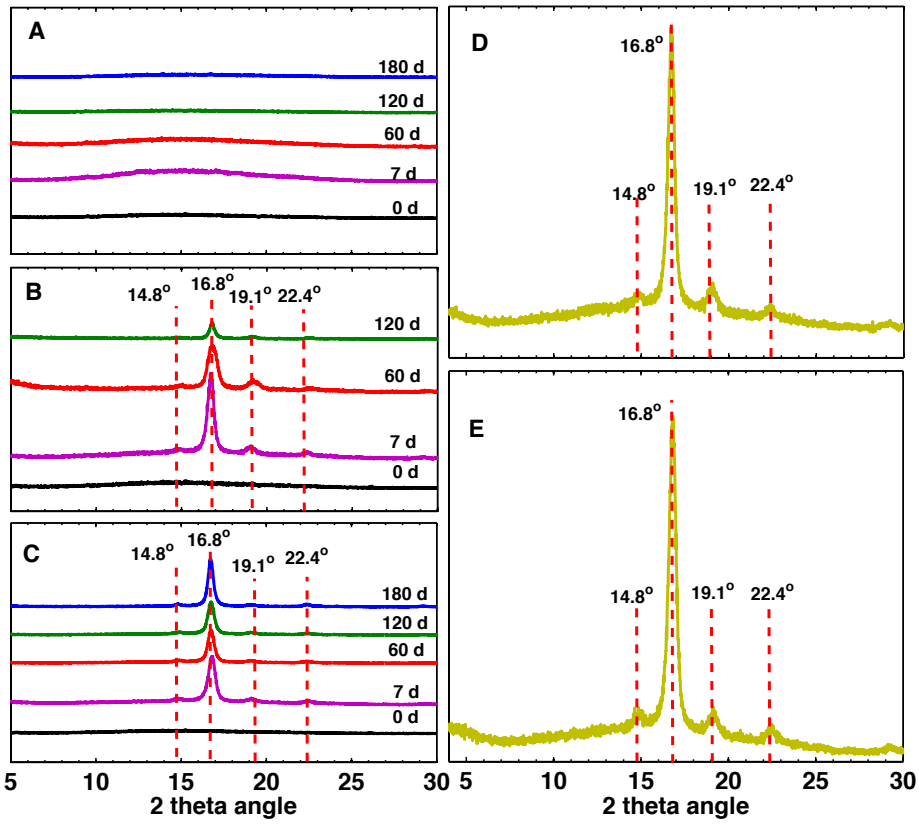


**Figure 3.6** XRD profiles of PLA films during hydrolytic degradation in (A) water, (B) 50% ethanol, (C) 95% ethanol and in the 3rd day of immersion in (D) 50% ethanol and (E) 95% ethanol at 40 °C. The numbers on each profile indicate days immersed.

Crystallinity results can be correlated with DSC thermograms of PLA before and after being hydrolyzed by water-ethanol solutions for various times (**Figure 3.7**). Before exposure, amorphous PLA showed a cold-crystallization temperature peak ($T_{cc}$) due to the rearrangement of polymer chains inducing crystallization during the DSC heating process. When PLA was exposed to pure water (**Figure 3.7A**), $T_{cc}$ shifted to a lower temperature. This can be attributed to chain scission and reduction in molecular weight

of the PLA matrix, which facilitates nucleation and growth of PLA crystals, improving chain segment mobility [43, 56]. Another explanation could be the production of locally ordered structures during hydrolysis, promoting the occurrence of cold crystallization at lower temperatures [56]. The double melting peaks could be attributed to the formation of two different crystalline structures formed during the DSC heating process [60, 61]. Some crystals that could be formed during crystallization from melt are the α and β-forms that have approximately the same energy and therefore the possibility to coexist [57, 62]. The high $T_m$ corresponds to melting of the more stable structure, which is the α-crystal, while the low $T_m$ is ascribed to the less perfect crystal that is the β-form [62]. For PLA exposed to ethanol solutions (**Figure 3.7B and C**), after the 3$^{rd}$ day, the samples did not show crystallization peaks, meaning that PLA had been crystallized in agreement with the XRD profiles, presenting α-form crystals (**Figure 3.6**). The α-form crystals are reflected in thermograms displaying only one melting peak over time. However, after 60 days of immersion, a small endothermal peak started to appear and became stronger over time. This phenomenon could be explained by hydrolysis process, which is reflected in the change of the molecular weight distribution (*MWD*) of PLA (**Figure 3H.1**, Appendix 3H). After 60 days, the *MWD* of PLA became broader due to polymer chain scission, resulting in shorter polymer chains and the presence of LA oligomers with different $T_m$'s compared to α-form crystals originated by the SIC process (regions I and II, **Figure 3.5**).

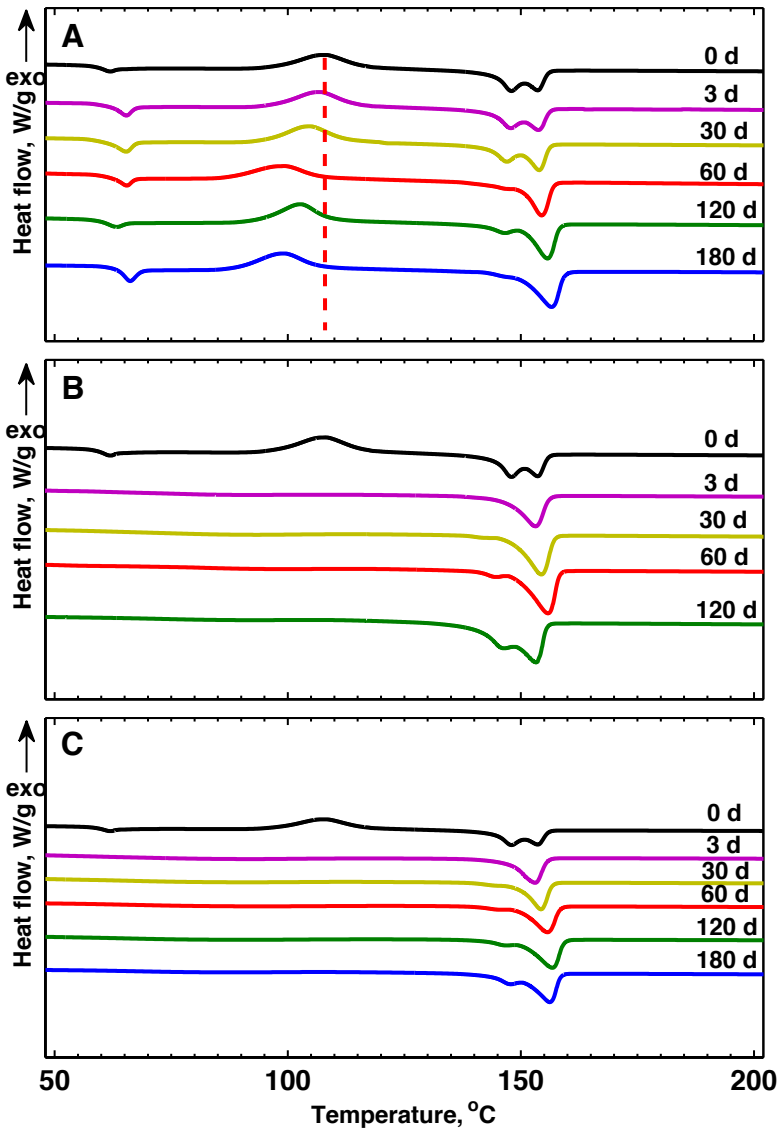


**Figure 3.7** DSC thermograms of PLA film during hydrolytic degradation in (A) water, (B) 50% ethanol and (C) 95% ethanol at 40 °C. The numbers on each thermogram indicate days immersed.

### 3.3.4 Lactic acid release

During hydrolysis of the amorphous regions of PLA, low molecular weight water-soluble oligomers and monomers are released. **Figure 3.8** shows the release of LA from PLA into water, 50% and 95% ethanol at 40 °C. During the first 40 days of exposure, the release of PLA monomers was higher when the polymer was in contact with 50% ethanol, followed by 95% ethanol and then by water (**Figure 3.8 insert**). After the second month of exposure, the release of LA increased exponentially for samples in contact with 50% ethanol. At 120 days, the concentration of LA in 50% ethanol was 700 µg/mL, meaning that approximately 30% of the PLA was hydrolyzed. Not long after that, the film disintegrated. Over the same period, the percentage of PLA hydrolyzed by water and 95% ethanol was 1.4 and 0.5%, respectively.

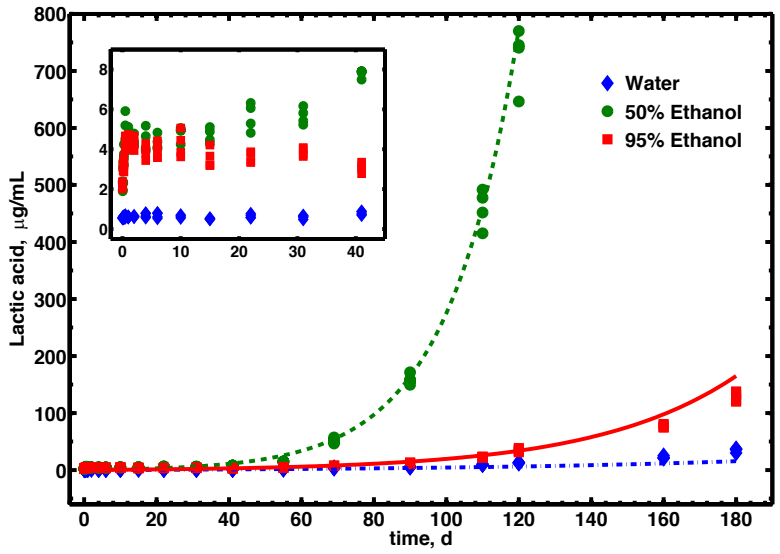


**Figure 3.8** Release of LA during hydrolytic degradation of PLA films in contact with water, 50% and 95% ethanol at 40 °C. Fitted lines indicate the prediction of **(Eq.** 3.4 to each solution.

The highest release of LA in 50% ethanol concurs with the fastest reduction in $M_n$ (**Figure 3.1**), since polymer chains in the amorphous regions are being hydrolyzed faster, as reflected by the increase in $\%X_c$ in region III (**Figure 3.5**).

A model that predicts LA release is proposed based on the process of chain scission into progressively lower molecular weights, followed by diffusion of LA-mers through the PLA matrix, followed by crossing the interface into the fluid, and finally dissolving into LA in the various water-ethanol solutions. The resulting concentration of LA in the solution is described by:

$$C_f = \frac{Q \cdot A}{V_f}[exp(Rkt) - 1] \quad \text{(Eq. 3.4)}$$

where $C_f$ is the concentration of LA in the solution, $Q$ and $R$ are constants, $A$ is the disk surface area, $V_f$ is fluid volume, $t$ is time, and $k$ is the rate constant in **(Eq.** 3.2. The development of the model is presented in the Appendix 3I. Fitting **(Eq.** 3.4 to the experimental data gave $Q = 0.9$ μg/cm$^2$ and $R = 2.232$. The predicted LA release from PLA hydrolysis immersed in water, 50% and 95% ethanol are the curves in **Figure 3.8**.

During LA release it is important to consider that the migration rate of molecules within the polymer matrix depends on several factors, including the size of the migrants, density, and the $T_g$ of the polymer [63, 64]. Therefore, changes in $T_g$ will affect the release of LA previously discussed since $T_g$ will determine the flexibility of polymer chains and the free volume within the matrix. When PLA was exposed to water ($T_g$= 53 °C) (**Figure 3.4**), the diffusion of LA and LA-mers took place in the glassy state because the experiments were conducted at 40°C. Below $T_g$, in the glassy state, the polymer is stiff and therefore less open to diffusion by LA molecules. For PLA immersed in ethanol solutions, diffusion of LA took place above $T_g$, in the rubbery state, where the

polymer molecules are flexible and open to diffusion [63, 65]. The higher the ethanol content, the lower the $T_g$ and the higher the diffusion rates of LA and LA-mers.

The main migrants from PLA are LA and LA-mers, which are degradation products from the hydrolysis of polymer chains. This study only carried out the quantification of alkali decomposition products based on the conversion of lactide and LA-mers to LA. A theoretical prediction for the rate of diffusion of oligomers up to 5 units was made based on the free volume theory as a function of the $T_g$ of the polymer during hydrolysis experiments (**Figure 3J.1**, Appendix 3J). Based on the predictions, the release of LA (90 g/mol) is faster when PLA is exposed to 95% ethanol. These results are not in full agreement with the experimental data since the estimated diffusion coefficient does not take in account hydrolysis of the polymer. It only considers the effect of $T_g$.

Predicted values showed that the smaller the molecular weight of the oligomer, the faster the diffusion through PLA. Therefore, the LA quantified during release experiments can be identified as mostly LA released from the PLA matrix and not from the alkali hydrolysis of LA-mers released from PLA in the solution. This finding could be supported by work conducted by Mutsuga et al. [40] who studied the long-term migration of LA-mers in water at 40 °C. Their results showed that until three months exposure to water, no LA-mers were detected. However, by six months, 3.46 μg/cm$^2$ of LA-mers up to 13 units were quantified. In our experiment, the initial presence of LA-mers in the PLA films were not detected by MALDI-TOF (data not shown). Therefore, at the early stages the LA quantified during the experiments can be attributed to the

hydrolytic degradation of PLA in contact with the water-ethanol solutions and release as mostly LA into solution.

### 3.4 Conclusions

The exposure of PLA disks to different water-ethanol solutions led to the hydrolytic degradation of the polymer with concurrent SIC. Hydrolysis was accelerated by the immersion of PLA in 50% ethanol, which showed a faster reduction in $M_n$ than in 95% ethanol and pure water. Hydrolysis is related to the amount of water molecules available to start chain scission, so NMR techniques were applied to study water sorption in PLA. Higher sorption of $D_2O$ was found when PLA was exposed to 50% ethanol, explaining the faster hydrolysis. A new model was proposed to explain the rate of hydrolysis, accounting for the effect of PLA swelling due to ethanol sorption. The rate of degradation for 50% ethanol was 0.0230 $gmol^{-1}$ $d^{-1}$. This was the maximum rate of decay in $M_n$, meaning that 50% concentration provides the optimal competitive balance between swelling and hydrolysis. During PLA hydrolysis the $\%X_c$ increased, indicating that SIC occurred in PLA when exposed to 50% and 95% ethanol. In the crystallization process of PLA, three different regions were identified. Regions I and II were due to SIC by ethanol. The Avrami equation was found to describe the crystallization process well. Region III was due to hydrolysis of the amorphous regions. XRD studies showed the formation of α-crystal during SIC. LA release was studied as an indication of hydrolysis of PLA. PLA immersed in 50% ethanol showed the highest release of LA, which is in accordance with the fastest decay in $M_n$ by hydrolysis. A model was proposed to predict LA release during hydrolysis when PLA is exposed to different ethanol-water solutions.

## 3.5 Acknowledgments

The authors thank Olivier Vitrac for assistance with estimating theoretical LA diffusion coefficients. I-F, F., thanks the Mexican National Council for Science and Technology (CONACYT), the Mexican Secretariat of Public Education (SEP) and the Government of Mexico for providing financial support through a Ph.D. fellowship. RA thanks partial support of the USDA National Institute of Food and Agriculture and Michigan AgBioResearch, Hatch project R. Auras.

# APPENDICES

## APPENDIX 3A: NMR Analysis

The $^{1}$H-NMR spectrum of PLA film with ethanol is shown in **Figure 3A.1**. The protons of ethanol $CH_3$ and $CH_2$ groups are located at 1.22 and 3.70 ppm, respectively. The $CH_2$ protons have some overlap with residual THF (3.72 ppm). These chemical shift values, however, demonstrate that ethanol does not overlap with the peaks of PLA protons. Based on these results, ethanol quantification in further experiments was carried out using the protons of the $CH_3$ group.

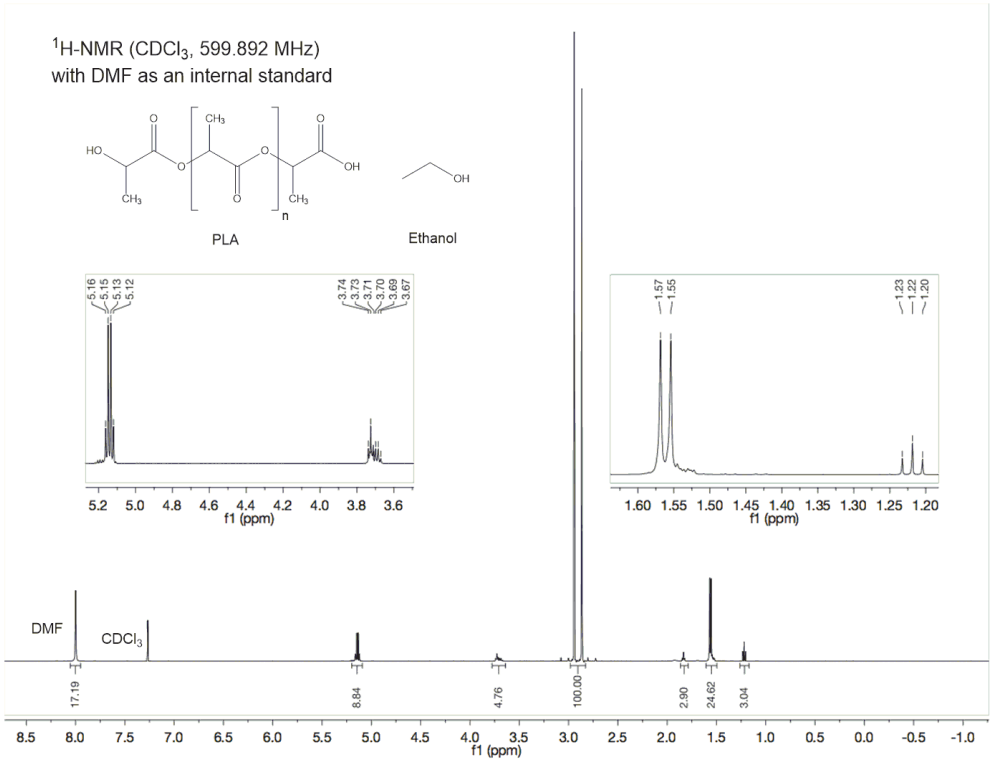


**Figure 3A.1** $^{1}$H-NMR spectrum of PLA with ethanol.

**Table 3A.1** $^{1}$H-NMR peaks and identification of ethanol in PLA.

| Compound | Group | Chemical Shift (ppm) | Multiplicity, coupling constant, #protons |
|---|---|---|---|
| PLA | -O-C***H***-$CH_3$-COO- | 5.14 | q, *J=7.1 Hz*, 1 |
| PLA | -O-CH-C***H$_3$***-COO- | 1.56 | d, *J=7.2 Hz*, 3 |
| Ethanol | C***H$_3$***-$CH_2$-OH | 1.22 | t, *J=7.0 Hz*, 3 |
| Ethanol | $CH_3$-C***H$_2$***-OH | 3.70 | q, *J=6.9 Hz*, 2 |

Water identification using the NMR technique led to some modifications in the media for quantification purposes. $^{1}$H-NMR spectra cannot provide direct evidence of the real amount of water sorbed in the experiments due to the inevitable contamination by environmental water, which would interfere with the actual concentration of water sorbed by the PLA film. If the sample is contaminated with water from the surroundings, it will show up around 1.56 ppm when PLA is dissolved in $CDCl_3$, where the chemical shift changes depending on the solvent used to dissolve the polymer under study [66]. Another issue is that the peaks of the water overlap with those of the $CH_3$ group of PLA at 1.56 ppm using $CDCl_3$ as the solvent according to **Table 3A.1**. Therefore, to quantify the amount in the sorption experiments, deuterated water ($D_2O$) was used (hydrogen isotopes $^{1}$H of $H_2O$ have been replaced by the deuterium isotope $^{2}$H) [67].

**Figure 3A.2** shows the D-NMR spectrum of PLA dissolved in THF when 50% ethanol was added. An additional peak in the spectrum at 3.44 ppm was observed. The $D_2O$ peak was tentatively assigned to 4.09 ppm. The reason for the presence of two peaks can be explained by the equilibrium between water and $D_2O$ with a proton

transfer from the ethanol to $D_2O$ and an exchange of deuterium between the hydroxyl group of the ethanol and water according to the following reaction [68]:

$$EtOH + D_2O \rightleftarrows EtOD + HOD$$

Typically, one would expect a single peak for the mixture due to rapid exchange between $D_2O$ and ethanol. This is not the case for these measurements because of the low concentration of the $D_2O$/EtOH mixture in the NMR tube, with the lowest concentration detected in sorption experiments of 0.08 μL/mL and 0.24 μL/mL ($8.88 \times 10^{-5}$ and $1.89 \times 10^{-4}$ g/mL) for $D_2O$ and EtOH, respectively. It is worth mentioning that with sorption experiments using 100% $D_2O$, two peaks were seen in the spectrum. In this situation, it could be assumed that there was a proton transfer from the end groups of PLA in the presence of $D_2O$. EXSY NMR (Exchange Spectroscopy) was carried out to verify that both peaks belong to the $D_2O$ in the system. Indeed, cross-peaks were observed between the resonances. Hence, for quantitative purposes, the two peaks were taken into consideration for water sorption in PLA since they represent the water content in the solvent systems under study.

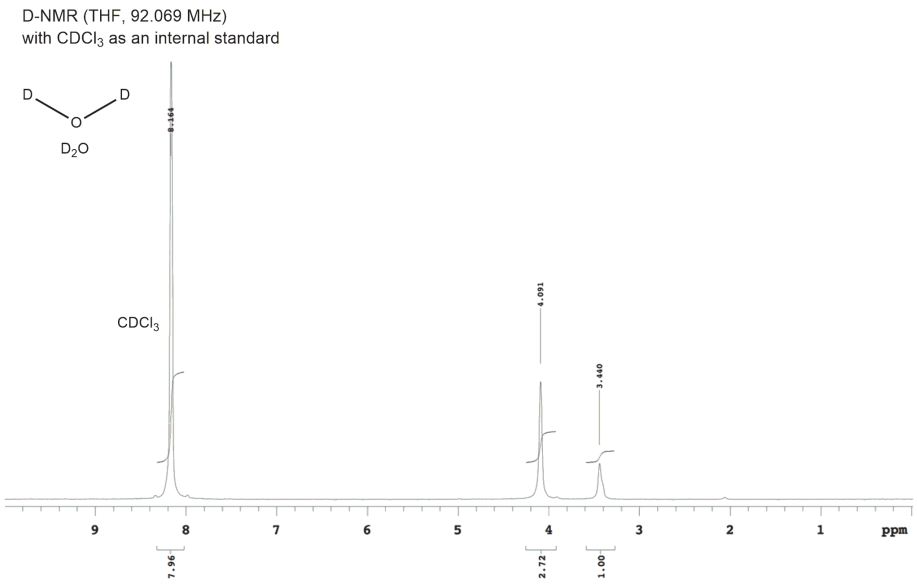


**Figure 3A.2** D-NMR spectrum of PLA with $D_2O$

**APPENDIX 3B: Optical images of PLA samples during hydrolytic degradation**

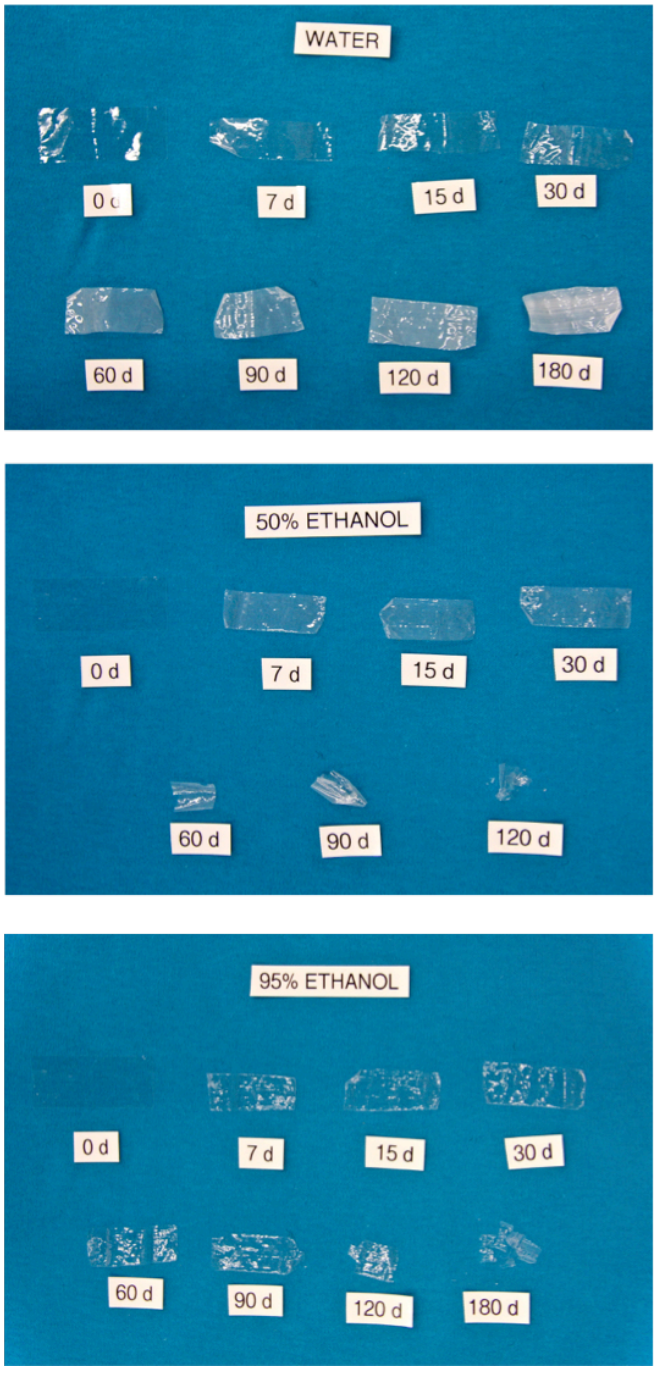


**Figure 3B.1** Optical images of PLA samples during hydrolytic degradation by water, 50% and 95% ethanol at 40 °C.

## APPENDIX 3C: Diffusion of $H_2O$ and $D_2O$ vapor in PLA film

*Methodology:* Diffusion of $H_2O$ and $D_2O$ vapor in PLA films were determined by gravimetric analysis using an SGA-100 from VTI Corp. (Hialeah, FL, USA). PLA films (15-20 mg) were exposed to 75% relative humidity ($p/p_o$) at 40 °C.

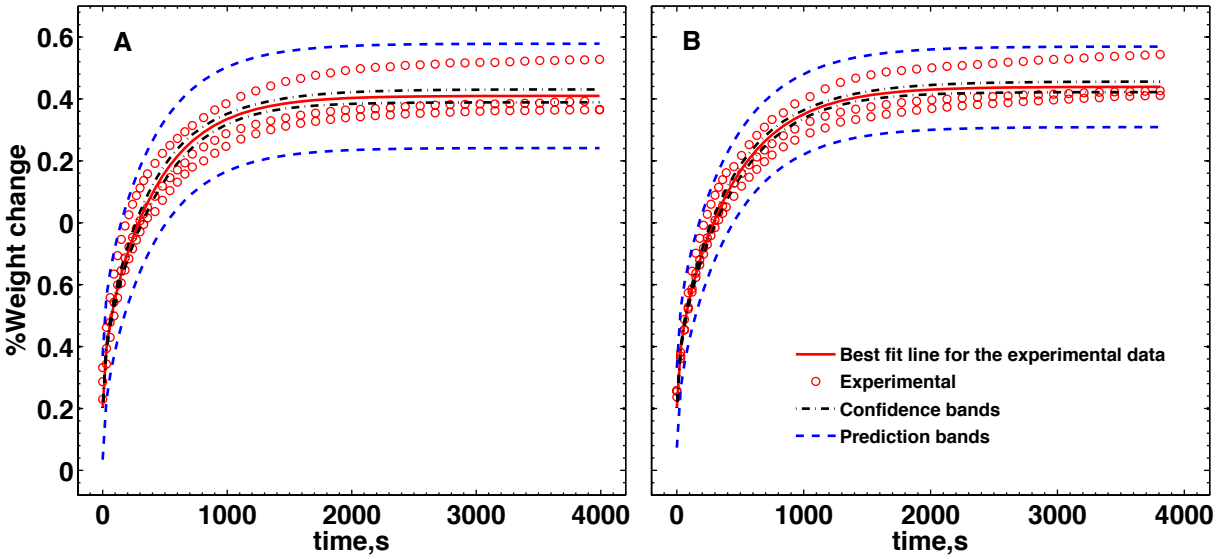


**Figure 3C.1** Diffusion of (A) $H_2O$ and (B) $D_2O$ vapor in PLA film at 75% relative humidity, 40 °C.

**Table 3C.1** Diffusion coefficient (*D*) of $H_2O$ and $D_2O$ vapor in PLA film at 75% relative humidity, 40 °C.

| **Vapor** | ***D* x $10^{13}$ ($m^2/s$)** |
|---|---|
| $H_2O$ | 5.09 ± 0.07 [a] |
| $D_2O$ | 4.75 ± 0.30 [a] |

Values with same letter are not statistically different (α=0.05 Tukey-Kramer Test)

Note: *D* values were calculated using $D = l^2/7.2\ t_{1/2}$ where $l$ is thickness and $t_{1/2}$ is the half time

**APPENDIX 3D: Sorption isotherms for $H_2O$ and $D_2O$ vapor in PLA film**

*Methodology:* $H_2O$ and $D_2O$ sorption isotherms for the PLA films were determined by gravimetric analysis using an SGA-100 from VTI Corp. (Hialeah, FL, USA). PLA films (15-20 mg) were exposed to relative humidities between 5 and 95% at 40 °C.

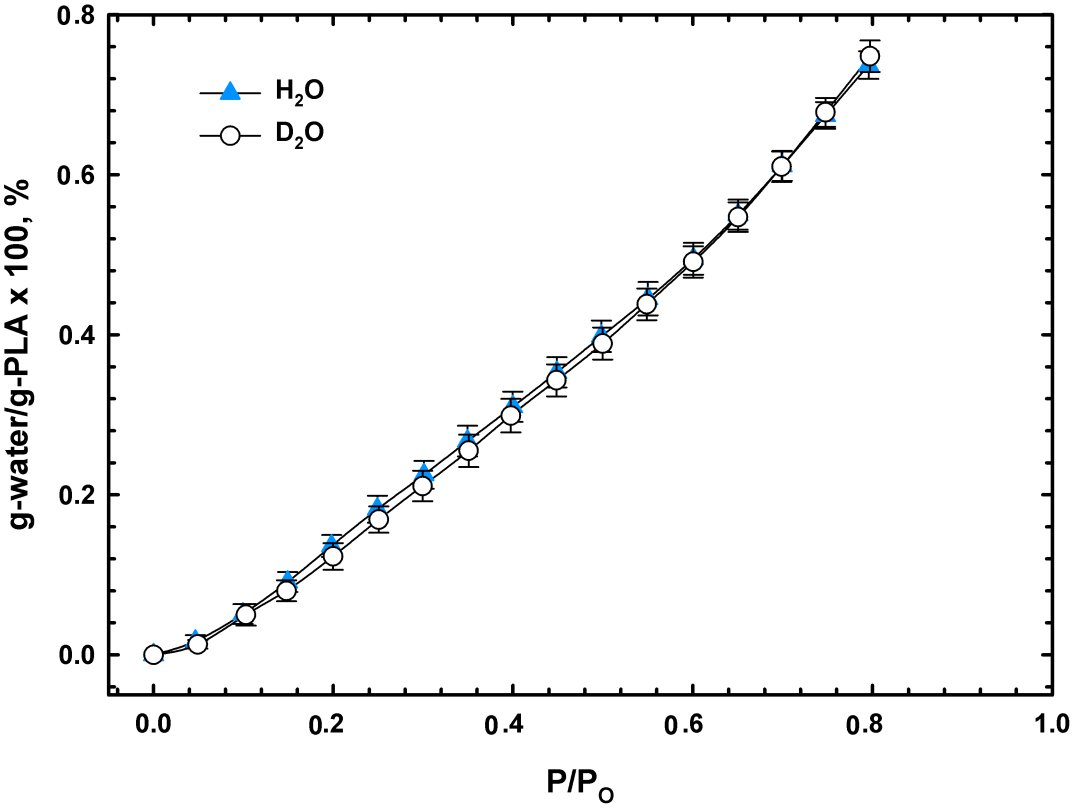


**Figure 3D.1** Sorption isotherms for $H_2O$ and $D_2O$ vapor in PLA film at 40 °C.

## APPENDIX 3E: Ethanol sorption into PLA films

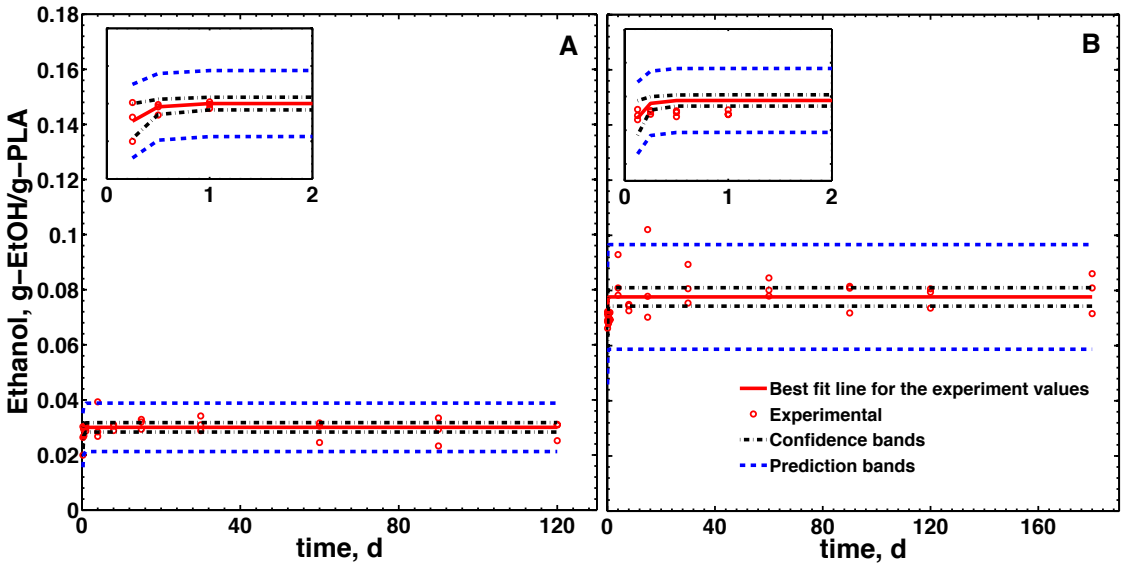


**Figure 3E.1** Ethanol sorption into PLA films in contact with: (A) 50% ethanol and (B) 95% ethanol at 40 °C. y-axis is in grams of ethanol sorbed divided by grams of PLA disk used for the $^{1}$H-NMR experiments.

**APPENDIX 3F: Expansion of PLA in contact with different volume fraction of ethanol**

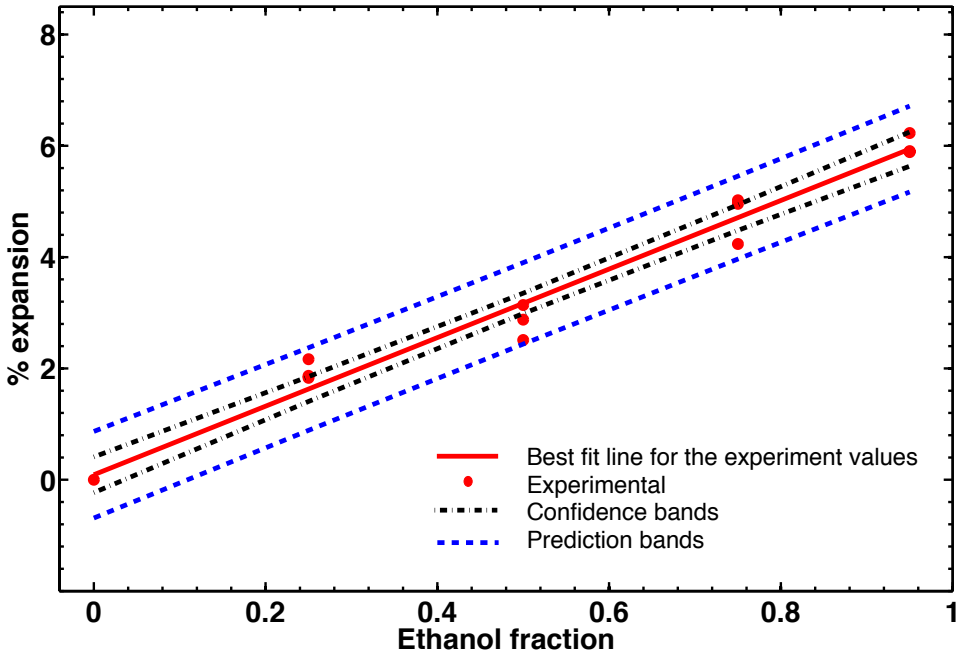


**Figure 3F.1** Expansion of PLA in contact with different volume fractions of ethanol (% expansion=6*p;* $R^2$=0.969, where *p* is the ethanol fraction by volume). The % expansion was determined as 100 times the volume of ethanol sorbed in PLA divided by the initial volume of the disk.

**APPENDIX 3G: Model for change in molecular weight, including polymer expansion**

Let *N* be the number of polymer chains in the disk at time $t$ and $M_t$ be the number-average molecular weight ($M_n$). In time $t + \Delta t$, scission during hydrolytic degradation will cause *n* cuts in the polymer chains, leaving $N - n$ chains uncut and 2 new chains. Since the total mass before and after scission is the same, the molecular weight at time $t + \Delta t$ is

$$M_{t+\Delta t} = M_t \frac{N}{(N-n)+(2n)} \qquad \text{Eq. 3G.1}$$

If $\Delta t$ is small, $n$ will be small compared to $N$. The equation above then reduces to

$$M_{t+\Delta t} = M_t \left(1 - \frac{n}{N}\right) \qquad \text{Eq. 3G.2}$$

so that

$$\frac{(M_{t+\Delta t} - M_t)}{M_t} = -\frac{n}{N} = -\left({}^{n}/_{V_d}\right) \Big/ \left({}^{N}/_{V_d}\right) \qquad \text{Eq. 3G.3}$$

where $V_d$ is the volume of the polymer disk. The quantity ${}^{N}/_{V_d}$ is related to the initial density of the PLA. The quantity ${}^{n}/_{V_d}$ is determined by the concentration $c$ of the water in the disk and by the contact time $\Delta t$ between the PLA and water. Then

$$\frac{\Delta M}{M} = -\beta c \Delta t \qquad \text{Eq. 3G.4}$$

where $c$ is the concentration of water and $\beta$ is a rate constant. In the limit as $\Delta t$ approaches zero,

$$\frac{dM}{M} = -\beta c dt$$ Eq. 3G.5

$$M = M_0 e^{-\beta \int_0^t c dt}$$ Eq. 3G.6

where $M_0$ is the initial $M_n$. If $c$ is constant due to fast diffusion,

$$M = M_0 e^{-\beta c t}$$ Eq. 3G.7

If diffusion of water and ethanol into the disk can be considered fast compared to the rate of scission, the mass of water occupying the voids inside the disk is:

$$c = \frac{mass\ of\ water}{V_d} = \frac{(1-p)(V_o + \Delta V)}{V_d}$$ Eq. 3G.8

where $p$ is the volume fraction of water in the ethanol-water mix surrounding the disk, $V_o$ is the total volume of voids initially in the disk, and $\Delta V$ is the increase in this volume due to expansion by ethanol.

If the expansion of the disk found earlier (.06$p$) is assumed to apply to only the voids, not the chains, then

$$c = (1-p)\left(\frac{V_o}{V_d} + \frac{\Delta V}{V_d}\right) = (1-p)\left(\frac{V_o}{V_d} + 0.06p\right)$$ Eq. 3G.9

$$= \left(\frac{V_o}{V_d}\right) + \left(0.06 - \frac{V_o}{V_d}\right)p - 0.06p^2$$

$$M = M_0 exp(-kt)$$ Eq. 3G.10

$$k = \beta\left[\frac{V_o}{V_d} + \left(0.06 - \frac{V_o}{V_d}\right)p - 0.06p^2\right]$$ Eq. 3G.11

**APPENDIX 3H: Molecular weight distribution (*MWD*) of PLA films during hydrolytic degradation**

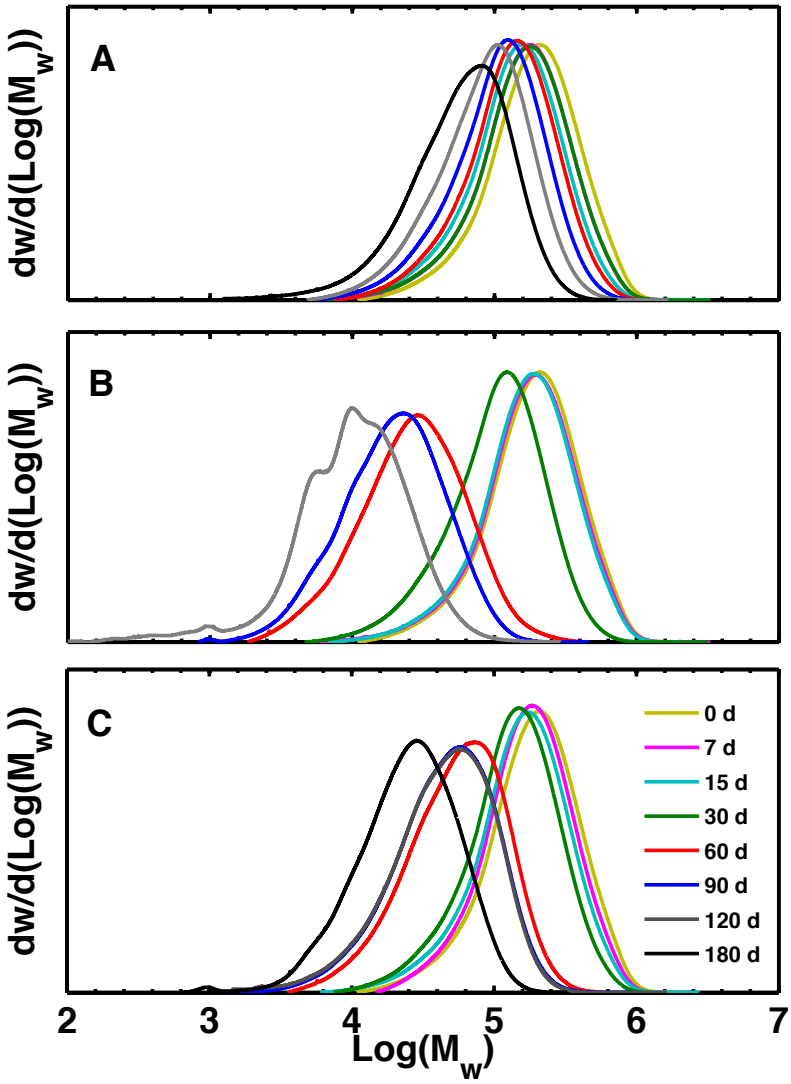


**Figure 3H.1** *MWD* of PLA films during hydrolytic degradation when in contact with: (A) water, (B) 50% ethanol and (C) 95% ethanol at 40 °C

**APPENDIX 3I: Model for LA release**

From the model for change in molecular weight, $M = M_0 exp(-kt)$ with $k = \beta\left[\frac{V_o}{V_d} + \left(0.06 - \frac{V_o}{V_d}\right)p - 0.06p^2\right]$. Fitting this model to the number molecular weight vs time data for all environments (water, 50% ethanol, 95% ethanol) gave $\beta = 1.05$ and $\frac{V_o}{V_d} = 0.0056$. With this information, a prediction for the release of LA can be proposed. The mechanism of LA release begins with chain scission inside the disk. This results in chains with very different molecular weights diffusing through the PLA matrix at the same time, crossing the interface some time later into the fluid, and further dissolving into LA monomers, mostly before leaving the PLA matrix. The increment of mass of PLA entering the fluid surrounding the disk in infinitesimal time $dt$ appears to follow the relationship:

$$dm \sim \frac{dt}{M^R} \qquad \text{Eq. 3I.1}$$

where $dm$ is the infinitesimal mass, $M$ is the molecular weight at time $t$, which is $M = M_o exp(-kt)$, and $R$ is a constant that accounts for all the above effects. When $t$ is small, $M$ is large and $dm$ is small. When $t$ is large, $M$ is small and $dm$ is large.

Since mass leaves the disk by diffusion, $dm$ should be proportional to the disk surface area $A$. It then enters the surrounding fluid volume $V_f$, and increases the LA concentration. The above relationship therefore becomes:

$$dC_f = \frac{B \cdot A \cdot dt}{V_f \cdot M^R} = \frac{B \cdot A}{V_f \cdot M_o^R} exp(Rkt)dt \qquad \text{Eq. 3I.2}$$

where $C_f$ is the concentration of PLA in the fluid and $B$ is another constant. Integrating and applying the boundary condition $m = 0$ at $t = 0$:

$$C_f = \frac{Q \cdot A}{V_f}[exp(Rkt) - 1] \qquad \text{Eq. 3I.3}$$

where $Q$ is a constant. The $^{A}/_{V_f}$ ratio used in the experiments reported was 1.79 $cm^2/mL$.

**APPENDIX 3J: Theoretical diffusion coefficients of LA-oligomers**

To predict the diffusion coefficients of LA and LA-mers, the free volume model/theory proposed by Ventras and Ventras [69] was applied. The diffusion coefficient ($D_1$) can be determined using the following equation, which depends on temperature, concentration, and the free-volume characteristics of the system [70, 71]:

$$D_1 = \overline{D}_0 exp\left[-\frac{E^*}{RT}\right] exp\left[-\frac{\omega_1 \hat{V}_1^* + \omega_2 \xi \hat{V}_2^*}{\hat{V}_{FH}/\gamma}\right] \quad \text{Eq. 3J.1}$$

where $\hat{V}_{FH}/\gamma$ is the term where the free-volume characteristics of the system are included, with $\hat{V}_{FH}$ being the average hole free volume per gram of mixture and $\gamma$ the average overlap factor for the mixture introduced, since the same free-volume is available to more than one jumping unit. To calculate the trace diffusion coefficient of LA, the mass fraction of LA in PLA film, $\omega_1$, is assumed to approach 0. Accordingly, the weight fraction of PLA in PLA film, $\omega_2$, is close to 1. $\xi$ is the ratio of critical molar volume of LA jumping unit to critical molar volume of PLA jumping unit, and $\hat{V}_1^*$ and $\hat{V}_2^*$ are the specific hole free volume of LA and PLA required for a jump, respectively.

$\hat{V}_{FH}/\gamma$ was calculated using the following equation:

$$\frac{\hat{V}_{FH}}{\gamma} = \omega_1 \frac{K_{11}}{\gamma_1}\left(K_{21} + T - T_{g1}\right) + \omega_2 \frac{\hat{V}_{FH2}}{\gamma_2} \quad \text{Eq. 3J.2}$$

where $K_{11}/\gamma_1$ and $K_{21} - T_{g1}$ are LA free volume parameters, $T$ is temperature in K, $\gamma_2$ is the overlap factor for the free volume of pure PLA, and $\hat{V}_{FH2}$ is the specific hole free

volume of the equilibrium liquid polymer at any temperature. $\hat{V}_{FH2}$ was calculated depending on the glass transition temperature of PLA ( $T_{g2}$):

$$\hat{V}_{FH2} = \hat{V}_2^0(T_{g2})\left[f_{H2}^G + \alpha_2(T - T_{g2})\right] \quad T \geq T_{g2} \qquad \text{Eq. 3J.3}$$

$$\hat{V}_{FH2} = \hat{V}_2^0(T_{g2})\left[f_{H2}^G + (\alpha_2 - \alpha_{c2})(T - T_{g2})\right] \quad T < T_{g2} \qquad \text{Eq. 3J.4}$$

where $\hat{V}_2^0(T_{g2})$ is the specific volume of the polymer at $T_{g2}$, $f_{H2}^G$ is the fractional hole free volume of PLA at $T_{g2}$, $\alpha_2$ is the thermal expansion coefficient for the equilibrium liquid polymer, and $\alpha_{c2}$ is the thermal expansion coefficient for the sum of the specific occupied volume and the specific interstitial free volume for the equilibrium liquid polymer. The following equations were used to calculate free volume parameters:

$$f_{H2}^G = \alpha_2 K_{22} \qquad \text{Eq. 3J.5}$$

$$\alpha_{c2} = \frac{\ln\left[\frac{\hat{V}_2^0(T_{g2})(1 - f_{H2}^G)}{\hat{V}_2^0(0)}\right]}{T_{g2}} \qquad \text{Eq. 3J.6}$$

$$\gamma_2 = \frac{\hat{V}_2^0(T_{g2})\alpha_2}{K_{12}/\gamma_2} \qquad \text{Eq. 3J.7}$$

$$\hat{V}_1^* = \hat{V}_1^0(0) \qquad \text{Eq. 3J.8}$$

$$\hat{V}_2^* = \hat{V}_2^0(0) \qquad \text{Eq. 3J.9}$$

$$\frac{K_{12}}{\gamma_2} = \frac{\hat{V}_2^*}{2.303\left(C_1^g\right)_2\left(C_2^g\right)_2} \qquad \text{Eq. 3J.10}$$

$$K_{22} = \left(C_2^g\right)_2 \qquad \text{Eq. 3J.11}$$

where $K_{12}/\gamma_2$ and $K_{22}$ are PLA free volume parameters, $\left(C_1^g\right)_2$ and $\left(C_2^g\right)_2$ are the Williams-Landel-Ferry (WLF) constants, $\hat{V}_1^0(0)$ and $\hat{V}_2^0(0)$ are the specific volume of equilibrium liquid of LA and PLA at 0 K, respectively.

Viscosity-temperature and density-temperature data for pure LA was used to determine $\overline{D}_0$, $K_{11}/\gamma_1$, and $K_{21} - T_{g1}$, using the following equation [72]:

$$\ln \eta_1 = \ln\left(\frac{0.124 \times 10^{-16} \tilde{V}_c^{2/3} RT}{M_1 \hat{V}_1^0}\right) - \ln\overline{D}_0 + \frac{\hat{V}_1^*}{\left(\frac{K_{11}}{\gamma_1}\right)\left(K_{21} + T - T_{g1}\right)} \quad \text{Eq. 3J.12}$$

where $\eta_1$ is viscosity, $\tilde{V}_c$ is the LA molar volume at the critical temperature, $M_1$ is the molecular weight of LA and $\hat{V}_1^0$ is the specific volume of the pure LA at $T$.

The diffusion coefficient of oligomers up to five units of LA was predicted using the scaling law [73]:

$$\frac{D(M,T)}{D(M_0,T)} = \left(\frac{M}{M_0}\right)^{-\alpha\left(T - T_g\right)} \quad \text{Eq. 3J.13}$$

where $M_0$ is the molecular weight of LA, $M$ is the molecular weight of the oligomers, $\alpha$ is a scaling exponent deviation to the Rouse theory, which depends on the geometry of the solute, polymer type and the temperature difference, $T$ and $T_g$.

**Table 3J.1** Parameters to predict the diffusion coefficient of LA and up to 5 LA-mers in PLA.

| Parameter | Value |
|---|---|
| $\hat{V}_1^0(0)$, $cm^3/mol$ | 69.2 |
| $\tilde{V}_c$, $cm^3/mol$ | 259.5 |
| $R$, J/Kmol | 8.314 |
| $M_1$, g/mol | 90 |
| $\overline{D}_0$, $cm^2/s$ | 2.146 $x10^{-9}$ |
| $K_{11}/\gamma_1$, $Kcm^3/g$ | 0.0145 |
| $K_{21} - T_{g1}$, K | 10.46 |
| $C_1^g$, $K^{-1}$ | 3.24 |
| $C_2^g$, K | 164.9 |
| $\alpha_2$, $C^{-1}$ | 7.4 $x10^{-4}$ |
| $\hat{V}_2^0(0)$, $cm^3/g$ | 0.7214, 0.7116 and 0.7024 * |
| $K_{12}/\gamma_2$, $cm^3/g$ | 5.863 $x10^{-4}$, 5.783 $x10^{-4}$ and 5.708 $x10^{-4}$ * |
| $\hat{V}_2^0(T_{g2})$, $cm^3/g$ | 0.8105, 0.7995 and 0.7892 * |
| $E^*$, J/mol | 2.4564 $x10^4$ |
| $\omega_1$ | 0 |
| $\omega_2$ | 1 |
| $\xi$ | 0.65 |
| $\alpha$ | 5.5, 4.2 and 3.3 * |

* Values for water, 50% and 95% ethanol, respectively.

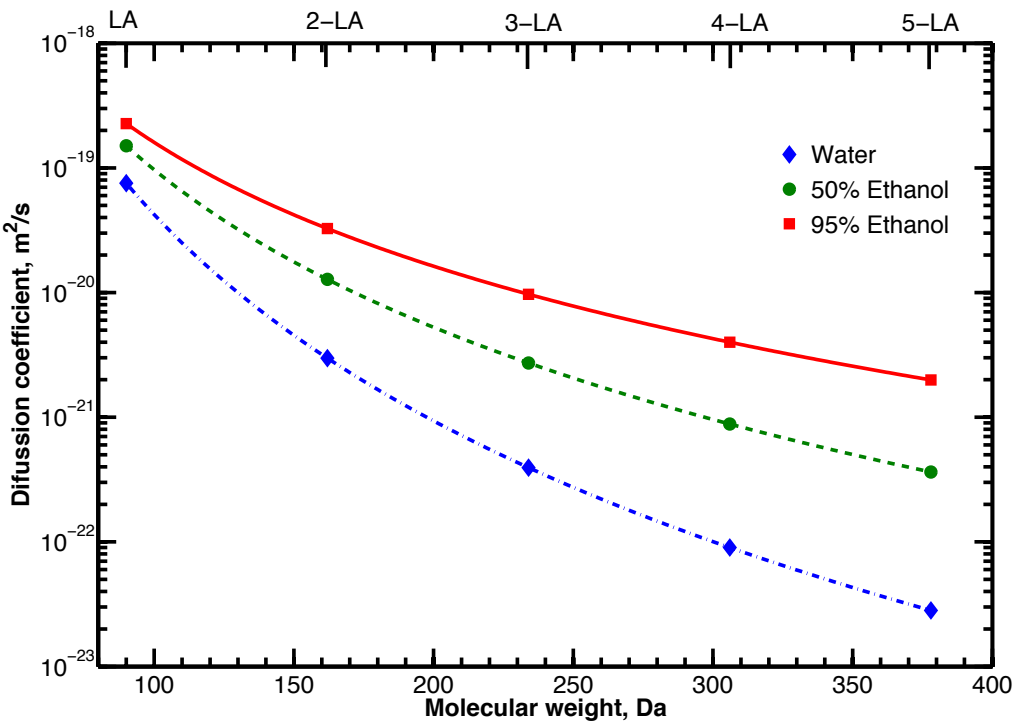


**Figure 3J.1** Theoretical estimated diffusion coefficients of LA and LA-mers in water, 50% and 95% ethanol. Fitted exponential decay lines are provided.

## APPENDIX 3K: Initial amount of lactic acid oligomers

Matrix-assisted laser desorption-ionization time-of-flight mass spectrometry (MALDI-TOF MS; Axima-CFR Plus, Shimadzu Europa, Duisburg, Germany) was used to analyze the presence of lactic acid oligomers in PLA film before hydrolysis through contact with water, 50% and 95% ethanol. α-cyano-4-hydroxycinnamic acid (10 mg/mL in 50/50 acetonitrile/water with 1 mg/mL diammonium hydrogen citrate) and dithranol (10 mg/mL in tetrahydrofuran) were used as MALDI matrix agents. Sample solutions of PLA in THF were prepared at concentrations of 0.1 and 0.01 mg/mL to be analyzed. The negative ion mode was used and the detector m/z range was 200-1500 Da.

# REFERENCES

## REFERENCES


[1] R. Auras, B. Harte, S. Selke, An overview of polylactides as packaging materials, Macromol. Biosci. 4 (2004) 835-864.

[2] E.T. Vink, S. Davies, Life Cycle Inventory and Impact Assessment Data for 2014 Ingeo™ Polylactide Production, Industrial Biotechnology 11 (2015) 167-180.

[3] N. Bleach, K. Tanner, M. Kellomäki, P. Törmälä, Effect of filler type on the mechanical properties of self-reinforced polylactide–calcium phosphate composites, J. Mater. Sci. Mater. Med. 12 (2001) 911-915.

[4] Y. Ikada, H. Tsuji, Biodegradable polyesters for medical and ecological applications, Macromol. Rapid Commun. 21 (2000) 117-132.

[5] J.-Y. Park, I.-H. Lee, Controlled release of ketoprofen from electrospun porous polylactic acid (PLA) nanofibers, J. Polym. Res. 18 (2011) 1287-1291.

[6] K.E. Uhrich, S.M. Cannizzaro, R.S. Langer, K.M. Shakesheff, Polymeric systems for controlled drug release, Chem. Rev. 99 (1999) 3181-3198.

[7] Y.-N. Chang, R.E. Mueller, E.L. Iannotti, Use of low MW polylactic acid and lactide to stimulate growth and yield of soybeans, Plant Growth Regul. 19 (1996) 223-232.

[8] R.G. Sinclair, Slow-release pesticide system. Polymers of lactic and glycolic acids as ecologically beneficial, cost-effective encapsulating materials, Environ. Sci. Technol. 7 (1973) 955-956.

[9] K.M. Nampoothiri, N.R. Nair, R.P. John, An overview of the recent developments in polylactide (PLA) research, Bioresour. Technol. 101 (2010) 8493-8501.

[10] D.G. Hayes, S. Dharmalingam, L.C. Wadsworth, K.K. Leonas, C. Miles, D. Inglis, Biodegradable agricultural mulches derived from biopolymers, in: C.S. Kishan Khemani (Ed.), Degradable polymers and materials: Principles and practice, American Chemical Society, Washington, DC, 2012, pp. 201-223.

[11] NatureWorks. NatureWorks PLA helps Delhaize extend environmentally-friendly packaging to Belgian costumers. http://cms.natureworksllc.com/News-and-Events/Press-Releases/2005/9-13-05-NatureWorks-PLA-Helps-Delhaize-Extend, 2015 (accessed 09.08.15).

[12] NatureWorks. Pacific Pre-cut enhances the freshness of its brand with NatureWorks PLA packaging for fresh-packed salads.

http://cms.natureworksllc.com/News-and-Events/Press-Releases/2005/6-5-05-Pacific-Pre-Cut-Enhances-the-Freshness-of-Its-Brand-With-NatureWorks-PLA-Packaging, 2015 (accessed 09.08.15).

[13] NaureWorks. SPAR Austria enhances freshness of produce with NatureWorks PLA. http://cms.natureworksllc.com/News-and-Events/Press-Releases/2005/9-8-05-SPAR-Austria-Enhances-Freshness-of-Produce-with-NatureWorks-PLA, 2015 (accessed 09.08.15).

[14] C.G. Pitt, M.M. Gratzl, A.R. Jeffcoat, R. Zweidinger, A. Schindler, Sustained drug delivery systems II: Factors affecting release rates from poly ( ε - caprolactone) and related biodegradable polyesters, Journal of Pharmaceutical Sciences 68 (1979) 1534-1538.

[15] M.-K. Lai, R.-C. Tsiang, Microencapsulation of acetaminophen into poly (L-lactide) by three different emulsion solvent-evaporation methods, J. Microencapsulation 22 (2005) 261-274.

[16] L. Zhang, C. Long, J. Pan, Y. Qian, A Dissolution - Diffusion Model and Quantitative Analysis of Drug Controlled Release from Biodegradable Polymer Microspheres, The Canadian Journal of Chemical Engineering 84 (2006) 558-566.

[17] C. Gualandi, M. Govoni, L. Foroni, S. Valente, M. Bianchi, E. Giordano, G. Pasquinelli, F. Biscarini, M.L. Focarete, Ethanol disinfection affects physical properties and cell response of electrospun poly (l-lactic acid) scaffolds, Eur. Polym. J. 48 (2012) 2008-2018.

[18] Z. Pan, J. Ding, Poly (lactide-co-glycolide) porous scaffolds for tissue engineering and regenerative medicine, Interface focus 2 (2012) 366-377.

[19] M. Ahmed, G. Punshon, A. Darbyshire, A.M. Seifalian, Effects of sterilization treatments on bulk and surface properties of nanocomposite biomaterials, Journal of Biomedical Materials Research Part B: Applied Biomaterials (2013).

[20] C. Xiang, A.G. Taylor, J.P. Hinestroza, M.W. Frey, Controlled release of nonionic compounds from poly (lactic acid)/cellulose nanocrystal nanocomposite fibers, J. Appl. Polym. Sci. 127 (2013) 79-86.

[21] M.K. Mitchell, D.E. Hirt, Degradation of PLA fibers at elevated temperature and humidity, Polym. Eng. Sci. (2014).

[22] S. De Jong, E.R. Arias, D. Rijkers, C. Van Nostrum, J. Kettenes-Van den Bosch, W. Hennink, New insights into the hydrolytic degradation of poly (lactic acid): participation of the alcohol terminus, Polymer 42 (2001) 2795-2802.

[23] H. Tsuji, K. Sumida, Poly (L‐lactide): v. effects of storage in swelling solvents on physical properties and structure of poly (L‐lactide), J. Appl. Polym. Sci. 79 (2001) 1582-1589.

[24] R.A. Auras, S.P. Singh, J.J. Singh, Evaluation of oriented poly (lactide) polymers vs. existing PET and oriented PS for fresh food service containers, Packag. Technol. Sci. 18 (2005) 207-216.

[25] H. Tsuji, Hydrolytic Degradation, in: R. Auras, L.-T. Lim, S. Selke, H. Tsuji (Eds.), Poly(lactic acid). Synthesis, Structures, Properties, Processing, and Applications, John Wiley & Sons, Inc., New Jersey, 2010, pp. 345-381.

[26] S. Sato, D. Gondo, T. Wada, S. Kanehashi, K. Nagai, Effects of various liquid organic solvents on solvent‐induced crystallization of amorphous poly (lactic acid) film, J. Appl. Polym. Sci. 129 (2013) 1607-1617.

[27] J. Gao, L. Duan, G. Yang, Q. Zhang, M. Yang, Q. Fu, Manipulating poly (lactic acid) surface morphology by solvent-induced crystallization, Applied Surface Science 261 (2012) 528-535.

[28] N. Wu, S. Lang, H. Zhang, M. Ding, J. Zhang, Solvent-Induced Crystallization Behaviors of PLLA Ultrathin Films Investigated by RAIR Spectroscopy and AFM Measurements, J. Phys. Chem. B 118 (2014) 12652-12659.

[29] S. Lee, Fourteen-year-old aging study of the effect of thickness on methanol transport in crosslinked poly (methyl methacrylate), Journal of materials research 11 (1996) 2403-2405.

[30] S.M. Aharoni, N.S. Murthy, Effects of Solvent-induced Crystallization on the Amorphous Phase of Polycarbonate of bisphenol A), International Journal of Polymeric Materials 42 (1998) 275-283.

[31] K. Tashiro, Y. Ueno, A. Yoshioka, M. Kobayashi, Molecular mechanism of solvent-induced crystallization of syndiotactic polystyrene glass. 1. Time-resolved measurements of infrared/Raman spectra and X-ray diffraction, Macromolecules 34 (2001) 310-315.

[32] K. Tashiro, A. Yoshioka, Molecular mechanism of solvent-induced crystallization of syndiotactic polystyrene glass. 2. Detection of enhanced motion of the amorphous chains in the induction period of crystallization, Macromolecules 35 (2002) 410-414.

[33] A. Yoshioka, K. Tashiro, Thermally-and solvent-induced crystallization kinetics of syndiotactic polystyrene viewed from time-resolved measurements of infrared spectra at

the various temperatures (1) estimation of glass transition temperature shifted by solvent absorption, Polymer 44 (2003) 6681-6688.

[34] W.-H. Lee, H. Ouyang, M.-C. Shih, M.-H. Wu, Kinetics of solvent-induced crystallization of poly (ethylene terephthalate) at the final stage, J. Polym. Res. 10 (2003) 133-137.

[35] H. Ouyang, W.-H. Lee, W. Ouyang, S.-T. Shiue, T.-M. Wu, Solvent-induced crystallization in poly (ethylene terephthalate) during mass transport: Mechanism and boundary condition, Macromolecules 37 (2004) 7719-7723.

[36] H. Ouyang, W.-H. Lee, M.-C. Shih, Three stages of crystallization in poly (ethylene terephthalate) during mass transport, Macromolecules 35 (2002) 8428-8432.

[37] ASTM, Standard 47544-11. Standard test method for two-sided liquid extraction of plastic materials using FDA migration cell. , ASTM International, West Conshohocken, PA, 2011.

[38] J. Crank, The Mathematics of Diffusion, 2nd ed., Oxford Science Publications, Oxford, 1975.

[39] E. Fischer, H.J. Sterzel, G. Wegner, Investigation of the structure of solution grown crystals of lactide copolymers by means of chemical reactions, Colloid Polym. Sci. 251 (1973) 980-990.

[40] M. Mutsuga, Y. Kawamura, K. Tanamoto, Migration of lactic acid, lactide and oligomers from polylactide food-contact materials, Food Addit. Contam. 25 (2008) 1283-1290.

[41] L. Di Maio, P. Scarfato, M.R. Milana, R. Feliciani, M. Denaro, G. Padula, L. Incarnato, Bionanocomposite polylactic acid/organoclay films: functional properties and measurement of total and lactic acid specific migration, Packag. Technol. Sci. 27 (2014) 535-547.

[42] N. Gulati, Use of QMC technology for measuring barrier properties of biodegradable packaging material, in: School of Packaging, Michigan State University, Michigan, 2008.

[43] W. Tham, B. Poh, Z.M. Ishak, W. Chow, Water Absorption Kinetics and Hygrothermal Aging of Poly (lactic acid) Containing Halloysite Nanoclay and Maleated Rubber, J. Polym. Environ. (2015) 1-9.

[44] G.L. Siparsky, K.J. Voorhees, J.R. Dorgan, K. Schilling, Water transport in polylactic acid (PLA), PLA/polycaprolactone copolymers, and PLA/polyethylene glycol blends, J. Environ. Polym. Degr. 5 (1997) 125-136.

[45] C. Chu, Hydrolytic degradation of polyglycolic acid: tensile strength and crystallinity study, J. Appl. Polym. Sci. 26 (1981) 1727-1734.

[46] C.G. Pitt, G. Zhong-wei, Modification of the rates of chain cleavage of poly (ϵ-caprolactone) and related polyesters in the solid state, Journal of controlled release 4 (1987) 283-292.

[47] X. Yuan, A.F. Mak, K. Yao, In vitro degradation of poly (L‐lactic acid) fibers in phosphate buffered saline, J. Appl. Polym. Sci. 85 (2002) 936-943.

[48] H. Tsuji, Y. Ikada, Properties and morphology of poly (L‐lactide). II. Hydrolysis in alkaline solution, J. Polym. Sci. A Polym. Chem. 36 (1998) 59-66.

[49] J. Cai, M. Liu, L. Wang, K. Yao, S. Li, H. Xiong, Isothermal crystallization kinetics of thermoplastic starch/poly (lactic acid) composites, Carbohydr. Polym. 86 (2011) 941-947.

[50] A. Kalkar, V. Deshpande, M. Kulkarni, Isothermal crystallization kinetics of poly (phenylene sulfide)/TLCP composites, Polym. Eng. Sci. 49 (2009) 397-417.

[51] G. Papageorgiou, D. Achilias, S. Nanaki, T. Beslikas, D. Bikiaris, PLA nanocomposites: effect of filler type on non-isothermal crystallization, Thermochim. Acta 511 (2010) 129-139.

[52] T. Ke, X. Sun, Melting behavior and crystallization kinetics of starch and poly (lactic acid) composites, J. Appl. Polym. Sci. 89 (2003) 1203-1210.

[53] W.-C. Tsai, M. Hedenqvist, Å. Laiback, H. Melin, M. Ngo, M. Trollsås, U. Gedde, Physical changes and sorption/desorption behaviour of amorphous and semi-crystalline PLLA exposed to water, methanol and ethanol, Eur. Polym. J. 76 (2016) 278-293.

[54] S. Sasaki, T. Asakura, Helix distortion and crystal structure of the α-form of poly (l-lactide), Macromolecules 36 (2003) 8385-8390.

[55] H. Marubayashi, S. Asai, M. Sumita, Complex crystal formation of poly (l-lactide) with solvent molecules, Macromolecules 45 (2012) 1384-1397.

[56] H.-m. Chen, Y. Shen, J.-h. Yang, T. Huang, N. Zhang, Y. Wang, Z.-w. Zhou, Molecular ordering and $\alpha'$ -form formation of poly (l-lactide) during the hydrolytic degradation, Polymer 54 (2013) 6644-6653.

[57] M. Yasuniwa, S. Tsubakihara, K. Iura, Y. Ono, Y. Dan, K. Takahashi, Crystallization behavior of poly (L-lactic acid), Polymer 47 (2006) 7554-7563.

[58] H. Zhou, T.B. Green, Y.L. Joo, The thermal effects on electrospinning of polylactic acid melts, Polymer 47 (2006) 7497-7505.

[59] X. Zhang, M. Espiritu, A. Bilyk, L. Kurniawan, Morphological behaviour of poly (lactic acid) during hydrolytic degradation, Polym. Degrad. Stab. 93 (2008) 1964-1970.

[60] K. Fukushima, C. Abbate, D. Tabuani, M. Gennari, G. Camino, Biodegradation of poly (lactic acid) and its nanocomposites, Polym. Degrad. Stab. 94 (2009) 1646-1655.

[61] K. Fukushima, D. Tabuani, G. Camino, Nanocomposites of PLA and PCL based on montmorillonite and sepiolite, Mater. Sci. Eng., C 29 (2009) 1433-1441.

[62] W. Hoogsteen, A. Postema, A. Pennings, G. Ten Brinke, P. Zugenmaier, Crystal structure, conformation and morphology of solution-spun poly (L-lactide) fibers, Macromolecules 23 (1990) 634-642.

[63] E. Helmroth, R. Rijk, M. Dekker, W. Jongen, Predictive modelling of migration from packaging materials into food products for regulatory purposes, Trends Food Sci. Tech. 13 (2002) 102-109.

[64] S.T. Ju, J.L. Duda, J.S. Vrentas, Influence of temperature on the diffusion of solvents in polymers above the glass transition temperature, Ind. Eng. Chem. Prod. Res. Dev. 20 (1981) 330-335.

[65] J. Vrentas, C. Vrentas, Fickian diffusion in glassy polymer‐solvent systems, J. Polym. Sci., Part B: Polym. Phys. 30 (1992) 1005-1011.

[66] G.R. Fulmer, A.J. Miller, N.H. Sherden, H.E. Gottlieb, A. Nudelman, B.M. Stoltz, J.E. Bercaw, K.I. Goldberg, NMR chemical shifts of trace impurities: common laboratory solvents, organics, and gases in deuterated solvents relevant to the organometallic chemist, Organometallics 29 (2010) 2176-2179.

[67] J. Tolgyessy, Chemistry and Biology of Water, Air and Soil: Environmental Aspects, Elsevier Science Publisher, Amsterdam, The Netherlands, 1993.

[68] J. Hine, C.H. Thomas, The Rate of Deuterium Exchange between Ethanol and Water. A Reinvestigation1, J. Am. Chem. Soc. 75 (1953) 739-740.

[69] J. Vrentas, C. Vrentas, Predictive methods for self-diffusion and mutual diffusion coefficients in polymer–solvent systems, Eur. Polym. J. 34 (1998) 797-803.

[70] J. Vrentas, C. Vrentas, Solvent self-diffusion in rubbery polymer-solvent systems, Macromolecules 27 (1994) 4684-4690.

[71] J. Vrentas, C. Vrentas, Solvent self-diffusion in glassy polymer-solvent systems, Macromolecules 27 (1994) 5570-5576.

[72] J. Vrentas, C. Vrentas, Energy effects for solvent self-diffusion in polymer-solvent systems, Macromolecules 26 (1993) 1277-1281.

[73] X. Fang, S. Domenek, V. Ducruet, M. Réfrégiers, O. Vitrac, Diffusion of aromatic solutes in aliphatic polymers above glass transition temperature, Macromolecules 46 (2013) 874-888.

# CHAPTER 4

## Chemical Recycling of Poly(Lactic Acid) by Water-Ethanol Solutions

A version of this chapter is published as:

F. Iñiguez-Franco, R. Auras, K. Dolan, S. Selke, D. Holmes, M. Rubino, H. Soto-Valdez, Chemical recycling of poly(lactic acid) by water-ethanol solution, Polymer Degradation and Stability 149 (2018) 28-38.

## 4.0 Abstract

The chemical recycling of poly(lactic acid) (PLA) by hydrolysis in water-ethanol solutions at moderate temperatures was investigated and the kinetic parameters of the hydrolysis, rate constant and activation energy ($E_a$) were assessed. Hydrolysis experiments of PLA in 50% ethanol at 40, 60, 70 and 80 °C were performed. Analyses of the molecular weight distribution (*MWD*) of PLA were performed by conducting a deconvolution of the *MWD* distribution since the *MWD* at the latter stages of the hydrolysis experiments was not normally distributed. Conducting this analysis allowed us to identify the more likely possible hydrolysis reactions and to estimate the prevalent rate of hydrolysis. A reparameterization of the Arrhenius equation was conducted for a better estimation of the $E_a$ with a low correlation coefficient between the parameters. No dependence of the hydrolysis rate with the change in *pH* for 50% ethanol was detected. For a better understanding of the effect of temperature on the hydrolytic degradation of PLA in water, hydrolysis experiments were also performed at 60, 70, 80 and 90 °C. The final $E_a$ values for the hydrolytic degradation of PLA in 50% ethanol and in water were 9.627 $x10^4$ and 10.474 $x10^4$ J/mol, respectively, that are within the same range of values reported in literature. The $E_a$ was 9% higher when PLA was hydrolyzed in water than in 50% ethanol. This study presents an alternative method for PLA chemical recycling using 50% ethanol.

## 4.1 Introduction

Production of plastics from fossil resources is no longer considered sustainable, so that pressure for a circular and bio-based economy of materials with lower

environmental footprint and from renewable resources is intensifying. Among these new bioplastics, PLA is one of the main commercial polymers that has increasingly gained acceptance [1, 2]. PLA is a thermoplastic aliphatic polyester, based on the ring opening polymerization of the lactic acid (LA) dimer - lactide - obtained from the fermentation of sugars derived from corn, potato or cassava starches [1, 2]. As pollution is becoming increasingly a concern, evaluation of the end of life (EoL) scenario is essential to understand the real environmental footprint of plastics such as PLA. PLA, besides being disposed through all the regular EoL scenarios (*i.e.*, recycling, incineration and landfill), can also be recovered through composting. One of the preferable disposal routes for all polymers including PLA is recycling, which can be either mechanical or chemical [2]. Mechanical recycling involves recovering, sorting, regrinding and reprocessing of PLA [3]. Although this process requires simpler technologies and it is easily implemented, it results in the deterioration of PLA's physical properties since the molecular weight is reduced due to shear and temperature, as well as foreign contaminants that are not completely removed [4]. Alternatively, chemical recycling converts PLA back to its monomer LA by hydrolysis and separate contaminants, so LA can then be used as raw material for new PLA production with the same properties as virgin PLA [4, 5].

Chemical recycling is a depolymerization method, which does not require severe operating steps. PLA and other polymers are generally depolymerized at high temperature using toxic solvents such as toluene, tetrahydrofuran, dichloromethane or chloroform [4, 6-8]. However, other methods have been developed for chemical recycling of PLA through alcoholysis by the solubilization of PLA in ethyl lactate followed by the hydrolysis of the lactic acid ester formed [9, 10]. Solubilization using acetone has

been explored [11]. New strategies for recycling PLA in aqueous phase at high temperatures has also been investigated [12, 13]. However, temperatures higher than the melting temperature ($T_m$) of PLA may trigger racemization and decomposition of the LA [12]. Therefore, hydrolysis of PLA at lower and medium temperature is preferred. The hydrolysis of PLA is mostly affected by the *pH* of the solution, temperature, and crystallinity of the original PLA material [6, 14].

A chemical recycling method using “green” solvents at moderate temperatures should be economically viable and preferred for recovery of PLA. We have demonstrated in our previous work [15] that the hydrolytic degradation of PLA in water-ethanol solutions was faster when PLA was exposed to 50% water-ethanol (v/v). This was attributed to the faster water penetration into the PLA matrix starting the chain cleavage after immediate swelling of the PLA matrix due to the presence of ethanol molecules. This proposed method could be used to safely recover PLA. However, the optimal process conditions to recycle PLA using water-ethanol solutions, as a “green” solvent, must be determined to generate a commercial opportunity. Furthermore, the parameters controlling this process such as the activation energy and temperature need to be fully assessed.

The effect of temperature on the hydrolytic and chemical recycling process of polymers is important to understand. $E_a$ is commonly used to describe how the kinetic rate of the reactions changes with temperature, and it is described by the Arrhenius equation. The $E_a$ is usually estimated by linearizing the Arrhenius equation using the natural logarithm to avoid numerical problems of having correlation between factors of the Arrhenius equation [12, 16-20]. This method, however, creates a high correlation

between the pre-exponential factor and the $E_a$ parameters of the equation. Therefore, in this study, we propose a reparameterization of the Arrhenius equation as previously suggested by other authors in other fields [21-28]. In this work, we applied reparameterization of the Arrhenius equation for estimating the $E_a$ of the hydrolytic degradation of PLA to obtain better estimates, low relative errors, and low correlation among the governing parameters. Thus, work aimed to understand and to analyze the hydrolytic degradation of PLA by water-ethanol solutions for the purpose of chemical recycling at moderate temperatures and to estimate the kinetic parameters, rate constant and activation energy that drives the hydrolytic degradation of PLA in these solutions.

## 4.2 Material and methods

### 4.2.1 Chemicals and reagents

PLA pellets (3.8 – 4.2 wt.% D-LA) were procured from NatureWorks LLC (Minnetonka, MN, USA). CAPS (3-(cyclohexylamino)-1-propanesulfonic acid), HEPES (N-(2-Hydroxyethyl)piperazine-N′-(2-ethanesulfonic acid)), sodium citrate, methanol, 1-butanol and ethanol HPLC grade were obtained from Sigma-Aldrich (St. Louis, MO, USA). Water HPLC grade and 1-propanol were acquired from J.T. Baker (Center Valley, PA, USA), respectively. Tetrahydrofuran (THF) reagent grade stabilized with BHT was procured from Pharmco-AAPER (North East, CA, USA).

### 4.2.2 Film production

PLA pellets were dried at 60 °C for 24 h under vacuum (85 kPa) and processed in a Randcastle cast film microextruder (Extrusion System, Inc., Cedar Grove, NJ, USA)

with a screw of 1.5875 cm diameter, 24/1 L/D ratio extruder, and 34 cc volume. The temperatures of extrusion for zone 1, 2, and 3, transfer tube and die were 193, 212, 215, 215 and 210 °C, respectively, with a rotation speed of 49 rpm. The film thickness was 27.9 ± 9.9 μm.

### 4.2.3 Molecular weight

To study the hydrolytic degradation of PLA film at different temperatures, migration cells as recommended by ASTM D4754-11 [29] were used. Each cell contained ten disks of PLA film, 2.0 cm of diameter, placed on a stainless steel wire and separated by glass beads [30]. Preliminary experiments on hydrolytic degradation of PLA were performed in different water-alcohol solutions: 50% ethanol, 50% methanol, 50% 1-propanol and 20% 1-butanol by volume at 70 °C. All the solutions were preconditioned before testing. After determining 50% ethanol as the main solvent to be used in the study of the $E_a$ of PLA hydrolytic degradation, migration cells containing 50% ethanol by volume were stored at 40, 60, 70 and 80 °C. All cells were first conditioned at the set temperature. Cells contained water were also conditioned and stored at 60, 70, 80 and 90 °C. Experiments designed to control the *pH* of the 50% ethanol solution during the hydrolytic degradation of PLA were performed at 80 °C with *pH* values of 4, 7 and 11, using sodium citrate (0.1 M), HEPES (0.3 M) and CAPS (0.1 M) as buffer solutions, respectively. Samples of film were retrieved periodically to assess number average molecular weight ($M_n$), weight average molecular weight ($M_w$) and polydispersity index (*PDI*). $M_n$ was assessed as previously described by the authors [15] where 10 mg of film were dissolved in THF (2 mg/mL) and tested using size exclusion chromatography (SEC). The measurements were conducted in triplicate.

The deconvolution of the molecular weight distribution (*MWD*) was carried out in Fityk (distributed under the terms of GNU General Public License) using nonlinear least-squares curve fitting for a LogNormal function [31, 32].

### 4.2.4 Nuclear Magnetic Resonance (NMR)

PLA samples, after hydrolysis in 50% ethanol at 80 °C, were analyzed by $^{13}C$ NMR (carbon nuclear magnetic resonance) on a 500 MHz Varian DirectDrive 2 Spectrometer equipped with 5 mm PFG OneNMR probe. The gHMBC (gradient heteronuclear multiple bond correlation) experiment was run on a Bruker Avance 900 MHz NMR spectrometer equipped with a 5 mm TCI triple-resonance cryoprobe operating at 898.76 and 226.02 MHz for $^{1}H$ and $^{13}C$, respectively. Samples were dissolved in $CDCl_3$ and run at ambient temperature. 7292 transients were collected for the carbon NMR with a 1.0 second recycle delay; data were zero-filled to 262144, and 0.5 Hz exponential multiplication was used. gHMBC data were collected with a 1.5 recycle delay, 96 scans per increment and 350 increments. Linear prediction and zero-filling were applied to the carbon dimension, and unshifted sine-bell squared windows were used in both dimensions.

### 4.2.5 Parameter estimation: Order of reaction

To calculate the order of the reaction for the hydrolytic degradation of PLA, the general rate law was used:

$$-\frac{dM_n}{dt} = kM_n^{\eta} \qquad \text{Eq. 4.1}$$

where $k$ is the rate constant of hydrolysis ($h^{-1}$) and $\eta$ is the order of reaction. The parameters $k$ and $\eta$ were estimated separately. One of the parameters was set at

different constant values in a range of possible values to obtain the estimate of the second parameter with the lowest root mean square error (RMSE).

After data analysis and to calculate the hydrolysis rate constant, the first order reaction equation was used:

$$M_n = M_{n_o} exp(-kt) \quad \text{Eq. 4.2}$$

where $M_{no}$ is the initial $M_n$.

### 4.2.6 Parameter estimation: Activation energy

#### 4.2.6.1 Step 1: Re-parameterization of the Arrhenius equation

The effect of temperature on the hydrolytic degradation of PLA can be described using the Arrhenius equation:

$$k = k_o exp\left(-\frac{E_a}{RT}\right) \quad \text{Eq. 4.3}$$

where $k_o$ ($h^{-1}$) is the pre-exponential factor, $R$ is the universal gas constant (8.314 J/mol·K), and $T$ is temperature (K). A reparameterization of the Arrhenius equation is proposed in this study to estimate $E_a$ and to avoid a high correlation between parameters $k_o$ and $E_a$ as previously explained [25-27]. This can be done by introducing the reference temperature ($T_{ref}$) that corresponds to the rate constant of hydrolysis ($k_{ref}$):

$$k = k_{ref} exp\left[-\frac{E_a}{R}\left(\frac{1}{T} - \frac{1}{T_{ref}}\right)\right] \quad \text{Eq. 4.4}$$

The hydrolytic degradation of PLA can be described by the change of $M_n$ as a function of time (**Eq. 4.2**). Then, to describe the effect of temperature on the hydrolysis of PLA, the following model is proposed by inserting **Eq. 4.4** in **Eq. 4.2**, resulting in:

$$M_n = M_{n_o} exp\left(-k_{ref} exp\left[-\frac{E_a}{R}\left(\frac{1}{T}-\frac{1}{T_{ref}}\right)\right]t\right) \quad \text{Eq. 4.5}$$

The hydrolytic degradation can also be *pH* dependent; therefore, the dependence of *pH* was introduced in **Eq. 4.5** as an empirical form of secondary model that has been applied similarly for water activity studies [33]:

$$M_n = M_{n_o} exp\left(-k_{ref} exp\left[-\frac{E_a}{R}\left(\frac{1}{T}-\frac{1}{T_{ref}}\right)+\beta\left(pH-pH_{ref}\right)\right]t\right) \quad \text{Eq. 4.6}$$

where $\beta$ is a constant which reflects the *pH* dependence of the hydrolytic degradation and $pH_{ref}$ is the reference *pH*.

To estimate $\beta$, experiments involving hydrolysis of PLA at one temperature and different *pH*'s were performed: 80 °C at *pH* 4, 7 and 11. The following equation was used to estimate $\beta$ and $pH_{ref}$:

$$M_n = M_{n_o} exp\left(-k_{ref} exp\left[\beta\left(pH-pH_{ref}\right)\right]t\right) \quad \text{Eq. 4.7}$$

#### 4.2.6.2 Step 2: Scaled sensitivity coefficient (X′)

When parameter estimation is performed, two or more parameters may be involved. Therefore, it is essential to determine if those parameters can be estimated accurately, easily and simultaneously. The sensitivity coefficient (SC) indicates the magnitude of change of the response due to perturbation in parameters, and is an important tool to determine the correlation among parameters. The SC is obtained by taking the first derivative of the dependent variable ($\mu$) with respect to the parameter of interest (*i.e.* $X_{E_a} = \partial\mu/\partial E_a$). However, for comparing parameters on the same scale, a scaled sensitivity coefficient (SSC) ($X'$) figure is often plotted. The SSC is provided by

multiplying the SC with the parameter itself [34]. For example, the *X′* of the activation energy can be obtained as follows:

$$X'_{E_a} = E_a \frac{\partial \mu}{\partial E_a} \quad \text{Eq. 4.8}$$

#### 4.2.6.2.1 Temperature simulation ($T_{sim}$)

$E_a$ indicates the sensitivity of the rate to temperature. When temperature is constant, it is not possible to estimate $E_a$, or to plot its SSC. Therefore, a new concept was developed to show the temperature-dependent SSC when there are multiple isothermal experiments. So, a $T_{sim}$ approach was proposed to plot *X′* of $E_a$ by inserting a linear increasing dynamic temperature function in the model:

$$T_{sim} = T_L + \frac{T_H - T_L}{t_{max}} t \quad \text{Eq. 4.9}$$

where $T_L$ is the lowest temperature (K), $T_H$ is the highest temperature (K), $t$ is time and $t_{max}$ is the maximum time duration.

#### 4.2.6.2.2 *pH* simulation ($pH_{sim}$)

For the SSC of **Eq. 4.6** and **Eq. 4.7** the same concept as $T_{sim}$ was applied since *pH* is changing during the hydrolysis reaction. So, a $pH_{sim}$ approach was proposed by inserting the following function in the models to plot *X′* when *pH* is changing over time:

$$pH_{sim} = pH_L + \frac{pH_H - pH_L}{t_{max}} t \quad \text{Eq. 4.10}$$

where $pH_L$ is the lowest *pH* and $pH_H$ is the highest *pH*.

### 4.2.6.3 Step 3: Estimation of the optimum $pH_{ref}$ and $T_{ref}$

The goal is to obtain near zero correlation among parameters for better estimation since by reducing the correlation, the relative errors will be reduced. To

reach the goal it was important to find the optimum $pH_{ref}$ and $T_{ref}$ as explained in the supporting information provided online.

To estimate $E_a$ in **Eq. 4.6**, assuming it is constant over all temperatures and over all *pH*, it was necessary to estimate $\beta$ from **Eq. 4.7** for later use as a fixed value in **Eq. 4.6**. In order to estimate $\beta$, the optimum $pH_{\text{ref}}$ was obtained from **Eq. 4.7** by plotting the correlation between $k_{ref}$ and $\beta$ versus a possible range of $pH_{\text{ref}}$. The optimum $pH_{\text{ref}}$ was used to estimate the parameters $k_{ref}$, $M_{no}$ and $\beta$. Once $\beta$ was estimated, the value was applied as a constant in Eq. 4.6 and $pH_{\text{ref}}$ used was the optimum $pH_{\text{ref}}$ previously estimated.

The optimum $T_{ref}$ was obtained from a plot of the correlation between $k_{ref}$ and $E_a$ as a function of the possible range of $T_{ref}$ using **Eq. 4.6** and **Eq. 4.5**. For the final estimation, the optimum $T_{ref}$ value was used to estimate the parameters $M_{no}$, $k_{ref}$ and $E_a$.

The nonlinear regression (*nlinfit*) function in MATLAB® 2016a (MathWorks, Natick, MA, USA) was used to estimate all the parameters. Mean comparisons of the studied parameters among treatments were done using the Tukey HSD test ($p$<0.05) with JMP® 9.0 (Cary, NC, USA) statistical software.

## 4.3 Results and discussion

### 4.3.1 Hydrolysis in different alcohol solutions

In our previous work, the hydrolytic degradation of PLA in contact with water-ethanol solutions was evaluated. PLA showed faster hydrolytic degradation when it was in contact with 50% ethanol at 40 °C [15]. This is due to the competitive balance between the swelling effect of ethanol expanding the PLA network allowing the maximum sorption of water into the PLA matrix and the cleavage of the main chain of

the polymer due to hydrolysis. To further explore the swelling effect of alcohol solutions, different alcohol solutions all at mostly 50% volume with water were used to evaluate the competitive balance between swelling and water sorption. **Figure 4.1** shows the change in $M_n$ with time when PLA was immersed in 50% ethanol, 50% methanol, 50% 1-propanol, and 20% 1-butanol at 70 °C. A lower ratio of 1-butanol was selected due to the low miscibility between 1-butanol and water. **Table 4A.1**, Appendix 4A, shows the order of reaction and hydrolysis rate for each of the water-alcohol solutions. Since the order of reaction for all the solvents was close to one, the approach to estimate the rate of reaction, $k$, was to assume as a first order behavior. The rate constants showed that the hydrolysis was slower when PLA was in contact with 50% methanol and no differences were found with 50% ethanol, 50% 1- propanol and 20% 1-butanol.

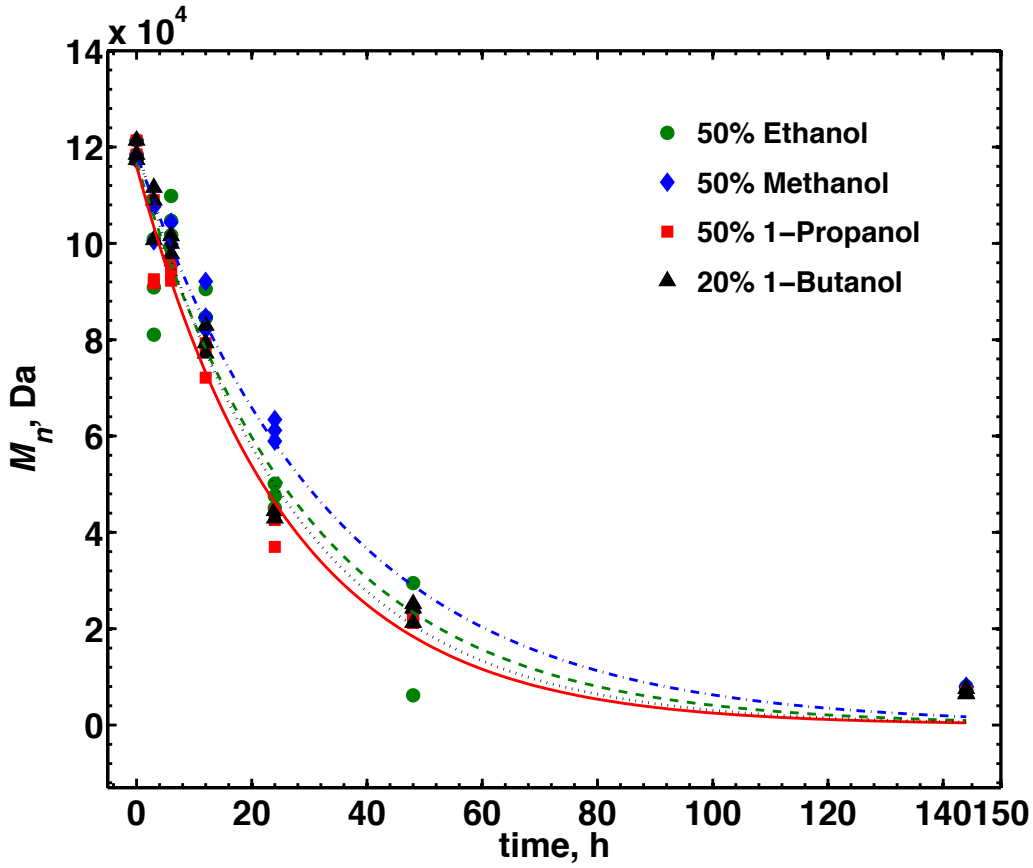


**Figure 4.1** $M_n$ as a function of time during hydrolytic degradation of PLA film immersed in 50% ethanol, 50% methanol, 50% 1-propanol and 20% 1-butanol at 70 °C. Lines indicate fitting of the first order reaction **Eq. 4.2** with $k$ = 0.0352 ± 0.0027, 0.0294 ± 0.0014, 0.0384 ± 0.0024 and 0.0367 ± 0.0017 $h^{-1}$, for 50% ethanol, 50% methanol, 50% 1-propanol and 20% 1-butanol, respectively.

Since no differences were found among the alcohols, except with methanol, which exhibited slower hydrolysis, 50% ethanol was used to assess the effect of temperature on the hydrolytic degradation of PLA and to calculate $E_a$. Ethanol was also selected since it can be produced from renewable resources such as sugar cane or

cornstarch, reducing the negative impact of using solvents derived from fossil resources for the recycling of PLA [35-37]. Additionally, the boiling point of 50% ethanol solution is higher than 50% 1-propanol (92 and 88 °C, respectively) and around the same as 20% 1-butanol (93 °C); thus, the hydrolysis and recycling can be performed at higher temperatures without reaching the boiling point, which would create process complications. Lastly, ethanol is a more economical choice than that of 1-propanol and 1-butanol [38].

### 4.3.2 Hydrolytic degradation of PLA in 50% ethanol

To study the effect of temperature on the hydrolytic degradation of PLA in 50% ethanol, PLA was exposed at different temperatures above the glass transition temperature ($T_g$) of the polymer immersed in 50% ethanol ($T_g$ = 36 °C [15]): 40, 60, 70 and 80 °C. **Figure 4.2** shows the *MWD* of PLA when it was exposed to hydrolysis in 50% ethanol. When the hydrolysis of PLA is via surface erosion the main peak of the *MWD* remains at the initial position with a reduced peak area. However, when PLA was exposed to hydrolysis at all temperatures, the *MWD* shifted away from its original position at time 0 h towards lower $M_n$. Canevarolo [39] and Tsuji and Ikada [40] found the same behavior indicating that degradation of PLA was preferentially carried out by chain scission in the bulk. At all temperatures, while the hydrolysis was progressing, the *MWD* peaks broaden and fragments of PLA chains were formed due to chain scission. Also, the *MWD* peaks at some point of the process changed from a monomodal distribution to double, triple or *n*-peaks distributions as seen in the *MWD*, indicating the formation of PLA oligomers. Tsuji and Ikada [40] studied the hydrolysis of different blends of crystalline and amorphous PLA. They found that the formation of another

peak is mostly due to the crystalline regions of PLA in the blends. Also, Tsuji et al. [13] in a comparative study on the hydrolytic degradation of PLA in the solid and in the melt found the formation of an additional peak during hydrolysis due to the degradation of the amorphous regions and presence of crystalline residues in the polymer matrix. So, the formation of additional peaks in the *MWD* during PLA degradation in 50% ethanol could be due to the crystalline residues from the hydrolysis process.

In our previous studies the crystallinity of PLA film immersed in 50% ethanol at 40 °C was analyzed during hydrolysis [15]. The degree of crystallinity of the film increased from around 3% to 25% after 168 h of immersion, and then between 360 h and 2880 h the crystallinity further increased to 50%. At the point that the *MWD* started to show more than one peak below 60 kDa, the crystallinity of the film was 40% corresponding to the region in which the crystallinity increases due to the hydrolysis of the amorphous regions of the PLA. This behavior could reflect complex kinetics where the ester bonds of PLA oligomer chains may have different susceptibility to cleavage. That means selective scission occurs where the degradation is not homogeneous and the accumulation of different low molecular weight fractions is more evident at prolonged hydrolysis time. In terms of chemical recycling of PLA, the crystalline residues could prolong the reaction period required for obtaining a high yield of LA [41-43].

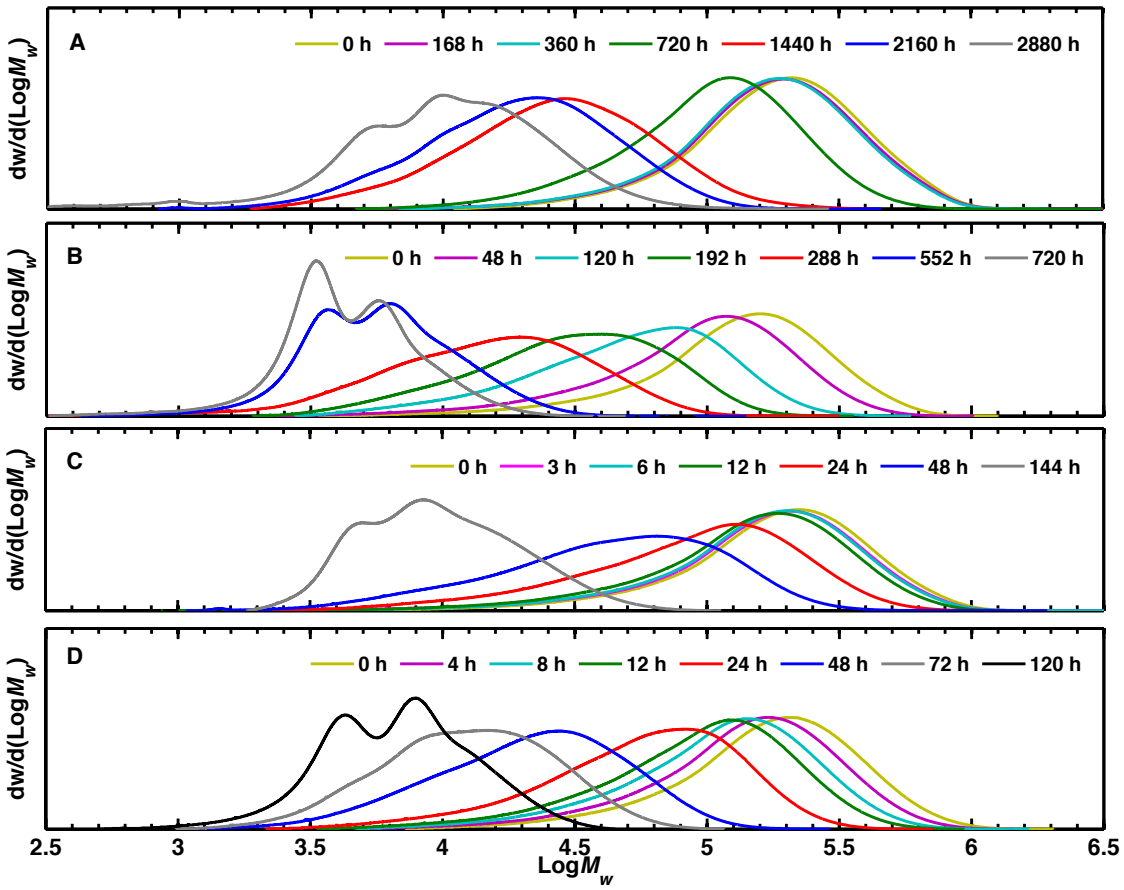


**Figure 4.2** *MWD* of PLA films during hydrolytic degradation when in contact with 50% ethanol at (A) 40, (B) 60, (C) 70 and (D) 80 °C.

To study the effect of temperature on the hydrolytic degradation of PLA in 50% ethanol, a deconvolution study of the *MWD* was performed to understand the reaction kinetics. Different deconvolution functions have been used such as Gaussian and Lorentzian functions [44-48]. However, it has been shown that these functions are not appropriate since the curves for solid-state reactions are asymmetrical, whereas LogNormal can properly fit asymmetric functions [32]. So, the LogNormal function was used to perform the deconvolution of the peaks followed by the kinetics analysis of the separated peaks to calculate the rate constants. The deconvolution of the peaks was

carried out when skewness of the distribution was observed and when more than one peak was detected in the *MWD*. This occurred when $M_n$ was below 60 kDa where the *MWD* distribution deviated from monomodal at all temperatures. **Figure 4.3** shows an example of the deconvolution of the last 5 curves of the hydrolytic degradation of PLA in 50% ethanol at 60 °C from **Figure 4.2B**. Different *MWD* can be observed from 120 h to 720 h of hydrolysis. The longer the exposure of PLA in solution, the more different lengths of polymer chains are formed. This means that while the PLA is exposed to 50% ethanol, selective chain scission occurs during the hydrolysis reactions.

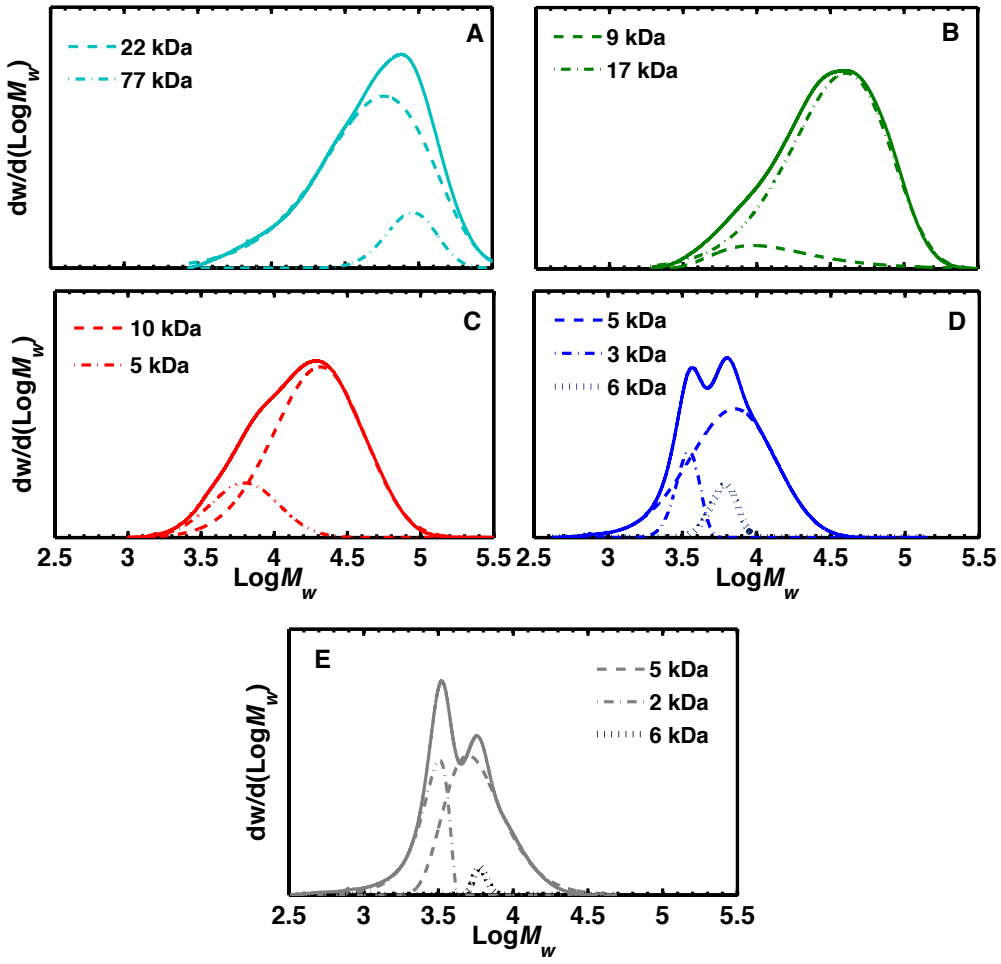


**Figure 4.3** Deconvolution of *MWD* of PLA for different hydrolysis times in 50% ethanol at 60 °C as shown in **Figure 4.2B**: (A) 120 h, (B) 192 h, (C) 288 h, (D) 552 h and (E) 720 h.

The hydrolytic degradation of PLA leads to random cleavage of the ester bonds where longer chains of the polymer are more susceptible to hydrolysis than the shorter chains [6]. The hydrolysis products of PLA contain fragments of water-soluble products like oligomers and LA fragments. To understand the hydrolysis of PLA, the proposed $M_n$ from the deconvoluted portions of the original *MWD* were plotted as a function of time

(**Figure 4.4**). The $M_n$ reduced to ~50 kDa when PLA was immersed for 720, 48, 24 and 12 h at 40, 60, 70, 80 °C, respectively, which is marked with a crossed dotted line (−•−) in **Figure 4.4**. Before that time, the *MWDs* were monomodal. After this point, increased skewness of the distributions and more than one peak were observed where the individual $M_n$ obtained from the deconvolution process were plotted.

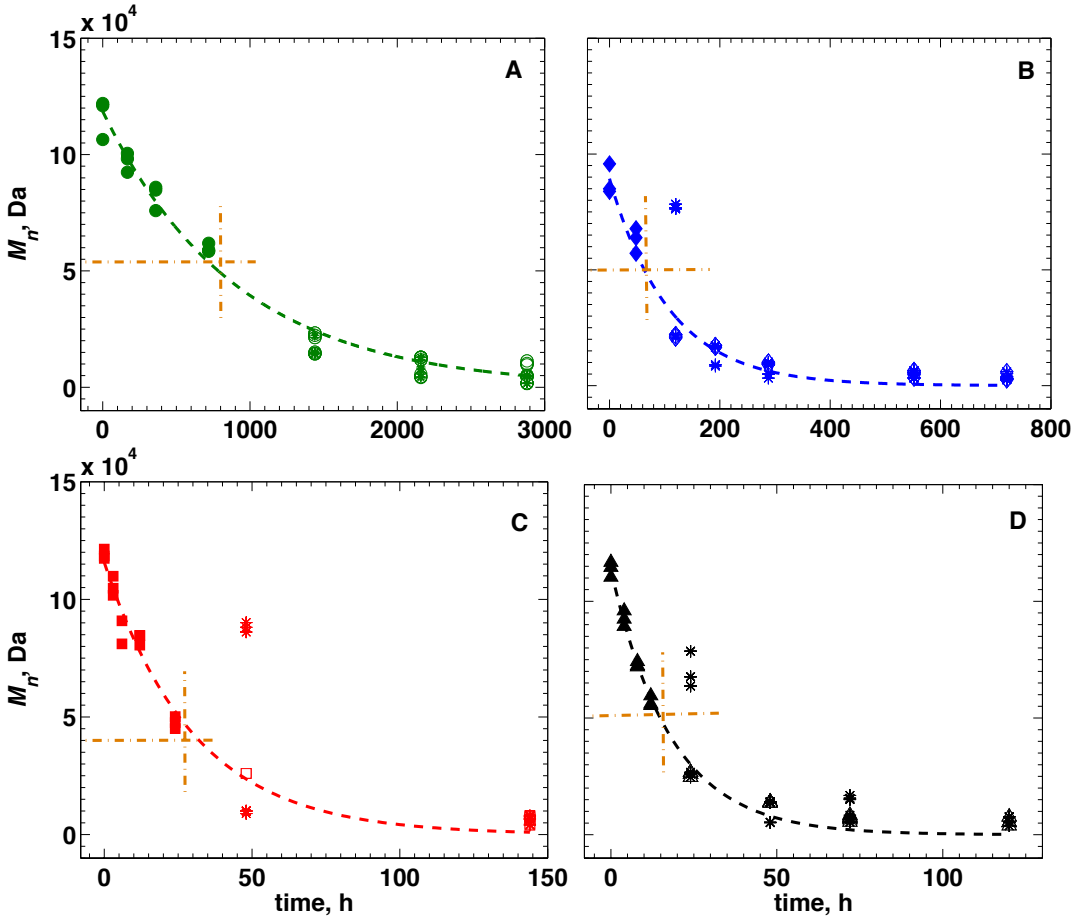


**Figure 4.4** $M_n$ as function of time during hydrolytic degradation of PLA film immersed in 50% ethanol at (A) 40, (B) 60, (C) 70 and (D) 80 °C. (•, ◆, ■, Δ) Filled markers indicate the main initial path of hydrolysis reaction. Unfilled markers indicate more likely side reactions. (*) Less prevalent side reactions. (−−−) Lines indicate fitting of **Eq. 4.2** for more likely reactions during PLA hydrolysis as determined by deconvolution.

To further understand PLA degradation, potentially different paths have been investigated. For instance, recombination reactions, which may result in crosslinking were considered [49, 50]. Recombination reactions of PLA have been seen when the polymer has been exposed to thermal degradation or degradation by composting [49, 51, 52]. They can also happen when cyclic oligomers recombine with linear molecules by ring opening reactions favoring the formation of longer chains [51, 52]. In this study, crosslinking was discarded as a side reaction after NMR experiments were carried out. In particular, gHMBC and $^{13}C$ NMR were run on PLA exposed to 50% ethanol at 80°C to probe for any new carbon resonances that may have formed that correspond to crosslinking (*e.g.,* carbon resonances around 100 ppm due to orthoesters). Aside from peaks attributable to PLA, oligomers and lactide, there was no evidence of crosslinking (**Figure 4B.1** and **Figure 4B.2**, Appendix 4B). **Figure 4.4B, C, D** showed a reduction in $M_n$ until 50 kDa with a subsequent increase in $M_n$ at 60, 70 and 80 °C, which could be attributed to recombination reactions. However, for the purposes of this study, these paths were not considered for determining the main order of reaction since these reactions are less prevalent side reactions and the fractional areas corresponding to their respective *MWD* are small. Other paths were also not considered when the $M_n$ of PLA showed an abrupt drop during hydrolysis and then $M_n$ stayed the same until the end of the experiment.

After the process of separating the individual data of the $M_n$ obtained by peak deconvolution, the kinetic analysis of selected $M_n$ as the most prevalent reaction was carried out for each temperature. **Table 4.1** shows the order of reaction of the selected $M_n$ during hydrolysis of PLA immersed in 50% ethanol at 40, 60, 70 and 80 °C. The

order of reaction for each temperature was close to a first order kinetic reaction. Therefore, the rate constants were calculated using **Eq. 4.2**. It is well known that hydrolytic degradation depends on the temperature, so the rate of hydrolysis of PLA increases with temperature. When the temperature increases, the time in which PLA was degraded to ~5 kDa decreased from 4 months at 40 °C to about 5 days at 80 °C. According to the SSC, which can be used to approximate the optimal time to accurately estimate the hydrolysis reaction rate, the hydrolytic degradation experiments should be run for 1000, 100, 33 and 16 h at 40, 60, 70 and 80 °C, respectively (**Figure 4C.1**, Appendix 4C). Therefore, the data for the decrease of $M_n$ before ~50 kDa, where the *MWD* does not exhibit skewness or multiple peaks, which is marked with a crossed dotted line (−•−) in **Figure 4.4**, should be sufficient to estimate the kinetic parameters for a first order reaction. At 60 °C, more initial experimental points should be taken to further improve the estimates since only two points were taken before 100 h.

**Table 4.1** Order of reaction ($\eta$) and rate constants for PLA films at different temperatures in 50% ethanol solution and water.

| Temperature | $\eta$ * | | $k$ ($h^{-1}$) ** | |
|---|---|---|---|---|
| (°C) | 50% Ethanol | Water | 50% Ethanol | Water |
| 40 | 1.016 ± 0.050 | nd | 0.0011 ± 0.00004 [a] | nd |
| 60 | 1.056 ± 0.073 | 1.054± 0.0977 | 0.0092 ± 0.0006 [b, A] | 0.0043 ± 0.0002 [a, B] |
| 70 | 1.039 ± 0.078 | 1.007 ± 0.0612 | 0.0331 ± 0.0019 [c, A] | 0.0181 ± 0.0007 [b, B] |
| 80 | 1.032 ± 0.042 | 1.043 ± 0.0732 | 0.0553 ± 0.0029 [d, A] | 0.0506 ± 0.0021 [c, A] |
| 90 | nd | 1.048 ± 0.0752 | nd | 0.0916 ± 0.0054 [d] |

* Fitting of general rate law **Eq. 4.1**

** Fitting of first order reaction **Eq. 4.2**

Values with the same lowercase letter within a column and capital letter within a row are not significantly different ($\alpha$=0.05)

Note: Not determined (nd) since water at 40 °C is below the $T_g$ of PLA, and ethanol at 90 °C is close to the boiling point of the solution

### 4.3.3 Effect of temperature on the hydrolytic degradation of PLA in 50% ethanol: Activation energy.

To evaluate the effect of temperature on the hydrolytic degradation of PLA for chemical recycling, the activation energy as stated by the Arrhenius equation should be estimated. Commonly, the effect of temperature on the hydrolysis of PLA is estimated by linearizing the Arrhenius equation **Eq. 4.3** by plotting the natural logarithm ln($k$) from the equation as a function of the reciprocal temperature to avoid fitting a non-linear equation [12, 16-20]. However, when the Arrhenius equation is used for parameter estimation, high correlation is found when $E_a$ and $k_o$ are simultaneously estimated, resulting in high relative error. **Table 4.2** shows the correlation matrix for the hydrolytic degradation of PLA in 50% ethanol using the Arrhenius equation as expressed in **Eq. 4.3**. A large correlation of the $E_a$ and $k_o$ for the hydrolysis reaction in 50% ethanol was found, with relative error for $E_a$ and $k_o$ of ~15 % and 328%, respectively. Therefore, a reparameterization of the Arrhenius equation as shown in **Eq. 4.4** has been recommended by several authors [21-28] to reduce the correlation between $E_a$ and $k_o$.

**Table 4.2** Correlation matrix of the estimated parameters using Arrhenius equation (**Eq. 4.3**) for the hydrolytic degradation of PLA in 50% ethanol.

| Parameter | $k_o$ | $E_a$ | Relative error, % |
|---|---|---|---|
| $k_o$ | 1 | 0.9998 | 328.45 |
| $E_a$ | 0.9998 | 1 | 14.94 |

During hydrolytic degradation of PLA, the number of carboxylic acid chain ends increases, making the hydrolysis a self-catalyzed reaction due to the accumulation of

the acidic polymer fragments in the specimens. So, the *pH* decreases over time, for example from *pH*=8.7 to *pH*=4.6 at 40 °C after 2800 h. Besides temperature, the hydrolysis mechanism of PLA may depend on the *pH* of the media due to the different susceptibility of the ester groups in lactic acid oligomers [14]. So, it is important first to study the influence of the *pH* on the hydrolysis rate constant of PLA. A parameter estimation approach was used to estimate the parameters of **Eq. 4.5** and **Eq. 4.6**. A detailed description of the methodology and the calculation steps are provided in the supporting information available online and elsewhere [53].

When PLA was immersed in 50% ethanol at 80 °C and different *pH*, the *MWD* shifted towards lower molecular weight as hydrolysis proceeded (**Figure 4F.1**, Appendix 4F). As in the hydrolysis of PLA in 50% ethanol without controlling the *pH* of the solution, the *MWD* at the latest stages of the degradation did not show a monomodal distribution. Therefore, for the analysis of the kinetics the same deconvolution procedure of the *MWD* was performed as in **Figure 4.3**, and then the analysis of the $M_n$ selecting the more likely side reactions to happen as in **Figure 4.4**. **Figure 4.5** shows the change in $M_n$ of PLA during hydrolytic degradation at constant *pH* after the deconvolution of the *MWD*. From **Table 4.3** we can observe that the order of reaction was close to one for the hydrolysis of PLA at *pH* 4, 7 and 11. Therefore, **Eq. 4.2** was applied to estimate the rate of hydrolysis. As was expected, when the *pH* of the media was basic (*pH* 11) the hydrolysis was faster than at acid (*pH* 4) and neutral (*pH* 7) conditions (**Table 4.3**). When PLA is exposed to basic conditions, the carbonyl carbon atoms of the polymer are susceptible to attack by the hydroxide ions and hydrolytic degradation and molecular weight reduction are more significant than in acid solutions [14, 54, 55].

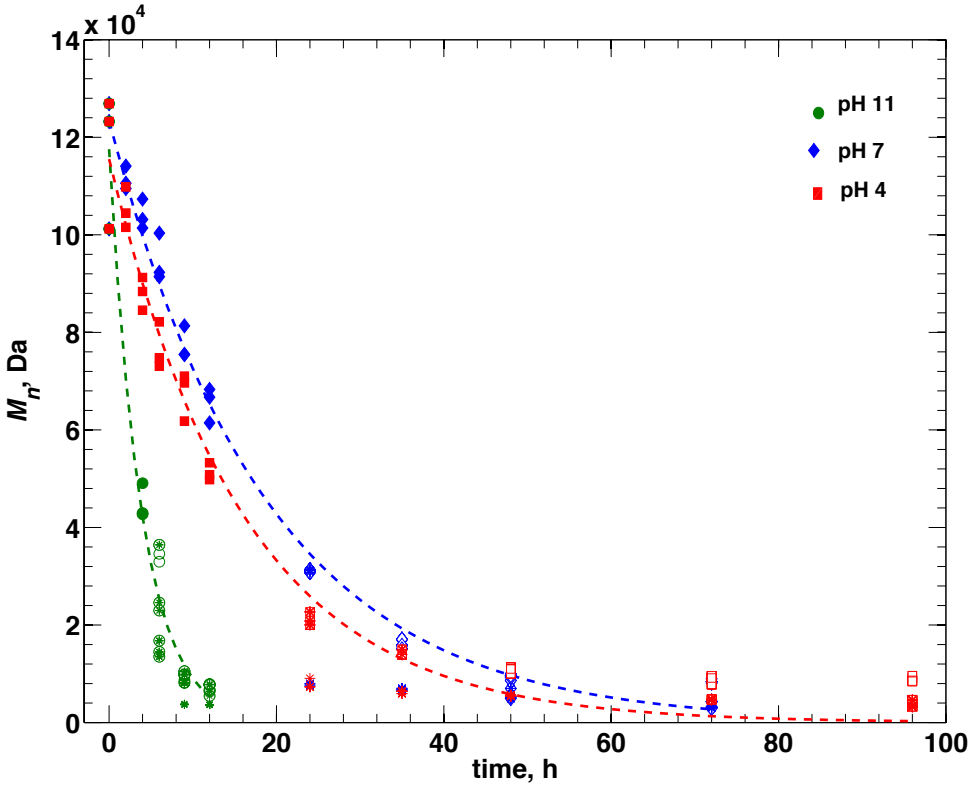


**Figure 4.5** $M_n$ as a function of time during hydrolytic degradation of PLA film immersed in 50% ethanol at 80 °C and different *pH*. (•,◆,■) Filled markers indicate the main initial path of hydrolysis reaction. Unfilled markers indicate more likely side reactions. (*) Less prevalent side reactions. (−−−) Lines indicate fitting of **Eq. 4.2** for more likely reactions during PLA hydrolysis.

**Table 4.3** Order of reaction ($\eta$) and rate constants for PLA films at 80 °C and different *pH* temperatures in 50% ethanol solution.

| ***pH*** | ***η*** * | ***k*** **($h^{-1}$)** ** |
|---|---|---|
| 4 | 1.002 ± 0.048 | 0.0623 ± 0.0032 [a] |
| 7 | 1.008 ± 0.044 | 0.0530 ± 0.0020 [a] |
| 11 | 1.001 ± 0.039 | 0.2563 ± 0.0139 [b] |

* Fitting of the general rate law **Eq. 4.1**

** Fitting of first order reaction **Eq. 4.2**

Values with different lower case letters are statistically different (α=0.05 Tukey-Kramer Test).

After the analysis of the hydrolytic degradation of PLA in 50% ethanol at different *pH* at 80 °C, where the rate increased exponentially with *pH*, thereby supporting the proposed equation, the estimation of $\beta$ using **Eq. 4.7** was carried out to be able to estimate $E_a$ from **Eq. 4.6**. For the estimation of $\beta$, it was necessary to find the optimum $pH_{ref}$ to have low correlation between parameters. Since there is no information on the $pH_{ref}$, the *pH* average was initially used ($pH_{ref}$ = 7.33). A final $pH_{ref}$= 7.697 was determined as explained in the supporting information. The optimum $pH_{ref}$ was used for the final estimation of the parameters presented in **Table 4.4** where $\beta$ was equal to 0.2153. The values of $\beta$ = 0.2153 and $pH_{ref}$ = 7.697 were used for the estimation of $E_a$ as a function of *pH* and temperature (**Eq. 4.6**).

**Table 4.4.** Final estimated parameters values at the optimum $pH_{ref}$ = 7.697 (**Eq. 4.7**).

| **Parameter** | **Estimates** | **RMSE, x10$^4$** |
|---|---|---|
| $k_{ref,}$ h$^{-1}$ | 0.1004 ± 0.0052 | 1.1737 |
| $M_{no}$, Da | 117,920 ± 2917 | |
| $\beta$ | 0.2153 ± 0.0148 | |

To estimate the $E_a$ as a function of *pH* using **Eq. 4.6**, it was necessary to find the optimum $T_{ref}$ to have low relative errors in the final estimation. The methodology to estimate the $T_{ref}$ is shown in the supporting information giving a $T_{ref}$ of 56.538 °C with a correlation coefficient of 4.1080 x10$^{-5}$ between $E_a$ and $k_{ref}$ and a relative error of 1.63 and 3.31%, respectively. **Table 4.5** shows the final estimated parameters for **Eq. 4.6** for the hydrolysis of PLA in 50% ethanol.

**Table 4.5** Final estimated parameter values at the optimum $T_{ref}$.

| Solution | $T_{ref}$, °C | Parameter | | | RMSE, x$10^3$ |
|---|---|---|---|---|---|
| | | $k_{ref}$, $h^{-1}$ | $M_{no}$, Da | $E_a$, x$10^4$, J/mol | |
| 50% Ethanol, *pH* correction * | 56.538 | 0.0093 ± 0.00031 | 114,480 ± 1879 | 9.589 ± 0.1559 [a] | 8.1062 |
| 50% Ethanol ** | 57.688 | 0.0076 ± 0.00027 | 110,840 ± 1625 | 9.341 ± 0.1669 [a] | 7.2478 |
| Water ** | 75.931 | 0.0276 ± 0.00078 | 115,290 ± 1744 | 10.143 ± 0.2228 [b] | 6.4603 |

* Estimated by using **Eq. 4.6**

** Estimated by using **Eq. 4.5**

Values with different lower case letters within a row are different ($\alpha$=0.05)

Note: $T_{ref}$ values are expressed with three decimals for parameter estimation purposes to get near zero correlation between $k_{ref}$ and $E_a$.

As previously mentioned, the hydrolytic degradation of PLA depends on the *pH* of the media. However, it is important to study whether the *pH* correction previously applied would affect the $E_a$ of hydrolysis. So, **Eq. 4.5** was applied to estimate $E_a$ without considering the change of *pH* during hydrolysis. For the non-linear regression estimation, the optimum $T_{ref}$ 57.688 °C with the lowest correlation was used for the final estimation of the parameters as presented in the supporting information giving a correlation coefficient of 1.2976 $x10^{-5}$ between $E_a$ and $k_{ref}$ and a relative error of 1.79 and 3.52%, respectively. The activation energy of the hydrolytic degradation of PLA in 50% ethanol without considering the change of *pH* during hydrolysis was 9.341 $x10^4$ J/mol (**Table 4.5**). After the reparameterization of the Arrhenius equation the $E_a$ was estimated as 9.589 $x10^4$ J/mol when dependence on *pH* was included. The difference between these values of $E_a$ was not statistically significant ($p$>0.05). Therefore, we were not able to detect dependence on *pH* of the $E_a$ for the hydrolytic degradation rate of PLA.

### 4.3.4 Hydrolytic degradation of PLA in water

For a better understanding of how 50% ethanol solution contributes to the hydrolytic degradation of PLA for chemical recycling purposes, the effect of temperature on the hydrolysis of PLA was also studied in water without ethanol. PLA films were immersed in water at different temperatures above the $T_g$: 60, 70, 80 and 90 °C. **Figure 4.6** shows the *MWD* of PLA during hydrolysis at these different temperatures. As in the hydrolysis of PLA in contact with 50% ethanol (**Figure 4.2**), the *MWD* shifted to lower molecular weight as the hydrolysis reactions took place. At all degradation temperatures, the broadness of the *MWD* increased and at the last stages several peaks appeared in the distributions. Even that the *MWD* shifted to lower molecular weight as hydrolysis

proceeded for PLA in water and in 50% ethanol, the evolution of the peaks was different. For example, during hydrolysis at 70 °C (**Figure 4.6B**), a peak was observed after 192 h of immersion in water ($M_n$ ≈ 4 kDa). Then, the peak shifted to lower molecular weight ($M_n$ ≈ 3.5 kDa) and the height of the peak increased after 264 h being the more predominant peak. However, for 50% ethanol (**Figure 4.2**) this peak was not as predominant as in water, which may be attributed to the difference on the chain scission selectivity during PLA hydrolysis process due to the swelling effect of the ethanol molecules. Future studies should be conducted to understand the difference in chain scission selectivity during hydrolysis reactions of PLA in water and 50% ethanol. The analysis of the effect of temperature on the hydrolysis of PLA in water was performed following the same procedure of deconvolution as in the hydrolysis of PLA in 50% ethanol to identify the side reactions and estimate the constant rates of the hydrolysis of PLA in water.

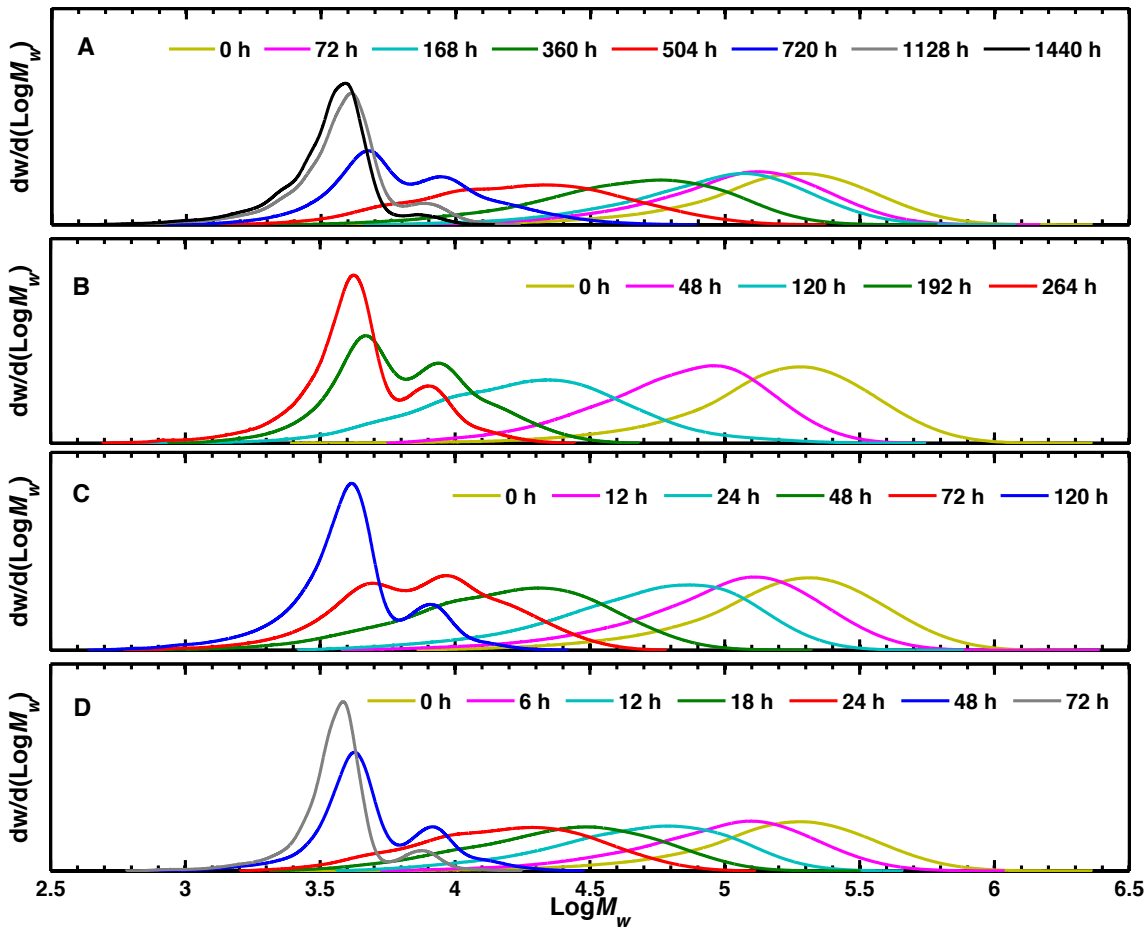


**Figure 4.6** *MWD* of PLA films during hydrolytic degradation when in contact with water at (A) 60, (B) 70, (C) 80 and (D) 90 °C

**Figure 4.7** shows the change in $M_n$ of PLA over time when it was immersed in water at 60, 70, 80 and 90 °C. After the deconvolution of the *MWD*, the more likely side reactions were selected following the same process as in 50% ethanol. The order of reaction of the selected $M_n$ for each temperature was close to 1 (**Table 4.1**). Therefore, the rate constants were estimated using the first order reaction **Eq. 4.2** as shown in **Table 4.1**. As expected, the higher the temperature the faster the hydrolysis. In this study, the hydrolytic degradation of PLA was faster when it was in contact with 50%

ethanol than in water at 60 and 70 °C ($p$<0.05); however, no statistical difference was detected on the rate of hydrolysis between 50% ethanol and water when PLA was exposed at 80 °C ($p$>0.05). This can be rationalized by the increased movement of the PLA chains at 80 °C resulting in the same rate of penetration of water molecules as the swelling of the matrix that occurs when PLA is exposed to 50% ethanol solution. **Figure 4.8** shows the rate constants of hydrolysis in 50% ethanol and water at the various temperatures of the experiments performed. The trend lines indicate that the higher the temperatures of the hydrolytic degradation in 50% ethanol and in water the faster the hydrolysis, increasing exponentially. To understand the effect of temperature on the hydrolytic degradation of PLA in water, the estimation of the $E_a$ was also carried out.

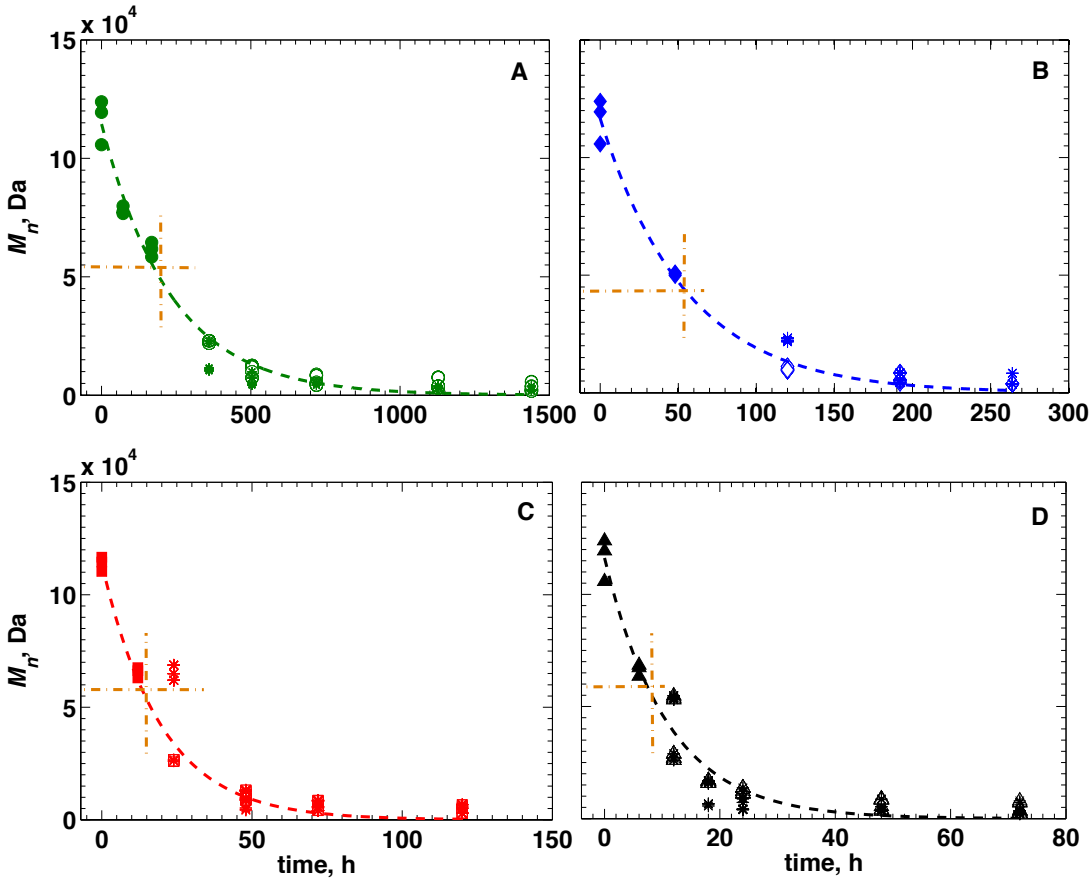


**Figure 4.7** $M_n$ as function of time during hydrolytic degradation of PLA film immersed in water at (A) 60, (B) 70, (C) 80 and (D) 90 °C. (•,◆,■, Δ) Filled markers indicate the main initial path of hydrolysis reaction. Unfilled markers indicate more likely side reactions. (*) Less prevalent side reactions. (−−−) Lines indicate fitting of **Eq. 4.2** for more likely reactions during PLA hydrolysis.

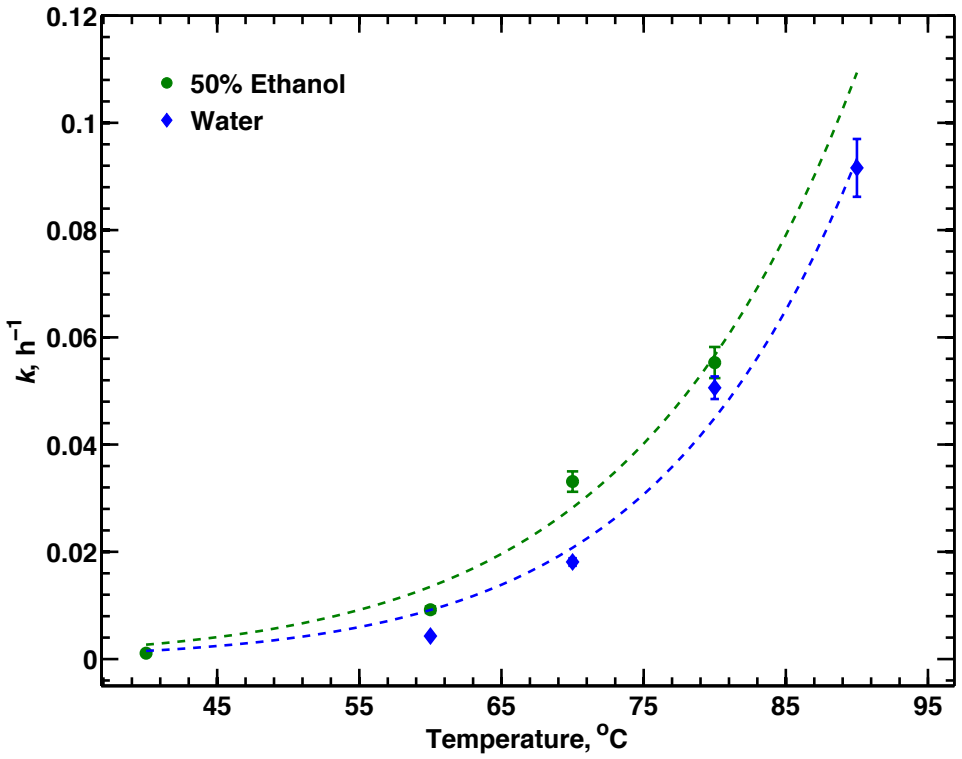


**Figure 4.8** Rate constants (*k*) of the hydrolytic degradation of PLA in 50% ethanol solution and water *vs.* temperature. Trend lines are used as a visual aid.

### 4.3.5 Effect of temperature on the hydrolytic degradation of PLA in water: Activation energy

To study the effect of the temperature on the hydrolytic degradation of PLA in contact with water, the activation energy was estimated using the reparameterization of the Arrhenius equation **Eq. 4.5** without considering the change of *pH* during hydrolysis since the *pH* did not have an effect on the $E_a$ of PLA when it was hydrolyzed by a 50% ethanol solution. So, it was assumed that it would not have an effect on the $E_a$ in water. The procedure for the estimation was the same as in 50% ethanol as shown in the

supporting information. For the final estimation of the parameters, the optimal $T_{ref}$ of 75.931 °C was used since it gave a correlation coefficient of 1.5516 x$10^{-5}$ between $E_a$ and $k_{ref}$ and a relative error of 2.48 and 2.20 %, respectively, which are acceptable and very low. The final estimation of the $E_a$ of the hydrolytic degradation of PLA in water was 10.143 x$10^4$ J/mol (**Table 4.5**).

Even though the values of the $E_a$ for the hydrolytic degradation of PLA in water and in 50% ethanol were different, these values are within the range of values (from 4 to 10 x$10^4$ J/mol) reported in the literature when PLA was exposed to different environments [12, 16-20, 55-57]. These environments include 100% relative humidity (40 – 80 °C) [16], steam high pressure (100 – 130 °C) [18], water high pressure (180 – 350 °C; 140 – 180 °C) [12, 57], *pH* 7 buffer solution (37 – 70 °C; 50 – 75 °C) [17, 56], basic media of *pH* 10 (50 – 70 °C) and acidic media of *pH* 2 (40 – 120 °C) [19, 20]. Some of the studies were performed using a range of temperatures below and above the $T_g$ that could affect the final estimations. However, the $T_g$ was not reported in solution, but of the initial PLA samples. It is also important to mention that the studies have also reported $E_a$ values from the linearized Arrhenius equation.

One of the main objectives of the present work was to provide an alternative method for chemical recycling of PLA. For that, it is important to consider the LA-oligomers yield during the hydrolysis reactions. $E_a$ values have been reported within the range of this study in aqueous phase but at higher temperatures (120 – 250 °C), obtaining high yields (~ 95%) of LA when hydrolysis was close to the $T_m$ [13, 57]. When PLA is hydrolyzed in the solid state, crystalline residues, as discussed for **Figure 4.2**, could prolong the reaction period required to obtain high yields of LA. However, Tsuji et

al. [13] reported that when PLA containing the crystalline residues is hydrolyzed in the solid state in water, the LA yield was comparable with the hydrolysis in the molten state without any crystalline residues where the time to get 95% LA yield at 120 °C was 72 h and at 180 °C was 2 h. In this study according to the rate constant estimated in **Table 4.1**, the time needed for 95% yield of LA at 80 °C in 50% ethanol should be 128 h. If the temperature of hydrolysis increased to 91 °C, below the boiling point of the 50% ethanol solution, the time would be reduced. Using the values estimated in **Table 4.1** the rate of hydrolysis at 91 °C and the time needed to get the 95% LA yield can be estimated using **Eq. 4.5** giving 0.1698 $h^{-1}$ and 41 h, respectively. The time of 41 h is comparable with the values obtained in water at 120 °C by Tsuji et al. [13]. However, it is important to further study the yield of LA-oligomers that can be used to start the re-polymerization of PLA from chemical recycling since it is not necessary to go to monomers if the goal is to re-polymerize PLA. In this case, the time needed to get 95% yield of LA-oligomers of 10 units in 50% ethanol at 91 °C would be around 29 h. So, this work presents a feasible method to achieve low $M_n$ PLA with green solvents at moderate temperatures using low energy and in a reasonable amount of time.

Future studies should be conducted to estimate the yield of LA-oligomers when PLA is hydrolyzed in 50% ethanol to re-polymerize PLA. It is important to study the crystallization behavior of PLA at high temperatures when PLA is immersed in 50% ethanol and how it will affect the yield of LA-oligomers for the chemical recycling of PLA and establish the separation process and purification of LA from the water-ethanol solution. It is expected that small increases in temperature can be translated into greater gain of LA-oligomers for recycling PLA.

## 4.4 Conclusions

The hydrolytic degradation of PLA by water-ethanol solutions for chemical recycling was studied. The hydrolysis of PLA at moderate temperatures above the $T_g$ was carried out in 50% ethanol solution and in water to study the effect of temperature. The analysis of the *MWD* indicated that the hydrolysis in 50% ethanol and water was preferentially carried out by bulk erosion showing a multi-modal distribution at the latter stages of the hydrolysis. The deconvolution of *MWD* indicated that multiple reaction pathways followed first order kinetics. The $E_a$ for the hydrolysis of PLA in water was around 9% higher than in 50% ethanol at moderate temperatures: 10.143 $x10^4$ and 9.341 $x10^4$ J/mol, respectively. These values were estimated after the reparameterization of the Arrhenius equation to obtain near zero correlation between parameters and therefore producing a better estimation. Also, the $E_a$ for the hydrolytic degradation of PLA in 50% ethanol was estimated taking in consideration the change of *pH*, however; no differences were found in the estimations. The $E_a$ values obtained in this work were within the same range of values reported in literature. This study presents an alternative method of using 50% ethanol to hydrolyze PLA at moderate temperatures for PLA chemical recycling.

## 4.5 Acknowledgements

I-F, F., thanks CONACYT (The Mexican National Council for Science and Technology), SEP (The Mexican Secretariat of Public Education), and the Government of Mexico for providing support funds for a Ph.D. fellowship. RA thanks the partial support of the USDA - and MI AgBioResearch, Hatch R. Auras.

# APPENDICES

**APPENDIX 4A: Rate constants and order of reaction for PLA films at 70 °C in water-alcohol solutions**

**Table 4A.1** Rate constants and order of reaction $\eta$ for PLA films at 70 °C in water-alcohol solutions.

| **Solvent** | $\eta$ * | $k$ * | $k$ ($h^{-1}$) ** |
|---|---|---|---|
| 50% Ethanol | 1.0246 ± 0.0054 | 0.0254 ± 0.0015 | 0.0352 ± 0.0027 [a] |
| 50% Methanol | 1.0111 ± 0.0035 | 0.0264 ± 0.0010 | 0.0294 ± 0.0014 [b] |
| 50% 1-Propanol | 1.3246 ± 0.0043 | 0.0008 ± 0.00004 | 0.0384 ± 0.0024 [a] |
| 20% 1-Butanol | 1.1323 ± 0.0034 | 0.0083 ± 0.0003 | 0.0367 ± 0.0017 [a] |

* Fitting of general rate law **Eq. 4.1**

** Fitting of first order reaction **Eq. 4.2**

Values with different lower case letters within a column are significantly different ($\alpha$=0.05)

## APPENDIX 4B: NMR Analysis

In order to investigate the possibility and extent of crosslinking of PLA during hydrolysis, $^{13}C$ and gHMBC (gradient heteronuclear multi-bond correlation) NMR experiments were carried out on PLA exposed to 50% ethanol at 80 °C. HMBC cross-peaks correlate protons to carbons that are 2-3 bonds removed. This allows determination of whether there are any new/unique $^{13}C$ resonances associated with the main PLA proton resonances (5.16 and 1.58 ppm for the CH and $CH_3$, respectively). The most probable structures resulting from crosslinking are orthoesters in which a carboxylic ester in PLA reacts with ethanol or water and the subsequent hemiacetal further reacts with another ester to form the orthoester. The resulting carbon with three alkoxy groups would have a unique carbon chemical shift (~100ppm), which would be easily detected in the HMBC experiment. **Figure 4B.1** shows the HMBC spectrum of the hydrolyzed PLA sample. No cross-peaks attributable to crosslinking were observed. There are resonances consistent with PLA and its oligomers as well as lactide. Inspection of the $^{13}C$ NMR confirms these results (**Figure 4B.2**)

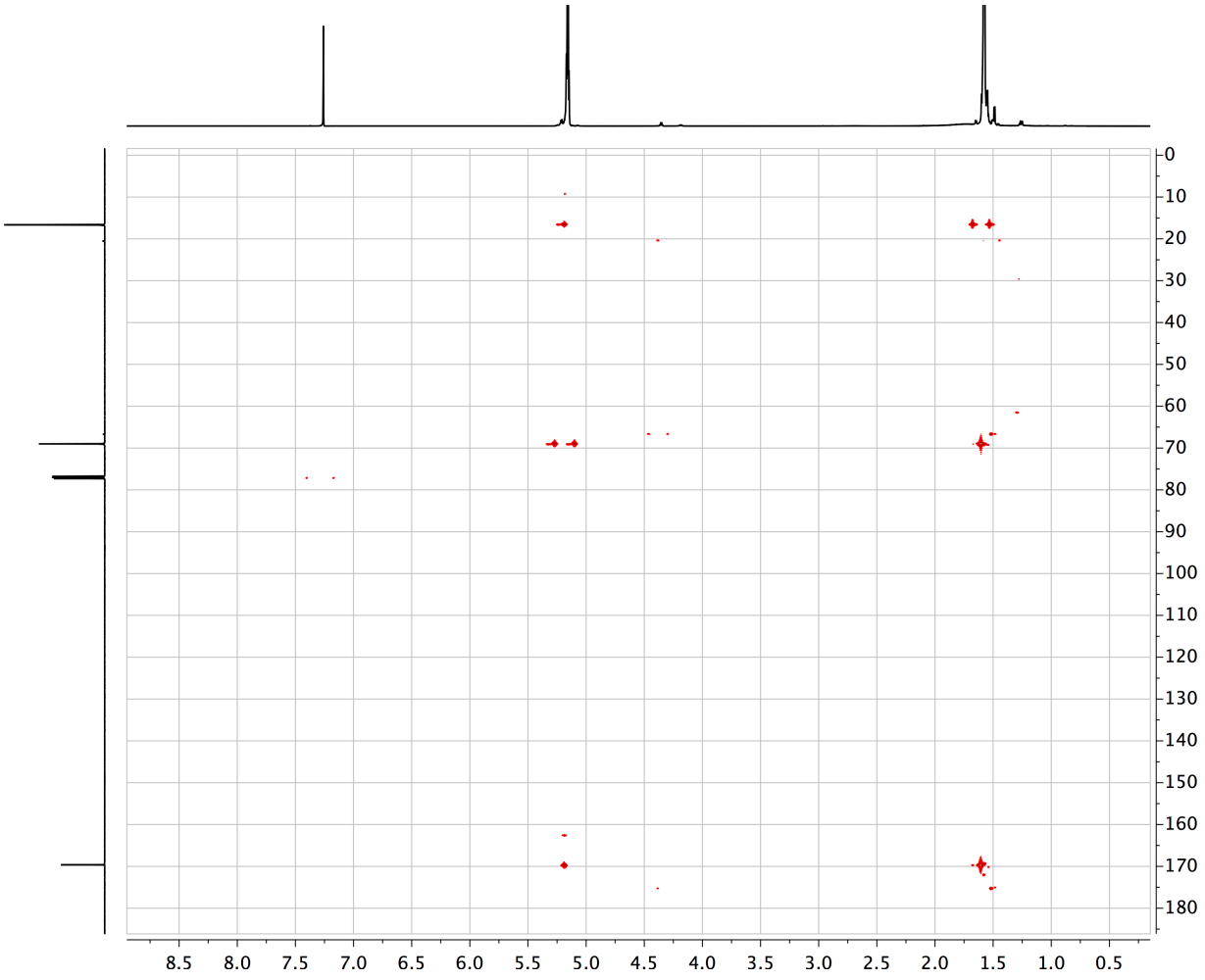


**Figure 4B.1** $^{1}H,^{13}C$-gHMBC of PLA exposed to 50% ethanol at 80 °C run on a Bruker Avance 900.

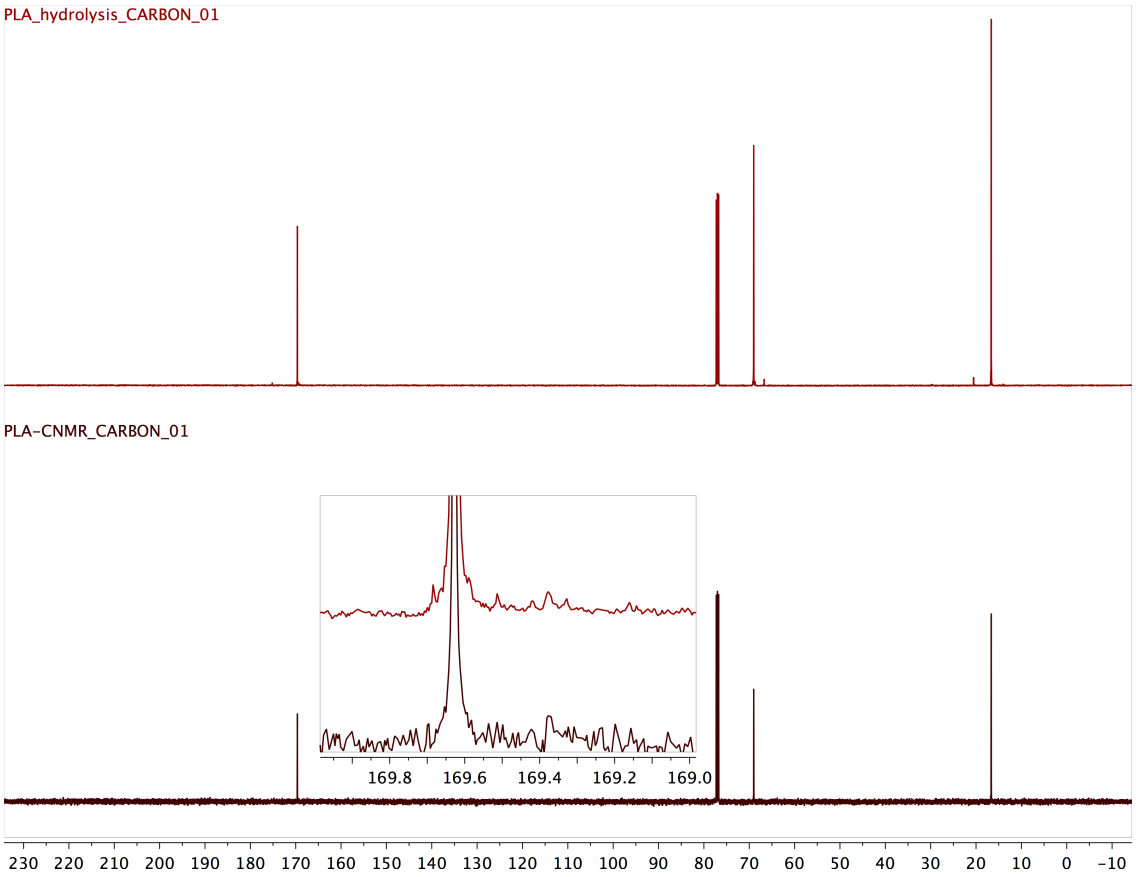


**Figure 4B.2** $^{13}C$ NMR of PLA prior to hydrolysis (top) and after hydrolysis in 50% ethanol at 80 °C (bottom). The expansion shows the carbonyl region and indicates additional small resonances around 169.4 ppm that are most likely attributable to PLA oligomers.

**APPENDIX 4C: Scale Sensitivity coefficient of hydrolytic degradation of PLA in 50% ethanol**

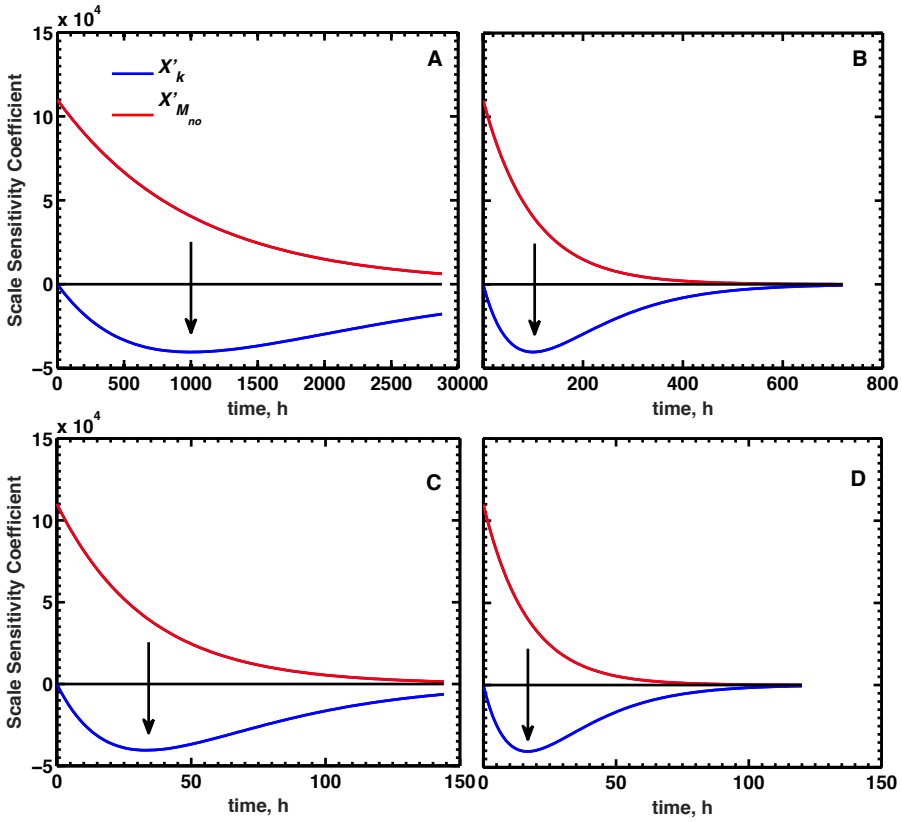


**Figure 4C.1** SSC of hydrolytic degradation of PLA in 50% ethanol using first order reaction equation **Eq. 4.2** at (A) 40, (B) 60, (C) 70 and (D) °80 C. Arrows indicate the optimal time to accurately estimate *k*.

## APPENDIX 4D: Parameter estimation of the $E_a$ for the hydrolysis of PLA in 50% ethanol

For the estimation of the activation energy for the hydrolysis of PLA in 50% ethanol, first it is necessary to plot SSC, which assists in the parameter identifiability of the model proposed. The SSC plot is needed to determine correlation among all the parameters of interest. Since there is no available information on the $T_{ref}$ and $pH_{ref}$ of the hydrolytic degradation of PLA to estimate $E_a$ using **Eq. 4.5** or **Eq. 4.6**, some authors have recommended using the average temperature in the case of $T_{ref}$ within the experimental temperature range [21, 25, 28, 58]. For this study, the initial $T_{ref}$ chosen was 62.5 °C, the average of the temperature range of study (40 to 80 °C) and for $pH_{ref}$ was the average of 4, 7, 11, corresponding to 7.33, later discussed.

To estimate $E_a$, taking the *pH* into consideration while hydrolysis reactions are taking place, first **Eq. 4.6** was used. **Figure 4D.1A** shows the SSC for the parameter estimation using **Eq. 4.6** with $\beta$ as a parameter to be estimated. From the $X'$ plot, $\beta$ and $E_a$ are identified as parameters that are correlated since their shape is similar with their maximum value at ~ 550 h meaning that the parameters need to be separately estimated. Therefore, it was proposed to fix $\beta$ as a constant. **Figure 4D.1B** shows the SSC of **Eq. 4.6** with $\beta$ fixed as a constant. From the $X'$ plot $M_{no}$ is identified as the parameter that is estimated with more accuracy with the lowest relative error followed by the $E_a$ and $k_{ref}$, meaning that the parameter with the largest error would be $k_{ref}$.

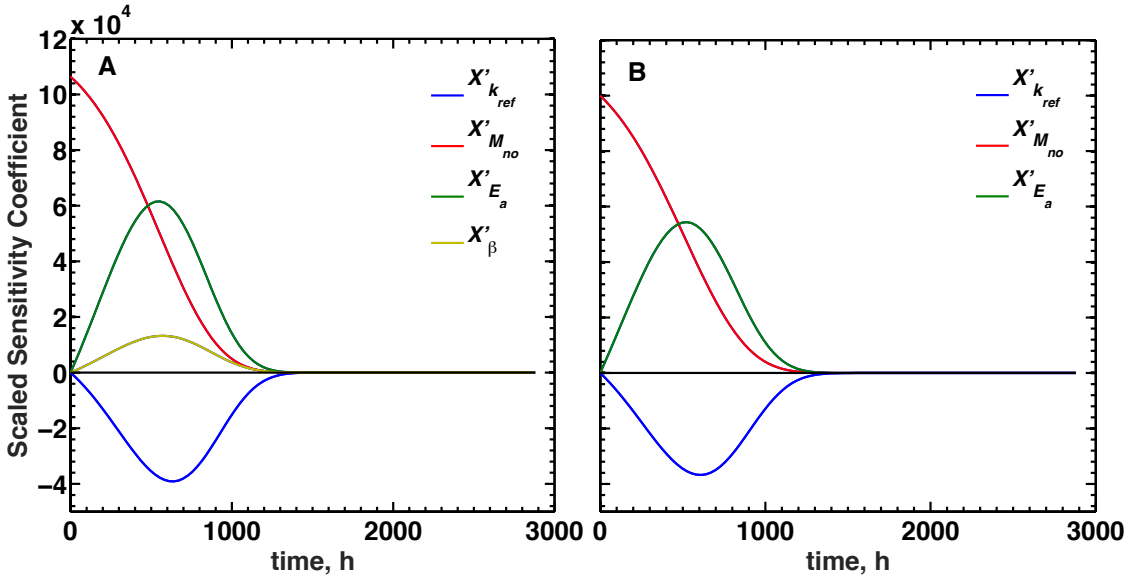


**Figure 4D.1** SSC of hydrolytic degradation of PLA in 50% ethanol using simulated dynamic temperature (**Eq. 4.9**) in **Eq. 4.6** at $T_{ref}$ = 62.5 °C and $pH_{ref}$ = 7.33. (A) $\beta$ as a parameter to estimate with initial guesses: $k_{ref}$ = 0.0099 $h^{-1}$, $M_{no}$ = 100,000 Da, $E_a$ = 9.04 x$10^4$ J.$mol^{-1}$, $\beta$ = 0.147. (B) $\beta$ as a constant with initial guesses: $k_{ref}$ = 0.01 $h^{-1}$, $M_{no}$ = 100,000 Da, $E_a$ = 9.04 x$10^4$ J.$mol^{-1}$.

To estimate $\beta$, **Eq. 4.7** was proposed where experiments at one temperature and different *pH* were performed. **Figure 4D.2** shows the SSC of **Eq. 4.7** where $M_{no}$ is the parameter identified as the easiest to be estimated with the lowest relative error, followed by $k_{ref}$ and then by $\beta$. To be able to estimate $\beta$, the hydrolytic degradation of PLA in 50% ethanol was performed at 80 °C controlling the *pH* during the experiment at three different values: 4, 7, and 11.

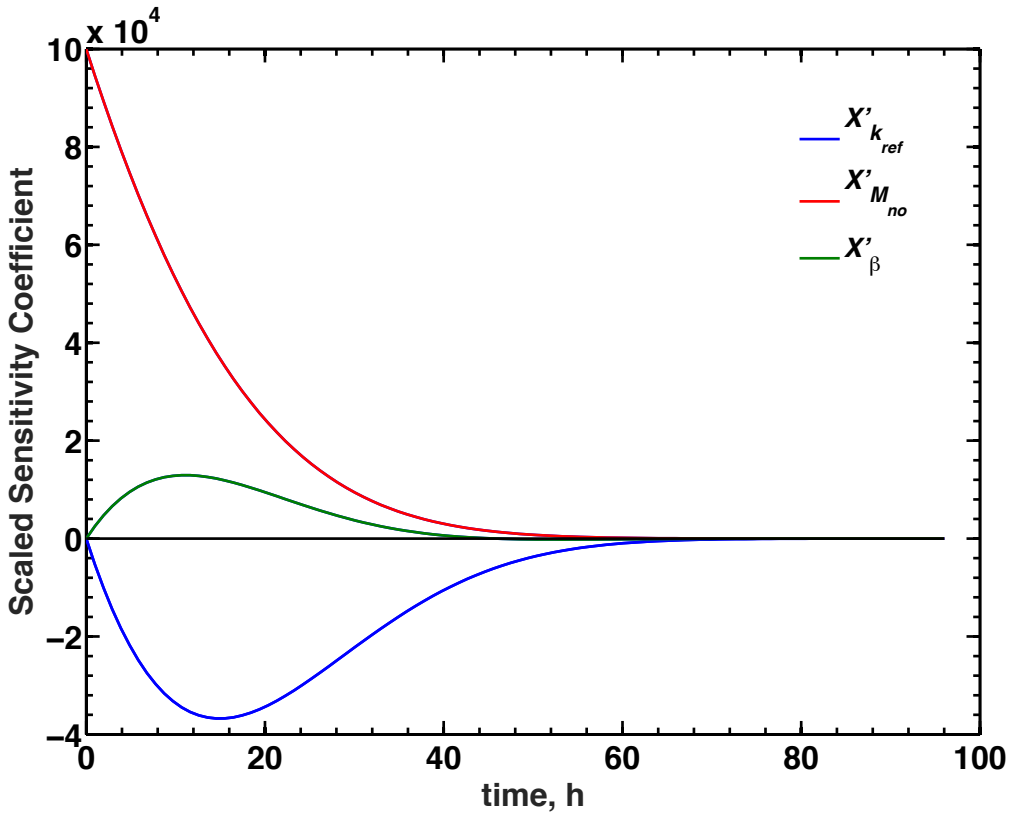


**Figure 4D.2** SSC of hydrolytic degradation of PLA in 50% ethanol at 80 °C and different *pH* using simulated dynamic *pH* (**Eq. 4.10**) in **Eq. 4.7** at $pH_{ref}$ = 7.33. Initial guesses: $k_{ref}$ = 0.093 $h^{-1}$, $M_{no}$ = 100,000 Da, $\beta$ = 0.147.

The correlation coefficient among the estimated parameters at average $pH_{ref}$ can be found in **Table 4D.1**. The correlation coefficient between $k_{ref}$ and $\beta$ was -0.1023. However, to perform a better estimation with a near zero correlation between $k_{ref}$ and $\beta$, an iterative search for $pH_{ref}$ was conducted until the correlation coefficient between $k_{ref}$ and $\beta$ showed near zero correlation. **Figure 4D.3** shows the plot of the correlation coefficient between $k_{ref}$ and $\beta$ using different $pH_{ref}$ values. The optimum $pH_{ref}$ was 7.697 with a correlation coefficient for $k_{ref}$ and $\beta$ of $-5.4879 \times 10^{-5}$ (**Table 4D.2**).

**Table 4D.1** Correlation matrix of the estimated parameters at the average $pH_{ref}$ = 7.33 (**Eq. 4.7**).

| Parameter | $k_{ref}$ | $M_{no}$ | $\beta$ | Relative error, % |
|---|---|---|---|---|
| $k_{ref}$ | 1.0000 | 0.5878 | -0.1023 | 5.21 |
| $M_{no}$ | 0.5878 | 1.0000 | -0.1787 | 2.47 |
| $\beta$ | -0.1023 | -0.1787 | 1.0000 | 6.74 |

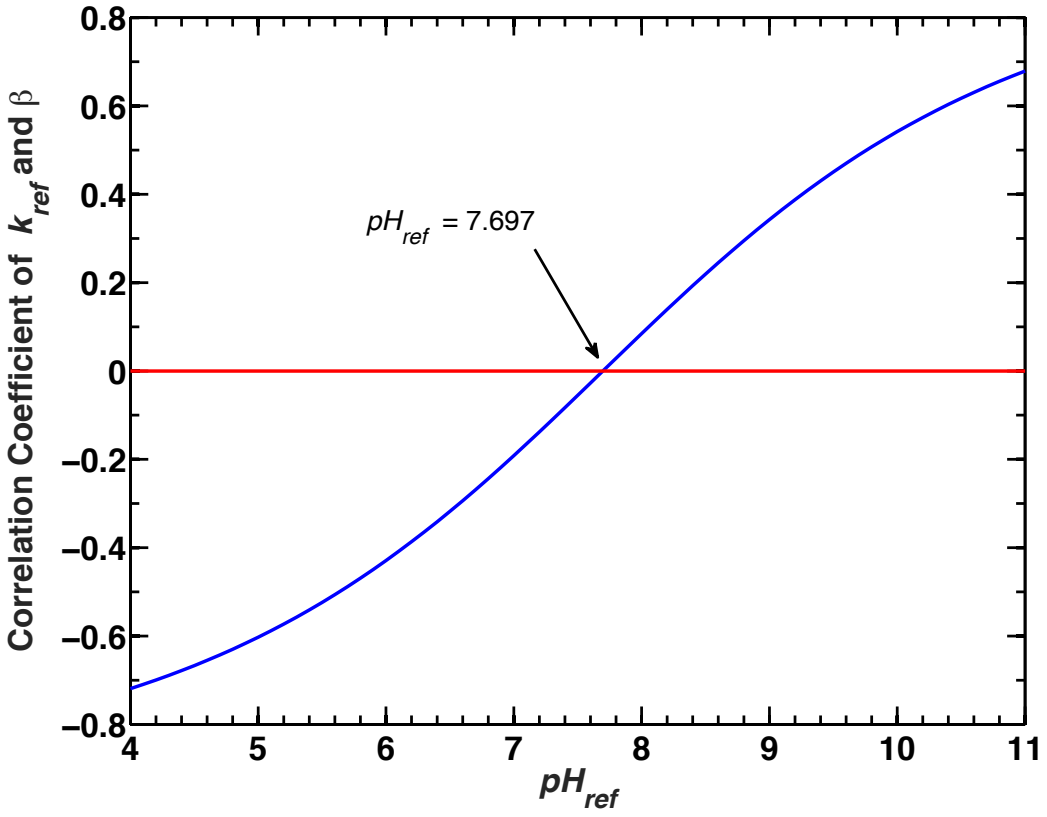


**Figure 4D.3** Plot of correlation coefficient of $k_{ref}$ and $\beta$ as a function of possible $pH_{ref}$ using **Eq. 4.7**.

**Table 4D.2** Correlation matrix of the estimated parameters at the optimum $pH_{ref}$ = 7.697 (**Eq. 4.7**).

| Parameter | $k_{ref}$ | $M_{no}$ | $\beta$ | Relative error, % |
|---|---|---|---|---|
| $k_{ref}$ | 1.0000 | 0.5726 | -0.0000* | 5.18 |
| $M_{no}$ | 0.5726 | 1.0000 | -0.1788 | 2.47 |
| $\beta$ | -0.0000* | -0.1788 | 1.0000 | 6.74 |

*$5.4879 \times 10^{-5}$

To estimate the $E_a$ as a function of $pH$ using **Eq. 4.6** with the final $\beta$ = 0.2153 and $pH_{ref}$ = 7.697 previously estimated, it is necessary to find the optimum $T_{ref}$**.** Since there is also no information regarding $T_{ref}$, the first value used for the estimation was the average temperature used in the experiments, 62.5 °C. **Table 4D.3** shows the correlation matrix of the estimated values at the average $T_{ref}$. The correlation coefficient between $E_a$ and $k_{ref}$ was 0.2920; however, near zero correlation needs to be achieved for a better estimation. After the iterative search of the correlation coefficient between $k_{ref}$ and $E_a$ was performed **(Figure 4D.4**), it was determined that the optimal $T_{ref}$ = 56.538 °C with a correlation between $k_{ref}$ and $E_a$ of $4.1080 \times 10^{-5}$ with relative errors of 3.31 and 1.63%, respectively (**Table 4D.4**). The non-linear estimation was performed using the optimum $T_{ref}$ resulting in an $E_a = 9.589 \times 10^4$ J/mol.

**Table 4D.3** Correlation matrix of the estimated parameters at the average $T_{ref}$ = 62.5 °C (**Eq. 4.6**).

| Parameter | $k_{ref}$ | $M_{no}$ | $E_a$ | Relative Error, % |
|---|---|---|---|---|
| $k_{ref}$ | 1.0000 | 0.5601 | 0.2920 | 3.46 |
| $M_{no}$ | 0.5601 | 1.0000 | 0.1278 | 1.64 |
| $E_a$ | 0.2920 | 0.1278 | 1.0000 | 1.63 |

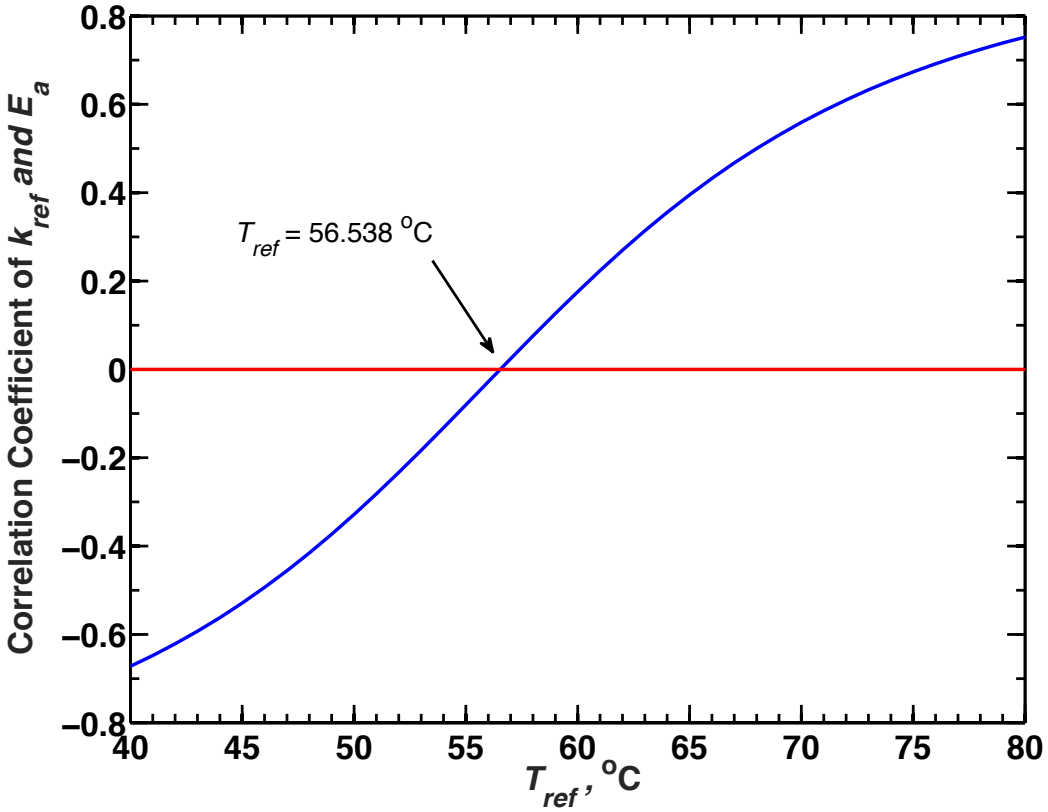


**Figure 4D.4** Plot of correlation coefficient of $k_{ref}$ and $E_a$ as a function of possible $T_{ref}$ using **Eq. 4.6**.

**Table 4D.4** Correlation matrix of the estimated parameters at the optimum $T_{ref}$ = 56.538 °C (**Eq. 4.6**).

| Parameter | $k_{ref}$ | $M_{no}$ | $E_a$ | Relative Error, % |
|---|---|---|---|---|
| $k_{ref}$ | 1.0000 | 0.5466 | 0.0000* | 3.31 |
| $M_{no}$ | 0.5466 | 1.0000 | 0.1278 | 1.64 |
| $E_a$ | 0.0000* | 0.1278 | 1.0000 | 1.63 |

*$4.1080 \times 10^{-5}$

To study whether the *pH* correction would affect the $E_a$ for the hydrolytic degradation of PLA in 50% ethanol, **Eq. 4.5** from the reparameterization of the Arrhenius equation was applied. The initial $T_{ref}$ applied for the estimation was the average of the experiments performed. **Figure 4D.5** shows the SSC constructed by the $T_{sim}$ approach (**Eq. 4.9**) consisting of the parameters $k_{ref}$, $M_{no}$ and $E_a$. From the *X´* plot $M_{no}$ is identified as the easiest parameter to be estimated and therefore the lowest relative error followed by $E_a$ and $k_{ref}$. **Table 4D.5** shows the correlation coefficient among the estimated parameters using $T_{ref}$ at the temperature average of 62.5 °C. The correlation coefficient between $E_a$ and $k_{ref}$ was 0.2401; however, near zero correlation is desired for a better estimation of $E_a$. Therefore, an iterative search for $T_{ref}$ was performed to find a near zero correlation between $E_a$ and $k_{ref}$. **Figure 4D.6** shows the iteration of different $T_{ref}$ with the respective correlation coefficient of $E_a$ and $k_{ref.}$ When $T_{ref}$ = 57.688 °C the correlation between $E_a$ and $k_{ref}$ was $1.2976 \times 10^{-5}$ with relative errors of 3.52 and 1.79, respectively (**Table 4D.6**).

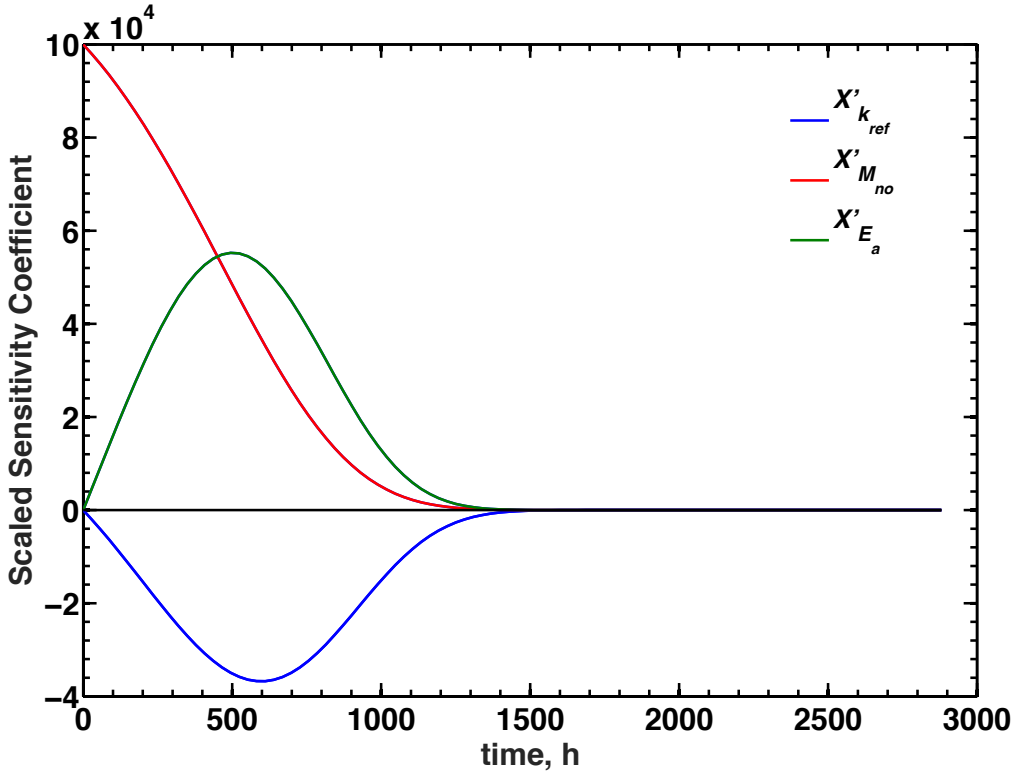


**Figure 4D.5** SSC of the activation energy estimation at $T_{ref}$ = 62.5 °C of hydrolytic degradation of PLA in 50% ethanol using simulated dynamic temperature (**Eq. 4.9**) in **Eq. 4.5**. Initial guesses: $k_{ref}$ = 0.007 $h^{-1}$, $M_{no}$ = 100,000 Da, $E_a$ = 9.04 x$10^4$ J.$mol^{-1}$.

**Table 4D.5** Correlation matrix of the estimated parameters at the average $T_{ref}$ = 62.5 °C for hydrolytic degradation of PLA in 50% ethanol solution (**Eq. 4.5**).

| **Parameter** | $k_{ref}$ | $M_{no}$ | $E_a$ | **Relative Error, %** |
|---|---|---|---|---|
| $k_{ref}$ | 1.0000 | 0.5619 | 0.2401 | 3.63 |
| $M_{no}$ | 0.5619 | 1.0000 | 0.1049 | 1.47 |
| $E_a$ | 0.2401 | 0.1049 | 1.0000 | 1.79 |

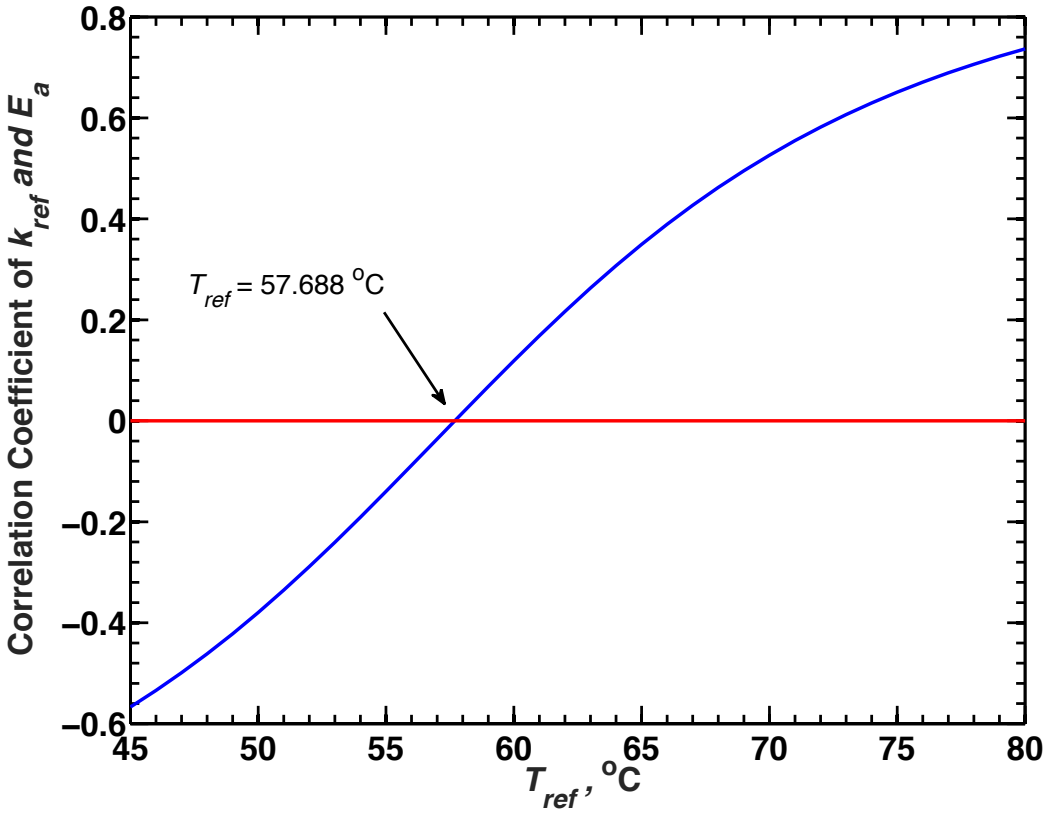


**Figure 4D.6** Plot of correlation coefficient of $k_{ref}$ and $E_a$ as a function of possible $T_{ref}$ for hydrolytic degradation of PLA in 50% ethanol solution (**Eq. 4.5**).

**Table 4D.6** Correlation matrix of the estimated parameters at the optimum $T_{ref}$ = 57.688 °C for hydrolytic degradation of PLA in 50% ethanol solution (**Eq. 4.5**).

| **Parameter** | $k_{ref}$ | $M_{no}$ | $E_a$ | **Relative Error, %** |
|---|---|---|---|---|
| $k_{ref}$ | 1.0000 | 0.5529 | 0.0000* | 3.52 |
| $M_{no}$ | 0.5529 | 1.0000 | 0.1049 | 1.47 |
| $E_a$ | 0.0000* | 0.1049 | 1.0000 | 1.79 |

*$1.2976 \times 10^{-5}$

## APPENDIX 4E: Parameter estimation of the $E_a$ for the hydrolysis of PLA in water

For initial estimations in water, the $T_{ref}$ selected was 75 °C, the average temperature of hydrolysis in water (60 – 90 °C, giving a correlation coefficient between $E_a$ and $k_{ref}$ of -0.0721 (**Table 4E.1**). After the iteration of different values of $T_{ref}$, the optimum value resulted in $T_{ref}$ = 75.931 °C (**Table 4E.1**) with a correlation coefficient of $1.5516 \times 10^{-5}$ between $E_a$ and $k_{ref}$ and relative errors of 2.39 and 3.43%, respectively (**Table 4E.2**).

**Table 4E.1** Correlation matrix of the estimated parameters at the average $T_{ref}$ = 75 °C for hydrolytic degradation of PLA in 50% ethanol solution (**Eq. 4.5**).

| **Parameter** | $k_{ref}$ | $M_{no}$ | $E_a$ | **Relative Error, %** |
|---|---|---|---|---|
| $k_{ref}$ | 1.0000 | 0.4877 | -0.0721 | 2.84 |
| $M_{no}$ | 0.4877 | 1.0000 | -0.0261 | 1.51 |
| $E_a$ | -0.0721 | -0.0261 | 1.0000 | 2.20 |

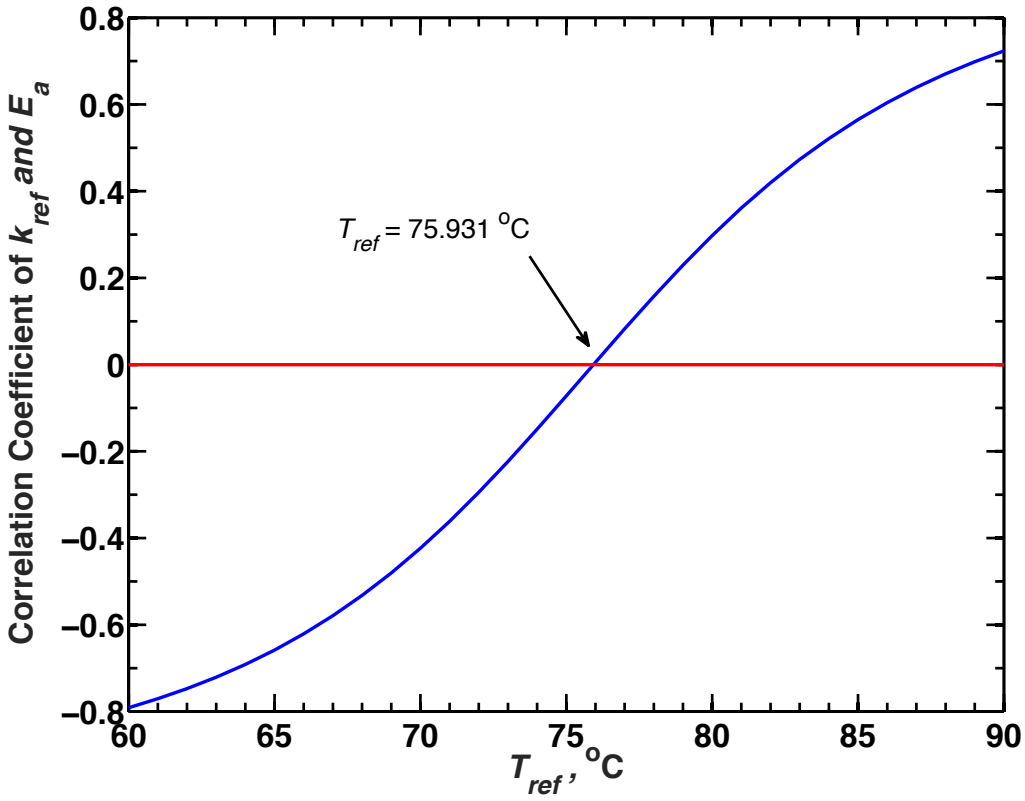


**Figure 4D.7** Plot of correlation coefficient of $k_{ref}$ and $E_a$ as a function of possible $T_{ref}$ for hydrolytic degradation of PLA in water (**Eq. 4.5**).

**Table 4E.2** Correlation matrix of the estimated parameters at the optimum $T_{ref}$ = 75.931 °C for hydrolytic degradation of PLA in water (**Eq. 4.5**).

| **Parameter** | $k_{ref}$ | $M_{no}$ | $E_a$ | **Relative Error, %** |
|---|---|---|---|---|
| $k_{ref}$ | 1.0000 | 0.4871 | 0.0000* | 2.48 |
| $M_{no}$ | 0.4871 | 1.0000 | -0.0261 | 1.51 |
| $E_a$ | 0.0000* | -0.0261 | 1.0000 | 2.20 |

*$1.5516 \times 10^{-5}$

**APPENDIX 4F: *MWD* of PLA films during hydrolytic degradation when in contact with 50% ethanol at 80 °C and different *pH***

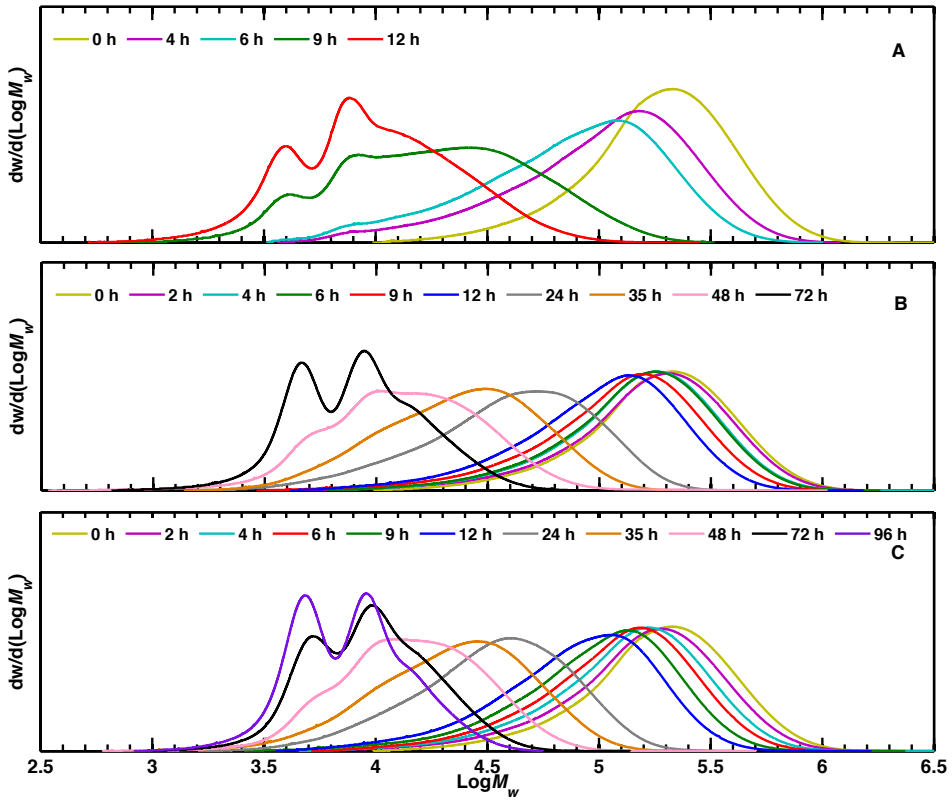


**Figure 4F.1** *MWD* of PLA films during hydrolytic degradation when in contact with 50% ethanol at 80 °C and different *pH*: (A) 11, (B) 7, and (C) 4.

# REFERENCES

## REFERENCES


[1] R. Auras, B. Harte, S. Selke, An overview of polylactides as packaging materials, Macromol. Biosci. 4 (2004) 835-864.

[2] E. Castro-Aguirre, F. Iñiguez-Franco, H. Samsudin, X. Fang, R. Auras, Poly (lactic acid)—Mass production, processing, industrial applications, and end of life, Adv. Drug Deliv. Rev. 107 (2016) 333-366.

[3] C. Chariyachotilert, S.E. Selke, R.A. Auras, S. Joshi, Assessment of the properties of poly (L-lactic Acid) sheets produced with differing amounts of post-consumer recycled poly (L-lactic Acid), J. Plast. Film Sheet. 28 (2012) 314-335.

[4] K. Hamad, M. Kaseem, F. Deri, Recycling of waste from polymer materials: An overview of the recent works, Polym. Degrad. Stab. 98 (2013) 2801-2812.

[5] V. Piemonte, S. Sabatini, F. Gironi, Chemical recycling of PLA: a great opportunity towards the sustainable development?, J. Polym. Environ. 21 (2013) 640-647.

[6] H. Tsuji, Hydrolytic Degradation, in: R. Auras, L.-T. Lim, S. Selke, H. Tsuji (Eds.), Poly(lactic acid). Synthesis, Structures, Properties, Processing, and Applications, John Wiley & Sons, Inc., New Jersey, 2010, pp. 345-381.

[7] K. Okamoto, K. Toshima, S. Matsumura, Degradation of poly (lactic acid) into repolymerizable oligomer using montmorillonite K10 for chemical recycling, Macromol. Biosci. 5 (2005) 813-820.

[8] Y. Tsuneizumi, M. Kuwahara, K. Okamoto, S. Matsumura, Chemical recycling of poly (lactic acid)-based polymer blends using environmentally benign catalysts, Polym. Degrad. Stab. 95 (2010) 1387-1393.

[9] P. Coszach, J.-C. Bogaert, J. Willocq, Chemical recycling of PLA by hydrolysis. United States Patent 8431683 B2, in, 2013.

[10] P. Coszach, J.-C. Bogaert, J. Willocq, Chemical recycling of PLA by alcoholysis. United States Patent 848675 B2, in, 2013.

[11] F. Gironi, S. Frattari, V. Piemonte, PLA Chemical Recycling Process Optimization: PLA Solubilization in Organic Solvents, J. Polym. Environ. 24 (2016) 328-333.

[12] H. Tsuji, H. Daimon, K. Fujie, A new strategy for recycling and preparation of poly (L-lactic acid): hydrolysis in the melt, Biomacromolecules 4 (2003) 835-840.

[13] H. Tsuji, T. Saeki, T. Tsukegi, H. Daimon, K. Fujie, Comparative study on hydrolytic degradation and monomer recovery of poly (L-lactic acid) in the solid and in the melt, Polym. Degrad. Stab. 93 (2008) 1956-1963.

[14] S. De Jong, E.R. Arias, D. Rijkers, C. Van Nostrum, J. Kettenes-Van den Bosch, W. Hennink, New insights into the hydrolytic degradation of poly (lactic acid): participation of the alcohol terminus, Polymer 42 (2001) 2795-2802.

[15] F. Iñiguez-Franco, R. Auras, G. Burgess, D. Holmes, X. Fang, M. Rubino, H. Soto-Valdez, Concurrent solvent induced crystallization and hydrolytic degradation of PLA by water-ethanol solutions, Polymer 99 (2016) 315-323.

[16] M.K. Mitchell, D.E. Hirt, Degradation of PLA fibers at elevated temperature and humidity, Polym. Eng. Sci. (2014).

[17] N. Weir, F. Buchanan, J. Orr, D. Farrar, G. Dickson, Degradation of poly-L-lactide. Part 2: increased temperature accelerated degradation, Proc. Inst. Mech. Eng. H J. Eng. Med. 218 (2004) 321-330.

[18] A.-F. Mohd-Adnan, H. Nishida, Y. Shirai, Evaluation of kinetics parameters for poly (L-lactic acid) hydrolysis under high-pressure steam, Polym. Degrad. Stab. 93 (2008) 1053-1058.

[19] Q. Zhou, M. Xanthos, Nanoclay and crystallinity effects on the hydrolytic degradation of polylactides, Polym. Degrad. Stab. 93 (2008) 1450-1459.

[20] F. Codari, S. Lazzari, M. Soos, G. Storti, M. Morbidelli, D. Moscatelli, Kinetics of the hydrolytic degradation of poly (lactic acid), Polym. Degrad. Stab. 97 (2012) 2460-2466.

[21] J. Ahmed, K. Dolan, D. Mishra, Chemical reaction kinetics pertaining to foods, in: Ahmed Jasim, M.S. Rahman (Eds.), Handbook of Food Process Design, Wiley & Blackwell-Publication, London, 2012, pp. 113-166.

[22] A.K. Agarwal, M.L. Brisk, Sequential experimental design for precise parameter estimation. 1. Use of reparameterization, Ind. Eng. Chem. Process Des. Dev. 24 (1985) 203-207.

[23] A.K. Agarwal, M.L. Brisk, Sequential experimental design for precise parameter estimation. 2. Design criteria, Ind. Eng. Chem. Process Des. Dev. 24 (1985) 207-210.

[24] D. Pritchard, D. Bacon, Statistical assessment of chemical kinetic models, Chem. Eng. Sci. 30 (1975) 567-574.

[25] M. Schwaab, J.C. Pinto, Optimum reference temperature for reparameterization of the Arrhenius equation. Part 1: Problems involving one kinetic constant, Chem. Eng. Sci. 62 (2007) 2750-2764.

[26] M. Schwaab, L.P. Lemos, J.C. Pinto, Optimum reference temperature for reparameterization of the Arrhenius equation. Part 2: Problems involving multiple reparameterizations, Chem. Eng. Sci. 63 (2008) 2895-2906.

[27] K.D. Dolan, D.K. Mishra, Parameter estimation in food science, Annu. Rev. Food Sci. Technol. 4 (2013) 401-422.

[28] H. Samsudin, Migration of antioxidants from poly (lactic acid), PLA, films into food simulants: A parameter estimation approach, in, Michigan State University, 2015.

[29] ASTM, Standard 4754-11. Standard test method for two-sided liquid extraction of plastic materials using FDA migration cell, ASTM International, West Conshohocken, PA, 2011.

[30] F. Iñiguez-Franco, R. Auras, M. Rubino, K. Dolan, H. Soto-Valdez, S. Selke, Effect of nanoparticles on the hydrolytic degradation of PLA-nanocomposites by water-ethanol solutions, Polym. Degrad. Stab. Accepted (2017).

[31] M. Wojdyr, Fityk: a general-purpose peak fitting program, J. Appl. Crystallogr. 43 (2010) 1126.

[32] A. Perejón, P.E. Sánchez-Jiménez, J.M. Criado, L.A. Pérez-Maqueda, Kinetic analysis of complex solid-state reactions. A new deconvolution procedure, J. Phys. Chem. B 115 (2011) 1780-1791.

[33] D.F. Smith, I.M. Hildebrandt, K.E. Casulli, K.D. Dolan, B.P. Marks, Modeling the Effect of Temperature and Water Activity on the Thermal Resistance of Salmonella Enteritidis PT 30 in Wheat Flour, J. Food Prot. 79 (2016) 2058-2065.

[34] J.V. Beck, K.J. Arnold, Parameter estimation in engineering and science, James Beck, 1977.

[35] B. Hahn-Hägerdal, M. Galbe, M.-F. Gorwa-Grauslund, G. Lidén, G. Zacchi, Bio-ethanol–the fuel of tomorrow from the residues of today, Trends Biotechnol. 24 (2006) 549-556.

[36] I. Muñoz, K. Flury, N. Jungbluth, G. Rigarlsford, L.M. i Canals, H. King, Life cycle assessment of bio-based ethanol produced from different agricultural feedstocks, Int. J. Life Cycle Assess. 19 (2014) 109-119.

[37] M. Balat, H. Balat, Recent trends in global production and utilization of bio-ethanol fuel, Appl. Energy 86 (2009) 2273-2282.

[38] ICIS. http://www.icis.com/chemicals/channel-info-chemicals-a-z/, 2017 (accessed September).

[39] S.V. Canevarolo, Chain scission distribution function for polypropylene degradation during multiple extrusions, Polym. Degrad. Stab. 70 (2000) 71-76.

[40] H. Tsuji, Y. Ikada, Blends of crystalline and amorphous poly (lactide). III. Hydrolysis of solution‐cast blend films, J. Appl. Polym. Sci. 63 (1997) 855-863.

[41] H. Tsuji, K. Nakahara, K. Ikarashi, Poly (L‐Lactide), 8. High‐Temperature Hydrolysis of Poly (L‐Lactide) Films with Different Crystallinities and Crystalline Thicknesses in Phosphate‐Buffered Solution, Macromol. Mater. Eng. 286 (2001) 398-406.

[42] H. Tsuji, K. Ikarashi, N. Fukuda, Poly (L-lactide): XII. Formation, growth, and morphology of crystalline residues as extended-chain crystallites through hydrolysis of poly (L-lactide) films in phosphate-buffered solution, Polym. Degrad. Stab. 84 (2004) 515-523.

[43] H. Tsuji, K. Ikarashi, In vitro hydrolysis of poly (l-lactide) crystalline residues as extended-chain crystallites: II. Effects of hydrolysis temperature, Biomacromolecules 5 (2004) 1021-1028.

[44] S. Bernard, K. Fiaty, D. Cornu, P. Miele, P. Laurent, Kinetic modeling of the polymer-derived ceramics route: investigation of the thermal decomposition kinetics of poly [B-(methylamino) borazine] precursors into boron nitride, J. Phys. Chem. B 110 (2006) 9048-9060.

[45] G.D. Sorarù, L. Pederiva, J. Latournerie, R. Raj, Pyrolysis kinetics for the conversion of a polymer into an amorphous silicon oxycarbide ceramic, J. Am. Ceram. Soc. 85 (2002) 2181-2187.

[46] V. Alvarez, A. Vázquez, Thermal degradation of cellulose derivatives/starch blends and sisal fibre biocomposites, Polym. Degrad. Stab. 84 (2004) 13-21.

[47] X. Yang, Z. Jiang, Kinetic studies of overlapping pyrolysis reactions in industrial waste activated sludge, Bioresour. Technol. 100 (2009) 3663-3668.

[48] C. Wagner, J. Vazquez, P. Villares, R. Jiménez-Garay, A theoretical method for resolving overlapping peaks in differential scanning calorimetry, Mater. Lett. 18 (1994) 280-285.

[49] G. Kale, R. Auras, S.P. Singh, Degradation of commercial biodegradable packages under real composting and ambient exposure conditions, J. Polym. Environ. 14 (2006) 317-334.

[50] G. Kale, R. Auras, S.P. Singh, R. Narayan, Biodegradability of polylactide bottles in real and simulated composting conditions, Polym. Test. 26 (2007) 1049-1061.

[51] O. Wachsen, K. Reichert, R.-P. Krüger, H. Much, G. Schulz, Thermal decomposition of biodegradable polyesters—III. Studies on the mechanisms of thermal degradation of oligo-l-lactide using SEC, LACCC and MALDI-TOF-MS, Polym. Degrad. Stab. 55 (1997) 225-231.

[52] O. Wachsen, K. Platkowski, K.-H. Reichert, Thermal degradation of poly-l-lactide—studies on kinetics, modelling and melt stabilisation, Polym. Degrad. Stab. 57 (1997) 87-94.

[53] H. Samsudin, R. Auras, D. Mishra, K. Dolan, G. Burgess, M. Rubino, S. Selke, H. Soto-Valdez, Migration of antioxidants from polylactic acid films: A parameter estimation approach and an overview of the current mass transfer models, Food Res. Int. (2017).

[54] J.H. Jung, M. Ree, H. Kim, Acid-and base-catalyzed hydrolyses of aliphatic polycarbonates and polyesters, Catal. Today 115 (2006) 283-287.

[55] K. Makino, H. Ohshima, T. Kondo, Mechanism of hydrolytic degradation of poly (L-lactide) microcapsules: effects of pH, ionic strength and buffer concentration, J. Microencapsulation 3 (1986) 203-212.

[56] H. Tsuji, K. Ikarashi, In vitro hydrolysis of poly (l-lactide) crystalline residues as extended-chain crystallites. Part I: long-term hydrolysis in phosphate-buffered solution at 37 C, Biomaterials 25 (2004) 5449-5455.

[57] V. Piemonte, F. Gironi, Kinetics of hydrolytic degradation of PLA, J. Polym. Environ. 21 (2013) 313-318.

[58] K. Dolan, Estimation of kinetic parameters for nonisothermal food processes, J. Food Sci. 68 (2003) 728-741.

# CHAPTER 5

## Effect of Nanoparticles on the Hydrolytic Degradation of PLA-Nanocomposites by Water-Ethanol Solutions

A version of this chapter is published as:

F. Iñiguez-Franco, R. Auras, M. Rubino, K. Dolan, H. Soto-Valdez, S. Selke. Effect of nanoparticles on the hydrolytic degradation of PLA-nanocomposites by water-ethanol solutions, Polymer Degradation and Stability 146 (2017) 287-297.

## 5.0 Abstract

Hydrolytic degradation of poly(lactic acid) (PLA-C) and PLA-nanocomposite produced with organomodified montmorillonite at 5 wt% (PLA-OMMT) were investigated in pure water, 50% and 95% ethanol solutions at 40 °C. The change in molecular weight, crystallinity, release of lactic acid (LA), and release of the organomodifier (QAC) were monitored. Ethanol sorption and glass transition temperature ($T_g$) *vs* ethanol fraction content were determined. Release of Al as a nanoclay marker was studied when PLA-OMMT was exposed to 50% ethanol solution. PLA-C and PLA-OMMT films had faster hydrolysis in 50% ethanol than in 95% ethanol and water. The incorporation of nanoclay did not have an effect on the hydrolytic degradation. The nanoclay doubled the sorption of ethanol into the film due to the sorption of ethanol into the nanoclay galleries. The nanoclay also acted as an anchor, restricting the movement of the polymer chains as evidenced by the $\Delta T_g$ and the crystallization behavior. Hydrolysis of PLA-C and PLA-OMMT was related with the release of LA during exposure. The release of QAC from PLA-OMMT films was higher in 95% ethanol at the early stages, but then it exponentially increased in 50% ethanol due to the faster hydrolytic degradation. The clay released from PLA-OMMT films during hydrolysis in 50% ethanol was 0.58% wt. at 90 d. of the initial amount of nanoclay in the PLA film.

## 5.1 Introduction

Global concern about environmental impacts of polymers has changed consumer preferences and led producers to decrease the use of plastics derived from fossil resources. Consequently, the production of novel plastics from renewable resources has increased. Poly (lactic acid), PLA, is a new bioplastic that has gained great attention

due to its lower environmental footprint and additional end of life scenario, composting [1, 2]. PLA, an aliphatic polyester, is manufactured by polymerization of lactic acid (LA) obtained by fermentation of corn or cassava starch [1, 2]. PLA has been used for an arrays of applications in broad and diverse industries for example medical [3-5], clothing [6], agricultural [7-10], and packaging [11-13]. However, PLA has some shortcomings such as low solvent resistant, brittleness, moderate barrier properties, and low thermal stability [2, 14].

Several approaches have been used to enhance PLA properties and to expand its applications. Some of these improvements have been achieved by the addition of fillers such as natural nanoclays, in particular, montmorillonite (MMT) with organomodifiers (OMMT) [15, 16]. MMT is a type of clay that belongs to the layered smectite group made up of several stacked layers with a thickness of 1 nm containing exchangeable cations (*e.g.*, $Na^+$, $K^+$, $Li^+$ and $Ca^{2+}$) in the interlayer space or gallery [17, 18]. The structure of the crystal is made of 2 silica tetrahedral sheets connected to an octahedral layer of alumina [16]. Since MMT is a hydrophilic clay, surface modification, by exchanging the cations in the galleries for organic cationic surfactants, increases the affinity of the nanoclay to polymers like PLA [16].

Although PLA-nanocomposites offer good mechanical, barrier and thermal properties, nanoparticles could have an effect on the hydrolytic degradation of PLA. The existence of nanoparticles in the polymer can increase the amount of water in the matrix accelerating the cleavage of the ester bonds on the main chain of the polymer due to the increase of the hydrophilicity of the polymer by the existence of the nanoparticles [19]. Other authors have also shown that the presence of the surfactant influences the

hydrolysis rate of PLA-nanocomposite materials. The faster degradation can be attributed to the hydroxyl groups of the surfactants improving the distribution of the clay in the polymer and resulting in easier water attack [20-22]. The hydrolysis rate depends on the dispersion of the filler, water uptake and the ability of hydrating by the fillers. Other studies have addressed the impact of OMMT on the hydrolytic degradation of PLA-nanocomposites in water and phosphate buffered solutions [19, 20, 23].

Nanocomposites can be used in different environments, such as organic compounds, acidic surroundings, mixtures of solvents, or different media for food applications (*e.g.*, juices, alcoholic beverage, cold-chain dairy products). PLA is susceptible to hydrolytic degradation under moist conditions, leading the reduction of molecular weight and the release of LA monomers and soluble LA oligomers [2, 24]. The presence of organic solvents, such as ethanol, plasticizes the PLA matrix, inducing the chain mobility and crystallization affecting the degradation rate of the polymer [25-31]. The transport of water-ethanol solutions into PLA-nanocomposites could differ from neat PLA where the release of nanoparticles and the surfactant could occur changing the hydrolysis behavior and therefore the durability and performance of PLA. Understanding the effect of nanoparticles on the hydrolysis of PLA in water-ethanol solutions and the interactions within the system is essential for the development of safe PLA-nanocomposites. The goal of this work was to understand the effect of adding nanoparticles and surfactant on the hydrolysis of PLA-nanocomposites in water-ethanol solutions and the interaction between PLA, nanoclay and solvent.

## 5.2 Materials and methods

### 5.2.1 Chemicals and reagents

From NatureWorks LLC (Minnetonka, MN, USA), PLA resin Ingeo™ 2003D (3.8 – 4.2 wt.% D-LA) was procured. The relative number ($M_n$) and weight ($M_w$) average molecular weight of the resin was 1.21 ± 0.08 x $10^5$ Da and 2.35 ± 0.07 x $10^5$ Da, respectively. The nanoclay used was Cloisite®30B (OMMT) obtained from BYK Additives Inc. (Gonzalez, TX, USA) having 73% wt MMT and 27% wt surfactant (QAC) (methyl, tallow, bis-2-hydroxyethyl, quaternary ammonium). The surfactant available on the nanoclay (Tomamine™Q-T-2 70%PG) was also obtained separately at 60 – 70% purity having 30 – 40% propylene glycol (Air Products and Chemicals Inc., Butler, IN, USA). The surfactant consists of methyl tallow ranging from 14 to 18 carbons (~60% C18; ~35% C16; ~5% C14). Ethanol, acetonitrile, methanol (all HPLC grade), formic acid and propyl hydroxy benzoate were procured (Sigma-Aldrich, St. Louis, MO, USA). Tetrahydrofuran (THF) was obtained from Pharmco-AAPER (North East, CA, USA). The HPLC grade water was obtained from J.T. Baker (Center Valley, PA, USA). Malonic acid was procured from Columbus Chemical Industries (Columbus, WI, USA). L(+) LA was obtained from Supelco (Bellefonte, PA, USA). The water used for the LC/MS/MS mobile phase was purified by a Milli-Q System (Millipore Corp., Bedford, MA, USA).

### 5.2.2 Production of films

PLA films were prepared by drying PLA pellets at 60 °C for 24 h and 85 kPa. PLA-OMMT (OMMT 5% wt) and PLA-QAC (surfactant 1.5% wt) films were processed in two stages. In the first stage masterbatches were prepared in a twin-screw extruder model ZSK 30 (Werner Pfleiderer, NJ, USA). PLA-OMMT masterbatch consisted of

80% wt of PLA dried pellets and 20% wt of Cloisite®30B with processing temperatures of 148 – 189 °C. For PLA-QAC masterbatch (surfactant 2.5% wt), the range of processing temperature was 148 – 185 °C. In the second stage the films were cast using a Randcastle microextruder (Extrusion System, Inc., Cedar Grove, NJ, USA) having a 1.5875 cm diameter screw, 34 cc volume, and 24/1 L/D ratio extruder. PLA-OMMT film was processed by mixing 25% wt of the masterbatch with 75% wt of PLA previously dried as mentioned. The extrusion temperatures for PLA-OMMT film were between 193 – 248 °C and 18 rpm. For PLA-QAC film lower temperature range of 143 – 173 °C and 30.5 rpm was used since QAC acted as a plasticizer during extrusion, lowering the processing temperature. A control film was produced (PLA-C) in the same cast film extruder as PLA-OMMT and PLA-QAC films with extrusion temperatures of 193 – 215 °C and 49 rpm. Each processing temperature range was selected to obtain good films for experimental methods. The thicknesses of the films were different where PLA-OMMT was the thinnest being 27.9 ± 9.9, 10.3 ± 1.5 and 35.9 ± 10.6 μm for PLA-C, PLA-OMMT and PLA-QAC, respectively.

### 5.2.3 Characterization of PLA-OMMT film

TEM (Transmission electron microscopy) and XRD (X-ray diffraction) were used to characterize the structure of PLA-OMMT films. TEM analyses were performed in a JEOL 100CX II TEM manufactured by JEOL, USA, Inc. (Peabody, MA, USA). To assess the spatial distribution of the nanoparticles, the PLA-OMMT films were embedded into a resin to provide support for the film during the ultramicrotomy and to retain the spatial organization of the specimen section on the TEM grid. The polymerization of the resin was carried out in an oven during two days at 60 °C.

Microtomed sections (100 nm) were obtained using an ultramicrotome RMC MYX (Boeckeler Instruments, Inc., Tucson, AZ, USA), and observed with an acceleration voltage of 120 kV in the bright field imaging mode.

XRD analyses were performed by a Rigaku Rotaflex Ru-200BH X-ray diffractomer with a Ni-filtered Cu Kα radiation source at 40 kV and 100 mA. PLA-OMMT and PLA-C films were analyzed using a 2θ range between 1.5° and 6° at 0.3 °/min with 0.01° increment. To evaluate the original interlayer space, clay powder was analyzed. The interlayer spacing was calculated according to Bragg's Law [32].

### 5.2.4 Storage experiments

Ten disks of 2.0 cm in diameter of PLA-C, PLA-OMMT and PLA-QAC films were inserted in wire made of stainless-steel and the disk were separated by glass beads. A schematic representation of the cells is in the Appendix 5B (**Figure 5B.1**). Then they were placed in cells containing different water-ethanol solutions previously conditioned at 40 °C: water, 50% ethanol, or 95% ethanol (v/v). The surface area to fluid volume ratio of the films was 1.79 $cm^2$/mL. The degradation through hydrolysis of PLA films and release tests were performed using a migration cell as indicated in ASTM D4754-11 at 40 °C [33]. Samples of the film were retrieved periodically to assess $M_w$ and $M_n$, and samples of the solution were also removed to evaluate LA and QAC release.

### 5.2.5 Molecular weight

$M_w$ and $M_n$ were tested as previously described by the authors [29]. In brief, film (10 mg) was taken from the vials and dissolved in THF (2 mg/mL) and tested using gel permeation chromatography (GPC). The measurements were conducted in triplicate.

To calculate the rate constants for the change in $M_n$ of PLA films, the experimental data was fitted using a first order reaction funded on the criteria that the expansion of the polymer material is because of the increase in emptied space as previously demonstrated by the authors when PLA was in contact with water-ethanol solutions [29]:

$$M_n = M_{n_0} exp(-kt) \quad \text{Eq. 5.1}$$

with

$$k = \beta \left[ \frac{V_o}{V_d} + \left( 0.06 - \frac{V_o}{V_d} \right) p - 0.06 p^2 \right] \quad \text{Eq. 5.2}$$

where $M_{n_0}$ is the initial $M_n$ (Da), $t$ is time (s), $k$ is the rate constant ($d^{-1}$), $V_o$ is the initial empty space that is in the PLA matrix ($cm^3$), $V_d$ is the disk volume ($cm^3$), $\beta$ is a constant, and $p$ is the fraction of ethanol ($p$ = 0, 0.5, 0.95). However, for better estimation of $k$, the Taylor series expansion was applied in this work following the same concept of the expansion of the polymer, replacing Eq. 2 by:

$$k = \frac{(p - p_{0.5})(p - p_{0.95})}{(p_0 - p_{0.5})(p_0 - p_{0.95})} k_{p=0} + \frac{(p - p_0)(p - p_{0.95})}{(p_{0.5} - p_0)(p_{0.5} - p_{0.95})} k_{p=0.5} + \frac{(p - p_0)(p - p_{0.5})}{(p_{0.95} - p_0)(p_{0.95} - p_{0.5})} k_{p=0.95} \quad \text{Eq. 5.3}$$

where $k_{p=0}, k_{p=0.5}$ and $k_{p=0.95}$ are rate constant for water, 50% and 95% ethanol, respectively. **Eq. 5.1** and **Eq. 5.3** were fitted in MATLAB® 2016a (MathWorks, Natick, MA, USA) using the nonlinear regression (*nlin-fit*), so $M_{n_0}$, $k_{p=0}$, $k_{p=0.5}$ and $k_{p=0.95}$ could

be estimated. Mean comparisons of the studied parameters among treatments were done by Tukey HSD test ($p<0.05$) using JMP® 9.0 (Cary, NC, USA) statistical software.

### 5.2.6 Water and ethanol sorption

Water vapor sorption isotherms of PLA-C and PLA-OMMT films were determined for relative humidity ranging from 5 to 95%. Ethanol vapor sorption isotherms for PLA-C, PLA-OMMT and clay (Cloisite®30B) were carried out at 40 °C with relative pressures (*i.e.*, partial ethanol vapor pressure/saturation ethanol vapor pressure) from 0.05 to 0.70. Isotherms were obtained by gravimetric analysis with a SGA-100 (VTI Corp., Hialeah, FL, USA). Between 15 and 20 mg of sample was used and the measurements were conducted in triplicate.

Ethanol sorption of PLA-C and PLA-OMMT films in contact with different volume fractions of water-ethanol solutions was evaluated at 40 °C. Samples were analyzed using $^{1}$H NMR (proton nuclear magnetic resonance) in a Varian Inova 600 MHz NMR-Spectrometer, which was equipped with a Nalorac 5 mm PFG switchable probe (599.892 MHz). A detailed description of the $^{1}$H NMR technique was previously provided [29]. The measurements were conducted in triplicate.

### 5.2.7 Dynamic mechanical analysis (DMA)

The loss factor (tan delta) *vs* temperature was analyzed to determine the glass transition temperature ($T_g$) of PLA-C and PLA-OMMT films where they were submerged in different water-ethanol solutions during the testing with a TA RSA-G2 (TA Instruments, New Castle, DE, USA) as previously described [29].

### 5.2.8 Differential scanning calorimetry (DSC)

The degree of crystallinity ($\%X_C$), crystallization temperature ($T_c$), $T_g$, and melting temperature ($T_m$) of PLA-C and PLA-OMMT films that had been immersed in 50% ethanol at 40 °C were obtained using a DSC (Q100, TA Instruments). The samples were retrieved periodically and dried before being analyzed. The samples were cooled from 25 to 5 °C and then run from 5 to 210 °C at 10 °C/min using a flow rate of purge nitrogen of 70 mL/min. The first run of the heat scan of the samples is reported. The measurements were conducted in triplicate.

### 5.2.9 Lactic acid release

LA release from PLA-C, PLA-OMMT and PLA-QAC films into water, 50% and 95% ethanol at 40 °C was determined as previously described by the authors [29]. In brief, 0.5 mL of solution from the test cells were retrieved regularly and then an alkali hydrolysis was performed. Samples with 50% and 95% ethanol were evaporated and later reconstituted with 0.5 mL of water. LA was evaluated using a LC/MS/MS system.

### 5.2.10 Surfactant release

The release of the surfactant (QAC) from PLA-OMMT and PLA-QAC films was studied using a LC/MS/MS system (AB/Sciex QTRAP 3200, Framingham, MA, USA) having a triple quadrupole/linear ion trap. Separation was performed on a Symmetry C18 (3.5 µm, 2.1 x 100 mm) reverse phase column (Waters, Milford, MA, USA) at a flow rate of 0.3 mL/min. The mobile phase was A: 1% formic acid and B: acetonitrile. The programming of the solvent was isocratic for 1.5 minutes with 1% B. Then a linear increase to 95% B up to 3.5 minutes was programmed, followed by an isocratic mode for 2.5 minutes. A linear gradient was done for 0.01 minutes to 5% B and held for 2 min

- isocratic mode. The oven temperature was kept at 40 °C. The analyses were carried out in the positive-ion mode using the ion spray method. The calibration curve was determined from solutions of 0.25 to 15 µg/mL using propyl hydroxy benzoate as the internal standard.

### 5.2.11 Nanoclay release

The release of nanoclay from PLA-OMMT films into 50% ethanol solution was determined using a graphite furnace atomic absorption spectrometry (GFAAS) (Perkin Elmer, Waltham, MA, USA). Al was selected as the nanoclay marker element. The nanoclay concentration was estimated by correlating with the concentrations of Al based on the elemental content in the nanoclay. The samples were prepared as previously described, but with the glass vials replaced as migration cells by 50 mL PP tubes and Teflon beads to avoid potential migration of aluminum from the glass. The experiment was conducted in quadruplicate.

## 5.3 Results and discussion

The influence of nanoparticles on the hydrolytic degradation of PLA-nanocomposites by different water-ethanol solutions, the variation in $M_n$ of PLA-C, PLA-OMMT and PLA-QAC was analyzed during exposure to water, 50% and 95% ethanol solutions to determine the rate of hydrolysis. Since water molecules influence the hydrolysis reactions, the sorption of water was determined for PLA-C and PLA-OMMT films using vapor isotherms. However, the presence of ethanol affects the water sorption due to PLA swelling. So, swelling studies were performed where the films were immersed into different volume fractions of water-ethanol. To study the possible

sorption of ethanol by the clays, ethanol sorption isotherms were determined for PLA-C, PLA-OMMT and clay powder. Crystallinity studies of PLA-C and PLA-OMMT were carried out over the exposure time in 50% ethanol to assess solvent induced crystallization (SIC) by ethanol molecules and to describe the crystalline and non-crystalline phases of the polymer during hydrolysis. LA and QAC release were evaluated for PLA-C, PLA-OMMT and PLA-QAC films when they were immersed in the different water-ethanol solutions. Finally, the release of clay from PLA-OMMT film to 50% ethanol was assessed during hydrolytic degradation.

### 5.3.1 Characterization of PLA-OMMT film

XRD patterns of OMMT clay powder, PLA-OMMT and PLA-C films between 2θ = 1.5° and 6° are shown in **Figure 5.1**. The spacing between the layers for the OMMT powder was 1.85 nm (2θ = 4.75 °). The *d*-spacing of the OMMT increased to 3.42 nm (2θ = 2.6) when embedded into the PLA matrix. The increase of the interlayer spacing and the displacement of the peak at a smaller angle indicated that the polymer entered the clay gallery, forming an intercalated nanocomposite. These results are consistent with other studies using OMMT at different concentrations within a PLA matrix resulting in intercalated nanocomposites [17, 34, 35]. The intercalated structure was confirmed by the TEM images (**Figure 5.2**) where the silicate monolayers are randomly distributed, but not well exfoliated in the PLA matrix.

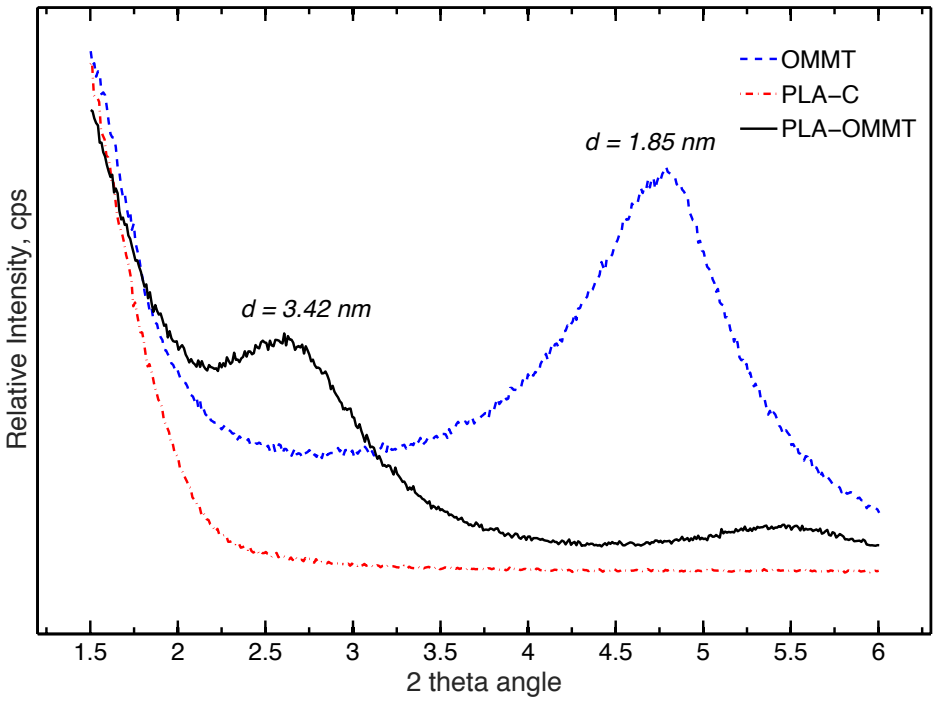


**Figure 5.1** Displacement of diffraction pattern of the OMMT clay when embedded in the PLA matrix. XRD patterns for OMMT clay powder, PLA-OMMT and PLA films.

(A)

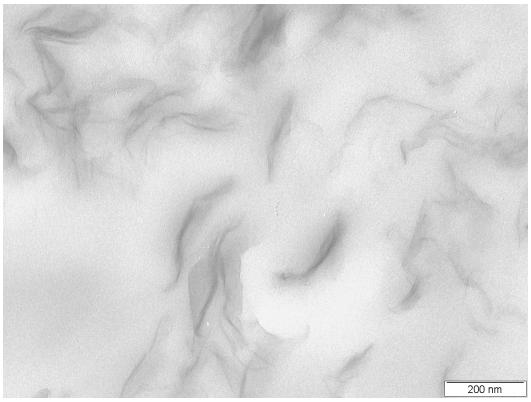


(B)

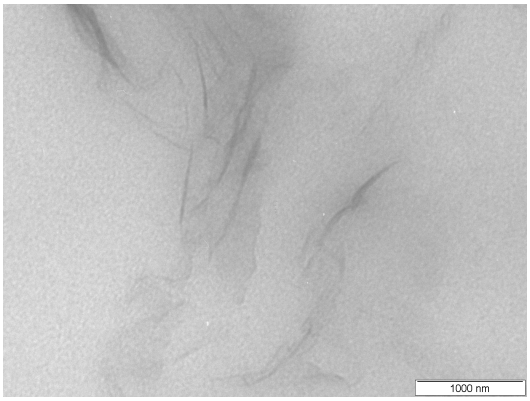


**Figure 5.2** Intercalation of OMMT in PLA matrix. TEM bright field images: (A) PLA-OMMT (x 100 000), (B) PLA-OMMT (x 270 000).

### 5.3.2 Molecular weight

**Figure 5.3** shows the $M_n$ *vs* time for PLA-C, PLA-OMMT and PLA-QAC films submerged in water, 50% and 95% ethanol at 40 °C. For the three films the molecular weight decreased over time due to the hydrolytic degradation of PLA. **Table 5.1** presents the rate constants $k$ ($d^{-1}$) for PLA-C, PLA-OMMT and PLA-QAC films exposed to the different solutions. It is important to note that after processing, the films showed different $M_{n_0}$. However, when the hydrolytic degradation rate was estimated, the $M_{n_0}$ of each of the film was taking into consideration. For the three films, when PLA films were immersed in 50% ethanol, the rate of hydrolysis was faster than in water and in 95% ethanol ($p$<0.05). When PLA is in contact with water-ethanol solutions, there is a competitive balance effect between the swelling caused by ethanol molecules and the water molecules that diffuse into the core of the polymer matrix starting the cleavage of the ester bonds. In our previous work, the maximum rate of decay in $M_n$ for PLA film was when the volume fraction of ethanol was around 0.50 where the swelling of the polymer was sufficient to allow the maximum sorption of water molecules to begin the hydrolysis [29]. For PLA-OMMT and PLA-QAC the 50% ethanol solution could have the same effect as in PLA-C film.

The addition of the QAC into PLA accelerated the rate of hydrolysis when PLA was in contact with water ($p$<0.05) (**Table 5.1**). The QAC acted as a plasticizer inducing movement of the polymer chains and therefore allowing the diffusion of water molecules trough the PLA to begin cleavage of the ester bonds. However, the presence of QAC decreased ($p$<0.05) the hydrolysis rate of PLA in 95% ethanol. This may be explained by a chemical reaction with water molecules and the ammonium from the QAC

depleting available water and so leaving few water molecules to participate in the hydrolysis reaction [36].

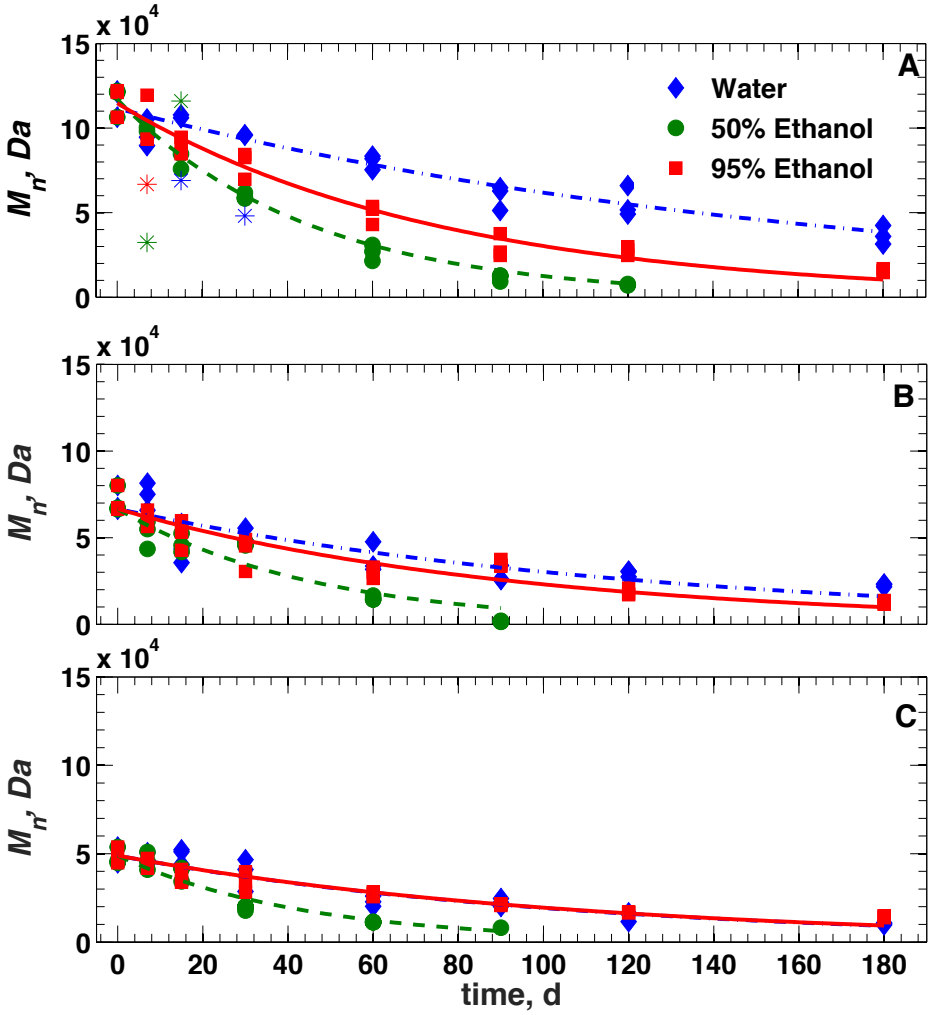


**Figure 5.3** First order reduction of $M_n$ for PLA-C, PLA-OMMT, and PLA-QAC films showing that the faster decay in $M_n$ was when the films were immersed in 50% ethanol. Lines indicate fitting of first order reaction with $k$ obtained from **Eq. 5.3**. $M_n$ as *vs* time during hydrolysis of (A) PLA-C, (B) PLA-OMMT and (C) PLA-QAC films submerged in water, 50% and 95% ethanol at 40 °C. Values indicated as * were considered outliers and therefore no used for fitting.

**Table 5.1** Hydrolytic degradation rate constants for PLA-C, PLA-OMMT and PLA-QAC films exposed to water-ethanol solutions at 40 °C.

| | $k$ ($d^{-1}$)* | | |
|---|---|---|---|
| **Solvent solution** | **PLA-C** | **PLA-OMMT** | **PLA-QAC** |
| Water | 0.0062 ± 0.0007 $^{a, A}$ | 0.0079 ± 0.0009 $^{a, AB}$ | 0.0093 ± 0.0008 $^{a, B}$ |
| 50% Ethanol | 0.0218 ± 0.0026 $^{b, A}$ | 0.0218 ± 0.0027 $^{b, A}$ | 0.0229 ± 0.0021 $^{b, A}$ |
| 95% Ethanol | 0.0125 ± 0.0014 $^{c, A}$ | 0.0106 ± 0.0011 $^{a, AB}$ | 0.0092 ± 0.0007 $^{a, B}$ |

*Fitting of first order reaction with $k$ obtained from **Eq. 5.3**

Note: Values with the same capital letter within a row and the same lowercase letter within a column are not different ($\alpha$=0.05)

The incorporation of nanoparticles into the PLA matrix did not affect the reduction of the $M_n$ when the polymer was immersed in each solvent ($p$>0.05). However, some authors have reported that nanoparticles have an effect on the hydrolysis of PLA, concluding that when the nanoparticles are within the PLA, there is an easier water attack since the volume and surface of the polymer in contact with the nanoparticles is higher [19, 21]. Therefore, even if the nanoparticles did not affect the hydrolysis rate, it is important to understand whether the incorporation of nanoparticles changes the solvent-polymer interaction affecting PLA morphology and its possible applications.

### 5.3.3 Water and ethanol sorption

Hydrolytic degradation of PLA begins with the diffusion of water through the PLA matrix cleaving the ester bonds of chains [24]. **Figure 5.4** shows similar sorption of $H_2O$ vapor in PLA-C and PLA-OMMT films indicating similar amount of water molecules sorb in the polymer matrix, which are then available to start the hydrolysis reactions, resulting in similar hydrolysis rates. The presence of ethanol changes the interaction of PLA and clay, so different sorption of water and ethanol can take place.

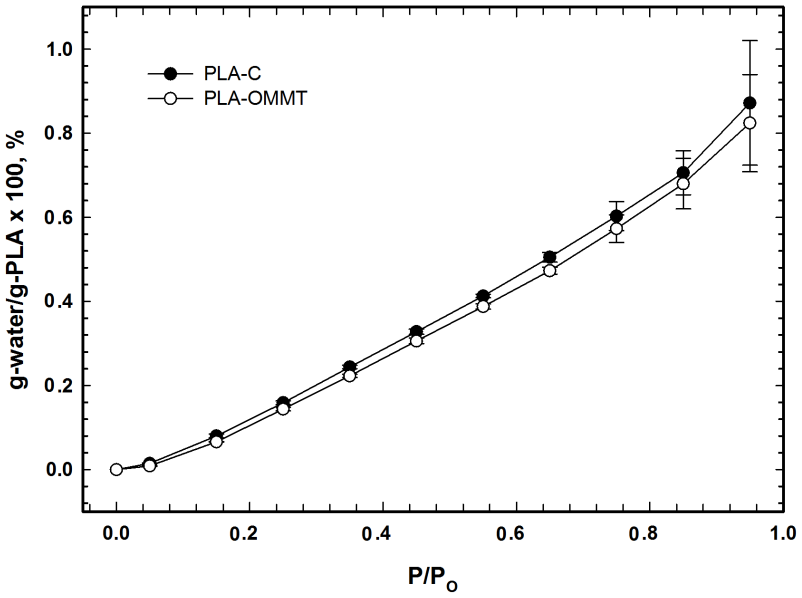


**Figure 5.4** Similar sorption of $H_2O$ vapor in PLA and PLA-OMMT films. Sorption isotherms for $H_2O$ vapor in PLA-C and PLA-OMMT films.

**Figure 5.5** presents the ethanol liquid sorption of the PLA films in contact with different volume fractions of ethanol as quantified by $^1H$ NMR. Sorption of ethanol in PLA-OMMT was almost double that in PLA-C. Therefore, to understand the higher sorption of ethanol in PLA-OMMT film, sorption isotherms of ethanol vapor in PLA-C,

PLA-OMMT and clay were carried out over a relative pressure ranging from 0.05 to 0.70 (**Figure 5.6**).

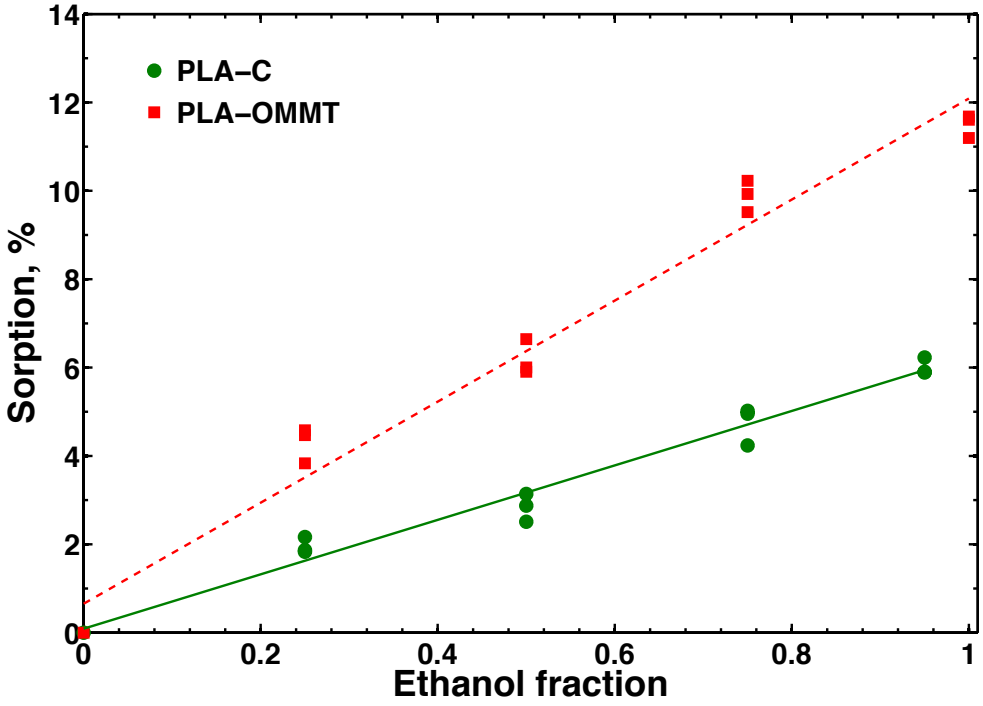


**Figure 5.5** Ethanol sorption of PLA-C (%sorption=6*p*; $R^2$=0.978) and PLA-OMMT (%sorption=12*p*; $R^2$=0.965) films in contact with different volume fractions of ethanol (*p* is the ethanol fraction by volume).

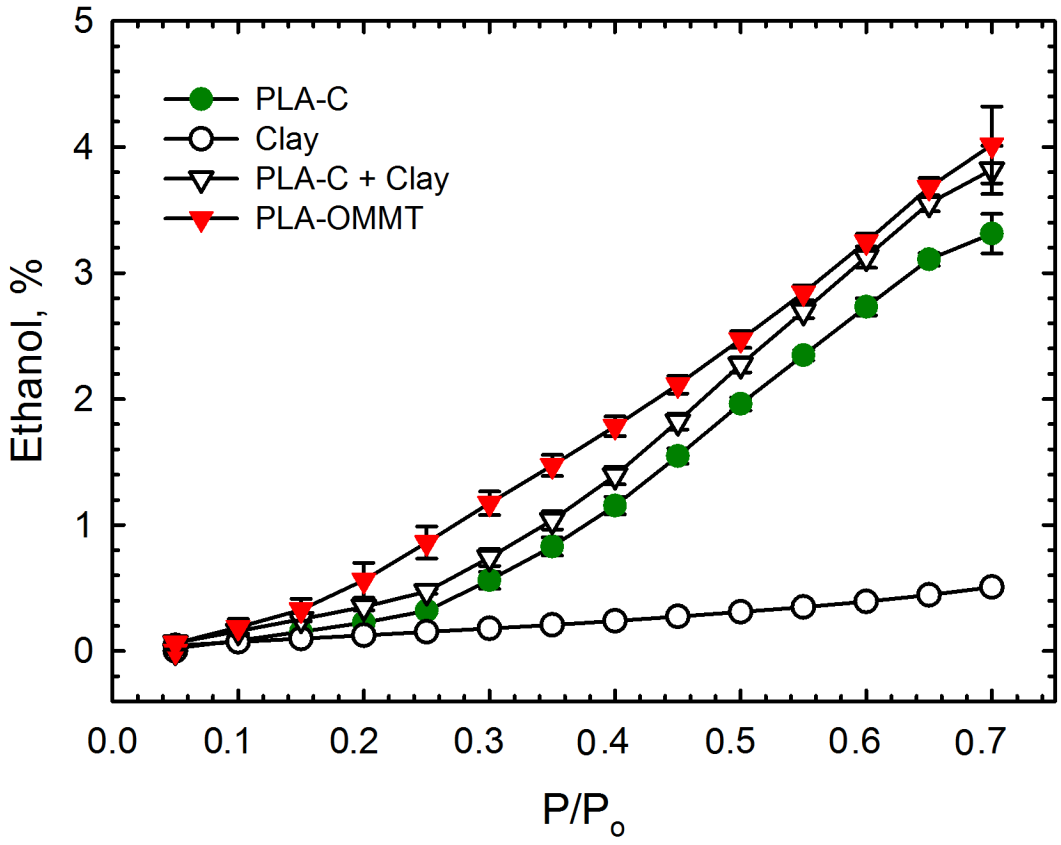


**Figure 5.6** Sorption isotherms of ethanol vapor in PLA-OMMT, PLA-C and clay particles. The sorption of PLA-C and clay correspond to the nominal composition of PLA-OMMT film (PLA:Clay = 95:5). PLA-C + Clay is the mathematical addition of ethanol sorption of PLA-C and clay.

In **Figure 5.6** the isotherms of PLA-C and clay represent the ethanol sorption corresponding to the nominal composition of PLA-OMMT film, which is 95% PLA film and 5% clay (PLA:Clay = 95:5). The PLA-OMMT isotherm showed higher ethanol sorption for all the $P/P_o$ range compared to the ethanol sorbed in 95% PLA-C and 5%

clay. To understand the influence of clay in PLA, the mathematical addition of the %ethanol sorbed by 95% PLA-C film and 5% clay is shown in **Figure 5.6** as PLAC + Clay. The computed %ethanol sorbed at high $P/P_o$ was similar to the ethanol sorption measured in PLA-OMMT. However, at low $P/P_o$ the computed ethanol sorbed was not similar to the measured %ethanol in PLA-OMMT film. The reason for this difference could be attributed to clustering of the clay powder particles while the clay layers in the PLA-OMMT film are intercalated (**Figure 5.2**) allowing easy sorption of ethanol into the clay galleries. Therefore, the higher sorption of ethanol in PLA-OMMT at volume fractions of ethanol between 0.2 and 0.5 (**Figure 5.5**) could be attributed to the sorption of ethanol into the galleries of the clay particles. Sorption of organic solvents by OMMT clays has been described by intercalation and clay swelling [37]. So, the higher sorption of ethanol by PLA-OMMT film could be explained by the sorption of ethanol between the clay galleries, since the sorption of ethanol in the PLA portion of PLA-OMMT is the same as in PLA-C film.

PLA plasticizes and crystallizes in the presence of ethanol, increasing chain mobility. In our previous work [29], when PLA was immersed in water-ethanol solutions, the decrease of the $T_g$ of PLA films was larger when the amount of ethanol in the solution augmented and swelling occurred immediately (**Figure 5.7A** and **Table 5.2**). The interaction of the PLA-OMMT with the solvent may be not the same as in neat PLA. **Figure 5.7B** and **Table 5.2** present the change in $T_g$ of PLA-OMMT when immersed in different amount of ethanol fractions. The $T_g$ of PLA-C and PLA-OMMT films were 64.7 ± 0.1 and 62.4 ± 0.1 °C, respectively, according to the DMA results. The lower $T_g$ of PLA-OMMT can be due to the free QAC in the matrix of the polymer, which was

released from the clay gallery during processing, softening the polymer. For PLA-OMMT immersed in 0, 25, 50, 75 and 95% ethanol, the $T_g$ dropped to 51.7, 47.6, 39.2, 33.4 and 17.8 °C, respectively. This indicated that the $T_g$ of the films decrease with the content of ethanol in the solution, inducing more movement of PLA polymer chains.

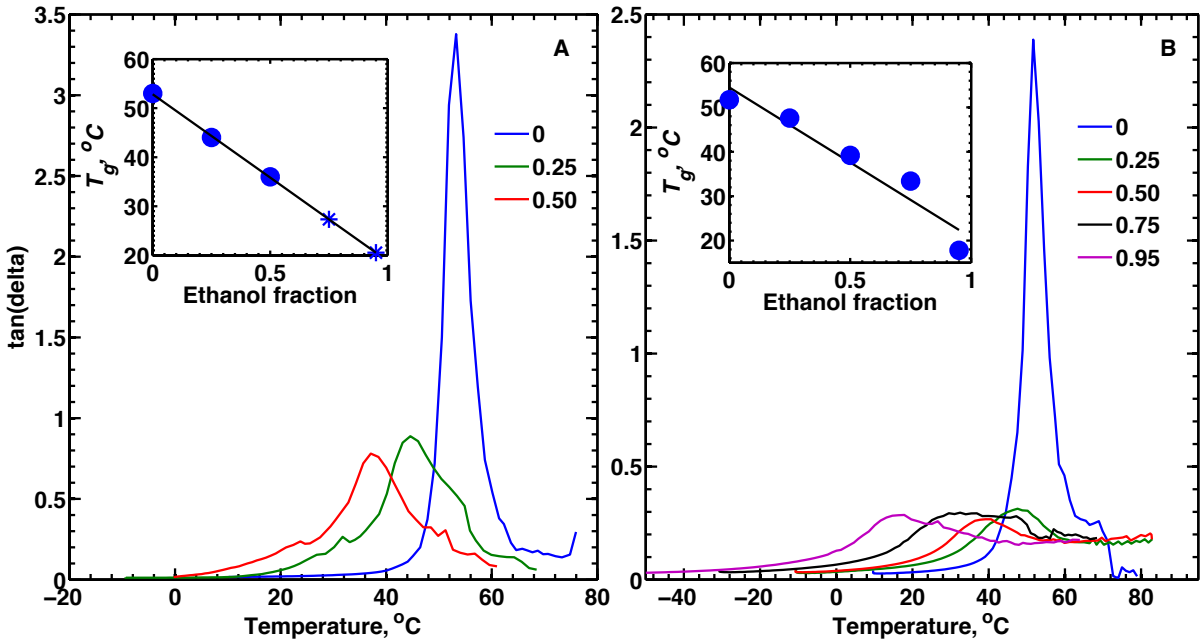


**Figure 5.7** $T_g$ of (A) PLA-C and (B) PLA-OMMT films submerged in different fractions of ethanol (v/v) from the DMA. Inserts: $T_g$ *vs* ethanol fraction ($p$); • experimental data, * estimated values that could not be experimentally measured, and – (fitted line) predicted values as (A) $T_g = -0.34p + 52.34;\ R^2 = 0.999$ (B) $T_g = -0.34p + 54.50;\ R^2 = 0.927$.

**Table 5.2** $T_g$ of PLA-C and PLA-OMMT films submerged in different fractions of ethanol (v/v) solution from DMA, and change in $T_g$ ($\Delta T_g$) with respect to non-immersed films.

| | PLA-C | | PLA-OMMT | |
|---|---|---|---|---|
| **Ethanol fraction** | **$T_g$, °C** | **$\Delta T_g$, °C** | **$T_g$, °C** | **$\Delta T_g$, °C** |
| No immersion | 64.7 ± 0.1 | | 62.4 ± 0.1 | |
| 0 | 52.6 | 12.1 | 51.7 | 10.7 |
| 0.25 | 44.2 | 20.5 | 47.6 | 14.8 |
| 0.50 | 36.8 | 27.9 | 39.2 | 23.2 |
| 0.75 | 27.3 | 37.4 | 33.4 | 29.0 |
| 0.95 | 20.2 | 44.7 | 17.8 | 44.6 |
| No immersion* | 59.8 ± 0.5 | | 55.8 ± 0.7 | |

*Values obtained by DSC.

Tan(delta) peaks in **Figure 5.7** could indicate interactions between the polymer-nanoparticle-solvent. The high of the tan(delta) peak is an indication of the interaction between the polymer chains and the solvent [38, 39]. Jonoobi et al. [38] found that when the concentration of nanofibers in PLA increased the tan(delta) peak decreased compared with PLA (neat), indicating that less chains of the polymer were contributing to the transition. In the case of PLA-OMMT film (**Figure 5.7B**), the peak was higher when it was immersed in water than when immersed in ethanol solutions. Lower peaks could indicate that the sorption of ethanol molecules enhanced the interaction with the polymer and the solvent, so the polymer became more elastic [39]. Also, the increase in

breadth proposes more particle-polymer interactions due to the broader distribution of relaxation time [39]. Therefore, when PLA-OMMT was exposed to ethanol solutions, the swelling of PLA enhanced the interaction of the polymer-solvent-nanoparticles. This interaction between the nanoparticles and solvent can be observed in **Figure 5.7B** in which the tan(delta) peak of water-ethanol solutions did not reach zero at the x-axis when temperature was high, unlike the PLA-C film (**Figure 5.7A**).

The presence of the OMMT nanoparticles in the PLA film could act as an anchor restricting the movement of PLA polymer chains. Klonos et al. [40] found that the presence of nanoparticles in PLA such as graphene oxide, carbon nanotubes and silica, immobilizes the polymer at the interfaces. It has also been studied that the presence of metal organic framework in PLA increases the toughness of the polymer matrix [41]. This restricted movement can be reflected in the change of $T_g$ ($\Delta T_g$) from DMA results (**Table 5.2**) where the change in $T_g$ was lower for PLA-OMMT than for PLA-C films for ethanol fraction < 0.75. For instance, the $\Delta T_g$ of the films immersed in 50% ethanol was 27.9 and 23.2 °C for PLA-C and PLA-OMMT, respectively. When the concentration of ethanol was higher than 75% there was not an anchor effect due to the presence of the clay. This might be because of the maximum swelling of the polymer matrix by the high concentration of ethanol limiting the restriction by the clays. Further studies have to be performed for the better understanding of the interaction between PLA-OMMT and ethanol solutions.

### 5.3.4 Crystallinity

The crystalline morphology of semi-crystalline PLA can be described by a model containing three phases, including the crystalline phase and the non-crystalline phase

that is subdivided into the mobile (MAF) and the rigid (RAF) amorphous fractions. Different authors have calculated the different fractions of PLA using DSC [42-46]. **Figure 5.8** shows the DSC thermograms of PLA-C and PLA-OMMT films during hydrolytic degradation in 50% ethanol at 40 °C.

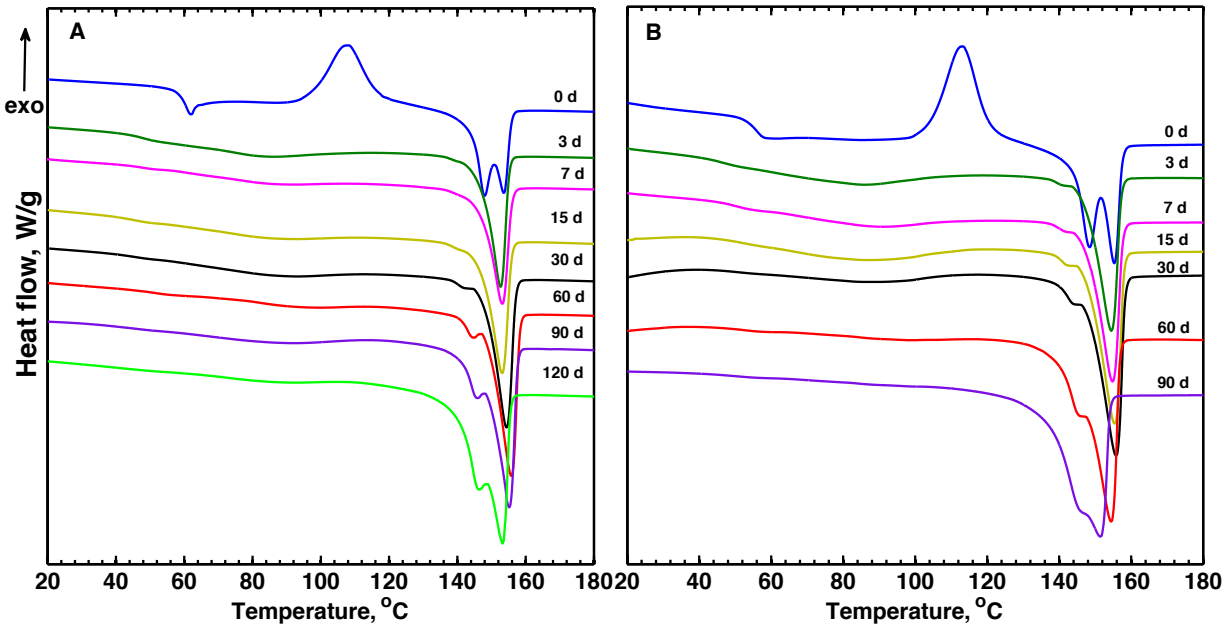


**Figure 5.8** DSC plots of (A) PLA-C and (B) PLA-OMMT films during hydrolytic degradation in 50% ethanol at 40 °C.

The crystallinity of PLA-C and PLA-OMMT films followed the same trend (**Figure 5C.2**, Appendix 5C). The evolution of $X_C$ for both films showed three different regions, where I and II can be attributed to the SIC and region III to the hydrolysis of the amorphous region. Regarding $X_{MAF}$ and $X_{RAF}$ the behavior was also similar for PLA-C and PLA-OMMT. A detail description of the methodology and evolution of the three phases, $X_C$, $X_{MAF}$ and $X_{RAF,}$ during the hydrolysis of PLA-C and PLA-OMMT in 50%

ethanol is explained in the Appendix 5C.

**Figure 5.9** shows the XRD profiles of PLA-OMMT film during hydrolysis in 50% ethanol at 40 °C. During SIC of PLA film in contact with 50% ethanol α-crystals were formed [29]. Similarly, the formation of crystals of PLA-OMMT took place when the film was exposed to the solvent solution for 3 days. The diffraction peaks observed were in accordance with the formation of α-crystals (orthorhombic unit cell with $a$= 1.06, $b$= 0.61, and $c$= 2.88 nm) [47]. Diffraction peaks at 22.7°, 19.2°, 16.9° and 15.0°correspond to the 102/210, 100/203, 110/200 and 010 plane reflections, respectively. Therefore, during SIC and hydrolytic degradation of the amorphous region of the polymer matrix the same form of crystals were present, meaning that the incorporation of nanoparticles into the PLA films did not interfere in the crystallization of the polymer.

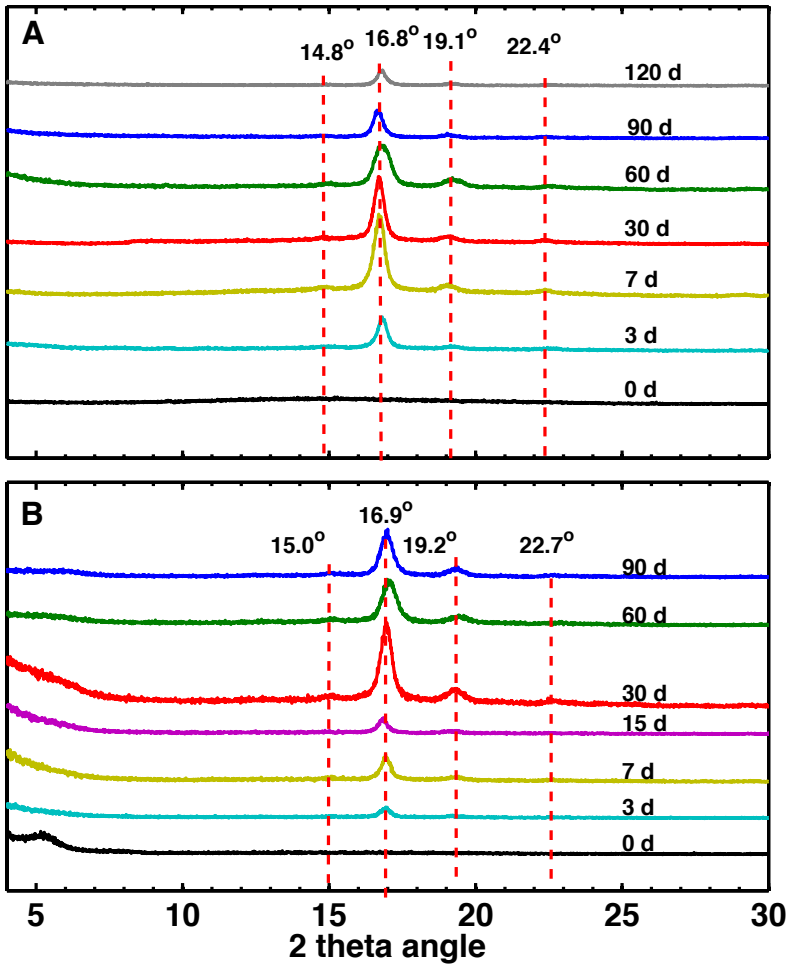


**Figure 5.9** XRD profiles of (A) PLA-C and (B) PLA-OMMT films during hydrolytic degradation in 50% ethanol at 40 °C. Immersed days are labeled.

The SIC during hydrolytic degradation of PLA when nanoparticles are incorporated can be correlated to the DSC thermograms (**Figure 5.8**). Due to the rearrangement of amorphous PLA-C and PLA-OMMT chains during the DSC heating process, the thermograms showed a cold-crystallization temperature peak ($T_{cc}$) at 0 d. After 3 days of exposure, the film sample did not show any $T_{cc}$, since PLA films crystallized after the 3$^{rd}$ day. Before and after 3 days of immersion in 50% ethanol, the

thermograms show a double melting peak. Different explanations have been discussed in the literature to explain this behavior. This could be attributed to the development of 2 different crystals during the heating process of DSC, α and β-forms [48, 49]. Also, during the hydrolysis process the additional melting peak can be associated with the formation of less perfect small crystals [21, 44]. Additionally, it has been proposed that the relaxation enthalpy of the more restricted amorphous region can be associated with the peak at high temperature, whereas the low temperature peak is due to the interspherulitic amorphous phase [50, 51].

The presence of nanoparticles increased the sorption of ethanol, which was sorbed between the clay galleries, where the clay acted as an anchor restricting the movement of the polymer chains. Crystallization was not affected, and consequently, the hydrolytic degradation was not affected by the presence of the clay.

### 5.3.5 Lactic acid release

Migrants from PLA during hydrolytic degradation may include different oligomers of LA, such as LA, lactoyl-lactic acid (linear dimer of LA), small oligomers of PLA (*e.g.*, trimers), and lactide (cyclic dimer of LA) [52]. **Figure 5.10** shows the release of LA from PLA-C, PLA-OMMT and PLA-QAC films into water, 50% and 95% ethanol at 40 °C. The highest release of LA was for the three films when they were immersed in 50% ethanol, in accordance with the fastest reduction in $M_n$ (**Figure 5.3**).

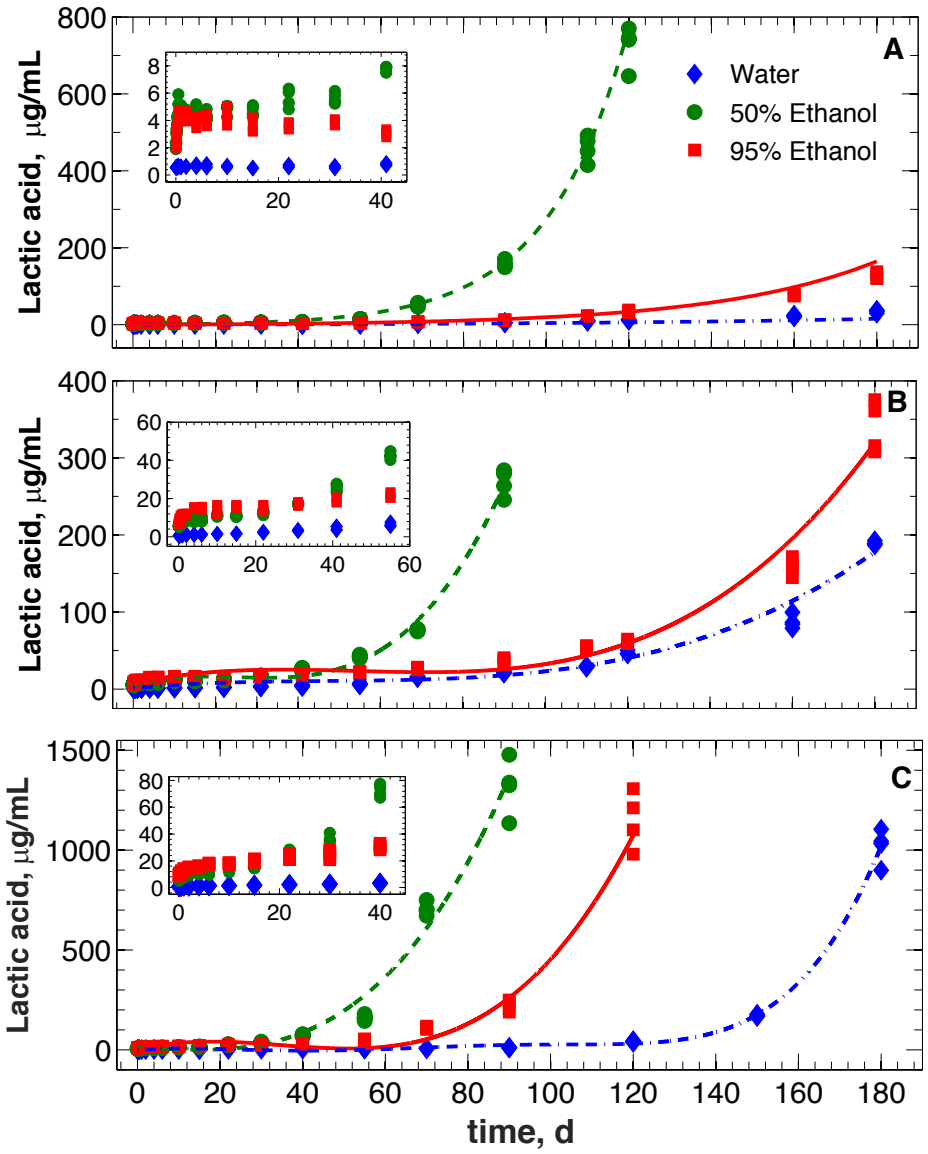


**Figure 5.10** Release of LA during hydrolysis at 40 °C of (A) PLA-C, (B) PLA-OMMT, (C) PLA-QAC films submerged in water, 50% and 95% ethanol. Lines are provided as a visual aid. Exponential increase of LA release when PLA films were immersed in 50% ethanol.

The initial phase of the exponential release of LA observed around 50 and 40 days for PLA-C and PLA-OMMT films, respectively, were in accordance with the increase of crystallinity after 30 days (**Figure 5C.2A**, Appendix 5C) because of the hydrolytic degradation of the amorphous regions remained after the SIC.

During the first month of exposure, for PLA-C film the release of LA was higher when PLA was exposed to 50% ethanol, then 95% ethanol and finally water (**Figure 5.10A insert**). However, the addition of the nanoclay in PLA matrix changed the initial LA release behavior during the first 30 d where the LA release was higher when PLA was immersed into 95% ethanol (**Figure 5.10B insert**). Similarly, the effect of the organomodifier (surfactant) on the hydrolysis of PLA, PLA-QAC film showed the same behavior as PLA-OMMT film during the early stages, where LA release was higher in 95% ethanol (**Figure 5.10C insert**). However, around 40 days of immersion of PLA-OMMT and PLA-QAC films in 50% ethanol the concentration of LA reached the amount released in 95% ethanol.

When the films were exposed to water, 50% and 95% ethanol the release of LA was higher for PLA-QAC film, followed by PLA-OMMT and then by PLA-C after 90 d of hydrolysis. In 50% ethanol where PLA has faster hydrolytic degradation, after 90 days of exposure 47% of the PLA-QAC film was hydrolyzed to LA while for PLA-OMMT and PLA-C films hydrolysis was 18% and 6%, respectively. The concentration of terminal carboxylic acid ends, which increases during hydrolysis making it a self-catalyzed reaction, was 15.2 ± 0.03 $x10^{-5}$ $mol/cm^3$ in accordance with the equation described by Pantani et al. [53]. For PLA-OMMT and PLA-C films, 18 and 6% of the films were hydrolyzed to LA, with a final concentration of terminal carboxylic acid ends of 73.2 ±

12.5 x$10^{-5}$ and 11.0 ± 2.1 x$10^{-5}$ mol/$cm^3$, respectively. Even though the decay in molecular weight was the same for the three films in contact with 50% ethanol, the release of LA was different. This could be due to the initial difference on $M_n$ of the films due to the processing conditions where the PLA-QAC film had the lowest initial $M_{n_o}$ of 4.82 x$10^4$ Da, followed by PLA-OMMT with 7.12 x$10^4$ Da, and finally PLA-C with 11.65 x$10^4$ Da. When PLA has low molecular weight the production of LA can be larger since the polymer has more molecular mobility, and the density of hydrophilic terminal groups (hydroxyl and carboxyl) are higher, increasing the hydrolysis [24].

### 5.3.6 Surfactant release

Surfactant in polymer nanocomposite systems can be identified as “free” or “bound” surfactant. The “free” surfactant is the surfactant able to be released from the clay surface, and the “bound” surfactant can be defined as the surfactant attached to the clay surface whose release is restricted by the clay particles [54]. The “free” surfactant defined in our system was 40.9 ± 6.9%, which was established after dissolving OMMT clay powder in 95% ethanol and quantified using the LC/MS/MS method previously described. The “free” surfactant was around the same range reported in polypropylene-clay and nylon-clay nanocomposites: 44.8 and 55.7%, respectively [54].

**Figure 5.11** shows the concentration of surfactant released from PLA-OMMT and PLA-QAC films during the hydrolytic degradation. The release of QAC from PLA-QAC was higher than from PLA-OMMT film. The higher release was due to the higher concentration of QAC in PLA-QAC film compared to QAC in the clay incorporated in the

PLA film. Also, the surfactant in PLA-QAC is all “free” and is not restricted by the clay. However, the release behavior for both films was similar.

The release of QAC from PLA-OMMT film is shown in **Figure 5.11A**. The concentration of QAC released into 50% ethanol after 90 d of exposure was 9.98 ± 0.71 µg/mL, and into 95% ethanol after 180 d was 10.18 ± 0.40 µg/mL. The “free” surfactant expected in our system was around 7.7 µg/mL, so the concentration of QAC release into 50% and 95% ethanol exceeds the “free” surfactant available in the clay. This additional QAC release could be attributed to the strong friction during film processing, which released the QAC from the clay into the film for further release during submersion.

The amount of QAC released at early stages was higher when PLA-OMMT film was immersed in 95% ethanol. Then, the release of QAC reached a steady state after 10 d and a further increase was observed after 30 d. The release remained constant from 30 to 60 d and after that the release of QAC increased again. In the last stage, the continuous release of QAC either in 50% or 95% ethanol can be explained by the hydrolysis of the amorphous regions allowing QAC to diffuse more easily through the polymer matrix.

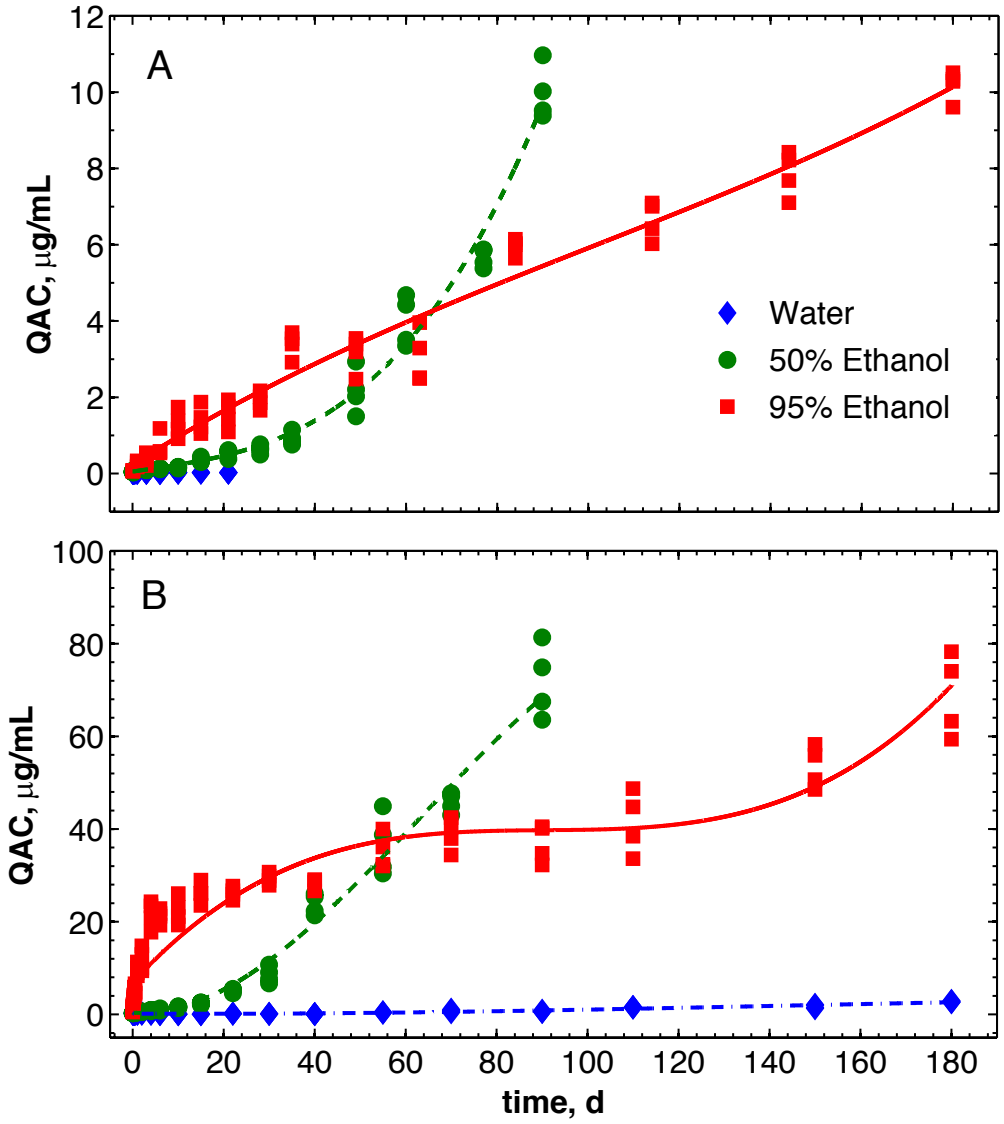


**Figure 5.11** Release of surfactant from PLA-OMMT and PLA-QAC films showing initial higher release in 95% ethanol but later the release was higher in 50% ethanol. Release of QAC during hydrolytic degradation at 40 °C of (A) PLA-OMMT and (B) PLA-QAC films submerged in water, 50% and 95% ethanol. Lines are provided as a visual aid.

The higher concentration of QAC released from 95% ethanol at the early stage of hydrolysis might be attributed to the higher sorption of ethanol into the PLA matrix, causing greater swelling and plasticization compared to 50% ethanol, which in turn facilitated the movement of the PLA chains [29]. After 30 d of immersion, the release of QAC exponentially increased for films immersed in 50% ethanol reaching and exceeding the concentration of QAC released into 95% ethanol at around 60 d. This could be explained by the higher hydrolysis in 50% ethanol allowing more QAC molecules to diffuse out.

The change in the release behavior of LA from PLA-OMMT and PLA-QAC compared to PLA-C in the early stages explained in the previous section (**Figure 5.10 inserts**) could be correlated with the presence of QAC in the MMT. The high release of QAC in 95% ethanol in the first 60 days could act as a plasticizer, softening the polymer matrix. In turn, this increases the movement of the chains and allows the easy diffusion of LA into the PLA films. After 40 d, the release of LA was higher in 50% ethanol than in 95% ethanol due to the higher hydrolysis taking place in 50% ethanol.

### 5.3.7 Release of clay

Since the hydrolytic degradation of PLA-OMMT film was fastest in 50% ethanol, we selected this system to quantify the release of the nanoclay. Nanoclay release from PLA-OMMT films was assessed by determining the concentration of Al as a nanoclay marker as a function of time using GFAAS (**Figure 5.12**). To ensure that the Al quantified belonged to the nanoclay particles in the nanocomposite, control samples with stainless steel wire and Teflon beads were run at the same time. The Al concentration detected from the control samples was subtracted from that measured

from the PLA-OMMT films. During the hydrolytic degradation of PLA-OMMT film, the concentration of Al increased over time indicating the release of nanoclay from the nanocomposite. The maximum concentration of Al was quantified after 90 d of hydrolysis as 22.7 ± 1.5 ppb, meaning that the concentration of clay released was 304.9 ± 19.5 ppb since the clay contains 7.46% wt. of Al. The release behavior showed two steady states, from 15 to 50 days and from 70 to 90 days. The first steady state from 15 to 50 days (clay = 125.26 ± 21.83 ppb) could be explained by the process of SIC region II (**Figure 5C.2**, Appendix 5C) where the crystallization rate is slow and the release of clay could be restricted by the secondary crystallization process. Then, the release of the clay increased due to hydrolysis of amorphous regions letting the clay be released until the concentration reached the second steady state. Even though PLA is a biodegradable polymer that hydrolyzed in contact with water, only 0.58% of the initial clay present in PLA was released (0.305 mg/L), which is comparable to the low concentration of nanoclay particles released from polypropylene (PP) and polyamide (PA6) nanocomposites (0.1 – 0.15 mg/L) [55]. The rest of the initial clay in the PLA could be trapped in the fragments of the film during hydrolysis or may have precipitated in the solution without detection, requiring further assessment.

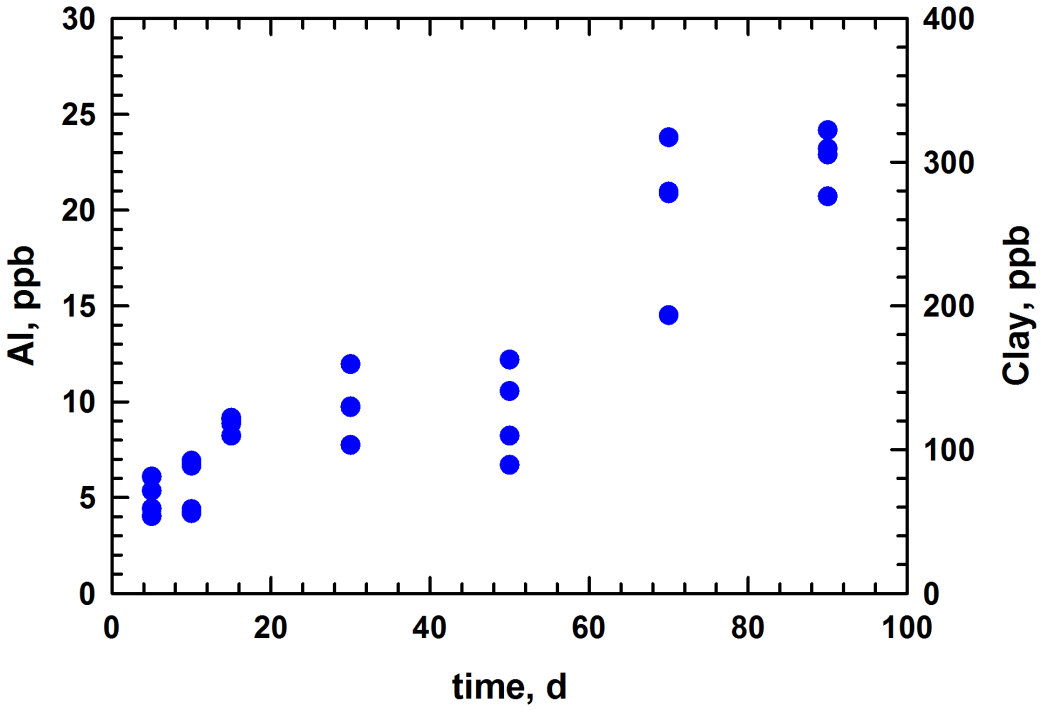


**Figure 5.12** Release of nanoclays from PLA-OMMT samples submerged in 50% ethanol at 40 °C.

PLA-OMMT film released a much greater amount of surfactant (9.98 µg/mL) than nanoclay particles (0.305 µg/mL) into 50% ethanol. The percentage released of surfactant and nanoclay of the initial amount of OMMT incorporated into the film was 51.76% and 0.58%, respectively. This difference is due to the difference in physical properties (*i.e.,* size, shape) between nanoclay particles and surfactant. In the release of surfactant and nanoclay particles from PP and PA6 nanocomposites Xia et al. [55] demonstrated that the molecular volume of the surfactant was around 661.1 Å or 0.661 $nm^3$ (radius < 1nm), significantly smaller than the size of the nanoclay particles, which ranged from a few tens of nm to hundreds of nm in the lateral dimension. Additionally,

Simon et al. [56] reported that the nanoparticles difficult to release from the polymer are the large ones. In this case, the surfactant can easily move through the polymer following the diffusing behavior of small molecules [55].

To verify the presence and release of nanoclay particles into the solvent during the PLA-OMMT film hydrolysis, TEM images were taken over time (**Figure 5.13**). The arrows in **Figure 5.13** indicate the presence of the clay particles, which are seen as several parallel lines that represent the clay layers. After 15 d of exposure of PLA-OMMT film to 50% ethanol, the clay released was detected in the TEM. EDS analysis at 15 d showed that the particle contained Si (34.4 wt%) and Al (6.1 wt%). The Al and Si contents quantified by EDS were changed to the content in the OMMT clay by multiplying by 73% since the surfactant content in the clay was 27%, and it does not contain Si and Al. So, the values were 25.1% Si and 4.4% Al, which approximately matched the values obtained by ICP Sodium Peroxide Fusion (18.1% Si and 7.46% Al). EDS analysis for 30, 50, 70 and 90 d (data not shown) gave a high content of Si, maybe due to some sort of contamination, as dust or impurities settling in the samples.

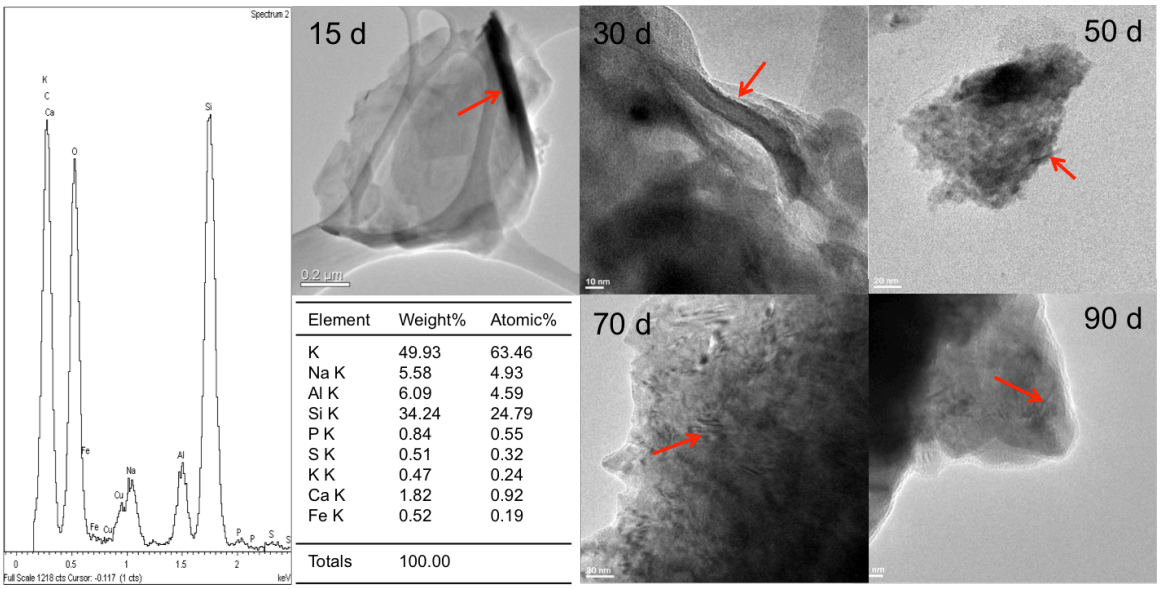


**Figure 5.13** TEM images of released nanoclay particles from PLA-OMMT film to 50% ethanol and the EDS analysis corresponding to particles in the image 15 d.

## 5.4 Conclusions

PLA-C and PLA-OMMT had faster hydrolysis when they were immersed in 50% ethanol due to the competitive balance effect between the swelling caused by the ethanol molecules and the water diffusing into the polymer matrix and starting the hydrolysis. The incorporation of nanoparticles in PLA films did not have an effect on the hydrolysis rates when films were exposed to water, 50 and 95% ethanol solutions. Similar sorption of $H_2O$ vapor in PLA-C and PLA-OMMT films was found, supporting the result of no difference in hydrolysis rates. In contrast, PLA-OMMT films sorbed double the amount of ethanol as PLA-C. This difference was due to the sorption of ethanol into the clay galleries and not to the expansion of the PLA matrix. The nanoclays acted as anchors restricting the movement of polymer chains, which is reflected in the $T_g$ and in

the similar behavior in the crystallization process where the changes in $X_C$, $X_{MAF}$ and $X_{RAF}$ were similar among the PLA and PLA-OMMT films with the presence of the same form of α-crystals. During hydrolysis, the release of LA and QAC were measured. LA release was higher in PLA-OMMT, attributed to the initial difference of $M_n$. The release of QAC at early stages was higher when PLA-OMMT was immersed in 95% ethanol. Then, in 50% ethanol the release exponentially increased due to the faster hydrolysis allowing QAC molecules to diffuse out more easily. The release of nanoclay was measured by quantifying Al in the 50% ethanol system, where the concentration at 90 d was 22.7 ppb of Al meaning that the clay released was 304.9 ppb (0.305 mg/L) corresponding to 0.58% of the initial clay incorporated into PLA.

## 5.5 Acknowledgments

I-F, F., thanks CONACYT (The Mexican National Council for Science and Technology), SEP (The Mexican Secretariat of Public Education), and the Government of Mexico for providing support funds for a Ph.D. fellowship. RA thanks the partial support of the USDA - and MI AgBioResearch, Hatch R. Auras. The authors express their gratitude to the Mass Spectrum & Metabolomics Core Facility and the Center for Advance Microscopy at MSU for their assistance with the development of the chromatography methods and TEM images. The authors also thank Daniel Holmes for his assistance with the development of $^1$H NMR method and Richard Staples for his assistance with XRD.

# APPENDICES

## APPENDIX 5A: Composition of masterbatch and films after processing

**Table 5A.1** Composition of masterbatch and films after processing.

| | ***Masterbatch*** | | ***Film*** | |
|---|---|---|---|---|
| | **OMMT, %** | **QAC, %** | **OMMT, %** | **QAC, %** |
| **PLA-C** | 0 | 0 | 0 | 0 |
| **PLA-OMMT** | 20 | 5.4 | 5 | 1.35 |
| **PLA-QAC** | 0 | 2.5 | 0 | 1.5 |

**APPENDIX 5B: Schematic representation of the cells for storage experiments**

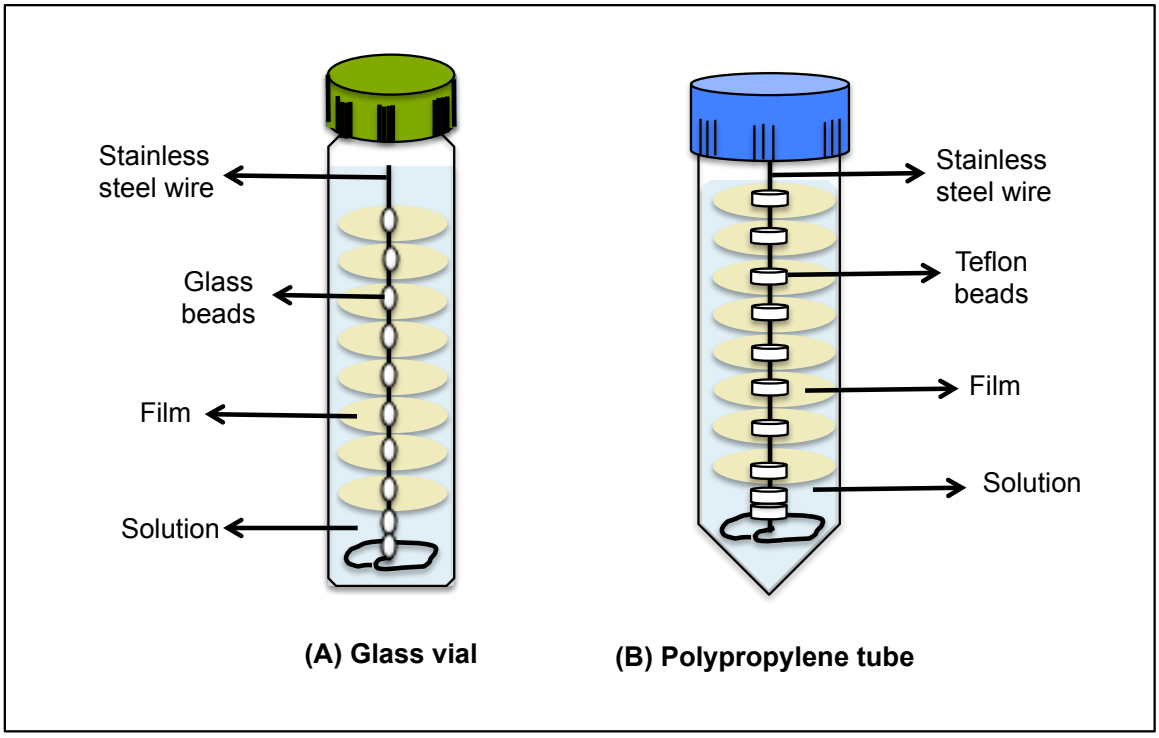


**Figure 5B.1** Schematic representation of (A) glass vial cells used for molecular weight experiments, LA release, surfactant release, and (B) PP tubes for nanoclay release experiments.

## APPENDIX 5C: Crystallinity

The crystalline fraction ($X_c$) and MAF fraction ($X_{MAF}$) were calculated using the following equations:

$$X_C = \frac{\Delta H_m - \Delta H_c}{\Delta H_f^*(1-\phi)} \quad \text{Eq. 5C.1}$$

$$X_{MAF} = \frac{\Delta C_p}{\Delta C_p^0} \quad \text{Eq. 5C.2}$$

where $\Delta H_m$ is the heat of melting, $\Delta H_c$ the cold crystallization heat, $\Delta H_f^*$ is the heat of fusion PLA when is 100% crystalline (93.7 J/g) [57], $\phi$ is the filler fraction, $\Delta C_p$ is the specific heat change at $T_g$ related to a mobile glass transition, and $\Delta C_p^0$ is the specific heat change at $T_g$ of the MAF ($\Delta C_p^0 = 0.639\, J/g\,℃$) [58]. Normally, the RAF fraction ($X_{RAF}$) is obtained from the remaining portion using the relationship:

$$X_{RAF} = 1 - X_C - X_{MAF} \quad \text{Eq. 5C.3}$$

However, **Figure 5.8** shows two different changes of heat-flow after 3 days of hydrolysis of PLA-C and PLA-OMMT films, where the heating at higher temperature, around 70 °C, can be related to the devitrification of the RAF ($T_g$) [44, 45]. Therefore, RAF was also estimated as follows:

$$X_{RAF} = \frac{\Delta C_{p2}}{\Delta C_p^0} \quad \text{Eq. 5C.4}$$

where $\Delta C_{p2}$ is the specific heat change at the second $T_g$. An example of the different $\Delta C_p$ taken from DSC plots to calculate $X_{MAF}$ and $X_{RAF}$ is shown in **Figure 5C.1**.

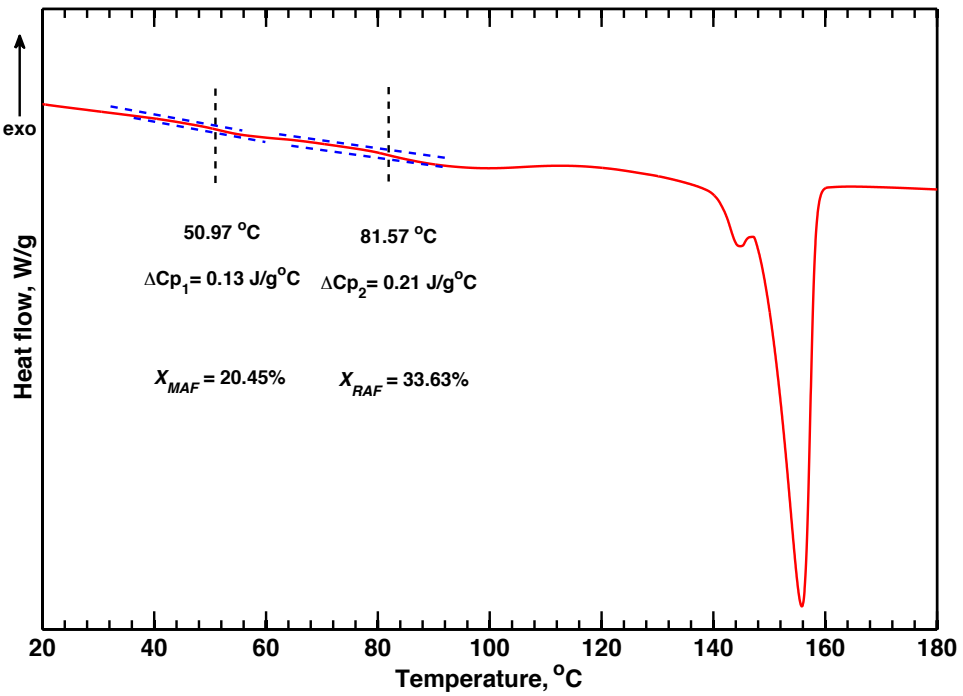


**Figure 5C.1** DSC plot of PLA-C film immersed during 60 d in 50% ethanol at 40 °C.

**Figure 5C.2** shows the evolution of the crystalline and non-crystalline phases of PLA-C and PLA-OMMT during the hydrolytic degradation in 50% ethanol at 40 °C. The $X_C$ of PLA-C increased from around 3 to 25% after 7 days of immersion and during the next 8 days the $X_C$ was constant. After the first 15 days of immersion, the $X_C$ started to increase again (**Figure 5C.2A**). From our previous work, during the study of the crystallization of PLA during hydrolysis in water-ethanol solutions, three regions were identified. The crystallinity in region I and II can be attributed to SIC by ethanol molecules, where region I corresponds to primary crystallization and region II to a secondary crystallization. On the other hand, the increase on crystalllinity in region III was because of the hydrolysis of the amorphous regions of the PLA [29]. The same

regions were identified for PLA-OMMT. The evolution of $X_{MAF}$ during hydrolysis decreased over time, meaning that the MAF is first depleted due to SIC and then hydrolyzed (**Figure 5C.2B**). However, $X_{RAF}$ (**Figure 5C.2C**) increased to around 0.5 in the first week corresponding to the primary crystallization (region I) due to SIC. Afterwards, $X_{RAF}$ began to slightly decrease for both films, PLA-C and PLA-OMMT, meaning that hydrolysis reactions over time could also be taking place in the RAF. It is worth mentioning that MAF has a rubbery character while RAF has reduced mobility. Thus, the free volume (FV) hole size and distribution are different in both amorphous regions [42, 43, 59]. It has been shown that the RAF increases the local diffusion of small molecules in PLA since it is constituted of low insufficiently decoupled tie chains between the amorphous and the crystalline regions that obstruct the relaxation. This causes the formation in RAF of a large number of small FV holes, accelerating the diffusion of water molecules [43]. Therefore, the similarities in the evolution of RAF for PLA-C and PLA-OMMT films indicate the same rate of hydrolytic degradation where the FV and therefore the diffusion of water molecules were similar.

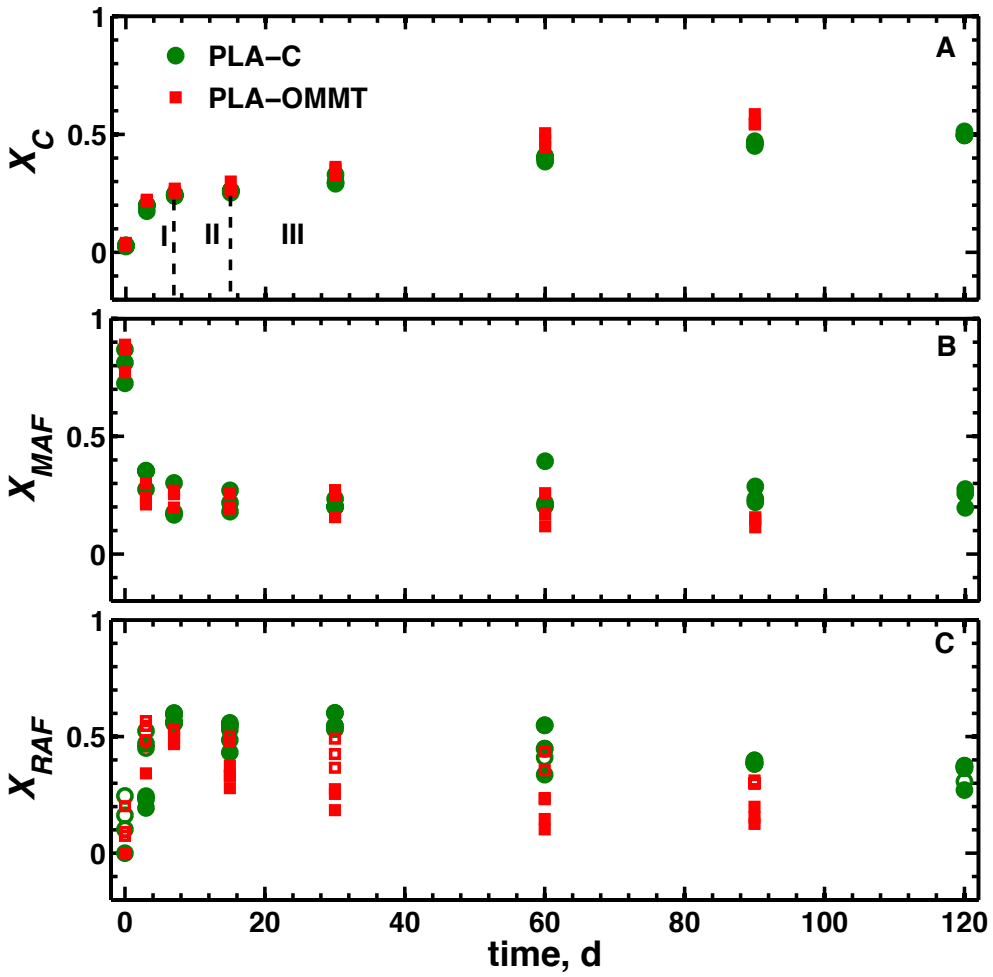


**Figure 5C.2** (A) Crystalline, (B) MAF, and (C) RAF during hydrolytic degradation of PLA-C and PLA-OMMT films immersed in 50% ethanol at 40 °C. I, II and III in (A) indicate different regions of PLA corresponding to the different crystallization processes. The main points in (A), (B) and (C) were obtained using **Eq. 5C.1**, **Eq. 5C.2** and **Eq. 5C.4**, respectively. Symbols □ and o in (C) represent the values obtained from **Eq. 5C.3**.

The crystalline fraction ($X_c$) of PLA-C and PLA-OMMT films during hydrolysis in 50% ethanol at 40 °C was also determined from XRD profiles from **Figure 5.9** (**Table**

**5C.1**). However, the crystallinity obtained from XRD profiles showed higher values compared to the values obtained from DSC (**Figure 5C.2A**). This difference was because of the difficulty of analyzing the data by baseline correction to get an accurate crystallinity due to the noise of the baseline.

**Table 5C.1** Crystallinity fraction ($X_c$) determined from XRD profiles during hydrolytic degradation of PLA-C and PLA-OMMT films in 50% ethanol at 40 °C.

| time, d | PLA-C | PLA-OMMT |
|---|---|---|
| 0 | 0.045 | 0.148 |
| 3 | 0.287 | 0.319 |
| 7 | 0.335 | 0.454 |
| 15 | 0.381 | 0.484 |
| 30 | 0.373 | 0.524 |
| 60 | 0.461 | 0.525 |
| 90 | 0.537 | 0.651 |
| 120 | 0.632 | |

Note: $X_c$ determined by XRD are not accurate due to the baseline noise. So, they may not match the DSC estimations.

# REFERENCES

## REFERENCES


[1] E. Castro-Aguirre, F. Iñiguez-Franco, H. Samsudin, X. Fang, R. Auras, Poly (lactic acid)—Mass production, processing, industrial applications, and end of life, Adv. Drug Deliv. Rev. 107 (2016) 333-366.

[2] R. Auras, B. Harte, S. Selke, An overview of polylactides as packaging materials, Macromol. Biosci. 4 (2004) 835-864.

[3] Y. Ikada, H. Tsuji, Biodegradable polyesters for medical and ecological applications, Macromol. Rapid Commun. 21 (2000) 117-132.

[4] J.-Y. Park, I.-H. Lee, Controlled release of ketoprofen from electrospun porous polylactic acid (PLA) nanofibers, J. Polym. Res. 18 (2011) 1287-1291.

[5] K.E. Uhrich, S.M. Cannizzaro, R.S. Langer, K.M. Shakesheff, Polymeric systems for controlled drug release, Chem. Rev. 99 (1999) 3181-3198.

[6] D. Farrington, J. Lunt, S. Davies, R. Blackburn, Poly (lactic acid) fibers, in: R. Blackburn (Ed.), Biodegradable and sustainable fibres, Woodhead Publishing Limeted, Cambridge, England, 2005, pp. 191-220.

[7] D.G. Hayes, S. Dharmalingam, L.C. Wadsworth, K.K. Leonas, C. Miles, D. Inglis, Biodegradable agricultural mulches derived from biopolymers, in: C.S. Kishan Khemani (Ed.), Degradable polymers and materials: Principles and practice, American Chemical Society, Washington, DC, 2012, pp. 201-223.

[8] K.M. Nampoothiri, N.R. Nair, R.P. John, An overview of the recent developments in polylactide (PLA) research, Bioresour. Technol. 101 (2010) 8493-8501.

[9] R.G. Sinclair, Slow-release pesticide system. Polymers of lactic and glycolic acids as ecologically beneficial, cost-effective encapsulating materials, Environ. Sci. Technol. 7 (1973) 955-956.

[10] Y.-N. Chang, R.E. Mueller, E.L. Iannotti, Use of low MW polylactic acid and lactide to stimulate growth and yield of soybeans, Plant Growth Regul. 19 (1996) 223-232.

[11] NatureWorks. SPAR Austria enhances freshness of produce with NatureWorks PLA. http://www.pressreleasefinder.com/NatureWorks/NWPR015/en/, 2018 (accessed 01/03/2018).

[12] NatureWorks. Pacific Pre-cut enhances the freshness of its brand with NatureWorks PLA packaging for fresh-packed salads.

http://cms.natureworksllc.com/News-and-Events/Press-Releases/2005/6-5-05-Pacific-Pre-Cut-Enhances-the-Freshness-of-Its-Brand-With-NatureWorks-PLA-Packaging, 2015 (accessed 09/08/2015).

[13] NatureWorks. NatureWorks PLA helps Delhaize extend environmentally-friendly packaging to belgian costumers. http://www.pressreleasefinder.com/NatureWorks/NWPR001/en/, 2018 (accessed 01/03/2018).

[14] S.S. Ray, M. Bousmina, Biodegradable polymers and their layered silicate nanocomposites: in greening the 21st century materials world, Prog. Mater Sci. 50 (2005) 962-1079.

[15] S.S. Ray, K. Yamada, M. Okamoto, K. Ueda, New polylactide-layered silicate nanocomposites. 2. Concurrent improvements of material properties, biodegradability and melt rheology, Polymer 44 (2003) 857-866.

[16] S.S. Ray, M. Okamoto, Polymer/layered silicate nanocomposites: a review from preparation to processing, Prog. Polym. Sci. 28 (2003) 1539-1641.

[17] J.-M. Raquez, Y. Habibi, M. Murariu, P. Dubois, Polylactide (PLA)-based nanocomposites, Prog. Polym. Sci. 38 (2013) 1504-1542.

[18] Y. Xi, R.L. Frost, H. He, T. Kloprogge, T. Bostrom, Modification of Wyoming montmorillonite surfaces using a cationic surfactant, Langmuir 21 (2005) 8675-8680.

[19] Q. Zhou, M. Xanthos, Nanoclay and crystallinity effects on the hydrolytic degradation of polylactides, Polym. Degrad. Stab. 93 (2008) 1450-1459.

[20] M.-A. Paul, C. Delcourt, M. Alexandre, P. Degée, F. Monteverde, P. Dubois, Polylactide/montmorillonite nanocomposites: study of the hydrolytic degradation, Polym. Degrad. Stab. 87 (2005) 535-542.

[21] K. Fukushima, C. Abbate, D. Tabuani, M. Gennari, G. Camino, Biodegradation of poly (lactic acid) and its nanocomposites, Polym. Degrad. Stab. 94 (2009) 1646-1655.

[22] A. Araújo, G. Botelho, M. Oliveira, A. Machado, Influence of clay organic modifier on the thermal-stability of PLA based nanocomposites, Appl. Clay Sci. 88 (2014) 144-150.

[23] K. Fukushima, D. Tabuani, M. Dottori, I. Armentano, J. Kenny, G. Camino, Effect of temperature and nanoparticle type on hydrolytic degradation of poly (lactic acid) nanocomposites, Polym. Degrad. Stab. 96 (2011) 2120-2129.

[24] H. Tsuji, Hydrolytic Degradation, in: R. Auras, L.-T. Lim, S. Selke, H. Tsuji (Eds.), Poly(lactic acid). Synthesis, Structures, Properties, Processing, and Applications, John Wiley & Sons, Inc., New Jersey, 2010, pp. 345-381.

[25] Z. Pan, J. Ding, Poly(lactide-*co*-glycolide) porous scaffolds for tissue engineering and regenerative medicine, Interface Focus 2 (2012) 366-377.

[26] H. Liu, J. Zhang, Research progress in toughening modification of poly (lactic acid), J. Polym. Sci. Part B Polym. Phys. 49 (2011) 1051-1083.

[27] H. Balakrishnan, A. Hassan, M. Imran, M.U. Wahit, Toughening of polylactic acid nanocomposites: A short review, Polym. Plast. Technol. Eng. 51 (2012) 175-192.

[28] S. Detyothin, A. Kathuria, W. Jaruwattanayon, S.E.M. Selke, R. Auras, Poly(lactic acid) Blends, in: R. Auras, L.T. Lim, S. Selke, H. Tsuji (Eds.), Poly(lactic acid). Synthesis, Structures, Properties, Processing, and Applications, John Wiley & Sons, Inc., New Jersey, 2010, pp. 227-266.

[29] F. Iñiguez-Franco, R. Auras, G. Burgess, D. Holmes, X. Fang, M. Rubino, H. Soto-Valdez, Concurrent solvent induced crystallization and hydrolytic degradation of PLA by water-ethanol solutions, Polymer 99 (2016) 315-323.

[30] H. Tsuji, A. Mizuno, Y. Ikada, Properties and morphology of poly (L‐lactide). III. Effects of initial crystallinity on long‐term in vitro hydrolysis of high molecular weight poly (L‐lactide) film in phosphate‐buffered solution, J. Appl. Polym. Sci. 77 (2000) 1452-1464.

[31] H. Tsuji, Y. Ikada, Properties and morphology of poly (L-lactide) 4. Effects of structural parameters on long-term hydrolysis of poly (L-lactide) in phosphate-buffered solution, Polym. Degrad. Stab. 67 (2000) 179-189.

[32] J.M. Cowley, Diffraction physics, Third ed., Elsevier Science B.V., Amsterdam, Holland, 1995.

[33] ASTM, Standard 47544-11. Standard test method for two-sided liquid extraction of plastic materials using FDA migration cell, ASTM International, West Conshohocken, PA, 2011.

[34] J. Feijoo, L. Cabedo, E. Giménez, J. Lagaron, J. Saura, Development of amorphous PLA-montmorillonite nanocomposites, J. Mater. Sci. 40 (2005) 1785-1788.

[35] D.D.S. Morais, R. Barbosa, K.M. Medeiros, E.M. Araújo, T.J.A. de Mélo, Preparation of Poly (Lactic Acid)/Bentonite Clay Bio-Nanocomposite, in: Materials Science Forum, Trans Tech Publ, 2014, pp. 233-237.

[36] W.L. Masterton, C.N. Hurley, Chemistry: Principles and Reactions, Sixth ed., Cengage Learning, CA, USA, 2008.

[37] X. Fang, Design and engineering of barrier materials including nano-adsorbents, in, AgroParisTech, 2013.

[38] M. Jonoobi, J. Harun, A.P. Mathew, K. Oksman, Mechanical properties of cellulose nanofiber (CNF) reinforced polylactic acid (PLA) prepared by twin screw extrusion, Compos. Sci. Technol. 70 (2010) 1742-1747.

[39] M. Abdalla, D. Dean, D. Adibempe, E. Nyairo, P. Robinson, G. Thompson, The effect of interfacial chemistry on molecular mobility and morphology of multiwalled carbon nanotubes epoxy nanocomposite, Polymer 48 (2007) 5662-5670.

[40] P. Klonos, Z. Terzopoulou, S. Koutsoumpis, S. Zidropoulos, S. Kripotou, G.Z. Papageorgiou, D.N. Bikiaris, A. Kyritsis, P. Pissis, Rigid amorphous fraction and segmental dynamics in nanocomposites based on poly (l–lactic acid) and nano-inclusions of 1–3D geometry studied by thermal and dielectric techniques, Eur. Polym. J. 82 (2016) 16-34.

[41] A. Kathuria, M.G. Abiad, R. Auras, Toughening of poly (l-lactic acid) with Cu 3 BTC 2 metal organic framework crystals, Polymer 54 (2013) 6979-6986.

[42] J. Del Rio, A. Etxeberria, N. Lopez-Rodriguez, E. Lizundia, J. Sarasua, A PALS contribution to the supramolecular structure of poly (L-lactide), Macromolecules 43 (2010) 4698-4707.

[43] S.F. Nassar, A. Guinault, N. Delpouve, V. Divry, V. Ducruet, C. Sollogoub, S. Domenek, Multi-scale analysis of the impact of polylactide morphology on gas barrier properties, Polymer 108 (2017) 163-172.

[44] A. Magoń, M. Pyda, Study of crystalline and amorphous phases of biodegradable poly (lactic acid) by advanced thermal analysis, Polymer 50 (2009) 3967-3973.

[45] E. Zuza, J.M. Ugartemendia, A. Lopez, E. Meaurio, A. Lejardi, J.-R. Sarasua, Glass transition behavior and dynamic fragility in polylactides containing mobile and rigid amorphous fractions, Polymer 49 (2008) 4427-4432.

[46] T.L. Nguyen, F. Bédoui, P.E. Mazeran, M. Guigon, Mechanical investigation of confined amorphous phase in semicrystalline polymers: case of PET and PLA, Polym. Eng. Sci. 55 (2015) 397-405.

[47] S. Sasaki, T. Asakura, Helix distortion and crystal structure of the α-form of poly (l-lactide), Macromolecules 36 (2003) 8385-8390.

[48] K. Fukushima, D. Tabuani, G. Camino, Nanocomposites of PLA and PCL based on montmorillonite and sepiolite, Mater. Sci. Eng., C 29 (2009) 1433-1441.

[49] M. Yasuniwa, S. Tsubakihara, K. Iura, Y. Ono, Y. Dan, K. Takahashi, Crystallization behavior of poly (L-lactic acid), Polymer 47 (2006) 7554-7563.

[50] N. Delpouve, M. Arnoult, A. Saiter, E. Dargent, J.M. Saiter, Evidence of two mobile amorphous phases in semicrystalline polylactide observed from calorimetric investigations, Polym. Eng. Sci. 54 (2014) 1144-1150.

[51] S. Montserrat, P. Cortes, Physical ageing studies in semicrystalline poly (ethylene terephthalate), J. Mater. Sci. 30 (1995) 1790-1793.

[52] R. Conn, J. Kolstad, J. Borzelleca, D. Dixler, L. Filer, B. LaDu, M. Pariza, Safety assessment of polylactide (PLA) for use as a food-contact polymer, Food Chem. Toxicol. 33 (1995) 273-283.

[53] R. Pantani, F. De Santis, F. Auriemma, C. De Rosa, R. Di Girolamo, Effects of water sorption on poly (lactic acid), Polymer 99 (2016) 130-139.

[54] Y. Xia, M. Rubino, R. Auras, Modeling of surfactant release from polymer-clay nanocomposites into ethanol, Polym. Test. 50 (2016) 57-63.

[55] Y. Xia, M. Rubino, R. Auras, Release of nanoclay and surfactant from polymer–clay nanocomposites into a food simulant, Environ. Sci. Technol. 48 (2014) 13617-13624.

[56] P. Simon, Q. Chaudhry, D. Bakos, from polymer packaging to food–a physicochemical view, J. Food Nutr. Res. 47 (2008) 105-113.

[57] E. Fischer, H.J. Sterzel, G. Wegner, Investigation of the structure of solution grown crystals of lactide copolymers by means of chemical reactions, Colloid Polym. Sci. 251 (1973) 980-990.

[58] M. Pyda, R. Bopp, B. Wunderlich, Heat capacity of poly (lactic acid), J. Chem. Thermodyn. 36 (2004) 731-742.

[59] G. Dlubek, A.S. Gupta, J. Pionteck, R. Häßler, R. Krause-Rehberg, H. Kaspar, K. Lochhaas, Glass transition and free volume in the mobile (MAF) and rigid (RAF) amorphous fractions of semicrystalline PTFE: a positron lifetime and PVT study, Polymer 46 (2005) 6075-6089.

# CHAPTER 6

## Control of Hydrolytic Degradation of Poly(Lactic Acid) by Incorporation of Chain Extender: from Bulk to Surface Erosion

A version of this chapter is published as:

F. Iñiguez-Franco, R. Auras, J. Ahmed, S. Selke, M. Rubino, K. Dolan, H. Soto-Valdez. Control of hydrolytic degradation of poly(lactic acid) by incorporation of chain extender: from bulk to surface erosion, Polymer Testing 67 (2018) 190-196.

## 6.0 Abstract

Poly(lactic acid) (PLA) was prepared by incorporating 1.5% wt. of chain extender to control the thermal stability of PLA during processing. PLA films were processed with three-selected residence times: 4, 8 and 16 min. The PLA film with highest molecular weight was processed with a residence time of 8 min; therefore, films processed at those conditions were selected for hydrolysis experiments. Results showed that the addition of the chain extender significantly increased the dynamic moduli of PLA, and the onset decomposition temperature decreased by 1 °C. These results were attributed to the different structures obtained after processing PLA with the chain extender resulting in long-chain branching. The hydrolytic degradation of PLA films at accelerated conditions was decreased by the presence of the chain extender, reducing the rate constant from 0.206 to 0.065 $h^{-1}$. This reduction was associated with differences in the degradation mechanism from bulk to surface erosion.

## 6.1 Introduction

Interest in using bio-based and biodegradable polymers, originating from renewable sources, has significantly increased due to the global awareness of material sustainability and to avoid the use of world oil resources. One of the main biodegradable polymers is PLA, a linear aliphatic polyester produced by the condensation polymerization of lactic acid (LA) derived by fermentation of sugars from corn [1, 2]. The high molecular weight PLA is, however, made from lactide monomer by the ring opening polymerization (ROP) using aluminum [3] and tin alkoxides [4] as catalysts for the polymerization of lactides. PLA has attracted considerable attention for

its biocompatibility, bioresorbability, biodegradability, and many others processability qualities [2].

The versatility of PLA has led to broad applications such as in the medical field, agriculture, and the packaging industry [1, 2, 5-10] in which PLA can be in contact with different environments that can lead to its degradation. Water molecules induce hydrolytic degradation of PLA by cleaving the ester groups, leading to a decrease in molecular weight and subsequently to the release of PLA oligomers and monomers [11]. The degradation mechanism of PLA can be either surface or bulk erosion depending on the competition between the diffusion of water molecules into PLA and the rate of the hydrolysis reactions [12]. Bulk erosion is a homogenous degradation process where the diffusion rate of water molecules is higher than the hydrolysis rate [11]. On the other hand, surface erosion takes place when the surface degradation rate is much higher than the diffusion of water molecules, so hydrolysis mainly occurs in the near-surface regions with no significant dependence on thickness of the rate of weight loss per unit surface area [13].

PLA degradation leads to changes in thermal and mechanical properties, morphology and molecular weight [14-17]. Depending on the intended application, degradation can be an advantage or a disadvantage. In the case of applications such as packaging, controlling the resistance to hydrolytic degradation is important since the properties of the container must remain intact during the shelf life of the product to maintain their quality.

Chain extenders such as epoxy-acrylic additives have been used for thermal stabilization of PLA during processing to minimize the reduction of molecular weight [18-

23]. The main mechanism of stabilization is chain extension from the formation of either longer linear or branched chains and some potential crosslinking structures [20, 24]. One of the commercially available epoxy based chain extenders is Joncryl® ADR-4368. Joncryl® ADR-4368 is an oligomeric copolymer based on glycidyl methacrylate, styrene and other acrylates with a functionality greater than four [25]. During PLA degradation two new chains are created with a carboxylic acid group and hydroxylic group on each of the ends of the chain. The epoxy groups of the Joncryl® chain extender can theoretically react with both the hydroxyl and carboxyl acid groups. However, studies have shown that the reaction with the carboxylic acid group is favored [26, 27]. Bikiaris and Karayannidis [28] suggested that the excess of epoxy groups could react with the hydroxyl end groups and with new hydroxyl groups from the joining of the epoxide and carboxyl groups. This work aimed to understand the effects of chain extenders into PLA during processing and its further impact on the hydrolytic degradation of modified PLA.

## 6.2 Materials and methods

### 6.2.1 Chemicals and reagents

PLA used in this study was Ingeo® PLA 4032D supplied by NatureWorks LLC (Minnetonka, MN, USA) with a weight and number average molecular weight ($M_w$, $M_n$) of 3.01 $\pm$ 0.01 x$10^5$ Da and 1.76 $\pm$ 0.04 x$10^5$ Da, respectively. Water HPLC grade was obtained from J.T. Baker (Center Valley, PA, USA). Ethanol HPLC grade and CAPS (3-(cyclohexylamino)-1-propanesulfonic acid) were acquired from Sigma-Aldrich (St. Louis, MO, USA). Tetrahydrofuran (THF) reagent grade stabilized with BHT was procured from Pharmco-AAPER (North East, CA, USA). The chain extender used was Joncryl® ADR-4368, a styrene-acrylic multi-functional epoxide oligomeric agent accepted by the USA

Food and Drug Administration (FDA) and provided by BASF (Florham Park, NJ, USA). The chemical structure of Joncryl® is shown in **Figure 6.1**.

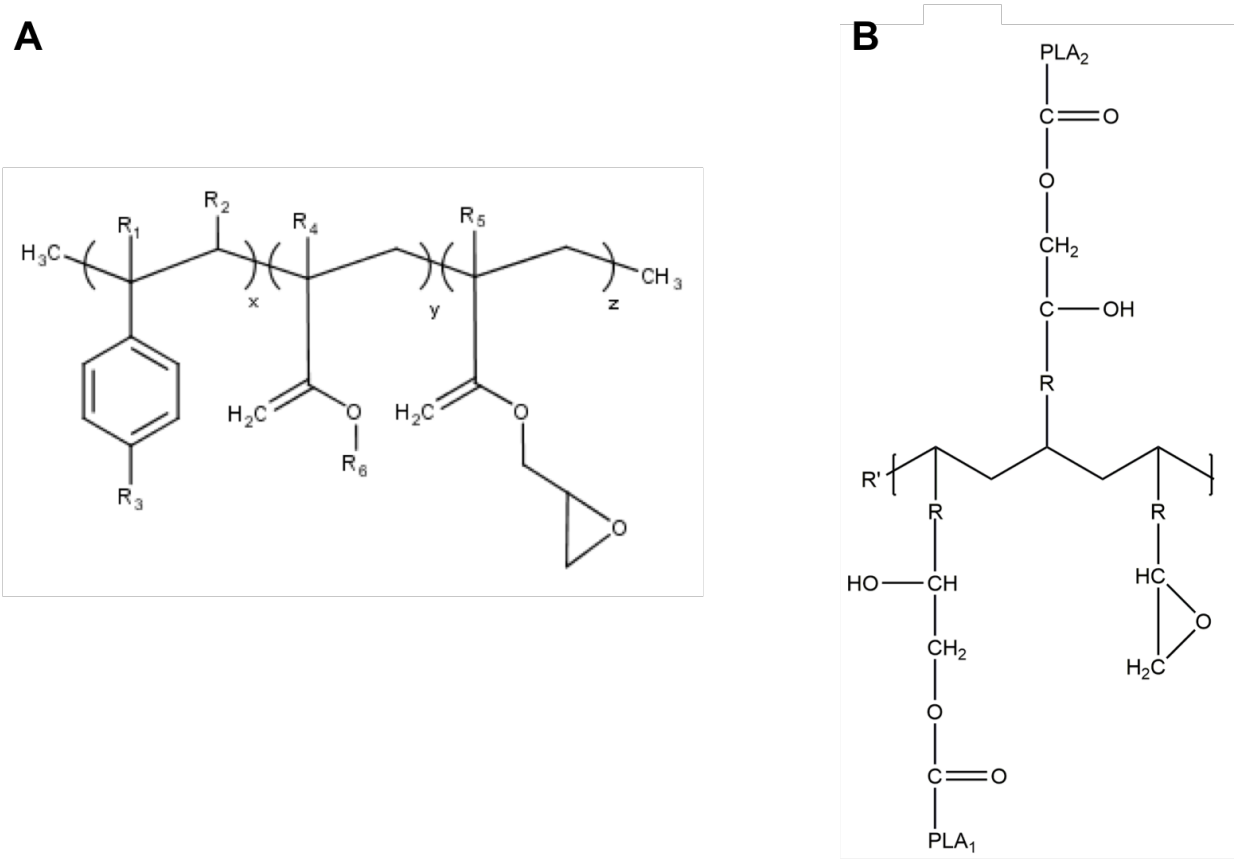


**Figure 6.1**(A) General structure of Joncryl® ADR, where $R_1$ – $R_5$ are H, $CH_3$, a higher alkyl group, or a combination; $R_6$ is an alkyl group, and x, y and z are each between 1 and 20. (B) Possible structure of PLA and Joncryl® according to Najafi et al. [18].

### 6.2.2 Film production

PLA pellets and Joncryl® ADR-4368 were initially dried at 60 °C for 12 h under vacuum (85 kPa) before processing. PLA with Joncryl® ADR-4368 films (PLA-J) were produced by first mixing PLA dried pellets with 1.5% wt. of Joncryl® ADR-4368 and then processing in a Randcastle cast film microextruder with a screw of 1.5875 cm diameter,

24/1 L/D ratio extruder, and 34 cc volume (Extrusion Systems, Inc., Cedar Grove, NJ, USA). PLA-J films were processed using different residence times: 4, 8 and 16 min with an extrusion temperature range of 182 – 196 °C from hopper to die. Control film (PLA-C) was processed at the same conditions as PLA-J films. The thicknesses of the films were 0.025 ± 0.001 and 0.021 ± 0.007 mm for PLA-C and PLA-J, respectively.

### 6.2.3 Molecular weight

PLA samples were dissolved in THF (2 mg/mL) to determine $M_n$, $M_w$, viscosity average molecular weight ($M_v$) and polydispersity index (*PDI*). The dissolved samples were analyzed using a size exclusion chromatograph (SEC) (Waters 1515, Waters, Milford, MA, USA) with a refractive index detector (Waters 2414) and a series of four columns of HR Styragel® (HR4, HR3, HR2 and HR1) (each 7.8 mm × 300 mm, Waters Styragel). The total run time for the sample was 50 min with a flow rate of THF of 1 mL/min and an injection volume of 100 µL. The temperature of the columns and the detector was 35 °C. The standards used for the calibration curve were polystyrene standards-Shodex SM-105 (Waters, Milford, MA) with a molecular weight ranging from $5.00x10^2$ to $2.48x10^6$ Da. The measurements were conducted in triplicate.

### 6.2.4 Characterization of films

Oscillatory melt rheology of PLA-based films (PLA-C and PLA-J) was evaluated using a Rheometer (Discovery Hybrid HR-3; TA Instruments, New Castle, DE, USA) attached with an electrically heated plate (EHP) at selected temperatures (160, 170, 180 and 190 °C). Compression molded film disk samples (diameter 25 mm and thickness 550 mm) were placed between the plates (measuring plate diameter 25 mm) at a gap set to 500-µm, and held for 5 min to relax the residual stresses before the

actual rheological measurement. The EHP system precisely controlled the sample temperature using a platinum resistance thermometer positioned at the center and in contact with the opposite face of the lower plate. Frequency sweep tests (0.1–10 Hz) were conducted within a linear viscoelastic range (LVR), at a constant strain (0.05%) at selected temperatures. Time dependency of the melt was measured at a constant frequency of 1 Hz and 170 °C for a period of 15 min. All rheological measurements were carried out in duplicate, and rheological parameters were obtained directly from the instrumental software (TRIOS, TA Instruments, New Castle, DE, USA).

Thermal gravimetric analysis (TGA) was performed using TGA (Q50, TA Instruments, New Castle, DE, USA). Samples of 5 – 10 mg were heated from 25 to 600 °C with a heating ramp of 10 °C/min in an inert atmosphere ($N_2$).

Thermal analysis was carried out using a differential scanning calorimetry (DSC) DSC (Q100, TA Instruments, New Castle, DE, USA), under nitrogen atmosphere to determine the degree of crystallinity ($\%X_C$), cold-crystallization temperature ($T_{cc}$), glass transition temperature ($T_g$), and melting temperature ($T_m$) of PLA-C and PLA-J films. The samples (5 -10 mg) were cooled from 25 to 5 °C and then run from 5 to 210 °C. An isothermal step for 3 min was carried out and then run to 5 °C; finally, a second heat run was performed from 5 to 210 °C. The ramp used was 10 °C/min with a flow rate of purge nitrogen of 70 mL/min. The degree of *%Xc* was calculated using the following equation:

$$\%X_C = \frac{\Delta H_m - \Delta H_C}{\Delta H_f^*(1-x)} \times 100 \qquad \text{Eq. 6.1}$$

where $\Delta H_m$ is the heat of melting, $\Delta H_C$ is the cold crystallization heat, $\Delta H_f^*$ is the heat of fusion of PLA when it is 100% crystalline (93.7 J/g) [29], and $x$ is the Joncryl® fraction. The measurements were conducted in triplicate and the results of the second heat are reported.

### 6.2.5 Hydrolytic degradation study

The hydrolysis studies were performed at 80 °C using 50% ethanol solution (ethanol/water ratio of 1:1 v/v) controlling the *pH* at 11 using CAPS (0.1 M) as a buffer solution. Ten disks of film (2 cm in diameter) were cut and then inserted in a stainless steel wire separated by glass beads and placed inside of a glass vial. Then the vials were filled with the solution previously conditioned at the experimental temperature. Films were retrieved periodically and then analyzed by SEC. The measurements were conducted in triplicate.

To estimate the rate constants for the change in $M_n$ of PLA films over time, the experimental data was fitted using the first order reaction since this was the best order reaction as previously demonstrated by the authors [30]:

$$M_n = M_{n_o} exp(-kt) \qquad \text{Eq. 6.2}$$

where $M_{no}$ is the initial $M_n$ (Da), $k$ is the rate constant ($h^{-1}$) and $t$ is time (h). **Eq. 6.2** was fitted using MATLAB® 2016a (MathWorks, Natick, MA, USA) nonlinear regression function (*nlinfit*).

### 6.2.6 Diffusion of water vapor

Diffusion of water vapor of PLA-C and PLA-J films was determined by gravimetric analysis using an SGA-100 from VTI Corp. (Hialeah, FL, USA). The test conditions were

40 °C and 70% relative humidity (RH). The experiments were conducted in triplicate. Diffusion coefficient (*D*) were calculated using the following equation:

$$D = l^2/7.2\ t_{1/2} \quad \text{Eq. 6.3}$$

where *l* is thickness (m) and $t_{1/2}$ is the half time (s).

Mean comparison of the *D* and *k* were done by Tukey HSD test with a significance level $\alpha$=0.05 (*p*-value, $p<0.05$) using JMP® 9.0 (Cary, NC, USA) statistical software.

## 6.3 Results and discussion

### 6.3.1 Processing of PLA films

**Figure 6.2** shows the $M_n$ after processing both PLA (PLA-C and PLA-J) films at selected residence times in the cast film extruder. When PLA-C film was processed at residence times of 4, 8, and 16 min, the $M_n$ values were found to be 141.8 ± 2.3, 136.9 ± 1.7, and 124.7 ± 3.4 kDa, respectively; indicating that the longest residence time of 16 min degraded the neat PLA film significantly ($p<0.05$). On the contrary, the $M_n$ values increased abruptly and even doubled the value observed for the neat PLA when 1.5% wt. of chain extender was incorporated into the PLA matrix. The $M_n$ values for 1.5% wt. chain extended incorporated to PLA were 240.3 ± 2.8, 272.7 ± 6.6, and 270.4 ± 1.2 kDa for a residence time of 4, 8, and 16 min, respectively. This demonstrates that the incorporation of the chain extender restricted the lowering of $M_n$ during processing by reconnecting cleaved chains, increasing the molecular weight of the PLA. This increase in molecular weight has been shown to be due to carboxyl end groups reacting with the epoxy functional groups of the chain extender via ring-opening polymerization reactions,

forming covalent bonds [18, 31].

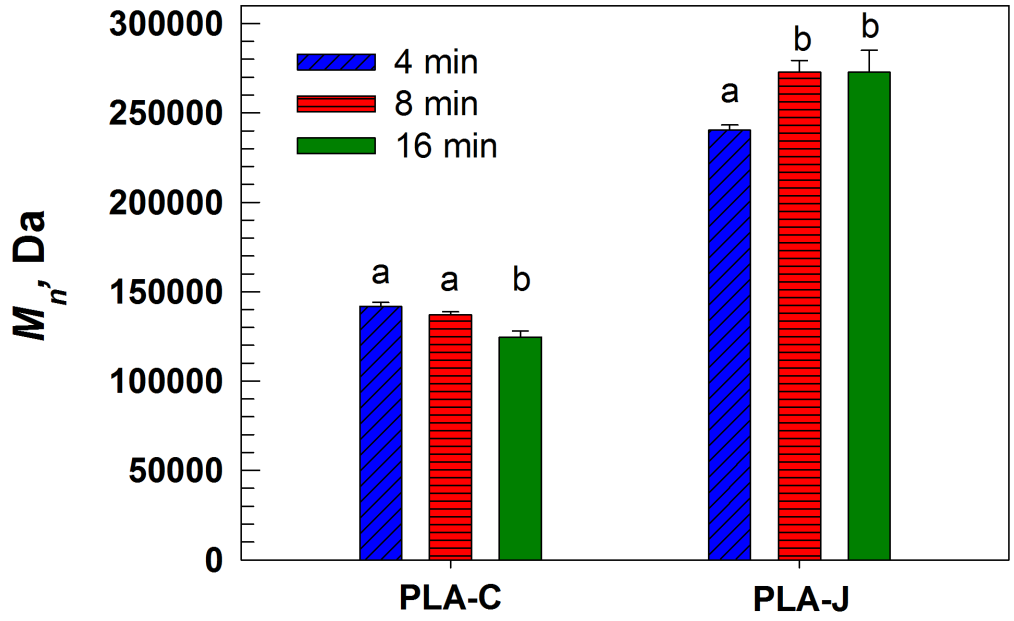


**Figure 6.2** $M_n$ of PLA-C and PLA-J films after processing at selected residence times. Values with different lower case letters within the same classification are statistically different ($\alpha$=0.05).

While comparing the $M_n$ values of PLA-J films produced with selected residence times, it was found that the highest $M_n$ was obtained at a residence time of 8 min, and the value insignificantly lowered ($p$>0.05) on further extension of time. So, it was inferred that 8 min was the minimum time required to activate the chain extender to reconnect chains of PLA matrix that had been cleaved during heat processing. Therefore, the PLA-J film with 8 min of residence time was selected for further characterization analysis and hydrolytic degradation studies having the highest $M_n$ with the lowest residence time of processing. For comparison purposes the PLA-C film processed at the same conditions as PLA-J was selected.

### 6.3.2 Characterization

#### 6.3.2.1 Rheological behavior

Films with the highest $M_n$ after processing with a residence time of 8 min were characterized by their rheological properties. The time dependency of viscosity of PLA-C and PLA-J films was investigated by oscillatory time sweep tests for a time period of 15 min at 170 °C. As shown in **Figure 6.3**, the complex viscosity ($\eta^*$) of the two types of samples behaved differently during the heating period; it decreased from 0.17 to 0.13 Pa.s for the PLA-C, while an increasing trend (1.5 to 1.9 Pa.s) was noticed for the PLA-J. The observed values clearly indicated a time-dependency for both samples. The test indicated a minor degradation of PLA samples happening because of the degradation of the polymer, whereas the addition of the chain extender improved the stability of the PLA matrix by affecting its melt-strength by means of chain extension/branching [20, 32].

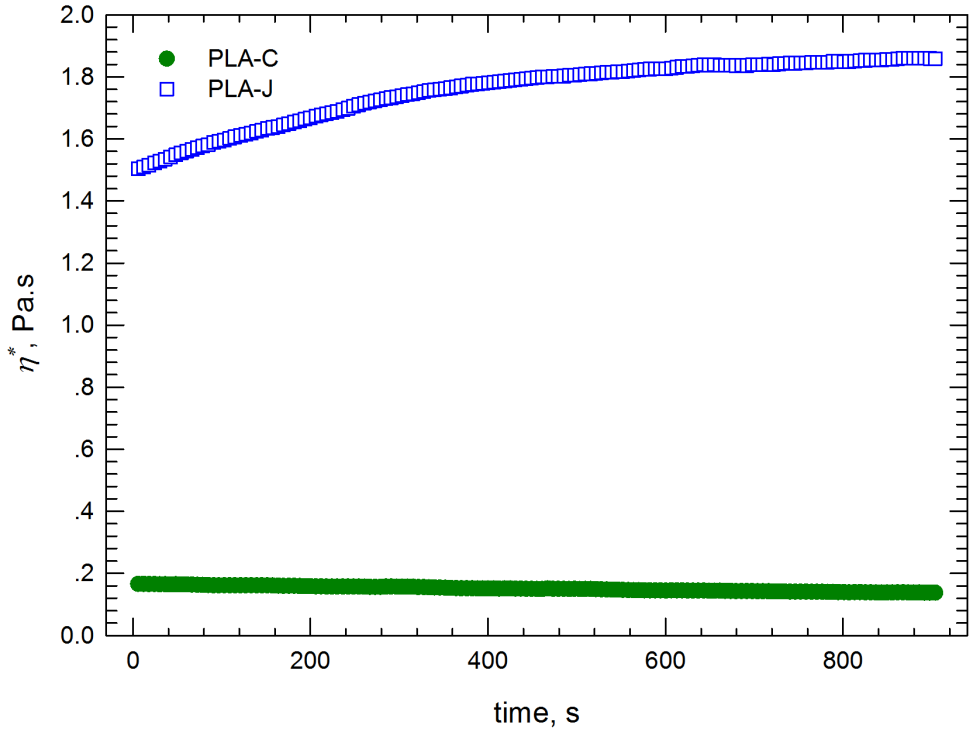


**Figure 6.3** Time dependency of PLA melt at 170 °C for a time period of 15 min.

The influence of the chain extender on the mechanical rigidity of PLA films at 170 °C is illustrated in **Figure 6.4**. PLA-C film at melt exhibited high-frequency dependency, and the loss modulus (*G″*) was significantly higher than the storage modulus (*G′*), confirming a predominating liquid-like characteristic of the melt. PLA-J, with incorporated chain extender, had significantly lower frequency-dependency of the dynamic moduli compared to the neat PLA. **Figure 6.4** shows that the slope of *G′* - *ω* of PLA-J at a terminal range of frequency is largely deviates from 2, and it is less than 1. The slope in the low-frequency range indicates the blend has a different morphology than the neat polymer. A power law behavior at low-frequency (slope <1) is one of the

characteristic dynamic responses of a co-continuous morphology [33]. Addition of chain extender markedly improved the mechanical properties of the PLA-J matrix as compared to the control sample. For the control sample, the liquid-like property predominates ($G''>G'$) throughout the frequency range, and a gel point was attained at the highest frequency (62.8 rad/s). Addition of Joncryl improved the $G'$ significantly, and the $G'$ exceeded the $G''$ above 1 rad/s with predominating solid-like property. The $G'$ of PLA-J increased almost 1-2 log cycles over the control sample within the studied frequency range, which was further confirmed by the low phase angle ($\delta$) data. A similar 30 times increase in the complex shear viscosity of PLA incorporated with 1 wt% chain extender (Joncryl®4368) in PLA blend (at an angular frequency of 0.1 rad/s) at 180 °C was previously reported [21]. Such a significant increase in the mechanical rigidity indicated that macromolecular chain extension had occurred during the extrusion compounding process [34]. The difference in storage modulus between neat PLA and PLA-J has been reported by other authors who attributed the difference to creation of a branched polymer [18, 19, 22, 35].

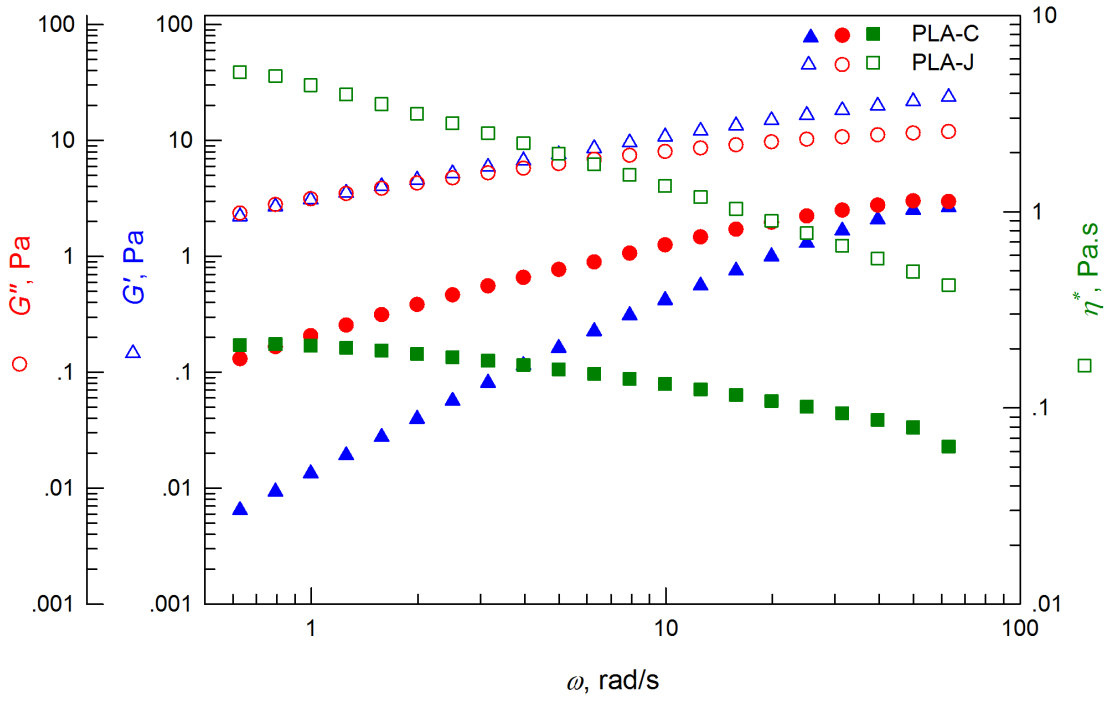


**Figure 6.4** Mechanical spectra of PLA-C and PLA-J films as a function of angular frequency at 170 °C.

A plot of phase angle, $\delta$ against the complex modulus ($G^*$) eliminates the effect of shifting along the frequency axis and yields temperature independent curves when time temperature superposition (TTS) holds [36]. **Figure 6.5** illustrates these plots for both PLA films at selected temperatures. All of the data were superimposed in one curve with a very characteristic shape although the superposition of the PLA-J sample was superior to that of the neat PLA polymer. At low values of $G^*$, $\delta$ is nearly 90° for PLA-C, indicating that the samples are viscous. The behavior of PLA-J was quite different from that of PLA-C, and the difference in the shape of the curves can be

related to the influence of chain extension or a change of topology from linear to branched polymer for PLA-J [21, 37, 38].

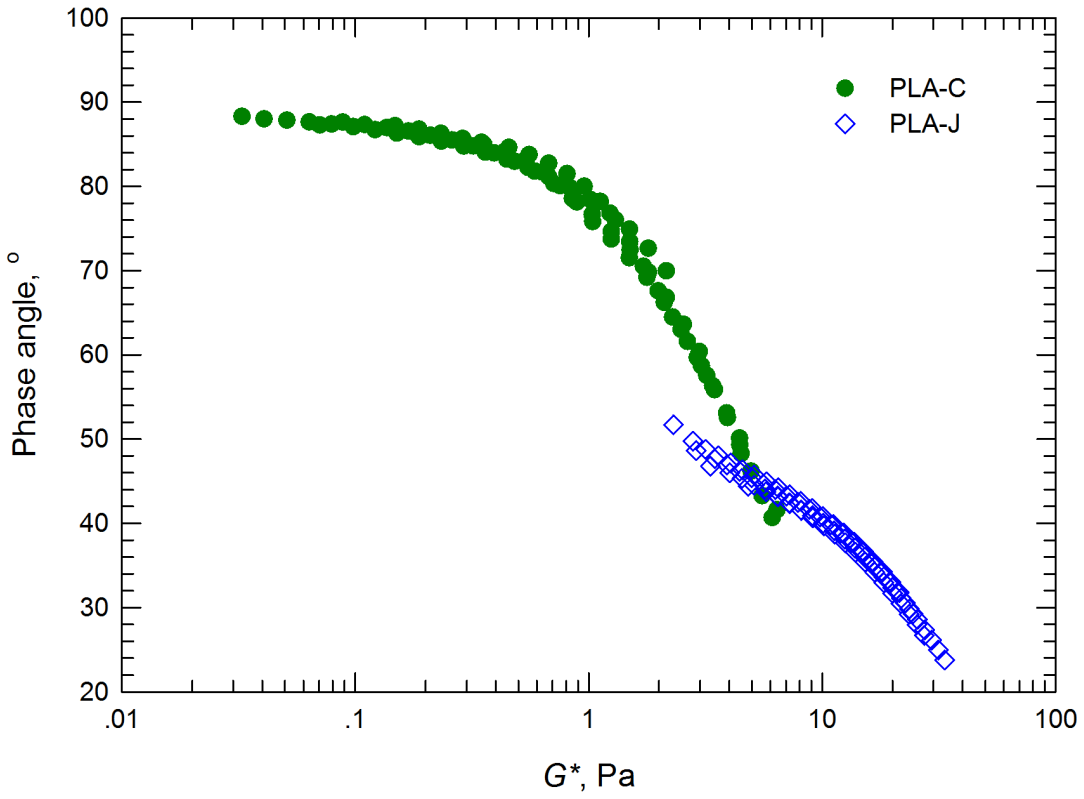


**Figure 6.5**. Van Gurp-Palmen plot of PLA-C and PLA-J samples obtained from master curves for a reference temperature of 180 °C.

### 6.3.2.2 Thermal properties

**Figure 6.6** displays the TGA thermograms of PLA-C and PLA-J films to investigate the effect of the chain extender on the thermal degradation behavior of PLA. The onset decomposition temperatures ($T_{onset}$) of PLA-C and PLA-J were 359.5 ± 0.3

and 358.4 ± 0.1 °C, respectively. A marginal decrease in the $T_{onset}$ was observed after the incorporation of the chain extender in PLA. Although the values were close, this could be attributed to branched structures of PLA-J film, which result in a higher concentration of hydroxyl groups as end groups, making the polymer less stable than the linear PLA. These results are in accordance with those researchers who studied the thermal stability of branched PLA with Joncryl® ADR-4368 and epoxidized soybean oil [18, 39].

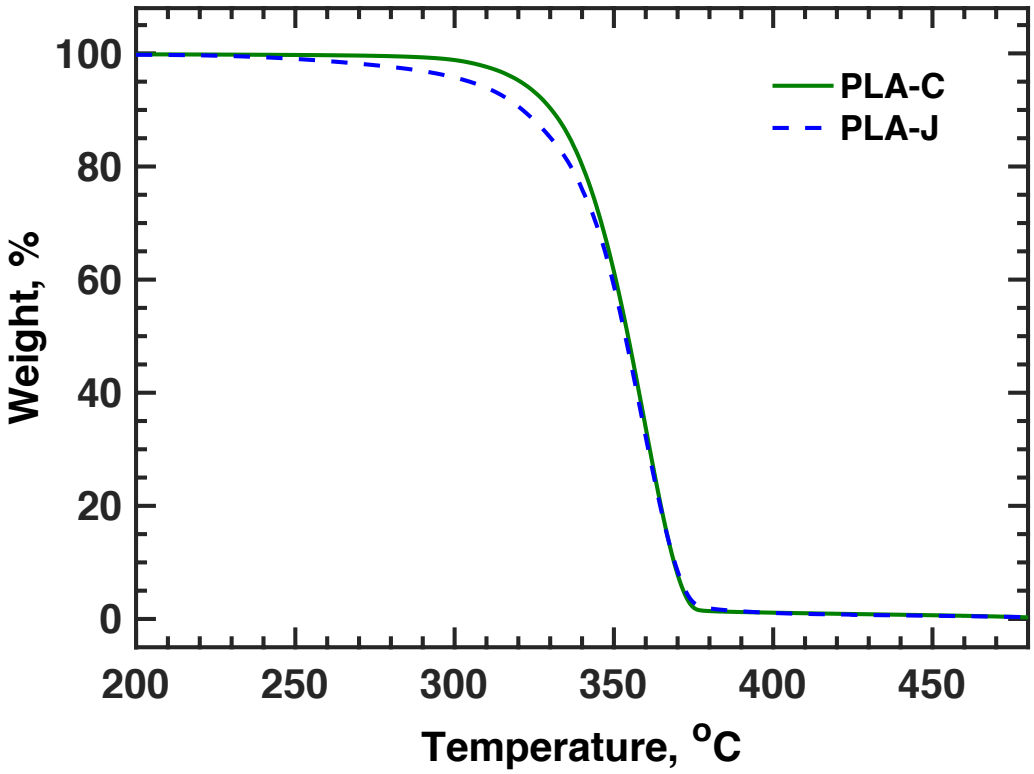


**Figure 6.6** TGA thermograms of PLA-C and PLA-J films.

**Figure 6.7** shows the DSC heating thermograms of PLA-C and PLA-J films. The thermal parameters are listed in **Table 6.1**. Incorporation of the chain extender did not

influence the $T_g$ of the PLA significantly. However, the $\%X_C$ slightly increased with the presence of the chain extender, and the $T_m$ and the $T_{cc}$ for PLA-J decreased by 1 °C. Even that the difference was marginal, branched polymers had faster cold crystallization rates than the linear PLA due to heterogeneous nucleation effect by the branching points [35, 40-42]. Although there was a nucleation effect of the chain extender, the $T_m$ showed a marginal decrease, which can be attributed to the formation of imperfect crystals in the PLA-J film sample. The presence of chain branches after processing PLA with the chain extender restricted the chain mobility, forming thinner and imperfect crystals with lower melting point [35].

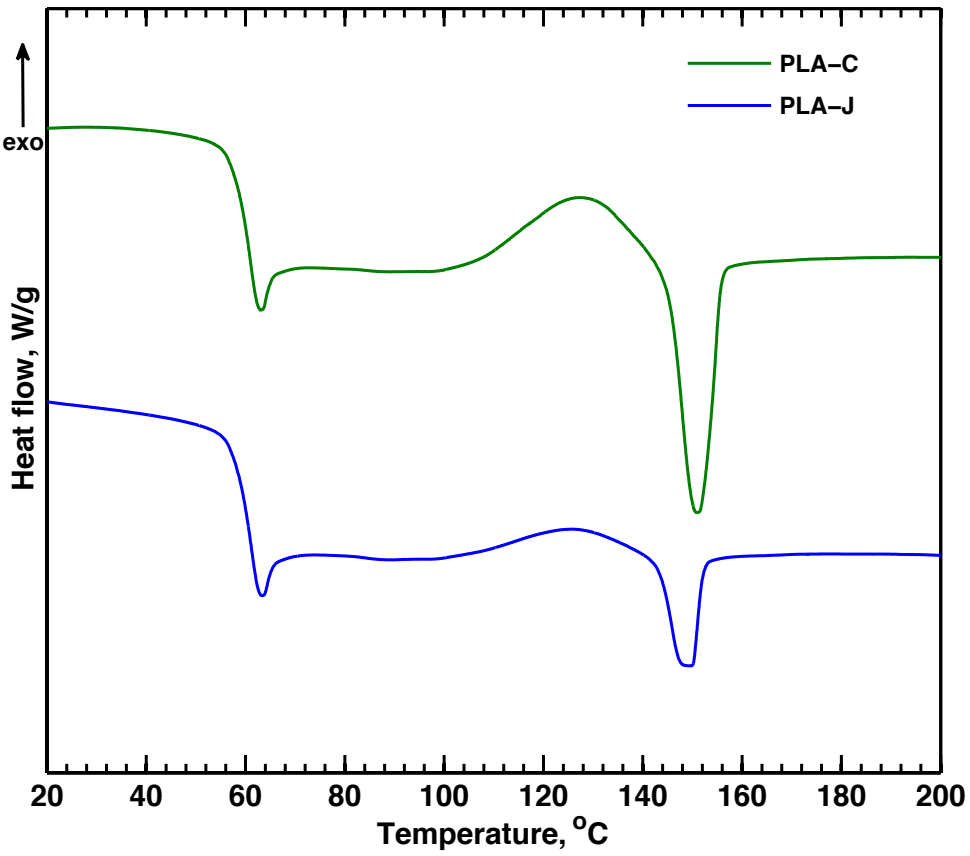


**Figure 6.7** DSC curves of the second heat scan of PLA-C and PLA-J films.

**Table 6.1** Thermal properties of the second heat scan of PLA-C and PLA-J films.

| Sample | $T_g$, °C | $T_{cc}$, °C | $T_m$, °C | $X_C$, % |
|---|---|---|---|---|
| PLA-C | 59.6 ± 1.2[a] | 126.8 ± 0.4[a] | 150.9 ± 0.1[a] | 0.2 ± 0.1[a] |
| PLA-J | 60.6 ± 0.3[a] | 125.5 ± 0.5[b] | 149.5 ± 0.2[b] | 0.7 ± 0.2[b] |

Values with different letter within the same column are different ($\alpha$=0.05).

### 6.3.3 Hydrolytic degradation study

To study the effect of the addition of chain extender on the hydrolytic degradation of PLA, PLA-C and PLA-J films were immersed in 50% ethanol solution at 80 °C and *pH* 11. These conditions were selected based on our earlier works to accelerate the hydrolysis of PLA films [43, 44]. It was found that the fast hydrolysis of PLA immersed in 50% ethanol solutions especially under basic conditions and high temperatures was very effective for the degradation [30]. **Figure 6.8** shows the molecular weight distribution (*MWD*) of PLA-C and PLA-J films during the hydrolysis in 50% ethanol at 80 °C and *pH* 11. In the beginning, before the hydrolysis started (time = 0), PLA-C showed a monomodal distribution with a *PDI* of 2.0 ± 0.2. However, PLA-J films exhibited a multimodal distribution with *PDI* of 2.2 ± 0.1, which could be associated with the presence of branches with different hydrodynamic volumes as a consequence of different chain topologies [21, 23]. Cailloux et al. [23] studied sheets of branched PLA with Joncryl®4300F where they attributed the peak at the lower molecular weight in the *MWD* of branched PLA to a linear population and the peak at the higher molecular weight to a branched chain population.

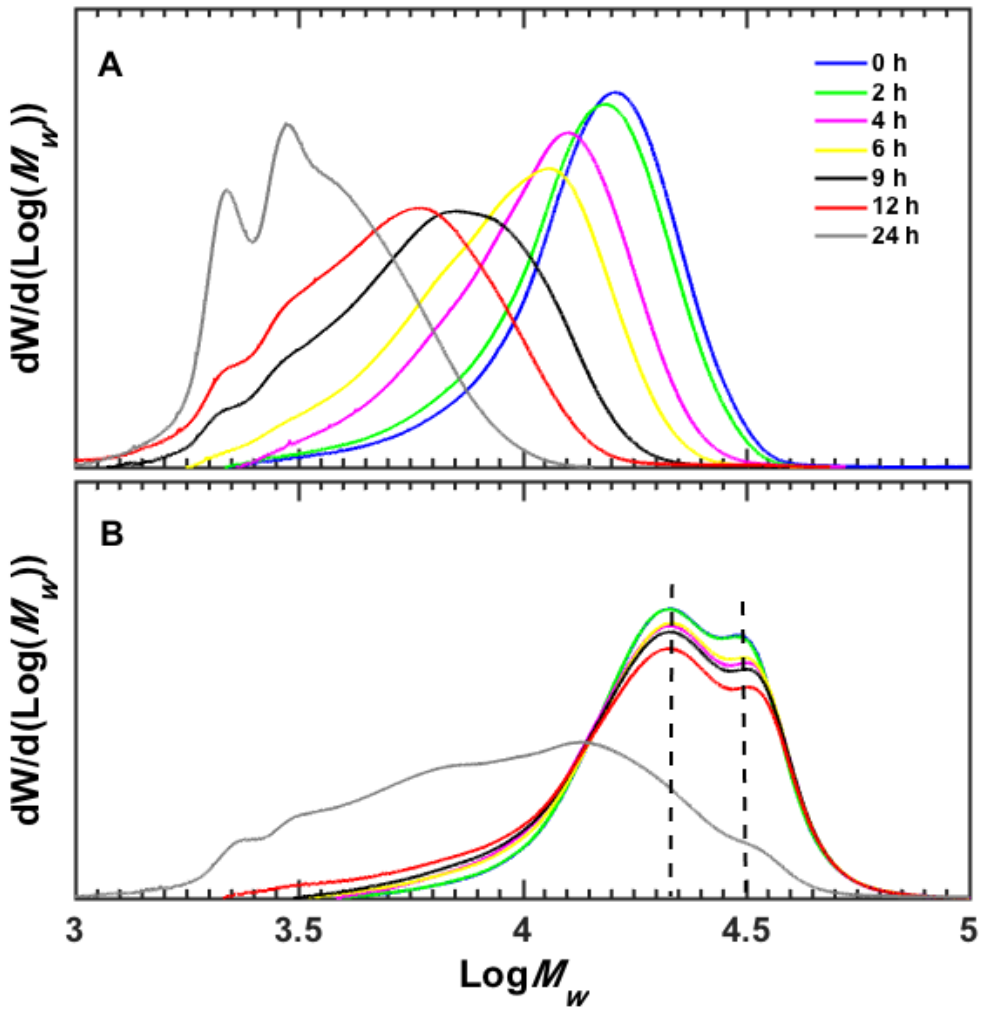


**Figure 6.8** *MWD* of (A) PLA-C and (B) PLA-J films during hydrolytic degradation in 50% ethanol at 80 °C, *pH* 11.

When PLA-C film was exposed to hydrolytic degradation in 50% ethanol for 24 h, the *MWD* shifted from its original position towards the lower molecular weight (**Figure 6.8A**). This behavior has been reported as degradation of PLA, which is preferentially carried out by the bulk erosion [45-48]. Optical images of PLA samples immersed in 50% ethanol solution can be found in Iñiguez-Franco et al. [43]. With progress of hydrolysis, the *MWD* peaks broadened and at some point changed from monomodal to

multimodal distribution. This could be explained by the fragments of PLA chains formed due to chain scission resulting in different molecular weights or due to the hydrolysis-resistant crystalline residues where the $M_n$ decrease slowed down during the hydrolysis process [45, 47, 48]. Different results have been found when PLA has been exposed to alkaline solutions at 37 °C where the hydrolysis of PLA proceeded via surface erosion mechanism [49]. In the case of the hydrolytic degradation of PLA-J the behavior of *MWD* was different than PLA-C film (**Figure 6.8B**); the *MWD* remained at the initial position and the lower molecular weight tail increased with a reduced peak area as hydrolysis was taking place. This change of behavior must correspond to hydrolysis of PLA-J via surface erosion where a significant weight loss occurs with no significant molecular weight decrease [50]. After 24 h, the *MWD* broadened with the formation of new peaks that can be attributed to chain scission and accumulation of PLA oligomers. Tsuji and Hayashi [50] studied the hydrolytic degradation of linear 2-arm and branched 4-arm PLA where the hydrolysis proceeded via bulk and surface erosion, respectively. The authors advocated that such a change happened due to the higher concentration of terminal hydroxyl groups in the branched PLA that can form hydrogen bonding among them. This interaction prevents the terminal hydroxyl group from interacting with water molecules where the cleavage is taking place in the ester groups around the terminal groups preventing the diffusion of water into the polymer core to start hydrolysis reactions.

To understand the effect of the branches on the hydrolytic degradation of PLA-J, water diffusion studies were performed by exposing the films to water vapor to determine the *D* as previously described by the authors [43, 51]. **Figure 6.9** shows

the %weight change profiles of PLA-C and PLA-J films exposed to water vapor at 40 °C and 70% RH. Experiments at 80°C were excluded because of the equipment limitation. Also, it is important to point out that crystallization could occur upon immersion at 80 °C as aforementioned in **Figure 6.8A**. At 40 °C and 70% RH, the estimated *D* in PLA-C was almost 1.5 times larger than in PLA-J (**Table 6.2**). The slower diffusion of water in PLA-J could be due to the presence of branches, supporting the hydrolysis mechanism via surface erosion where there is an interaction of water molecules with the terminal hydroxyl groups in the surface of the polymer.

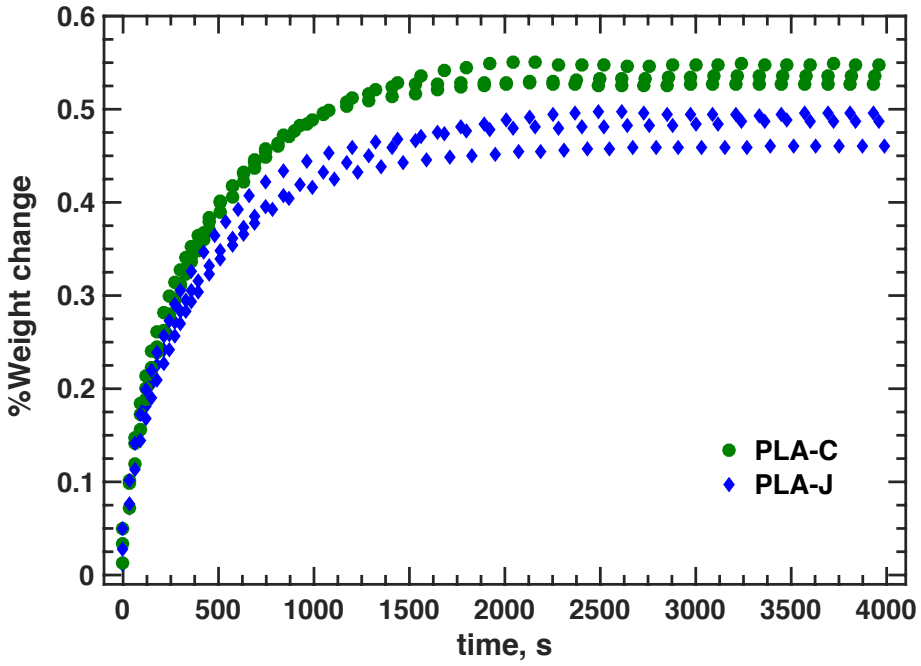


**Figure 6.9** %Weight change of PLA-C and PLA-J films exposed to water vapor at 40 °C, 70% RH.

**Table 6.2** Hydrolysis rate constants for PLA films immersed in 50% ethanol at 80 °C, *pH* 11, and *D* of water vapor at 40 °C, 70% RH.

| Film | $k$ ($h^{-1}$)* | $D$ x$10^{-13}$ ($m^2/s$)** |
|---|---|---|
| PLA-C | 0.206 ± 0.014 [a] | 4.14 ± 0.27 [a] |
| PLA-J | 0.065 ± 0.008 [b] | 2.88 ± 0.13 [b] |

* Fitting of **Eq. 6.2**. For PLA-J, this is considered as a pseudo-first order reaction for practical comparison purpose.

** *D* values were calculated using **Eq. 6.3**.

Values with different lower case letters are statistically different ($\alpha$=0.05).

When a deconvolution analysis of the *MWD* of PLA-J (**Figure 6.8A**) was performed using a LogNormal function as previously discussed by the authors [48, 52], two main different $M_n$ peaks were identified. At time 0 the peaks corresponded to different $M_n$: 12.28 x$10^5$ and 2.35 x$10^5$ Da. However, for the estimation of *k,* the experimental data of the highest $M_n$ peak of PLA-J sample did not follow the first order equation reaction (Eq. 2). Therefore, for purposes of this study and for practical comparison reasons a pseudo $M_n$ of PLA-J film was used to fit Eq. 2. Applying a first order reaction kinetics for PLA-C samples and a pseudo first order reaction for PLA-J film, different rate constants were estimated (**Table 6.2**). When the chain extender was introduced into the PLA matrix, the $M_n$ increased and the hydrolysis decreased around 70% ($p$<0.05). The branched chain extension changes the hydrolysis from bulk to surface erosion. When surface erosion happens the diffusion of water molecules is lower than the degradation rate of the polymer. The behavior of the molecular weight

reduction of PLA-C and PLA-J films can also be seen in **Figure 6.10B**, which shows the $M_v/M_{vo}$ during hydrolysis in 50% ethanol. A steady reduction in $M_v$ of PLA-J film and the absence of an abrupt drop were observed associated with a surface reaction pattern of hydrolysis [53]. The reduction in $M_v$ was only 26.2% after 12 h for PLA-J while the reduction for PLA-C was 84.9%. Such difference in $M_v$ could be associated with the hydrolysis occurring mainly in the near surface region for PLA-J film, in which the backbone cleavage rate is much higher than the diffusion of water, and therefore the decrease in the molecular weight is not as fast as in bulk erosion.

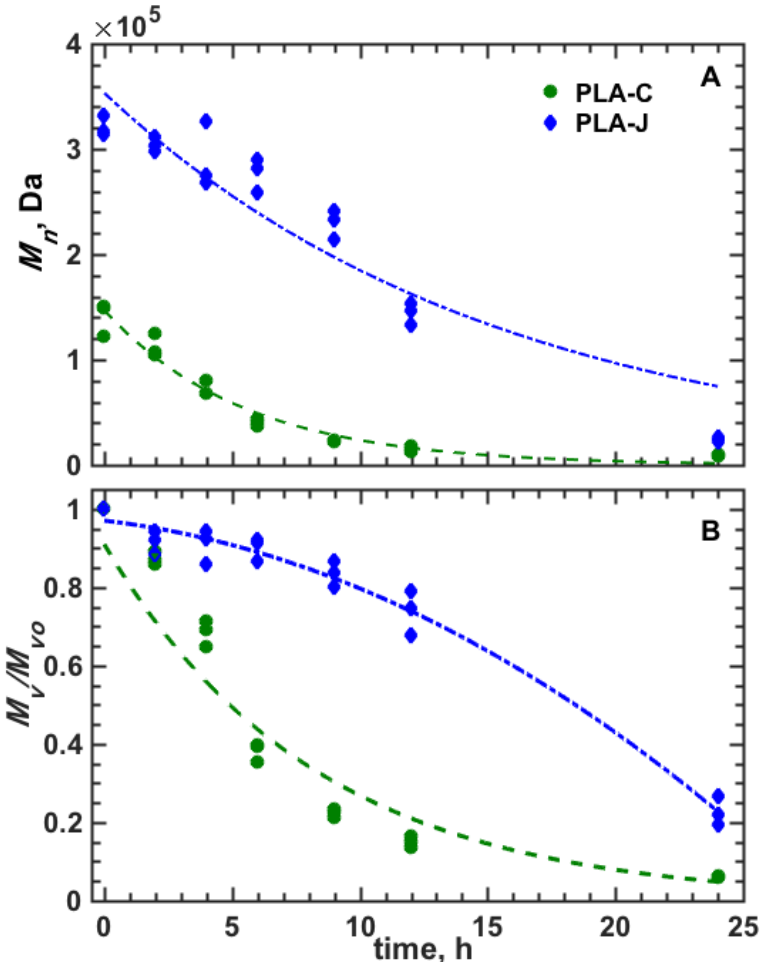


**Figure 6.10** (A) $M_n$ and (B) $M_v/M_{vo}$ as a function of time during hydrolytic degradation of PLA films immersed in 50% ethanol at 80 °C, *pH* 11. Lines in (A) are fitting of the first order reaction equation while lines in (B) are used as visual aid.

## 6.4 Conclusions

This study showed the effect of including an epoxy-acrylic additive on PLA films and its effect on the hydrolytic degradation of PLA. Epoxy-acrylic compounds have being widely studied as a chain extender for the thermal stabilization of PLA during processing. However, not much information has been provided about their effect on PLA hydrolytic behavior. PLA processed at a residence time of 8 min with 1.5% wt. of

chain extender was adequate to allow the epoxy groups of the chain extender to retard the PLA degradation and to provide a PLA with high $M_n$ Rheological and thermal data revealed that chain extension led to the formation of branched chain structures improving the dynamic moduli and decreasing the onset temperature of PLA. When PLA films were exposed to hydrolytic degradation, the hydrolysis mechanism of linear PLA-C and branched PLA-J films were different. The PLA-C film hydrolysis proceeded mainly via bulk erosion while surface erosion was taking place in PLA-J films. This mechanism was identified based on the different *MWD* behavior during hydrolysis of the films. These results can be attributed to the high concentration of terminal hydroxyl groups in the branched PLA that could form hydrogen bonds between each other. Thus, preventing the diffusion of water molecules into to the core of the PLA matrix to start the bulk hydrolysis reaction process. PLA modified with chain extender can prolong the service life of the PLA products by decreasing its hydrolytic degradation during storage and usage and changing its mechanism of hydrolytic failure. However, further studies should be conducted at normal shelf life conditions to study the fait of chain extenders compounds during the hydrolytic degradation of PLA and their possible migration to the environment ensuring the safety of the modified PLA material.

## 6.5 Acknowledgements

I-F, F., thanks CONACYT (The Mexican National Council for Science and Technology), SEP (The Mexican Secretariat of Public Education), and the Government of Mexico for providing support funds for a Ph.D. fellowship. R. Auras thanks the partial support of USDA and Michigan AgBioResearch, Hatch project R. Auras.

# REFERENCES

## REFERENCES


[1] R. Auras, B. Harte, S. Selke, An overview of polylactides as packaging materials, Macromol. Biosci. 4 (2004) 835-864.

[2] E. Castro-Aguirre, F. Iñiguez-Franco, H. Samsudin, X. Fang, R. Auras, Poly (lactic acid)—Mass production, processing, industrial applications, and end of life, Adv. Drug Deliv. Rev. 107 (2016) 333-366.

[3] P. Dubois, N. Ropson, R. Jérôme, P. Teyssié, Macromolecular engineering of polylactones and polylactides. 19. Kinetics of ring-opening polymerization of ε-caprolactone initiated with functional aluminum alkoxides, Macromolecules 29 (1996) 1965-1975.

[4] K. Jamshidi, S.-H. Hyon, Y. Ikada, Thermal characterization of polylactides, Polymer 29 (1988) 2229-2234.

[5] N. Bleach, K. Tanner, M. Kellomäki, P. Törmälä, Effect of filler type on the mechanical properties of self-reinforced polylactide–calcium phosphate composites, J. Mater. Sci. Mater. Med. 12 (2001) 911-915.

[6] Y. Ikada, H. Tsuji, Biodegradable polyesters for medical and ecological applications, Macromol. Rapid Commun. 21 (2000) 117-132.

[7] J.-Y. Park, I.-H. Lee, Controlled release of ketoprofen from electrospun porous polylactic acid (PLA) nanofibers, J. Polym. Res. 18 (2011) 1287-1291.

[8] Y.-N. Chang, R.E. Mueller, E.L. Iannotti, Use of low MW polylactic acid and lactide to stimulate growth and yield of soybeans, Plant Growth Regul. 19 (1996) 223-232.

[9] R.G. Sinclair, Slow-release pesticide system. Polymers of lactic and glycolic acids as ecologically beneficial, cost-effective encapsulating materials, Environ. Sci. Technol. 7 (1973) 955-956.

[10] K.M. Nampoothiri, N.R. Nair, R.P. John, An overview of the recent developments in polylactide (PLA) research, Bioresour. Technol. 101 (2010) 8493-8501.

[11] H. Tsuji, Hydrolytic Degradation, in: R. Auras, L.-T. Lim, S. Selke, H. Tsuji (Eds.), Poly(lactic acid). Synthesis, Structures, Properties, Processing, and Applications, John Wiley & Sons, Inc., New Jersey, 2010, pp. 345-381.

[12] S. Lyu, J. Schley, B. Loy, D. Lind, C. Hobot, R. Sparer, D. Untereker, Kinetics and time-temperature equivalence of polymer degradation, Biomacromolecules 8 (2007) 2301-2310.

[13] X. Yuan, A.F. Mak, K. Yao, Surface degradation of poly (L-lactic acid) fibres in a concentrated alkaline solution, Polym. Degrad. Stab. 79 (2003) 45-52.

[14] M.K. Mitchell, D.E. Hirt, Degradation of PLA fibers at elevated temperature and humidity, Polym. Eng. Sci. (2014).

[15] S. De Jong, E.R. Arias, D. Rijkers, C. Van Nostrum, J. Kettenes-Van den Bosch, W. Hennink, New insights into the hydrolytic degradation of poly (lactic acid): participation of the alcohol terminus, Polymer 42 (2001) 2795-2802.

[16] H. Tsuji, K. Sumida, Poly (L‐lactide): v. effects of storage in swelling solvents on physical properties and structure of poly (L‐lactide), J. Appl. Polym. Sci. 79 (2001) 1582-1589.

[17] R.A. Auras, S.P. Singh, J.J. Singh, Evaluation of oriented poly (lactide) polymers vs. existing PET and oriented PS for fresh food service containers, Packag. Technol. Sci. 18 (2005) 207-216.

[18] N. Najafi, M. Heuzey, P. Carreau, P.M. Wood-Adams, Control of thermal degradation of polylactide (PLA)-clay nanocomposites using chain extenders, Polym. Degrad. Stab. 97 (2012) 554-565.

[19] R. Al-Itry, K. Lamnawar, A. Maazouz, Improvement of thermal stability, rheological and mechanical properties of PLA, PBAT and their blends by reactive extrusion with functionalized epoxy, Polym. Degrad. Stab. 97 (2012) 1898-1914.

[20] Q. Meng, M.-C. Heuzey, P.J. Carreau, Control of thermal degradation of polylactide/clay nanocomposites during melt processing by chain extension reaction, Polym. Degrad. Stab. 97 (2012) 2010-2020.

[21] Y.-M. Corre, J. Duchet, J. Reignier, A. Maazouz, Melt strengthening of poly (lactic acid) through reactive extrusion with epoxy-functionalized chains, Rheol. Acta 50 (2011) 613-629.

[22] R. Al-Itry, K. Lamnawar, A. Maazouz, Reactive extrusion of PLA, PBAT with a multi-functional epoxide: Physico-chemical and rheological properties, Eur. Polym. J. 58 (2014) 90-102.

[23] J. Cailloux, O.O. Santana Pérez, E.A. Franco Urquiza, J. Bou, F. Carrasco, J. Gámez Pérez, M.L. Maspoch, Sheets of branched poly (lactic acid) obtained by one

step reactive extrusion calendering process: Melt rheology analysis, Express Polym. Lett. (2013).

[24] W.G. Blasius Jr, G.A. Deeter, M.A. Villalobos, Oligomeric chain extenders for processing, post-processing and recycling of condensation polymers, synthesis, compositions and applications. United States Patent 6984694 B2, in, 2006.

[25] M. Villalobos, A. Awojulu, T. Greeley, G. Turco, G. Deeter, Oligomeric chain extenders for economic reprocessing and recycling of condensation plastics, Energy 31 (2006) 3227-3234.

[26] S. Japon, L. Boogh, Y. Leterrier, J.-A. Månson, Reactive processing of poly (ethylene terephthalate) modified with multifunctional epoxy-based additives, Polymer 41 (2000) 5809-5818.

[27] A. Haralabakopoulos, D. Tsiourvas, C. Paleos, Chain extension of poly (ethylene terephthalate) by reactive blending using diepoxides, J. Appl. Polym. Sci. 71 (1999) 2121-2127.

[28] D.N. Bikiaris, G.P. Karayannidis, Chain extension of polyesters PET and PBT with two new diimidodiepoxides. II, J. Polym. Sci. A Polym. Chem. 34 (1996) 1337-1342.

[29] E. Fischer, H.J. Sterzel, G. Wegner, Investigation of the structure of solution grown crystals of lactide copolymers by means of chemical reactions, Colloid Polym. Sci. 251 (1973) 980-990.

[30] F. Iñiguez-Franco, R. Auras, K. Dolan, S. Selke, D. Holmes, M. Rubino, H. Soto-Valdez, Chemical recycling of poly(lactic acid) by water-ethanol solutions, Polym. Degrad. Stab. Accepted (2017).

[31] Q.T. Nguyen, S. Japon, A. Luciani, Y. Leterrier, J.A.E. Månson, Molecular characterization and rheological properties of modified poly (ethylene terephthalate) obtained by reactive extrusion, Polym. Eng. Sci. 41 (2001) 1299-1309.

[32] Q.-K. Meng, M.-C. Heuzey, P. Carreau, Effects of a multifunctional polymeric chain extender on the properties of polylactide and polylactide/clay nanocomposites, Int. Polym. Proc. 27 (2012) 505-516.

[33] I. Vinckier, H.M. Laun, Manifestation of phase separation processes in oscillatory shear: droplet-matrix systems versus co-continuous morphologies, Rheol. Acta 38 (1999) 274-286.

[34] M. Mihai, M.A. Huneault, B.D. Favis, Rheology and extrusion foaming of chain‐branched poly (lactic acid), Polym. Eng. Sci. 50 (2010) 629-642.

[35] V. Ojijo, S.S. Ray, Super toughened biodegradable polylactide blends with non-linear copolymer interfacial architecture obtained via facile in-situ reactive compatibilization, Polymer 80 (2015) 1-17.

[36] M. Van Gurp, J. Palmen, Time-temperature superposition for polymeric blends, Rheol. Bull 67 (1998) 5-8.

[37] S.G. Hatzikiriakos, Long chain branching and polydispersity effects on the rheological properties of polyethylenes, Polym. Eng. Sci. 40 (2000) 2279-2287.

[38] G. Fleury, G. Schlatter, R. Muller, Non linear rheology for long chain branching characterization, comparison of two methodologies: Fourier transform rheology and relaxation, Rheol. Acta 44 (2004) 174-187.

[39] C. Fu, B. Zhang, C. Ruan, C. Hu, Y. Fu, Y. Wang, Improved hydrolytic stability of poly (dl-lactide) with epoxidized soybean oil, Polym. Degrad. Stab. 95 (2010) 485-490.

[40] L. Wang, X. Jing, H. Cheng, X. Hu, L. Yang, Y. Huang, Blends of linear and long-chain branched poly (l-lactide) s with high melt strength and fast crystallization rate, Ind. Eng. Chem. Res. 51 (2012) 10088-10099.

[41] M. Nofar, W. Zhu, C.B. Park, J. Randall, Crystallization kinetics of linear and long-chain-branched polylactide, Ind. Eng. Chem. Res. 50 (2011) 13789-13798.

[42] J. You, L. Lou, W. Yu, C. Zhou, The preparation and crystallization of long chain branching polylactide made by melt radicals reaction, J. Appl. Polym. Sci. 129 (2013) 1959-1970.

[43] F. Iñiguez-Franco, R. Auras, G. Burgess, D. Holmes, X. Fang, M. Rubino, H. Soto-Valdez, Concurrent solvent induced crystallization and hydrolytic degradation of PLA by water-ethanol solutions, Polymer 99 (2016) 315-323.

[44] F. Iñiguez-Franco, R. Auras, M. Rubino, K. Dolan, H. Soto-Valdez, S. Selke, Effect of nanoparticles on the hydrolytic degradation of PLA-nanocomposites by water-ethanol solutions, Polym. Degrad. Stab. 146 (2017) 287-297.

[45] H. Tsuji, T. Saeki, T. Tsukegi, H. Daimon, K. Fujie, Comparative study on hydrolytic degradation and monomer recovery of poly (L-lactic acid) in the solid and in the melt, Polym. Degrad. Stab. 93 (2008) 1956-1963.

[46] S.V. Canevarolo, Chain scission distribution function for polypropylene degradation during multiple extrusions, Polym. Degrad. Stab. 70 (2000) 71-76.

[47] H. Tsuji, Y. Ikada, Blends of crystalline and amorphous poly (lactide). III. Hydrolysis of solution‐cast blend films, J. Appl. Polym. Sci. 63 (1997) 855-863.

[48] F. Iñiguez-Franco, R. Auras, K. Dolan, S. Selke, D. Holmes, M. Rubino, H. Soto-Valdez, Chemical recycling of poly (lactic acid) by water-ethanol solutions, Polym. Degrad. Stab. 149 (2018) 28-38.

[49] H. Tsuji, Y. Ikada, Properties and morphology of poly (L‐lactide). II. Hydrolysis in alkaline solution, J. Polym. Sci. A Polym. Chem. 36 (1998) 59-66.

[50] H. Tsuji, T. Hayashi, Hydrolytic degradation of linear 2-arm and branched 4-arm poly (dl-lactide) s: effects of branching and terminal hydroxyl groups, Polym. Degrad. Stab. 102 (2014) 59-66.

[51] S. Selke, J.D. Culter, R.J. Hernandez, Plastic packaging, properties, processing, applications, and regulations, 2nd ed., Hanser, Cincinnati, OH, 2004.

[52] E. Castro-Aguirre, R. Auras, S. Selke, M. Rubino, T. Marsh, Impact of Nanoclays on the Biodegradation of Poly (Lactic Acid) Nanocomposites, Polymers 10 (2018) 202.

[53] T. Kijchavengkul, R. Auras, M. Rubino, E. Alvarado, J.R.C. Montero, J.M. Rosales, Atmospheric and soil degradation of aliphatic–aromatic polyester films, Polym. Degrad. Stab. 95 (2010) 99-107.

# CHAPTER 7

## Overall Conclusion and Recommended Future Work

### 7.0 Overall Conclusion

PLA is a biodegradable polymer that has been used to replace the use of fossil-based polymers for specific applications, such as in the medical field, agriculture and food packaging industries [1]. PLA during its life cycle can be exposed to various solvents such as water and alcohol, leading to hydrolytic degradation and structural changes [2, 3]. The hydrolytic degradation of PLA has widely been studied. However, the synergetic effect of different water-ethanol solutions is not well understood to control and develop its applications and tailor its uses.

First, the parameters and factors affecting the hydrolysis of PLA in water-ethanol solutions were studied (Chapter 3). Experimental studies of the SIC and hydrolytic degradation of PLA films were performed at 40 °C in contact with water, 50% ethanol, and 95% ethanol. This study found that PLA films in contact with 50% ethanol showed faster degradation than in water and 95% ethanol. This result was attributed to the competitive balance between the swelling when ethanol was present, and the hydrolysis due to the sorption of water molecules to start the degradation reactions. During the study, it was confirmed that the water sorption was higher during hydrolysis of PLA exposed to 50% ethanol solution. The faster hydrolysis in 50% ethanol was confirmed by LA release. Furthermore, when PLA was exposed to water-ethanol solutions, the polymer experienced SIC where the crystallinity increased dramatically in the first stage due to the primary crystallization where a large number of crystals were formed, and

then the system experienced saturation where the crystallization rate was slow, corresponding to secondary crystallization. At the last stage, the crystallinity started to increase attributed to the hydrolysis of amorphous regions being higher when PLA was exposed to 50% ethanol, which was in accordance to the faster hydrolytic degradation of PLA.

Depending on the application, the hydrolytic degradation of PLA can be seen as an advantage or a disadvantage. PLA hydrolysis can be used for chemical recycling to recover PLA back to its monomer for new PLA production [4, 5]. After demonstrating that the hydrolytic degradation of PLA in water-ethanol solutions was faster when PLA was exposed to 50% ethanol, a method to safely perform the chemical recycling of PLA using a “green” solvent was developed (Chapter 4). For that, it was necessary to estimate the kinetic parameters, rate constant and activation energy driving PLA’s hydrolytic degradation. The hydrolysis of PLA was carried out above $T_g$ in 50% ethanol and water. The hydrolysis in these two systems was through a bulk erosion mechanism proven by the analysis of the *MWD* with a multimodal distribution at the latter stages of the hydrolysis. The analysis of the deconvolution showed multiple reaction pathways that followed the first order reaction kinetics. The $E_a$ was estimated using a reparameterization of the Arrhenius equation to obtain a better estimation with near zero correlation among the parameters. The $E_a$ values obtained were within the same range of values reported in literature when PLA has been exposed to different media, such as alkaline media, water or acidic media. The results indicated that 50% ethanol could be used as a potential solution alternative to perform the chemical recycling of PLA.

PLA has some limitations such as poor toughness and impact strength [6].

Nanoparticles have been incorporated into the PLA matrix to enhance its mechanical, thermal and barrier properties [7]. PLA-nanocomposites during their life cycle can be exposed to various solvents such as water and alcohol. Therefore, there is a critical need to understand the effect of the organo-clay filler on the hydrolytic degradation of PLA-nanocomposites and the potential release of the nanoparticles from different environments representing prolonged exposures. Chapter 5 showed the results of the hydrolytic degradation of PLA-nanocomposites by water, 50 and 95% ethanol solutions at 40 °C. PLA-nanocomposite film exposed to 50% ethanol solution had a faster rate of degradation and higher release of LA than in 95% ethanol and water due to the synergetic effect of the swelling of the matrix and water diffusion. No difference in the rate of degradation was found with OMMT incorporation into the PLA films. This was explained by the similar water vapor sorption in neat PLA and PLA-OMMT films. However, the effect of the nanoparticles in PLA affected the sorption of ethanol as almost the double amount of ethanol sorption occurred into the clay galleries without expansion of the PLA matrix. The presence of nanoparticles restricted the movement of the PLA chains showing similar behavior in the crystallization process to neat PLA. During the hydrolytic degradation of PLA-nanocomposite, the release of surfactant was detected, being higher in the 50% ethanol system. The release of nanoclay was measured by quantifying Al in the 50% ethanol solution corresponding to 304.9 ppb of nanoclay released after 90 d of exposure, which was 0.58% of the initial clay added into PLA.

PLA is susceptible to thermal degradation during melt processing [8]. Addition of chain extenders can ameliorate PLA's thermal degradation during processing [9-12].

However, studies evaluating the effect of chain extenders on the hydrolytic degradation of PLA are limited. Chapter 6 studied the effect of epoxy-acrylic additives (Joncryl® 1.5% wt.) used as a chain extender in the hydrolytic degradation of PLA. The hydrolysis was performed in accelerated condition, 50% ethanol at 80 °C and *pH* 11. The incorporation of the chain extender increased the molecular weight after processing indicating that the carboxylic end groups of PLA, as a product of the degradation, were reconnected by the epoxy groups of the chain extender. Results revealed that the chain extension led to the formation of a branched structure. The change of the molecular architecture affected the hydrolysis mechanism. The hydrolytic degradation was delayed with the presence of chain extender showing a surface erosion mechanism while the linear neat PLA presented bulk erosion. The surface erosion process was attributed to the lower diffusion of water molecules into the core of the polymer due to the presence of PLA branches. The branches increased the number of terminal hydroxyl groups that can interact with each other, preventing the interaction with water molecules, and therefore the diffusion into the bulk to start hydrolysis reactions. PLA modified by chain extender can prolong the service life of the material by delaying the hydrolysis reactions during storage and use.

## 7.1 Recommended Future Work

Future work should focus on the chemical recycling of PLA using 50% ethanol solution to optimize the commercial and industrial process. To successfully commercialize this chemical recycling process; the yield of LA-oligomers during the hydrolysis reactions should be fully understood. Efficient depolymerization of PLA would be around 95% yield of LA-oligomers in a short period. However, these studies are

missing along with the investigation of induced crystallization during hydrolysis. Crystal residuals present or formed during the hydrolysis can delay the recover process. To have a better overview of the recovery process, the separation of phases, water-ethanol, along with the LA-oligomers from the solution should be investigated to consider the cost-benefit of the process using a "green" solvent during the chemical recycling of PLA.

Besides the layered silicate-based nanoparticle studied in this dissertation, different nanoparticles have been added into PLA to improve its properties such as sepiolite and halloysite nanotubes [13]. The study of the effect of these nanoparticles on the hydrolytic degradation of PLA by water-ethanol solutions is recommended to be investigated to understand the different PLA-nanoparticles interactions for possible applications of PLA-nanocomposites. The transport of water-ethanol solutions into the different PLA-nanocomposites can differ where the release of nanoparticles could occur changing the hydrolysis behavior and therefore the durability and performance of the material. These changes may influence the release of the nanoparticles, but also the release could be affected by the hydrolytic degradation of PLA-nanocomposites by water-ethanol solutions.

This dissertation has also left for future work a better understanding of the possible fate of the chain extender during the hydrolytic degradation of modified PLA. Migration studies of the chain extenders should be performed looking for a possible diffusion of epoxy-acrylic chain extenders from PLA that can reach different environments encountered for consumer and non-consumer goods. Further studies should be conducted on understanding if the presence of the chain extenders affects the biodegradation of the final material.

# REFERENCES

## REFERENCES


[1] L.-T. Lim, R. Auras, M. Rubino, Processing technologies for poly (lactic acid), Prog. Polym. Sci. 33 (2008) 820-852.

[2] H. Tsuji, Hydrolytic Degradation, in: R. Auras, L.-T. Lim, S. Selke, H. Tsuji (Eds.), Poly(lactic acid). Synthesis, Structures, Properties, Processing, and Applications, John Wiley & Sons, Inc., New Jersey, 2010, pp. 345-381.

[3] H. Tsuji, K. Sumida, Poly (L‐lactide): v. effects of storage in swelling solvents on physical properties and structure of poly (L‐lactide), J. Appl. Polym. Sci. 79 (2001) 1582-1589.

[4] K. Hamad, M. Kaseem, F. Deri, Recycling of waste from polymer materials: An overview of the recent works, Polym. Degrad. Stab. 98 (2013) 2801-2812.

[5] V. Piemonte, S. Sabatini, F. Gironi, Chemical recycling of PLA: a great opportunity towards the sustainable development?, J. Polym. Environ. 21 (2013) 640-647.

[6] K.S. Anderson, K.M. Schreck, M.A. Hillmyer, Toughening polylactide, Polymer Reviews 48 (2008) 85-108.

[7] S.S. Ray, K. Yamada, M. Okamoto, K. Ueda, New polylactide-layered silicate nanocomposites. 2. Concurrent improvements of material properties, biodegradability and melt rheology, Polymer 44 (2003) 857-866.

[8] H. Nishida, Thermal Degradation, in: R. Auras, L.-T. Lim, S. Selke, H. Tsuji (Eds.), Poly(lactic acid). Synthesis, Structures, Properties, Processing, and Applications, John Wiley & Sons, Inc., New Jersey, 2010, pp. 401-412.

[9] N. Najafi, M. Heuzey, P. Carreau, P.M. Wood-Adams, Control of thermal degradation of polylactide (PLA)-clay nanocomposites using chain extenders, Polym. Degrad. Stab. 97 (2012) 554-565.

[10] R. Al-Itry, K. Lamnawar, A. Maazouz, Improvement of thermal stability, rheological and mechanical properties of PLA, PBAT and their blends by reactive extrusion with functionalized epoxy, Polym. Degrad. Stab. 97 (2012) 1898-1914.

[11] Y.-M. Corre, J. Duchet, J. Reignier, A. Maazouz, Melt strengthening of poly (lactic acid) through reactive extrusion with epoxy-functionalized chains, Rheol. Acta 50 (2011) 613-629.

[12] J. Cailloux, O.O. Santana Pérez, E.A. Franco Urquiza, J. Bou, F. Carrasco, J. Gámez Pérez, M.L. Maspoch, Sheets of branched poly (lactic acid) obtained by one step reactive extrusion calendering process: Melt rheology analysis, Express Polym. Lett. (2013).

[13] J.-M. Raquez, Y. Habibi, M. Murariu, P. Dubois, Polylactide (PLA)-based nanocomposites, Prog. Polym. Sci. 38 (2013) 1504-1542.